



THE UNIVERSITY OF  
**WAIKATO**  
*Te Whare Wānanga o Waikato*

Research Commons

<http://researchcommons.waikato.ac.nz/>

## Research Commons at the University of Waikato

### Copyright Statement:

The digital copy of this thesis is protected by the Copyright Act 1994 (New Zealand).

The thesis may be consulted by you, provided you comply with the provisions of the Act and the following conditions of use:

- Any use you make of these documents or images must be for research or private study purposes only, and you may not make them available to any other person.
- Authors control the copyright of their thesis. You will recognise the author's right to be identified as the author of the thesis, and due acknowledgement will be made to the author where appropriate.
- You will obtain the author's permission before publishing any material from the thesis.

**Modelling temporal dynamics of discharge and  
nutrient loading from a mixed land use  
catchment, and interactions with a eutrophic,  
temperate lake under climate change**

A thesis  
submitted in fulfilment  
of the requirements for the degree  
of  
**Doctor of Philosophy in Biological Sciences**  
at  
**The University of Waikato**  
by  
**Wang Me**



THE UNIVERSITY OF  
**WAIKATO**  
*Te Whare Wānanga o Waikato*

2017

## Abstract

Understanding anthropogenic-induced changes in catchment water discharge and nutrient loads is critical for eutrophication assessment and sustainable management of receiving environments. Anthropogenic activities have increased nutrient export from terrestrial systems to lakes, where they may lead to eutrophication. Impacts of excess nutrients may be exacerbated by a warming climate. A variety of catchment models has been developed to gain insight into the temporal and spatial variations in discharge, and suspended sediment and nutrient transport in response to climate forcing and rainfall-runoff. These models can be used to predict the effects of different land management strategies and climate change on discharge and losses of particulate and dissolved constituents of the discharge. The integration of individual components of the modelling framework, including climate, catchment and aquatic ecosystem models, enables simulation and prediction of present and future states of freshwater ecosystems, including their spatial and temporal dynamics.

The study area for this thesis is the Lake Rotorua catchment (~410 km<sup>2</sup>; Bay of Plenty, North Island, New Zealand). Commencement in 1991 of spray irrigation of treated wastewater (10 mm d<sup>-1</sup>) from Rotorua city in the Whakarewarewa Forest was envisaged as a solution to eutrophication of Lake Rotorua (surface area ~80 km<sup>2</sup>) where treated wastewater (to secondary treatment level) had previously been discharged. The Waipa Stream draining the irrigated area (~2 km<sup>2</sup>) discharges to the Puarenga Stream, ultimately entering Lake Rotorua. The Puarenga Stream is the second-largest surface inflow to Lake Rotorua and drains a catchment of 77 km<sup>2</sup>. Land use in the Puarenga Stream catchment is mostly plantation forest within which there are 16 blocks for spray irrigation of wastewater. The catchment has an area of pastoral farmland (8 km<sup>2</sup>) that is typically fertilised with nitrogen (N) and phosphorus (P), as well as being irrigated with cowshed washdown which also contributed N and P.

The overarching aim of this study was to utilize advanced modelling technologies to simulate the discharge and sediment and nutrient loads from a mixed land use catchment of Puarenga Stream, part of which is spray-irrigated with wastewater in Waipa Stream catchment, and to model and understand the impacts and effects of different management regimes on the receiving waterbody; a

temperate eutrophic lake (Rotorua). To achieve this, the study encompassed three main areas of research: 1) a process-based catchment model (Soil and Water Assessment Tool) application in the Puarenga catchment of Lake Rotorua under different hydrologic conditions, testing the influence of parameter sensitivity; 2) improvements to the catchment model (SWAT) to represent high-frequency (daily and hourly) variability of nutrient discharges and to simulate different land and wastewater irrigation management strategies; and 3) an application of the improved catchment model (from (2) above) combined with the lake model (DYRESM-CAEDYM) to predict the response of Lake Rotorua to future climate in 2090 and catchment nutrient discharge.

The objective of the first research component (Chapter 2) was to examine the applicability of SWAT2009 model (version rev488) to the Puarenga catchment. The research included quantifying model performance and parameter sensitivity during different hydrologic conditions. A Sequential Uncertainty Fitting (SUFI-2) procedure was used to auto-calibrate unknown parameter values in the SWAT2009 model for years 2004–2008. Model validation was performed using: 1) monthly instantaneous measurements of suspended sediment (SS), total phosphorus (TP) and total nitrogen (TN) concentrations (1994–1997); and 2) daily discharge-weighted mean concentrations calculated from high-frequency event-based samples for concentrations of SS (nine events), TP and TN (both 14 events) at 1 h or 2 h frequency (2010–2012). Model error associated with quick-flow was underestimated (44% bias for SS, 70% bias for TP) compared with monthly measurements derived predominantly from base flow measurements (< 1% bias for SS, 24% bias for TP). The use of low-frequency base flow measurements for model calibration provided poor simulation results for “flashy” lower-order streams. The model results highlight the importance of using high-frequency, event-based monitoring data for calibration, to alleviate the potential for underestimation of storm-driven fluxes. A manual procedure (one-at-a-time sensitivity analysis) was used to quantify parameter sensitivity for the two hydrologically-separated regimes. Parameters relating to tuning of main channel processes (e.g., lateral flow slope length and travel time) were more sensitive for base flow estimates (particularly discharge and SS), while those relating to overland processes (e.g., Manning's *n* value for overland flow) were more sensitive for the quick flow estimates. Separating discharge and loads of sediments and nutrients into a base flow and a

quick flow component provided important insights into uncertainties in parameter values. This research has important implications for performance of hydrological models applied to catchments with large fluctuations in stream flow, and in cases where models are used to examine scenarios that involve substantial changes to the existing flow regime.

The SWAT2009 model described in Chapter 2 did not have algorithms to simulate a complex irrigation operation. The objective of the second research chapter (Chapter 3) was therefore to develop a capability to simulate the irrigated sub-catchment and examine alternatives for managing the wastewater. A modified version of the SWAT2012 code (rev629) using hourly routing algorithms was adapted to the Waipa Stream sub-catchment within the Puarenga catchment. A similar configuration to Chapter 2 was applied for the modelling except that a finer temporal resolution of rainfall records was used in Chapter 3. Hourly records at Kaituna rain gauge, which is outside of the irrigated sub-catchment, were used to allocate weekly records at Red Stag gauge, which is within the irrigated sub-catchment, to hourly rainfall values. The modified SWAT2012 model was run at an hourly time step for a 10-year (2003–2012) period using the daily irrigation routine, then calibrated and validated by comparing weekly average predictions with measurements. The optimised values of parameters were different from those in Chapter 2. A range of statistical metrics indicated that the SWAT2012 model performed well using hourly routing with respect to 10-year (2003–2012) daily simulations that were averaged to the weekly measurements for comparison of discharge ( $r \geq 0.81$ ;  $p < 0.001$ ) and TN load ( $r \geq 0.73$ ;  $p < 0.001$ ), but it did not perform so well for simulations of both SS ( $0.43 \leq r \leq 0.54$ ;  $p < 0.001$ ) and TP load ( $0.45 \leq r \leq 0.54$ ;  $p < 0.001$ ) in both the calibration and validation periods. Hourly routing gave high temporal variability of TN load, although lower than the variability of SS and TP loads (i.e.,  $SS > TP > TN$  variability). Simulations were run using daily outputs for an unirrigated scenario and for a range of other management options including changes in the area, frequency and amount of irrigation. Increasing the irrigation area decreased TP and TN loads in the simulation. The impact of changing irrigation frequency from daily to one day each week was small for annual TP load simulations. Annual TN load increased considerably under weekly irrigation. Compared with low-frequency, high-volume wastewater applications (once every seven days), the current strategy of daily

wastewater irrigation minimises TN leaching and reduces saturation of the subsurface layer. Improvements to the SWAT2012 model and the use of hourly routing to capture high-frequency (daily and hourly) variability of nutrient discharges and simulations of different wastewater irrigation management regimes may assist with future strategies to mitigate P and N losses from the irrigated area by refining the area, timing, frequency and amount of irrigation.

In Chapter 4 the primary objective was to combine the modified SWAT2012 model from Chapter 3 with the lake model (DYRESM–CAEDYM version 4.0) to simulate the trophic state of Lake Rotorua (mean depth 10.8 m), in response to nutrient load reductions from wastewater-irrigated forest and farmland in the Puarenga Stream catchment under present and future climates. Initial parameter values required for the setup of both models were based on the monitoring data that were measured close to the start date of the simulation period. A range of statistical metrics indicated that the SWAT2012 model performed well ( $r \geq 0.88$ ,  $p < 0.001$ ) with respect to comparisons of monthly catchment discharge, TN and TP loads, and less so ( $r = 0.78$ ,  $p < 0.01$ ) for TN concentration, and not at all well for TP concentration ( $r = 0.17$ ,  $p > 0.05$ ) for the 4-year (2006–2010) simulation period. SWAT2012 model simulations were used for the Puarenga Stream input to the DYRESM–CAEDYM model of Lake Rotorua while other inflows used either measured data or values derived from other studies. Considering the 1.5-year lake residence time for Lake Rotorua, the DYRESM–CAEDYM model was validated using monthly data collected at two sites during 2008–2010. The DYRESM–CAEDYM model performed well ( $r \geq 0.63$ ;  $p < 0.01$ ) for surface water TP and TN concentrations in both the calibration and validation periods, but not for bottom-water nutrient concentrations. Effects of land management practice were then examined by simulating four nutrient application scenarios relating to wastewater irrigation and farmland fertilisation within the Puarenga catchment. Under the scenario of removing nutrient applications from both wastewater irrigation and farmland fertilisation, nutrient load reductions were 39.5% for TP and 75.2% for TN in the Puarenga catchment but these had much lesser effect on nutrient concentrations in the lake, with reduction of 3.5% for TP, 5.7% for TN, and 4.1% for chlorophyll *a* (Chl *a*; as a proxy for phytoplankton biomass) in surface waters. Based on the Intergovernmental Panel on Climate Change Fifth Assessment report, for the projected future climate of 2090 under the RCP8.5 scenario (equivalent to a

short-wave radiation increase of  $8.5 \text{ W m}^{-2}$ ), annual mean precipitation and solar radiation increase by 2.8% and 1.4%, respectively, humidity decreases by 0.6%, and air temperature increases by 2.7 °C. Downscaled climate projections for 2090 were derived from 22 general circulation models and used as input to SWAT and DYRESM–CAEDYM models of the catchment and lake, respectively. Simulations using a projected climate for 2090 had moderate impact on catchment nutrient loads (6% increase for TP, 7.6% decrease for TN), but concentrations in surface waters were predicted to increase by 45.9% for TP, 44.5% for TN, and 44.9% for Chl *a* from 2010 to 2090, suggesting that future climate change would increase eutrophication. Increased water temperatures would cause more frequent and longer periods of thermal stratification in polymictic lakes such as Rotorua, which would likely result in greater depletion of dissolved oxygen and possible anoxia of hypolimnetic waters. This overarching effect of climate change is likely to be through a physical response of the lake in the form of increased stratification and greater levels of internal nutrient loading.

This thesis has demonstrated the effects of different hydrologic conditions on SWAT2009 model performance and parameter sensitivity using an application to a small, mixed land use catchment, Lake Rotorua, New Zealand. By using the hourly routing algorithms and modifying relevant model code to simulate complex catchment irrigation operations, the SWAT2012 model performance was improved, particularly for high-frequency simulation of SS, TP and TN loads to the receiving lake. Finally, the modified SWAT2012 model combined with the lake model (DYRESM–CAEDYM) predicted that future climate change should be factored into assessments of the future trophic state of Lake Rotorua.

## **Acknowledgements**

The completion of this thesis is only made possible by the Grace of God. He alone began this good work and made many ways for me to finish this work. I am very grateful to Lord Jesus. My deepest gratitude also belongs to my parents for all of their support and patience through four and half years.

I thank God for my chief supervisor Prof. David Hamilton. I am very grateful to him being a father figure in directing my research papers and in taking care of a homesick girl always. Thank you for initially providing me the opportunity to visit New Zealand. My great gratitude to you for supporting my PhD study transfer, from Hohai University, Nanjing, China to the University of Waikato, Hamilton, New Zealand. I thank you for trusting me in this modelling study and pushing me forward to seek solutions and to present results in front of people. I am very grateful for your patience in detailed review and sparing your precious time to sit beside me and improve my English writing. I thank you for all your efforts made for my scholarship applications and for raising external student awards twice during my study. I thank you for being mindful of me and showing your smile always.

I would like to thank Associate Prof. Liancong Luo (Nanjing Institute of Geography and Limnology, Chinese Academy of Sciences). You initially introduced this study to me through your collaboration with David and brought me far from motherland to overseas. Your kindness to me will never be forgotten. Also my sincere deep thanks go to Dr Jonathan Abell (formerly University of Waikato, currently Ecofish Research Ltd, British Columbia, Canada). I thank you for your technical advice and valuable suggestions no matter whether you were in New Zealand or in Canada. I am deeply grateful to your steadfast help in encouraging my study in New Zealand and improving my English writing.

I also thank my co-supervisor Prof. Brendan Hicks for providing advice and helpful comments on finalising each chapter of my thesis. I greatly appreciate your understanding, patience, and help.

Sincere thanks also go to the Bay of Plenty Regional Council (BoPRC), Rotorua Lake Council (RLC) and Timberlands Limited for assistance with data collection. In particular, I thank Alison Lowe (RLC), Craig Putt (BoPRC), Alastair MacCormick (BoPRC), Penny MacCormick (BoPRC), Kim Lockie (RLC), Cheryl Hindle (Timberlands Limited) and Ian Hinton (Timberlands Limited).

I particularly thank Dr Chonghua Yin, Dr Yinpeng Li, and Dr Meng Wang from CLIMsystems for assistance with future climate projections using the SimCLIM software, and Dr Chonghua Yin for assistance with code modification for the catchment model. I also wish to send my special thanks to Chris McBride (the University of Waikato). You kindly helped me with understanding and modelling lake nutrient dynamics. Heartfelt thanks also to you for helping with the lake modelling work.

To the water quality people in LERNZ group at the University of Waikato, thank you for the friendly and collaborative environment through years – Dr Theodore Alfred Kpodonu, Dr Arianto Santoso, Simon Stewart, Kohji Muraoka, Dr Hannah Mueller, Vanessa Cotterill, Katie Noakes, and Dr Grant Tempero, Dr Mat Allan, Dr Moritz Lehmann, Dr Chris Data, Dr Adam Hartland, and Dr Aroon Parshotam,

My sincere respect and great gratitude to Liz Hartnell (the University of Waikato) and Andy Bruere (BoPRC). Thank you for being supportive and encouraging me through years of my stay in New Zealand. Thank you for always giving me warm hugs.

My special gratitude to my pastor Reverend Dr Theodore Alfred Kpodonu. This thesis would not have come this far without your shepherding. I thank God for giving me you as my spiritual father. Thank you for being unshakable and always standing by my side in good or bad times. Thank you for being my primary counsellor in both study and life experiences. Great thanks also to your merciful family, your wife Rita, four kids, Nichole, Nikao, Nanetta, and Zane, and everyone in our church family for giving me homelike love.

Finally, I thank Jinrui (Jason) Zhu for so much faithful support.

Praise God for His Goodness and Mercy.

# Table of Contents

Abstract .....	ii
Acknowledgements .....	vii
Table of Contents .....	ix
List of Figures .....	xii
List of Tables.....	xvi
Preface.....	xx
1 Introduction.....	1
1.1 Background and motivation .....	1
1.1.1 Climate, catchment and lake interactions.....	1
1.1.2 Hydrologic cycle and nutrient dynamics .....	3
1.1.3 Impacts of climate change on the lake catchment.....	5
1.1.4 Catchment and lake models .....	6
1.1.5 Study area.....	14
1.2 Thesis objectives .....	15
1.3 Thesis overview.....	15
1.4 References .....	20
2 Effects of hydrologic conditions on SWAT model performance and parameter sensitivity for a small, mixed land use catchment in New Zealand.....	27
2.1 Abstract .....	27
2.2 Introduction .....	28
2.3 Methods .....	31
2.3.1 Study area.....	31
2.3.2 Model configuration.....	33
2.3.3 Model calibration and validation .....	37
2.3.4 Hydrograph and contaminant load separation.....	45
2.3.5 Model evaluation.....	46
2.4 Results .....	49
2.4.1 Model performance and uncertainty .....	49
2.4.2 Separated parameter sensitivity.....	57
2.5 Discussion .....	60
2.5.1 Temporal dynamics of model performance .....	60
2.5.2 Key uncertainties.....	62

2.5.3	Temporal dynamics of parameter sensitivity .....	63
2.6	References .....	65
3	Water quality effects of treated municipal wastewater application to a temperate forested catchment: Insights from SWAT modelling.....	71
3.1	Abstract .....	71
3.2	Introduction .....	72
3.3	Methods .....	75
3.3.1	Study catchment .....	75
3.3.2	Sampling measurements.....	76
3.3.3	Model configuration and code modification .....	77
3.3.4	Parameter sensitivity and calibration .....	81
3.3.5	Model evaluation.....	82
3.3.6	Irrigation scenarios.....	83
3.4	Results .....	85
3.4.1	Sensitive and optimised parameters .....	85
3.4.2	Model performance .....	86
3.4.3	Irrigation scenarios simulations .....	97
3.5	Discussion .....	101
3.5.1	Effectiveness and uncertainties of modified SWAT2012 code ....	101
3.5.2	Impacts of temporal and spatial variations in management practices	103
3.6	References .....	105
4	Simulating variations in discharge and nutrient loads from a mixed land use catchment to a eutrophic lake: Effects of nutrient reductions and future climate	109
4.1	Abstract .....	109
4.2	Introduction .....	110
4.3	Methods .....	113
4.3.1	Study area and measured data .....	113
4.3.2	Model configuration.....	116
4.3.3	Model calibration and validation .....	119
4.3.4	Model scenarios .....	120
4.4	Results .....	124
4.4.1	Calibration and model performance.....	124
4.4.2	Catchment and lake scenarios: current climate.....	136

4.4.3	Catchment and lake scenarios: 2090 climate .....	141
4.5	Discussion .....	146
4.5.1	Model performance and sensitivity .....	146
4.5.2	Reducing nutrient loads to the Puarenga Stream catchment.....	148
4.5.3	Climate change impacts on catchment and lake .....	149
4.6	References .....	153
5	Concluding discussion and synthesis .....	160
5.1	Overview .....	160
5.2	Key findings and recommendations .....	160
5.3	Environmental implications .....	164
5.4	References .....	165
	Appendix 1 Code modifications made in SWAT2012_rev629 .....	168

## List of Figures

- Figure 1.1** A conceptual framework for the connected and interactive elements of climate, catchment (land and stream) and the lake, showing the main processes of hydrological and nutrient cycling. After Poole et al. (2002). Land considerations include land cover, soils, geology and topography. .... 2
- Figure 1.2** Key biogeochemical processes for nitrogen in soils, streams and lakes (dashed line indicates nitrate leaching only in water movement through soils). Adapted from Amatya et al. (2013). .... 4
- Figure 1.3** Key biogeochemical processes for phosphorus in soils, streams and lakes (dashed line indicates soluble phosphorus leaching only in water movement in soils). Adapted from Radcliffe et al. (2015). .... 5
- Figure 2.1** (a) Location of Puarenga Stream surface catchment in New Zealand, Kaituna rain gauge, climate station and managed land areas for which management schedules were prescribed in SWAT, and (b) location of the Puarenga Stream, major tributaries, monitoring stream-gauges, two cold-water springs and the Whakarewarewa geothermal contribution. Measurement data (Table 2.3) used to calibrate the SWAT model were from the Forest Research Institute (FRI) stream-gauge and were considered representative of the downstream/outlet conditions of the Puarenga Stream. .... 32
- Figure 2.2** Flow chart of methods used to separate hydrograph and contaminant loads and to quantify parameter sensitivities for: Q (discharge), SS (suspended sediment), MINP (mineral phosphorus), ORGN (organic nitrogen),  $\text{NH}_4\text{-N}$  (ammonium-nitrogen), and  $\text{NO}_3\text{-N}$  (nitrate-nitrogen). NSE: Nash-Sutcliffe efficiency. .... 47
- Figure 2.3** Regression of measured and simulated (a) discharge (Q), concentrations of (b) suspended sediment (SS), (c) total phosphorus (TP), and (d) total nitrogen (TN) including lower and upper 95% confidence limits (LCL and UCL) and lower and upper 95% prediction limits (LPL and UPL). Note that the “choppy” shape of confidence limits shown in figures b–d resulted from the few data points (< 50) in the regressions of measured and simulated SS, TP and TN concentrations. .... 50
- Figure 2.4** Measurements and daily mean simulated values of discharge, suspended sediment (SS), total phosphorus (TP) and total nitrogen (TN) during calibration (a–d) and validation (e–h). Measured daily mean discharge was calculated from 15-min observations and measured concentrations of SS, TP and TN correspond to monthly grab samples. .... 52
- Figure 2.5** Example of a storm event showing derivation of discharge (Q)-weighted daily mean concentrations (dashed horizontal line) based on hourly measured concentrations (black dots) of suspended sediment

(SS), total phosphorus (TP) and total nitrogen (TN) over two days (a–c). Comparisons of Q-weighted daily mean concentrations with simulated daily mean estimates of SS, TP and TN (scatter plot, d–f). The horizontal bars show the ranges in hourly measurements during each storm event in 2010–2012..... 54

**Figure 2.6** Measurements and simulations derived using the calibrated set of parameter values. Data are shown separately for base flow and quick flow. (a) Daily mean base flow and quick flow; (b) suspended sediment (SS) load; (c) total phosphorus (TP) load; (d) total nitrogen (TN) load. Vertical lines in b–d show the contaminant load in quick flow. Time series relate to calibration (2004–2008) and validation (1994–1997) periods (note time discontinuity). Measured instantaneous loads of SS, TP, and TN correspond to monthly grab samples..... 55

**Figure 2.7** The standard deviation (STD) of the ln-transformed Nash–Sutcliffe efficiency (NSE) used to indicate parameter sensitivity based on one-at-a-time (OAT) sensitivity analysis for separate base and quick flow components: (a) Q (discharge); (b) SS (suspended sediment); (c) MINP (mineral phosphorus); (d) NO<sub>3</sub>-N (nitrate-nitrogen); (e) ORGN (organic nitrogen); (f) NH<sub>4</sub>-N (ammonium-nitrogen). A median value (0.2) derived from the STD of ln-transformed NSE was chosen as a threshold above which parameters were deemed to be “sensitive”. Definitions of each parameter are shown in Table 2.4..... 58

**Figure 3.1** Study catchment drained by the Waipa Stream, Rotorua, New Zealand. Treated wastewater is spray-irrigated onto 14 blocks within the Whakarewarewa Forest, upstream of Lake Rotorua. .... 77

**Figure 3.2** Diagram of the modification of SWAT2012 code required for the Waipa irrigated forestry catchment. Components in the first row indicate the processes for which code modifications were required. Components in the second row describe each process. Components in the third row indicate the specific FORTRAN files where the SWAT2012 code was modified (see Appendix 1)..... 81

**Figure 3.3** Weekly mean values derived from simulated daily outputs for (a–b) discharge (Q) and (c–d) suspended sediment (SS) load, compared with weekly flow-proportional measurements at the Waipa D/S hydrometric station. The comparisons were undertaken by using a modified SWAT2012 code based on hourly routing (left) and daily routing (right). The calibration period was from 2003 to 2010 and the validation period was from 2011 to 2012. The model underestimated SS peaks when high rainfall occurred either during (A1–A3) or after (B) harvest of multiple blocks, as indicated by the number of harvested blocks in the upper panel of (c). .... 90

**Figure 3.4** Weekly mean values derived from simulated daily outputs for loads of (a–b) mineral phosphorus (MINP), (c–d) organic phosphorus (ORGP), and (e–f) total phosphorus (TP), compared with weekly

flow-proportional measurements at the Waipa D/S hydrometric station. The comparisons were undertaken by using a modified SWAT2012 code based on hourly routing (left) and daily routing (right). Calibration was from 2003 to 2010 and validation from 2011 to 2012. Underestimates of TP peaks were related to a lagged response to high rainfall only (C), high rainfall following (D) or during (E) harvest of more blocks, only during harvest of more blocks without high rainfall (F), and high TP in wastewater during harvest of multiple blocks at once (G), as indicated by the number of harvested blocks in the upper panel of (c)..... 91

**Figure 3.5** Weekly mean values derived from simulated daily outputs for loads of (a–b) organic nitrogen (ORGN) and (c–d) ammonium–nitrogen (NH<sub>4</sub>–N), compared with weekly flow-proportional measurements at the Waipa D/S hydrometric station. The comparisons were undertaken by using a modified SWAT2012 code based on hourly routing (left) and daily routing (right). The calibration period was from 2003 to 2010 and the validation period was from 2011 to 2012. 92

**Figure 3.6** Weekly average values derived from simulated daily outputs for loads of (a–b) nitrate–nitrogen (NO<sub>3</sub>–N) and (c–d) total nitrogen (TN), compared with weekly flow-proportional measurements at the Waipa D/S hydrometric station. The comparisons were undertaken by using a modified SWAT2012 code based on hourly routing (left) and daily routing (right). The calibration period was from 2003 to 2010 and the validation period was from 2011 to 2012. Several underestimates of peaks in TN load were related to consecutive wet days (H1–H3) and high TN in wastewater (I). ..... 93

**Figure 3.7** Example of a storm event for the period 10–12 October 2011 showing variability of hourly SWAT2012 simulations of (a) discharge (Q), (b) suspended sediment (SS), (c) total phosphorus (TP) and (d) total nitrogen (TN) loads over three days. The horizontal red lines show daily mean values. Rainfall (inverted scale) is shown in (a)..... 95

**Figure 3.8** Multiyear (2003–2012) mean of total annual measured and simulated (a) total phosphorus (TP) and (b) total nitrogen (TN). S0 is 10–14 blocks irrigated daily, S1 is decreased irrigated area, S2 is reassigned irrigation from high rainfall ( $\geq 20 \text{ mm d}^{-1}$ ) days to low rainfall days, S3 is reduced irrigation frequency to one day per week and S4 is no irrigation. Boxes denote interquartile ranges (i.e., 25% and 75%); whiskers denote minimum and maximum values; horizontal lines denote median values. .... 98

**Figure 3.9** Daily mean load simulations of (a) mineral phosphorus (MINP), (b) total phosphorus (TP), (c) nitrate–nitrogen (NO<sub>3</sub>–N), and (d) total nitrogen (TN) under actual irrigation and no irrigation. .... 100

**Figure 4.1** Lake Rotorua surface topographic catchment showing the major sub-catchments. The Puarenga Stream catchment modelled in this study

is located in the south. The only outlet from Lake Rotorua is the Ōhau Channel. Inset: Map of New Zealand showing location of Rotorua.. 114

**Figure 4.2** Monthly median change factors (square marker) applied in 22 general circulation models (GCMs) that were used to generate 2090 regional climate data for modelling the Puarenga Stream catchment and Lake Rotorua. (a) precipitation; (b) solar radiation; (c) mean air temperature; (d) relative humidity; (e) maximum temperature; and (f) minimum temperature. Error bars indicate the range of monthly changes derived from the 22 GCMs. .... 123

**Figure 4.3** Comparison of measurements taken at the FRI stream-gauge and SWAT2012 model outputs of (a) discharge (Q), concentrations of (b) suspended sediment (SS), (c) organic phosphorus (ORGP), (d) dissolved reactive phosphorus (DRP), (e) total phosphorus (TP), (f) organic nitrogen (ORGN), (g) ammonium-nitrogen (NH<sub>4</sub>-N), (h) nitrate-nitrogen (NO<sub>3</sub>-N) and (i) total nitrogen (TN) during calibration (July 2006 to June 2009) and validation (July 2009 to June 2010) periods..... 130

**Figure 4.4** Comparisons of concentrations simulated with DYRESM-CAEDYM of (a-b) phosphate (PO<sub>4</sub>-P), (c-d) total phosphorus (TP), (e-f) ammonium-nitrogen (NH<sub>4</sub>-N), (g-h) nitrate-nitrogen (NO<sub>3</sub>-N), (i-j) total nitrogen (TN), and (k) chlorophyll *a* (Chl *a*) with the measurements taken at the surface (0-6 m) and the bottom (19 m) water of Lake Rotorua, during calibration (January 2008 to June 2009) and validation (July 2009 to June 2010) period..... 134

**Figure 4.5** Measurements at monthly intervals and simulated concentrations on corresponding days in the surface and bottom waters of Lake Rotorua under the current climate (CC0) during calibration (2008-2009) and validation (2009-2010); daily simulated concentrations in the surface and bottom waters of Lake Rotorua under current climate (CC0) relative to four nutrient load scenarios (S1-S4) during a baseline period (2008-2010), and under 2090 climate changes to catchment only (CC1) and changes to both catchment and lake (CC2). (a)-(b) TP: total phosphorus, (c)-(d) TN: total nitrogen, and (e) Chl *a*: chlorophyll *a*. Nutrient load scenarios are described in the Methods. Boxes denote interquartile ranges (i.e., 25% and 75%); whiskers denote minimum and maximum values; horizontal lines denote median values..... 138

## List of Tables

<b>Table 1.1</b> Comparisons of a selection of catchment models. The SWAT model was applied in this thesis.....	12
<b>Table 1.2</b> Comparisons of a selection of lake models. DYRESM–CAEDYM was applied in this thesis.....	13
<b>Table 1.3</b> Description of data used to configure, calibrate and validate the SWAT model for each chapter. SS: suspended sediment; DRP: dissolved reactive phosphorus; TP: total phosphorus; NO <sub>3</sub> –N: nitrate–nitrogen; NH <sub>4</sub> –N: ammonium–nitrogen; TKN: total Kjeldahl nitrogen (NH <sub>4</sub> –N + organic N); TN: total nitrogen.....	17
<b>Table 2.1</b> Description of data used to configure the SWAT model.....	34
<b>Table 2.2</b> Prior–estimated parameter values for three dominant types of land–cover in the Puarenga Stream catchment. Values of other land use parameters were based on the default values in the SWAT database..	36
<b>Table 2.3</b> Description of data used to calibrate the SWAT model. Data were measured at the Forest Research Institute (FRI) stream–gauge and were considered representative of the downstream/outlet conditions of the Puarenga Stream.....	39
<b>Table 2.4</b> Summary of calibrated SWAT parameters. Discharge (Q), suspended sediment (SS) and total nitrogen (TN) parameter values were assigned using auto–calibration, while total phosphorus (TP) parameters were manually calibrated. SWAT default ranges and input file extensions are shown for each parameter. Parameters are unitless unless otherwise specified. “revap” indicates water movement into the overlying unsaturated layers.....	42
<b>Table 2.5</b> Criteria for model performance. Note: $o_n$ is the $n^{\text{th}}$ observed datum, $s_n$ is the $n^{\text{th}}$ simulated datum, $\bar{o}$ is the observed mean value, $\bar{s}$ is the simulated daily mean value, and N is the total number of observed data. Performance rating criteria are based on Moriasi et al. (2007) for Q: discharge, SS: suspended sediment, TP: total phosphorus and TN: total nitrogen. Moriasi et al. (2007) derived these criteria based on extensive literature review and analysing the reported performance ratings for recommended model evaluation statistics. $r$ : Pearson product moment correlation coefficient; NSE: Nash–Sutcliffe efficiency; PBIAS: percent bias.....	48
<b>Table 2.6</b> Model performance ratings for simulations of discharge (Q), concentrations of suspended sediment (SS), total phosphorus (TP) and total nitrogen (TN). n indicates the number of measurements. Q–weighted mean concentrations were calculated using Eq. (1). $r$ : Pearson product moment correlation coefficient; NSE: Nash–Sutcliffe efficiency; PBIAS: percent bias. The significance of correlations between simulations and measurements was quantified based on the $p$ value (see Section 2.3.5). $*p < 0.05$ ; $**p < 0.01$ ; $***p < 0.001$ .....	53
<b>Table 2.7</b> Model performance statistics for simulations of discharge (Q), and loads of suspended sediment (SS), total phosphorus (TP) and total nitrogen (TN). Statistics were calculated for both overall and	

separated simulations.  $Q_{all}$  and  $L_{all}$  indicate the overall simulations;  $Q_b$  and  $L_b$  indicate the base flow simulations;  $Q_q$  and  $L_q$  indicate the quick flow simulations.  $r$ : Pearson product moment correlation coefficient; NSE: Nash–Sutcliffe efficiency; PBIAS: percent bias. The significance of correlations between simulations and measurements was quantified based on the  $p$  value (see Section 2.3.5). \* $p < 0.05$ ; \*\* $p < 0.01$ ; \*\*\* $p < 0.001$ ..... 56

**Table 2.8** Rankings of relative sensitivities of parameters (from most to least) for variables (header row) of Q (discharge), SS (suspended sediment), MINP (mineral phosphorus), ORGN (organic nitrogen),  $NH_4-N$  (ammonium–nitrogen), and  $NO_3-N$  (nitrate–nitrogen). Relative sensitivities were identified by randomly generating combinations of values for model parameters and comparing modelled and measured data with a Student’s t test ( $p \leq 0.05$ ). Bold text denotes that a parameter was deemed sensitive relative to more than one simulated variable. Shaded text denotes that parameter deemed insensitive to any of the two flow components (base and quick flow; see Figure 2.7) using one–at–a–time sensitivity analysis. Definitions and units for each parameter are shown in Table 2.4..... 59

**Table 3.1** Statistics used to evaluate model performance. Note:  $o_n$  is the  $n^{th}$  observed datum,  $s_n$  is the  $n^{th}$  simulated datum,  $\bar{o}$  is the observed mean value,  $\bar{s}$  is the simulated daily mean value, and N is the total number of observed data. .... 83

**Table 3.2** Descriptions and specifications of treated municipal wastewater irrigation scenarios used for SWAT2012 simulations. .... 84

**Table 3.3** Optimised values and default ranges for the most sensitive parameters for discharge (Q), suspended sediment (SS), organic phosphorus (ORGP), mineral phosphorus (MINP), organic nitrogen (ORGN), ammonium–nitrogen ( $NH_4-N$ ), and nitrate–nitrogen ( $NO_3-N$ ) load simulations using a modified SWAT2012 code. The parameters marked with an asterisk have an optimised value outside of the SWAT default range. Parameters are unitless unless otherwise specified..... 87

**Table 3.4** Statistical values of Pearson product moment correlation coefficient ( $r$ ), root mean square error (RMSE), mean absolute error (MAE), and percent bias (PBIAS), used to indicate the SWAT model performance for daily simulations averaged to weekly time scale of discharge (Q), loads of suspended sediment (SS), mineral phosphorus (MINP), organic phosphorus (ORGP), total phosphorus (TP), organic nitrogen (ORGN), ammonium–nitrogen ( $NH_4-N$ ), nitrate–nitrogen ( $NO_3-N$ ) and total nitrogen (TN). The statistical values were calculated using a modified SWAT2012 code based on (I) hourly routing and (II) daily routing. The significance of correlation is asterisked where  $p < 0.05$ , otherwise  $p < 0.001$ . Units are relevant to RMSE and MAE values.... 94

**Table 3.5** Multi–year monthly mean aggregated from SWAT2012 hourly simulations for discharge (Q), suspended sediment (SS), total phosphorus (TP) and total nitrogen (TN) loads. Std.Dev. is standard deviation. .... 96

**Table 3.6** Change of annual total phosphorus (TP) and total nitrogen (TN) loads under four different irrigation scenarios from the simulations under

the actual irrigation scenario (S0: 10–14 blocks irrigated daily) during 2003–2012..... 99

**Table 4.1** Inflows to Lake Rotorua represented in the model. Six inflows were classified as surface (S) water-dominated catchments and four as groundwater (G)-dominated catchments (see Section 4.3.2). Mean annual inflow water temperature ( $T_{inf}$ ), discharge, concentrations of total phosphorus (TP) and total nitrogen (TN), and percentage of inflow volume, TP and TN load contributions were derived from Abell et al. (2015) for July 2006 to June 2010..... 118

**Table 4.2** Statistics used to evaluate model performance. Note:  $o_n$  is the  $n^{th}$  observed datum,  $s_n$  is the  $n^{th}$  simulated datum,  $\bar{o}$  is the observed mean value,  $\bar{s}$  is the simulated daily mean value, and N is the total number of observed data. .... 121

**Table 4.3** The 22 general circulation models (GCMs) used in this study and the country where each GCM originated. See IPCC (2013)..... 123

**Table 4.4** Optimised parameter values with input file extensions for the whole Puarenga Stream catchment for discharge (Q), suspended sediment (SS), total phosphorus (TP), and total nitrogen (TN) concentration simulations. The asterisked values were adjusted beyond the SWAT default range (see text). Input file extensions are shown for each parameter. Parameters are unitless unless otherwise specified. “revap” indicates water movement into the overlying unsaturated layers. .... 126

**Table 4.5** Statistical values of Pearson product moment correlation coefficient ( $r$ ), root mean square error (RMSE), mean absolute error (MAE), and percent bias (PBIAS), used to assess SWAT2012 model performance for daily mean simulations of discharge (Q), loads and concentrations of suspended sediment (SS), organic phosphorus (ORGP), dissolved reactive phosphorus (DRP), total phosphorus (TP), organic nitrogen (ORGN), ammonium-nitrogen ( $NH_4-N$ ), nitrate-nitrogen ( $NO_3-N$ ) and total nitrogen (TN) from the Puarenga Stream catchment. The significance of correlations between simulations and measurements was quantified based on the  $p$  value (see Section 4.3.2). \*  $p < 0.05$ ; \*\*  $p < 0.01$ ; \*\*\*  $p < 0.001$ . Units are relevant to RMSE and MAE values only..... 131

**Table 4.6** Sensitive DYRESM-CAEDYM parameter values that were adjusted from Abell et al. (2015)..... 133

**Table 4.7** Model performance of DYRESM-CAEDYM for daily mean concentrations of phosphate ( $PO_4-P$ ), total phosphorus (TP), ammonium-nitrogen ( $NH_4-N$ ), nitrate-nitrogen ( $NO_3-N$ ) and total nitrogen (TN) for surface (0–6 m) and bottom (19 m) waters of Lake Rotorua and surface water chlorophyll  $a$  (Chl  $a$ ) during calibration (January 2008 to June 2009) and validation (July 2009 to June 2010). Values of Pearson product moment correlation coefficient ( $r$ ), level of significance ( $p$ ), root mean square error (RMSE), mean absolute error (MAE), and percent bias (PBIAS) were used to indicate model performance. \*\* $p < 0.01$ . Units are relevant to RMSE and MAE values only. .... 135

**Table 4.8** Measured sampling days and corresponding simulation days with changes in surface and bottom water temperature ( $\Delta T$ )  $> 0.5$  °C, with

bottom water dissolved oxygen (DO) concentrations  $< 2 \text{ mg L}^{-1}$ , and with surface water chlorophyll *a* (Chl *a*) concentrations  $> 15 \text{ } \mu\text{g L}^{-1}$ , and TLI3 values under the current climate during calibration (2008–2009) and validation (2009–2010); daily simulated number of days with  $\Delta T > 0.5 \text{ } ^\circ\text{C}$ ,  $\text{DO} < 2 \text{ mg L}^{-1}$ ,  $\text{Chl } a > 15 \text{ } \mu\text{g L}^{-1}$ , and mean TLI3 values under current climate (CC0) relative to four nutrient load scenarios (S1–S4) during baseline period (2008–2010), and under 2090 climate changes to catchment only (CC1) and changes to both catchment and lake (CC2). Nutrient load scenarios are described in the Methods. The TLI3 is a three–variable Trophic Level Index function derived from concentrations of total nitrogen, total phosphorus and Chl *a*, which is used to indicate the lake trophic state (Burns et al., 1999)..... 137

**Table 4.9** Model results under current climate (CC0) for four nutrient load scenarios comprising changes to total phosphorus (TP) and total nitrogen (TN) loads from the Puarenga Stream catchment and in–stream TP and TN loads during baseline period (July 2006 to June 2010); changes to TP and TN concentrations in surface and bottom waters, and surface water chlorophyll *a* (Chl *a*) concentrations of Lake Rotorua during the baseline period (January 2008 to June 2010). Percentage change denotes changes to the simulations under scenarios S2–S4 relative to the simulations under the “reference” scenario S1. Nutrient load scenarios (S1–S4) are described in the Methods. S1–Irr1Pas1: both nutrient applications, S2–Irr0Pas1: pasture fertilisation only, S3–Irr1Pas0: wastewater irrigation only, S4–Irr0Pas0: no nutrient applications..... 140

**Table 4.10** Changes in inflow (Q) and nutrient loadings of suspended sediment (SS), mineral phosphorus (MINP), organic P (ORGP), ammonium–N ( $\text{NH}_4\text{–N}$ ), nitrate–N ( $\text{NO}_3\text{–N}$ ), organic N (ORGN), total P (TP), and total N (TN) in response to the 2090 climate impacts on catchment only, and changes of nutrient concentrations in Lake Rotorua. The value of TLI3, the three–variable Trophic Level Index calculated by concentrations of TN, TP and chlorophyll *a* (Chl *a*), is used to indicate the lake trophic state (Burns et al., 1999). The colour scale was specified for each variable in each column and indicates the range of % changes..... 142

**Table 4.11** Precipitation (PCP), solar radiation (SLR), air temperature ( $T_a$ ), humidity (HMD), evaporation ( $E_a$ ), water temperatures of inflows from groundwater discharge sub–catchments ( $T_{\text{gw}}$ ) and from surface water sub–catchments ( $T_{\text{sw}}$ ), and changes in nutrient concentrations in Lake Rotorua in response to a projected 2090 climate, for both Lake Rotorua catchment and lake. The increase in  $T_{\text{gw}}$  was 88% of the increase in  $T_a$  while the increase in  $T_{\text{sw}}$  was from the SWAT output. The TLI3 is a three–variable Trophic Level Index function derived from concentrations of total nitrogen (TN), total phosphorus (TP) and chlorophyll *a* (Chl *a*), which used to indicate the lake trophic state (Burns et al., 1999). The colour scale was specified for each variable in each column and indicates the range of % change..... 145

## **Preface**

This thesis has five chapters. Chapters 2–4 have been written in the style of scientific papers for publication in peer-reviewed scientific journals. This style necessitates some repetition of description of the study area and methodology. Except where referenced, the work in this thesis, including model applications, data analyses and writing, was undertaken by me while under the supervision of Professors David Hamilton and Brendan Hicks (the University of Waikato). All co-authors listed below have reviewed relevant chapters and provided editorial and scientific advice.

Chapter 2 is modified from Me, W., Abell, J.M., and Hamilton, D.P.: Effects of hydrologic conditions on SWAT model performance and parameter sensitivity for a small, mixed land use catchment in New Zealand, *Hydrol. Earth Syst. Sc.*, 19, 4127–4147, 2015.

Chapter 3 is in preparation for submission to the *Journal of Environmental Management* under the title “Water quality effects of treated municipal wastewater application to a temperate forested catchment: Insights from SWAT modelling” by Wang Me, David P. Hamilton, Jonathan M. Abell, and Alison Lowe.

Chapter 4 is in preparation for submission to *Environmental Modelling and Software* under the title “Simulating variations in discharge and nutrient loads from a mixed land use catchment to a eutrophic lake: Effects of nutrient reductions and future climate” by Wang Me, David P. Hamilton, Chris G. McBride, Jonathan M. Abell, and Brendan J. Hicks.

The thesis preparation used the consistent formatting style based on the guidelines in “Hydrology and Earth System Sciences” where Chapter 2 was published.

# **1 Introduction**

## **1.1 Background and motivation**

### **1.1.1 Climate, catchment and lake interactions**

A lake-based focus of limnology has historically been led by the view of *The Lake as a Microcosm* (Forbes, 1887), with limited consideration of the lake catchment. However, the physical combination of climate and catchment (land, streams and groundwater), as well as the lake, defines the processes that control lake water quantity and water quality (Wetzel, 2001). Land considerations include land cover, soil, geology, and topography. Contemporary limnology emphasizes a pluralistic view of aquatic ecosystems as connected and interactive elements rather than the traditional concept of island-like aquatic ecosystems (Jenkins, 2014). Climate variability directly controls lake stratification and mixing through solar radiation, air temperature, and wind on a day-to-day basis (Fee et al., 1996). Lake water quantity responds to precipitation, discharge of inflows and groundwater recharge, while lake water quality responds most strongly to inputs of phosphorus (P) and nitrogen (N) from the atmosphere and the associated suspended sediment (SS), P and N loads from surface and subsurface inflows from the catchment (Leavitt et al., 2009). A conceptual framework for the interactions between climate, catchment and lake ecosystems which is considered in this thesis is shown in Fig. 1.1.

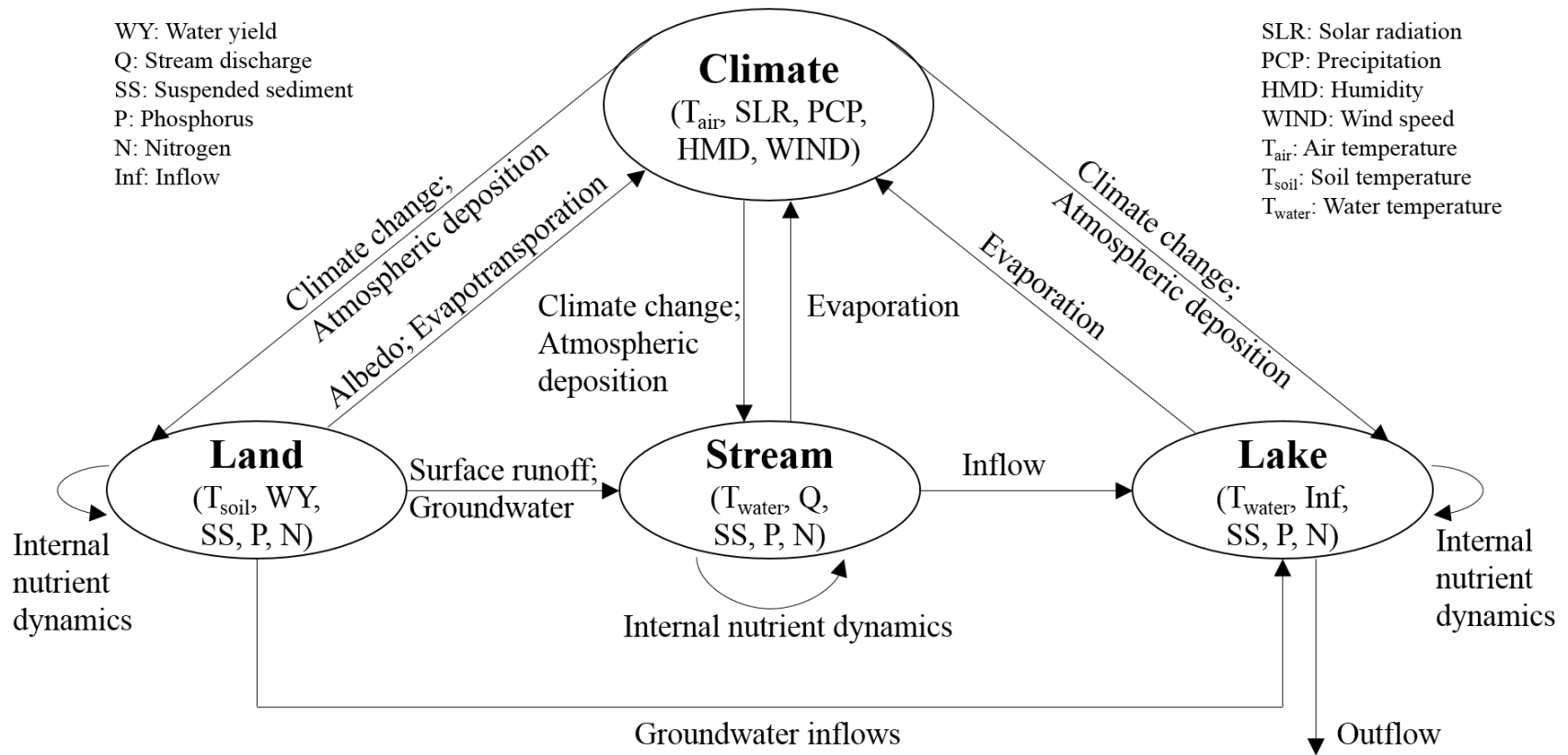
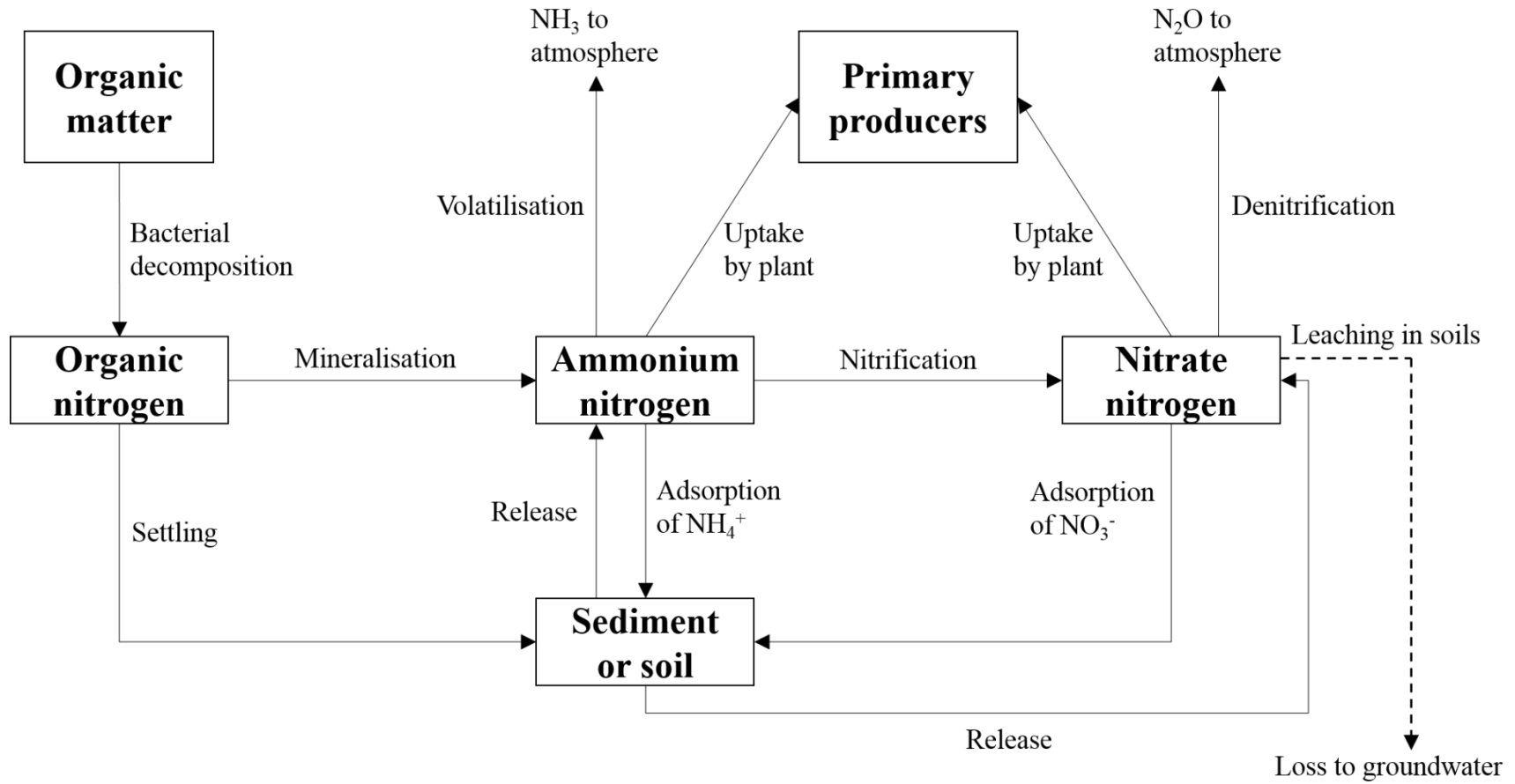


**Figure 1.1** A conceptual framework for the connected and interactive elements of climate, catchment (land and stream) and the lake, showing the main processes of hydrological and nutrient cycling. After Poole et al. (2002). Land considerations include land cover, soils, geology and topography.

### **1.1.2 Hydrologic cycle and nutrient dynamics**

The main components in the hydrological cycle are precipitation, interception by vegetation, evapotranspiration, soil water percolation, lateral flow recharge, groundwater recharge, surface runoff, water supply and seepage (Kuchment, 2004). Some of these processes are shown in Fig. 1.1. A catchment is a basin-shaped area of land that contributes to surface and groundwater (Bogaart and Troch, 2006). It receives water from precipitation, and is drained by dendritic stream networks at the land surface and by subsurface waters, which transport sediment, nutrients and other organic and inorganic compounds (Winter et al., 1998). Smaller streams of lower order converge into mainstream systems. The drainage area of a tributary is referred to as its sub-catchment, a number of which occur within a whole catchment. Water movement driven by rainfall and runoff determines the catchment shape and the extent of soil erosion. Soil texture and its drainage capacity, together with evaporative fluxes, determine the amount of water lost from the catchment (Tarboton, 2003). Inflow water sources and outflow type determine lake hydrological types, which can be classified into seepage lakes (mainly fed by precipitation), drainage lakes (mainly fed by groundwater or surface runoff and groundwater together), and impounded lakes (artificially controlled) (Shaw et al., 2004).

Nutrient biogeochemical processes in soils, streams and lakes are similar, mediated principally by plant uptake and organic matter processing in soils (Haider et al., 1989) and algae and bacteria in streams and lakes (Hickman and Penn 1977). Key biogeochemical processes influencing nitrogen cycling include 1) decomposition, 2) organic N mineralisation, 3) settling, 4) ammonium nitrification, 5) sediment release, 6) sediment adsorption, 7) plant uptake, 8) volatilisation, 9) nitrate denitrification, and 10) leaching (Fig. 1.2; Amatya et al., 2013). Key biogeochemical processes influencing phosphorus cycling include 1) decomposition, 2) organic P mineralisation, 3) settling, 4) mineral P sediment desorption/release, 5) adsorption, 6) plant uptake and 7) leaching (Fig. 1.3; Radcliffe et al., 2015).



4

**Figure 1.2** Key biogeochemical processes for nitrogen in soils, streams and lakes (dashed line indicates nitrate leaching only in water movement through soils). Adapted from Amatya et al. (2013).

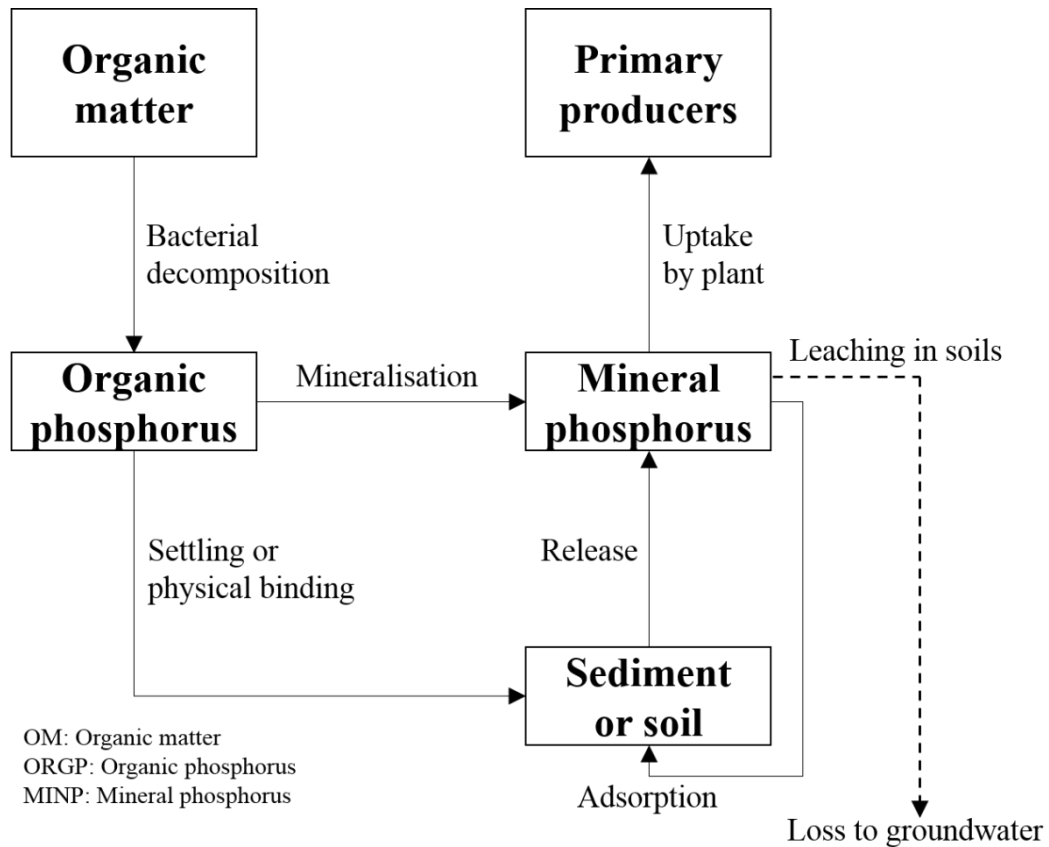


**Figure 1.3** Key biogeochemical processes for phosphorus in soils, streams and lakes (dashed line indicates soluble phosphorus leaching only in water movement in soils). Adapted from Radcliffe et al. (2015).

Hydrological and biogeochemical processes in both terrestrial and in-stream environments are affected by a number of different meteorological and physical conditions (Abell et al., 2013). Drainage patterns of catchments are also determined by the spatial variances of geomorphology and land use (Mulligan, 2004), which can result in spatial differences between lakes (Chen et al., 2012). Temporal variations in climate affect surface runoff and groundwater recharge in a catchment, and the resultant discharges to the lake. In turn, lake water density controls water column mixing and stratification, which largely control the internal distribution of nutrients (Shaw et al., 2004).

### 1.1.3 Impacts of climate change on the lake catchment

Projections of future climate include increasing air temperature coupled with changes in the seasonality of precipitation (IPCC, 2013). These changes will affect the hydrological cycle and nutrient biogeochemical cycling for both catchment

(land and stream) and lake environments (Schneiderman et al., 2010) (see Fig. 1.1). Warmer air temperatures will warm lake water and increase phytoplankton growth in surface waters, leading to changes in in-lake nutrient dynamics (Arnell et al., 2015). They will also increase soil and in-stream water temperature, which will influence terrestrial and in-stream nutrient processing, indirectly affecting lake water quality by altering the magnitude and seasonality of nutrient delivery to lakes (Whitehead et al., 2009). Future climate impacts may have a synergistic effect on in-lake nutrient dynamics through potential increases of nutrient loadings from catchment, increases of phytoplankton growth and greater strength and duration of stratification in lakes (Hamilton et al., 2016). However, nutrient loadings from catchments may decrease with climate warming because warmer air temperatures increase evaporation, resulting in less runoff (e.g., Robertson et al., 2016). There may also be potential for antagonistic interactions amongst lakes and catchments in terms of responses to climate change.

#### **1.1.4 Catchment and lake models**

The growing availability of advanced modelling technologies makes it possible to better replicate and simulate the natural hydro-biogeochemical system (Bouwman et al., 2013). Individual modelling components include the climate, catchment and aquatic ecosystem. The integration of these tools enables the simulation and prediction of present and future states of freshwater ecosystems, including their spatial and temporal dynamics, however, there is potential for uncertainties from the catchment model output to be amplified in lake model simulations (Couture et al., 2014).

Various catchment models have been developed and applied to evaluate the effects of variability in climate and soil properties on catchment hydrology and nutrient mass export (Devi et al., 2015). Generally, there are four types of catchment models (Pechlivanidis et al., 2011); empirically-based, conceptually-simplified, process-based, and semi-empirical process-based (i.e., intermediate between empirically-based and process-based). Relevant examples of four types of catchment models are shown in Table 1.1. Catchment information required for empirical models can vary with the questions being asked of the model but is mostly fairly simple. For other model types, the data requirements generally include 1) climate data including precipitation, air temperature, solar radiation, relative

humidity, and wind; 2) catchment topographic information; 3) soil properties; 4) land use type; 5) land management practices; 6) point sources nutrient discharges; and 7) other physical parameters representing specific catchment properties, some of which may be specific to a model.

Model selection largely depends on the relationship between the predictability of each individual model and the specific research objectives (Marshall et al., 2006). Empirically-based catchment models use statistical relationships in the observed data (Merz et al., 2006). These relationships are commonly calculated using statistical or neural network methods between the variables of interest and other environmental factors related to climate conditions, land use types and soil properties. Empirically-based catchment models may have difficulty when spatial and temporal variances fall outside of those tested by the model and there will be limited confidence for predictions in other catchments (Bouwman et al., 2013). TOPMODEL (Topography MODEL) is a simplified rainfall-runoff conceptual model (Beven et al., 1995). It estimates water content in saturated soils by assuming that the gradient of hydraulic conductivity is equal to the surface land slope. However, the application of TOPMODEL is limited to catchments that have moderate slope and short dry periods (Piñol et al., 1997). Process-based models reflect the temporal variances arising from different climatic conditions (such as low rainfall or storm events) and the spatial distributions of different geomorphologies, land uses and soil characteristics throughout the simulated catchment (Garambois et al., 2013). Process-based models predict values of state variables for simulations over a range of time scales from hourly, daily and monthly to annual time. Borah and Bera (2003) verified that process-based models of MIKE SHE (MIKE Système Hydrologique Européen; Refsgaard and Storm, 1995), SWAT (Soil and Water Assessment Tool; Arnold et al., 1998) and HSPF (Hydrologic Simulation Program FORTRAN; Donigian et al., 1995) can be used to predict hydrology and sediment and nutrient loadings from large and complex catchments.

MIKE SHE is a commercial model that uses numerical methods to simulate the interactions between stream flow and groundwater flow (Refsgaard and Storm, 1995). The model is used for long-term simulations and large-size catchments (Graham and Butts, 2005). It requires large amounts of input data and a large number of physical parameters. Similarly, the HSPF model also requires extensive

input data information but also has lumped parameters, which results in time-consuming model calibration procedures (Im et al., 2003). The HSPF model does not include spatially explicit calibration for land use and soil datasets, and depends on the empirical relationships for physical process simulations (Yang and Wang, 2010). This could limit HSPF applications to catchments with coarse resolution of spatial datasets or gaps in hydrologic or climate data. By contrast, the SWAT model requires moderate amounts of information for model configuration and calibration. It includes spatially-distributed land use and soil datasets and can be applied for different sizes of catchments (e.g., Ostojski et al., 2014). The SWAT model is more effective for applications to catchments where available data are scarce (Xie and Lian, 2013) and it is better suited for extending optimised parameters from one catchment to other similar catchments or to future climate projections (van Liew and Garbrecht, 2003). Both SWAT and HSPF models use a Hydrologic Response Unit (HRU) concept to divide sub-catchments into smaller units. The SWAT model predicts runoff and nutrient transport independently for each HRU, with predictions summed to obtain the total for each sub-catchment (Bryant et al., 2006). By contrast, HSPF simulates discharge and nutrients by routing successively to downslope HRUs (Yang and Wang, 2010). Saleh and Du (2004) compared the performance of the SWAT and HSPF models on an intensive dairy area in central Texas and verified that the SWAT model provided better simulations of daily mean nutrient load than the HSPF simulations.

Semi-empirical process-based models (e.g., SPARROW; SPATIally Referenced Regression on Watershed attributes) combine statistical regression with model physical structure to generate relationships between in-stream measured data and catchment spatial data (Smith et al., 1997). However, the SPARROW does not deal with temporal variances of different simulated variables. Model simulations are suitable for long time periods and large-size catchment where there can be a steady state approximation (Preston et al., 2011).

The SWAT model was selected for this thesis due to its ability to simulate different catchment land management practices and to reproduce the temporal and spatial variability in catchment discharge and nutrient loadings (Neitsch et al., 2011). The SWAT model was developed by the Agricultural Research Services of the United States Department of Agriculture (USDA ARS, Arnold et al., 1998). It requires a digital elevation model (DEM), spatially-distributed land use and soil

information, and meteorological data for simulations. The minimum meteorological data requirements to run SWAT are hourly or daily precipitation, and daily minimum and maximum air temperature. The SWAT model integrates spatially-distributed information into a GIS (Geographic Information System) platform. SWAT delineates a study catchment and divides it into sub-catchments based on DEM data and a stream digital map is used to “burn-in” channel locations to create accurate flow routings. The model then creates numerous HRUs, each based on specific topographic conditions, land use types and soil properties. Model simulations are at the HRU level, with temporal (ranging from hourly to annual) and spatial (ranging unlimited) variances then summarised for each sub-catchment. SWAT passes sub-catchment output to the relevant stream channel and calculates the in-stream discharge and nutrient transport to the catchment outlet. The main hydrological components in SWAT are interception by vegetation, evapotranspiration, soil water percolation, lateral flow recharge, groundwater recharge, surface runoff, water supply and seepage.

Two methods can be chosen for the calculation of surface runoff in SWAT. The use of Green-Ampt (Green and Ampt, 1911) infiltration method is used in this thesis for surface runoff simulations. Alternately, a semi-empirical the Soil Conservation Service (SCS) curve number (CN) method (USDA-SCS, 2004) can be used for surface runoff simulations. Sediment yield is estimated using the modified universal soil loss equation (MUSLE; Williams, 1975). Different forms of nitrogen and phosphorus within soil profiles are also simulated based on soil temperature, which the key factor for nutrient cycling in SWAT. Temperature of a soil layer is estimated as a function of minimum and maximum air temperature, soil surface temperature, and damping depth (i.e., the soil depth at which soil temperature no longer varies with climate). SWAT also has decay functions for in-stream nutrient transport simulations where water temperature determines nutrient biogeochemical processes in stream flows.

Two sets of routing algorithms (hourly and daily) can be used to calculate hydrological and nutrient transport processes in SWAT. The use of each set of algorithms is related to the temporal resolution (daily and hourly) of hydrological forcing data. Daily routing is commonly used and fits with most hydrological forcing data available at daily scale. Hourly routing is required for both hourly hydrological forcing data and the Green and Ampt infiltration method (Green and

Ampt, 1911), to simulate flow routing at an hourly time step. Hourly routing has been tested in simulating discharge and sediment load at hourly intervals (Jeong et al., 2010; Jeong et al., 2011). The SWAT model has also been used to evaluate impacts of land management practices on discharge and nutrient transport from agricultural areas (White et al., 2009; Aouissi et al., 2014). Our study site, a wastewater-irrigated forestry area in Rotorua, New Zealand, is steep and the discharge responds rapidly to rainfall events. Hourly routing algorithms in the SWAT model were therefore applied to simulate discharge and both dissolved and total nutrient species fluxes. Forcing data at hourly time steps may be able to better represent the dynamics of nutrients transported in steep areas of small catchments (Jeong et al., 2011).

With regards to modelling nutrient concentrations and the response in receiving water bodies to catchment inputs, the traditional approach has been to use a mass balance with empirically based parameters and an assumption of steady-state equilibrium (Vollenweider, 1975). These models assume the lake is mixed completely with invariant concentrations, which is applicable only to a subset of the entire time. For New Zealand, complete lake mixing occurs in winter. The assumption of equilibrium is also contrary to the real system which is dynamic according to changes in, for example, climate and invasive species (Rahel and Olden, 2008). By contrast, process-based aquatic ecosystem models use numerical equations to examine the effects of internal and external nutrient dynamics on in-lake biogeochemical processes (Kim et al., 2014). Relevant examples of empirically-based and process-based aquatic ecosystem models are shown in Table 1.2. The input-output lake model (Vollenweider, 1975) is empirically-based, using input and output loads as a basis for calculations. CE-QUAL-W2 model is a two-dimensional (longitudinal and vertical) process-based ecosystem model with hydrodynamic and water quality components (Cole and Wells, 2006). It assumes lateral homogeneity and hydrostatic approximation for the vertical momentum equation, and it is designed for long and narrow water bodies which may be considered as laterally invariant in water quality constituents. Another water quality model, WASP (Water Quality Analysis Simulation Program) runs with spatial delineation from one to three dimensions (Di Toro et al., 1983), however, it assumes complete lake mixing and requires extensive data information for model calibration (Kannel et al., 2011).

DYRESM–CAEDYM is a one–dimensional (1–D) hydrodynamic–biogeochemical aquatic ecosystem model and can be used to simulate vertical gradients of lake water characteristics (Hamilton and Schladow, 1997) such as Lake Rotorua which has simple morphometry. The DYRESM model was developed at the Centre for Water Research of the University of Western Australia (Imberger et al., 1978). DYRESM–CAEDYM comprises DYRESM (DYnamic REservoir Simulation Model) and CAEDYM (Computational Aquatic Ecosystem DYnamics Model) and can be run over the time periods varying from hours to decades. DYRESM uses the horizontal Lagrangian layer structure, i.e., the thickness of horizontal layers remains homogeneous within the user–defined limits. Layer mixing is driven by the surface wind causing both momentum and turbulent kinetic energy to be transmitted to each horizontal layer. CAEDYM simulates nutrient concentrations, dissolved oxygen, suspended sediments and phytoplankton biomass. DYRESM–CAEDYM requires information on lake morphology, meteorological data, inflow information (e.g., water temperature, discharge volume, nutrient concentrations), and withdrawal water volume to calculate a water balance. DYRESM–CAEDYM is used in this thesis because of its ability to accurately simulate vertical distributions of lake water temperature and density and ecological interactions between phytoplankton species and other biogeochemical variables over long (i.e., multi–annual) time scales (Hamilton and Schladow, 1997).

DYRESM–CAEDYM has not been previously integrated with outputs from the SWAT model for New Zealand lakes. Offline coupling of these two models (i.e., output from SWAT as input for DYRESM–CAEDYM to simulate variables of interest) would enable evaluation of the impacts of catchment–based land use practices on water quality and trophic state of receiving lakes (Hamilton et al., 2016). Initial parameter values required for both models were based on the monitoring data that were measured close to the start date of the simulation period. For the study catchment in this thesis, some catchment hydrological and nutrient parameters in SWAT were derived from existing data or knowledge gained in other studies. Others were assigned during a calibration process. For the DYRESM–CAEDYM application to the study lake in this thesis, lake water quality parameters were derived with reference to previous work done for Lake Rotorua (Rutherford et al., 1996; Burger et al., 2008; Hamilton et al., 2012; Abell et al., 2015).

**Table 1.1** Comparisons of a selection of catchment models. The SWAT model was applied in this thesis

Model type	Empirically-based	Conceptually-simplified	Process-based			Semi-empirical process-based
Catchment model	ANN	TOPMODEL	MIKE SHE	HSPF	SWAT	SPARROW
Model description	Artificial Neural Network (backpropagation algorithm)	Topography MODEL	MIKE Système Hydrologique Européen	Hydrologic Simulation Program FORTRAN	Soil and Water Assessment Tool	SPAtially Referenced Regression on Watershed attributes
Model source	Rumelhart and McClelland (1986)	Beven and Kirkby (1979)	Refsgaard and Storm (1995)	Donigian et al. (1995)	Arnold et al. (1998)	Smith et al. (1997)
Method	Statistical relationships between the variable of interest and other environmental factors	Assuming the gradient of hydraulic conductivity is equal to the surface land slope	Numerical methods for simulating the interactions between stream flow and groundwater flow	Numerical methods: Hydrologic Response Unit (HRU)	Numerical methods: HRU concept	Combines statistical regression with model physical structure
Limitations and strengths	1) Not able to reproduce the spatial and temporal variances of simulations; 2) Not applicable to other catchments without re-calibration	Limited to the catchment that has moderate geomorphology and brief dry periods	1) Requires large amounts of input data and model physical parameters; 2) Suitable for long-term period and large-size catchment	1) Numerous parameters for model setup; 2) Time consuming in calibrations 3) Not able to apply to the catchment where there are gaps or coarse resolution of datasets	1) Open source code 2) Able to apply for short-term periods and for small or moderate-size catchment 3) Able to apply to catchments where data are sparse	1) Not able to reproduce the temporal variances of simulations; 2) Suitable for long time periods and large-size catchments to provide a steady state condition

**Table 1.2** Comparisons of a selection of lake models. DYRESM–CAEDYM was applied in this thesis.

Model type	Empirically–based		Process–based	
Lake model	The input–output model	CE–QUAL–W2	DYRESM–CAEDYM	WASP
Model description	Reference to the phosphorus loading concept in limnology	Hydrodynamic and water quality model	DYnamic REservoir Simulation Model–Computational Aquatic Ecosystem DYnamics Model	Water Quality Analysis Simulation Program
Model source	Vollenweider (1975)	Cole and Wells (2006)	Imberger et al. (1978) Hipsey et al. (2006)	Di Toro et al. (1983)
Method	Mass balance approach under a steady–state equilibrium	Two dimensional (longitudinal and vertical)	One dimensional (vertical)	Three dimensional (horizontal, longitudinal and vertical)
Limitations and strengths	Assuming complete lake mixing with no spatial variations in concentration	1) Assuming lateral homogeneity and hydrostatic for vertical momentum equation; 2) Designed for long and narrow water bodies	1) Assuming the thickness of horizontal layers remains homogeneous; 2) Model running from hours to decades	1) Assuming lake complete mixing; 2) Requires extensive data information for model calibration

### 1.1.5 Study area

The study area for this thesis is the Lake Rotorua catchment (Bay of Plenty, North Island, New Zealand), the results of which form the focus of Chapters 2–4. The Rotorua area is located in North Island, New Zealand and has a warm, temperate climate. Annual mean precipitation of 1252 mm, air temperature 12.6 °C, relative humidity 81%, short-wave radiation 170 W m<sup>-2</sup> and wind speed 3.6 m s<sup>-1</sup> (at 10 m above the water surface) for Lake Rotorua were estimated for July 2006 – June 2010 (National Climatic Database; available at <http://cliflo.niwa.co.nz/>). Lake Rotorua is a large (area 80.8 km<sup>2</sup>), shallow (mean depth 10.8 m), polymictic lake with nine major inflows (mean annual discharge, 0.3–2.6 m<sup>3</sup> s<sup>-1</sup>) and nine minor inflows (mean annual discharge, 0.01–0.06 m<sup>3</sup> s<sup>-1</sup>). The only outflow (mean annual discharge 18.5 m<sup>3</sup> s<sup>-1</sup>) is the Ōhau Channel (Hoare, 1980). Mean annual discharge of inflows and the outflow were based on the measured or estimated hydrologic data in Abell et al. (2015). The residence time of Lake Rotorua is 1.5 year, provided by multiplying lake area by mean depth and dividing by the outflow discharge.

As a nationally–iconic water body, Lake Rotorua plays a significant role in recreation and tourism in New Zealand (Hamilton et al., 2012). However, the water quality of Lake Rotorua has declined over several decades due to increasing inputs of N and P (Mueller et al., 2015). The Rotorua City sewage treatment plant was one of the contributors to this water quality decline through direct inputs of treated wastewater into the lake prior to 1991. The Rotorua Lakes Council commenced a scheme of spray irrigation disposal of treated municipal wastewater within the Whakarewarewa Forest in 1991, aiming to reduce loads of N and P entering Lake Rotorua (Lowe et al., 2007). The average municipal wastewater (10 mm d<sup>-1</sup>) from Rotorua City is first treated at the Rotorua Wastewater Treatment Plant and is then pumped to holding ponds before being spray–irrigated through above–ground sprinklers onto a forest area of 193 ha. The applied N is partially removed by plant uptake and microbial denitrification (Barton et al., 2005), while the applied P is mostly removed through the highly adsorptive soil that has a high P retention (Beets et al., 2013). Nutrients not removed from these processes will generally be discharged from the Waipa Stream sub–catchment, ultimately entering Lake Rotorua via the Puarenga Stream. The Puarenga Stream is the second–largest surface inflow to Lake Rotorua and drains a catchment of 77 km<sup>2</sup>. It has an area of pastoral farmland (8 km<sup>2</sup>) that is typically fertilised with N and P to increase productivity (Anastasiadis et al., 2011).

## **1.2 Thesis objectives**

The objective of this thesis was to use numerical model applications to enhance understanding of the temporal dynamics of N and P loads to Lake Rotorua, to investigate how delivery of these nutrients affects water quality of the lake, and to examine the effect of different catchment nutrient management regimes and projected climate change. To achieve this, the study encompassed 1) a process-based catchment model (SWAT) application to the Puarenga catchment of Lake Rotorua under different hydrologic conditions, testing the influence of parameter sensitivity; 2) improvements to the SWAT model to represent high-frequency (daily and hourly) variability of nutrient discharges and to simulate different land management and wastewater irrigation management strategies; and 3) an application of the improved catchment model (from (2) above) combined with the lake model to predict the response of eutrophic, temperate Lake Rotorua to future climate and catchment nutrient discharge.

## **1.3 Thesis overview**

This thesis encompasses three main research chapters (Chapters 2–4), which have been written individually in a style of scientific papers.

Chapter 2 quantifies SWAT model performance and parameter sensitivity during different hydrologic conditions. Model evaluation was performed using two data sets: low-frequency data collected from monthly instantaneous measurements and high-frequency data measured during rainfall events. Simulated discharge, SS, total P (TP) and total N (TN) loads were partitioned into base flow and quick flow components. Parameter sensitivity for the two hydrologically-separated regimes was quantified.

Chapter 3 further develops the catchment model used in Chapter 2 to investigate the impacts of wastewater irrigation on discharge and water quality of the major stream draining the irrigated area. This study developed a sub-catchment modelling approach to allow for examination of high-frequency (daily and hourly) variability of nutrient discharges and alternatives for managing the wastewater. Scenario simulations were designed to improve the understanding of the impacts of wastewater irrigation by refining the area, timing and frequency of irrigation.

Chapter 4 applies the catchment model from Chapter 3 and simulates effects of nutrient reductions and future climate on Lake Rotorua. The objective of this study was to use combined climate-catchment-lake models to simulate the effect

on lake trophic state of nutrient load reductions from wastewater-irrigated forest and farmland under present and future climates. Downscaled climate projections for 2090–2099 were used as input to the improved catchment model and one-dimensional lake water quality model.

The SWAT model was used in Chapters 2–4 for the catchment simulations, and the lake model (DYRESM–CAEDYM) was used in Chapter 4 for the temporal assessments of receiving environment responses to catchment inputs. A description of data used to configure and calibrate the SWAT model for each chapter is shown in Table 1.3. This comparison allows the reader to assess the differences in optimised parameter values between chapters and the statistical values used to indicate model performance.

The source code of the catchment model (SWAT) has undergone major improvements since the thesis commenced in 2012. The original source code of SWAT2009\_rev488 version (released in November 2011) was applied in Chapter 2 to provide insights into the parameter sensitivity and model performance varying for two hydrologically-separated regimes. Along with the development of SWAT and GIS user interfaces, the latest version of SWAT2012\_rev629 source code (released in July 2014) was then applied in the further chapters. However, neither the original SWAT2012\_rev629 source code was found to be able to simulate a complex irrigation operation. Therefore, SWAT2012\_rev629 source code was modified and applied in Chapter 3 for two purposes; 1) to simulate the complex irrigation schedules and 2) to examine the high-frequency variability of discharge and nutrient mass export from the catchment using hourly routing algorithms. Optimised parameter values were also re-examined with the modified SWAT2012\_rev629 executable code which was applied in Chapter 4 and combined with the lake model (DYRESM–CAEDYM, version 4.0) to simulate the effects of catchment land use and management changes on the lake trophic state under both present and future climate.

The statistic Nash–Sutcliffe efficiency (NSE) used in Chapter 2 was substituted by root mean square error (RMSE) and mean absolute error (MAE) in Chapters 3–4 because of the findings in Krause et al. (2005) and Price et al. (2012). They recommended modified forms of NSE should be used for model evaluation based on the measurements and simulations that are driven by different climate conditions (e.g., low rainfall versus storm events). The scientific objectives in Chapters 3–4 were to use RMSE and MAE to provide statistical measures of model fit (e.g., Abell et al., 2015).

**Table 1.3** Description of data used to configure, calibrate and validate the SWAT model for each chapter. SS: suspended sediment; DRP: dissolved reactive phosphorus; TP: total phosphorus; NO<sub>3</sub>-N: nitrate–nitrogen; NH<sub>4</sub>-N: ammonium–nitrogen; TKN: total Kjeldahl nitrogen (NH<sub>4</sub>-N + organic N); TN: total nitrogen.

	<b>(I) Catchment measured data</b>		
	Chapter 2	Chapter 3	Chapter 4
Study catchment	Both Puarenga Stream catchment and Waipa Stream catchment	Waipa Stream catchment	Puarenga Stream catchment and Waipa Stream catchment separately
Rain gauge used	Kaituna rain gauge	Red Stag rain gauge and Kaituna rain gauge	Red Stag rain gauge and Kaituna rain gauge
Rainfall data frequency	Hourly records	Hourly records at Kaituna rain gauge used to proportion weekly records at Red Stag to hourly rainfall	Hourly records at Kaituna rain gauge used to proportion weekly records at Red Stag to hourly rainfall
Key land management area	Wastewater–irrigated area and pastoral farmland	Wastewater–irrigated area	Wastewater–irrigated area and pastoral farmland
Soil properties	Allophanic and pumice soils	Allophanic soils	Allophanic and pumice soils
Monitoring site used	FRI stream–gauge	Waipa downstream station	FRI stream–gauge
Stream discharge measurements used	15–min stream discharge data aggregated as daily mean values (1994–1997; 2004–2008)	Weekly flow–proportional samplings converted to weekly mean discharge data (2003–2012)	15–min stream discharge data aggregated as daily mean values (2006–2010)
Stream water quality measurements used	1) Monthly samples of SS, TP and TN concentrations assumed constant for the month (1994–1997; 2004–2008); 2) Daily discharge–weighted mean concentrations calculated from high–frequency event–based samples for concentrations of SS (nine events), TP and TN (both 14 events) at 1–2 h frequency (2010–2012)	Weekly mean load calculated from weekly flow–proportional measurements of SS, DRP, TP, NO <sub>3</sub> -N, NH <sub>4</sub> -N, TKN, and TN concentrations (2003–2012)	Monthly samples of SS, DRP, TP, NO <sub>3</sub> -N, NH <sub>4</sub> -N, TKN, and TN concentrations assumed constant for the month (2006–2010)

**Table 1.3** (continued) Description of data used to configure, calibrate and validate the SWAT model for each chapter. *r*: Pearson product moment correlation coefficient; NSE: Nash–Sutcliffe efficiency; RMSE: root mean square error; MAE: mean absolute error; PBIAS: percent bias.

	<b>(II) Catchment model used data</b>		
	Chapter 2	Chapter 3	Chapter 4
Study catchment	Both Puarenga Stream catchment and Waipa Stream catchment	Waipa Stream catchment	Puarenga Stream catchment and Waipa Stream catchment separately
Model code used	SWAT2009_rev488 unmodified code	SWAT2012_rev629 modified code	SWAT2012_rev629 modified code
Model routing used	Hourly routing	Hourly routing	Hourly routing
Calibration period	2004–2008	2003–2010	2006–2009
Validation period	1) 1994–1997; 2) 2010–2012	2011–2012	2009–2010
Modelled data frequency	Daily mean discharge and nutrient load simulations from which nutrient concentrations calculated	Daily mean discharge and nutrient load simulations averaged to weekly time scale	Daily and hourly mean discharge and nutrient load simulations from which nutrient concentrations calculated
Statistics used for model performance	<i>r</i> , NSE, PBIAS	<i>r</i> , RMSE, MAE, PBIAS	<i>r</i> , RMSE, MAE, PBIAS

**Table 1.3** (continued) Description of data sources used to configure, calibrate and validate the SWAT model for each chapter.

Data	Source
Digital elevation model (DEM) and digitised stream network	Bay of Plenty Regional Council (BoPRC)
Meteorological data and rainfall data	National Climate Database (available at <a href="http://cliflo.niwa.co.nz/">http://cliflo.niwa.co.nz/</a> ); BoPRC
Land use	New Zealand Land Cover Database Version 2; BoPRC
Soil characteristics	New Zealand Land Resource Inventory & digital soil map (available at <a href="http://smap.landcareresearch.co.nz">http://smap.landcareresearch.co.nz</a> )
Stream discharge and water quality measurements	BoPRC; Abell et al., 2013

## 1.4 References

- Abell, J.M., Hamilton, D.P., and Rutherford JC.: Quantifying temporal and spatial variations in sediment, nitrogen and phosphorus transport in stream inflows to a large eutrophic lake, *Environ. Sci. Processes Impacts*, 15, 1137–1152, 2013.
- Abell, J.M., McBride, C.M., and Hamilton, D.P.: Lake Rotorua wastewater discharge: environmental effects study, ERI Report No. 80, Client report prepared for Rotorua Lakes Council, Environmental Research Institute, Faculty of Science and Engineering, the University of Waikato, Hamilton, New Zealand, 122 pp., 2015.
- Amatya, D.M., Rossi, C.G., Saleh, A., Dai, Z., Youssef, M.A., Williams, R.G., Bosch, D.D., Chescheir, G.M., Sun, G., Skaggs, R.W., Trettin, C.C., Vance, E.D., Nettles, J.E., and Tian, S.: Review of nitrogen fate models applicable to forest landscapes in the southern U.S., *T. ASABE*, 56, 1731–1757, 2013.
- Anastasiadis, S., Nauleau, M-L., Kerr, S., Cox, T., and Rutherford, K.: Water quality management in Lake Rotorua: a comparison of regulatory approaches using the NManager Model, *Proceedings of the 52<sup>nd</sup> Annual Conference of the New Zealand Association of Economists*, Wellington, New Zealand, 46 pp., 2011.
- Aouissi, J., Benabdallah, S., Chabaâne, Z.L., and Cudennec, C.: Modeling water quality to improve agricultural practices and land management in a Tunisian catchment using the Soil and Water Assessment Tool, *J. Environ. Qual.*, 43, 18–25, 2014.
- Arnell, N.W., Halliday, S.J., Battarbee, R.W., Skeffington, R.A., and Wade, A.J.: The implications of climate change for the water environment in England, *Prog. Phys. Geog.*, 39, 93–120, 2015.
- Arnold, J.G., Srinivasan, R., Muttiah, R.S., and Williams, J.R.: Large area hydrologic modeling and assessment Part I: Model development, *J. Am. Water Resour. As.*, 34, 73–89, 1998.
- Barton, L., Schipper, L.A., Barkle, G.F., McLeod, M., Speir, T.W., Taylor, M.D., McGill, A.C., van Schaik, A.P., Fitzgerald, N.B., and Pandey, S.P.: Land application of domestic effluent onto four soil types: plant uptake and nutrient leaching, *J. Environ. Qual.*, 34, 635–643, 2005.
- Beets, P.N., Gielen, G., Oliver, G.R., Pearce, S.H., and Graham, J.D.: Determination of the level of soil N and P storage and soil health at the Rotorua Land Treatment site, *Scion Report 50659*, New Zealand Forest Research Institute Limited, Rotorua, New Zealand, 39 pp., 2013.
- Beven, K.J., and Kirkby, M.J.: A physically based variable contributing area model of basin hydrology, *Hydrol. Sci. Bull.*, 24, 43–69, 1979.

- Beven, K.J., Lamb, R., Quinn, P., Romanowicz, R., and Freer, J.: TOPMODEL, in: *Computer Models of Watershed Hydrology*, edited by: Singh, V.P., Water Resource Publications, Colorado, pp. 627–668, 1995.
- Bogaart, P.W., and Troch, P.A.: Curvature distribution within hillslopes and catchments and its effect on the hydrological response, *Hydrol. Earth System Sci.*, 10, 925–936, 2006.
- Borah, D.K., and Bera, M.: Watershed-scale hydrologic and nonpoint-source pollution models: review of mathematical bases, *T. ASAE.*, 46, 1553–1566, 2003.
- Bouwman, A.F., Bierkens, M.F.P., Griffioen, J., Hefting, M.M., Middelburg, J.J., Middelkoop, H., and Slomp, C.P.: Nutrient dynamics, transfer and retention along the aquatic continuum from land to ocean: towards integration of ecological and biogeochemical models, *Biogeosciences*, 10, 1–22, 2013.
- Bryant, R.B., Gburek, W.J., Vieth, T.L., and Hively, W.D.: Perspectives on the potential for hydrogeology to improve watershed modeling of phosphorus loss, *Geoderma*, 131, 299–307, 2006.
- Burger, D.F., Hamilton, D.P., and Pilditch, C.A.: Modelling the relative importance of internal and external nutrient loads on water column nutrient concentrations and phytoplankton biomass in a shallow polymictic lake, *Ecol. Model.*, 21, 411–423, 2008.
- Chen, X., Yang, X., Dong, X., and Liu, E.: Influence of environmental and spatial factors on the distribution of surface sediment diatoms in Chaohu Lake, Southeast China, *Acta Bot. Croat.*, 71, 299–310, 2012.
- Cole, T.M. and Wells, S.A.: CE-QUAL-W2: A two dimensional, laterally averaged, hydrodynamic and water quality model, version 3.5, Instruction Report EL-06-1, US Army Engineering and Research Development Center, Vicksburg, MS, the United States, 680 pp., 2006.
- Couture, R.M., Tominaga, K., Starrfelt, J., Moe, S.J., Kaste, O., and Wrigh, R.F.: Modelling phosphorus loading and algal blooms in a Nordic agricultural catchment-lake system under changing land-use and climate, *Environ. Sci. Processes Impacts*, 16, 1588–1599, 2014.
- Devi, G.K., Ganasri, B.P., and Dwarakish, G.S.: A review on hydrological models, International conference on water resources, coastal and ocean engineering (ICWRCOE2015), *Aquat. Proc.*, 4, 1001–1007, 2015.
- Di Toro, D.M., Fitzpatrick, J.J., and Thomann, R.V.: Documentation for Water Quality Analysis Simulation Program (WASP) and Model Verification Program (MVP), Contract No. 68-01-3872, U.S. Environmental Protection Agency, Duluth, Minnesota, the United States, 156 pp., 1983.

- Donigian, A.S.Jr., Bicknell, B.R., and Imhoff, J.C.: Hydrological simulation program - FORTRAN (HSPF), Chapter 12 in: *Computer Models of Watershed Hydrology*, edited by: Singh, V.P., Water Resources Publications, Highlands Ranch, CO., the United States, pp. 395–442, 1995.
- Fee, E.J., Hecky, R.E., Kasian, S.E., and Cruikshank D.R.: Effects of lake size, water clarity, and climatic variability on mixing depths in Canadian Shield Lakes, *Limnol. Oceanogr.*, 41, 912–920, 1996.
- Forbes, S.A.: The lake as a microcosm, *Bulletin of the Peoria Scientific Association, Illinois Natural History Survey, IL, the United States*, 15, 537–550, 1887.
- Garambois, P.A., Roux, H., Larnier, K., Castaings, W., and Dartus, D.: Characterisation of process-oriented hydrologic model behavior with temporal sensitivity analysis for flash floods in Mediterranean catchments, *Hydrol. Earth Syst. Sci.*, 17, 2305–2322, 2013.
- Graham, D.N., and Butts, M.B.: Flexible, integrated watershed modelling with MIKE SHE, in: *Watershed Models*, edited by: Singh, V.P., and Frevert, D.K., CRC Press, the United States, pp. 245–272, 2005.
- Green, W.H. and Ampt, G.A.: Studies on soil physics, part I – the flow of air and water through soils, *J. Agr. Sci.*, 4, 1–24, 1911.
- Haider, K., Heinemeyer, O., and Mosier, A.R.: Effects of growing plants on humus and plant residue decomposition in soil; uptake of decomposition products by plants, *Sci. Total Environ.*, 81, 661–670, 1989.
- Hamilton, D.P., and Schladow, S.G.: Prediction of water quality in lakes and reservoirs. Part I – Model description. *Ecol. Model.*, 96, 91–110, 1997.
- Hamilton, D.P., Özkundakci, D., McBride, C.G., Ye, W., Luo, L., Silvester, W., and White, P.: Predicting the effects of nutrient loads, management regimes and climate change on water quality of Lake Rotorua, University of Waikato Report 005, Environmental Research Institute, University of Waikato, Hamilton, New Zealand, 73 pp., 2012.
- Hamilton, D.P., Salmaso, N., and Paerl, H.W.: Mitigating harmful cyanobacterial blooms: strategies for control of nitrogen and phosphorus loads, *Aquat. Ecol.*, 50, 351–366, 2016.
- Hickman, M., and Penn, I.D.: The relationship between planktonic algae and bacteria in a small lake, *Hydrobiologia*, 52, 213–219, 1977.
- Hipsey, M.R., Romero, J.R., Antenucci, J.P., and Hamilton, D.P.: Computational aquatic ecosystem dynamic model: CAEDYM v2.3 science manual, Centre for Water Research, University of Western Australia, 102 pp., 2006.

- Hoare, R.A.: Inflows to Lake Rotorua, *Journal of Hydrology (NZ)*, 19, 49–59, 1980.
- Im, S., Brannan, K.M., and Mostaghimi, S.: Simulating hydrologic and water quality impacts in an urbanizing watershed, *J. Am. Water Resour. As.*, 39, 1465–1479, 2003.
- Imberger, J., Patterson, J.C., Hebbert, B., and Loh, I.: Dynamics of reservoir of medium size, *J. Fluid Mech.*, 104, 725–743, 1978.
- IPCC: *Climate Change 2013: The Physical Science Basis*, in: *Contribution of Working Group I to the Fifth Assessment Report of the Intergovernmental Panel on Climate Change*, edited by: Stocker, T.F., Qin, D., Plattner, G.-K., Tignor, M.M.B., Allen, S.K., Boschung, J., Nauels, A., Xia, Y., Bex, V., and Midgley, P.M., Cambridge University Press, Cambridge, New York, the United States, 1535 pp., 2013.
- Jenkins, D.G.: Lakes and rivers as microcosms, version 2.0, *J. Limnol.*, 73, 20–32, 2014.
- Jeong, J., Kannan, N., Arnold, J., Glick, R., Gosselink, L., and Srinivasan, R.: Development and integration of sub-hourly rainfall–runoff modeling capability within a watershed model, *Water Resour. Manag.*, 24, 4505–4527, 2010.
- Jeong, J., Kannan, N., Arnold, J.G., Glick, R., Gosselink, L., Srinivasan, R., and Harmel, R.D.: Development of sub-daily erosion and sediment transport algorithms for SWAT, *T. ASABE.*, 54, 1685–1691, 2011.
- Kannel, P.R., Kanel, S.R., Lee, S., Lee, Y.S., and Gan, T.Y.: A review of public domain water quality models for simulating dissolved oxygen in rivers and streams, *Environ. Model. Assess.*, 16, 183–204, 2011.
- Kim, D.-K., Zhang, W., Watson, S., and Arhonditsis, G.B.: A commentary on the modelling of the causal linkages among nutrient loading, harmful algal blooms, and hypoxia patterns in Lake Erie, *J. Gt. Lakes Res.*, 40, 117–129, 2014.
- Krause, P., Boyle, D.P., and Bäse, F.: Comparison of different efficiency criteria for hydrological model assessment, *Adv. Geosci.*, 5, 89–97, 2005.
- Kuchment, L.S.: The hydrological cycle and human impact on it, *Water Resour. Manage.*, *Encyclopedia of Life Support Systems (EOLSS)*, Abu Dhabi, the United Arab Emirates, 40 pp., 2004.
- Leavitt, P.R., Fritz, S.C., Anderson, N.J., Baker, P.A., Blenckner, T., Bunting, L., Catalan, J., Conley, D.J., Hobbs, W., Jeppesen, E., Korhola, A., McGowan, S., Rühland, K., Rusak, J.A., Simpson, G.L., Solovieva, N., and Werne, J.: Paleolimnological evidence of the effects on lakes of energy and mass transfer from climate and humans, *Limnol. Oceanogr.*, 54, 2330–2348, 2009.

- Lowe, A., Gielen, G., Bainbridge, A., and Jones, K.: The Rotorua Land Treatment Systems after 16 years, in: New Zealand Land Treatment Collective – Proceedings for the 2007 Annual Conference, 14–16 March 2007, Rotorua, New Zealand, pp. 66–73, 2007.
- Marshall, L., Sharma, A., and Nott, D.: Modelling the catchment via mixtures: issues of model specification and validation, *Water Resour. Res.*, 42, W11409, 2006.
- Merz, R., Blöschl, G., and Parajka, J.: Regionalisation methods in rainfall-runoff modelling using large samples, IAHS publication no. 307, IAHS, Wallingford, United Kingdom, pp. 117–125, 2006.
- Mueller, H., Hamilton, D.P., and Doole, G.J.: Response lags and environmental dynamics of restoration efforts for Lake Rotorua, New Zealand, *Environ. Res. Lett.*, 10, 074003, 2015.
- Mulligan, M.: Modelling catchment hydrology, in: *Environmental Modelling: Finding simplicity in complexity*, edited by: Wainwright, J., and Mulligan, M., John Wiley & Sons Ltd, Chichester, United Kingdom, 15 pp., 2004.
- Neitsch, S.L., Arnold, J.G., Kiniry, J.R., and Williams, J.R.: Soil and Water Assessment Tool theoretical documentation version 2009, Texas Water Resources Institute Technical Report No. 406, Texas A&M University System, College Station, Texas, the United States, 647 pp., 2011.
- Ostojski, M.S., Niedbala, J., Orlińska-Wozniak, P., Wilk, P., and Gebala, J.: SWAT model calibration results for different catchments sizes in Poland, *J. Environ. Qual.*, 43, 132–144, 2014.
- Pechlivanidis, I.G., Jackson, B.M., McIntyre, N.R., and Wheater, H.S.: Catchment scale hydrological modelling: a review of model types, calibration approaches and uncertainty analysis methods in the context of recent developments in technology and applications, *Global Nest J.*, 13, 193–214, 2011.
- Piñol, J., Beven, K.J., and Freer, J.: Modelling the hydrological response of Mediterranean catchments, Prades, Catalonia. The use of distributed models as aid to hypothesis formulation, *Hydrol. Process.*, 11, 1287–1306, 1997.
- Poole, G.C.: Fluvial landscape ecology: addressing uniqueness within the river discontinuum, *Freshwater Biol.*, 47, 641–660, 2002.
- Preston, S.D., Alexander, R.B., Schwarz, G.E., and Crawford, C.G.: Factors affecting stream nutrient loads: a synthesis of regional SPARROW model results for the continental United States, *J. Am. Water Resour. Assoc.*, 47, 891–915, 2011.

- Price, K., Purucker, T., Kraemer, S.R., and Babendreier, J.E.: Tradeoffs among watershed model calibration targets for parameter estimation, *Water Resour. Res.*, 48, W10542, 2012.
- Radcliffe, D.E., Reid, D.K., Blombäck, K., Bolster, C.H., Collick, A.S., Easton, Z.M., Francesconi, W., Fuka, D.R., Johnson, H., King, K., Larsbo, M., Youssef, M.A., Mulkey, A.S., Nelson, N.O., Persson, K., Ramirez-Avila, J.J., Schmieder, F., and Smith, D.R.: Applicability of models to predict phosphorus losses in drainage fields: A review, *J. Environ. Qual.*, 44, 614–628, 2015.
- Rahel, F.J. and Olden, J.D.: Assessing the effects of climate change on Aquatic invasive species, *Conserv. Biol.*, 22, 521–533, 2008.
- Refsgaard, J.C., and Storm, B.: MIKE SHE, Chapter 23 in: *Computer Models of Watershed Hydrology*, edited by: Singh, V.P., Water Resources Publications, Highlands Ranch, CO, the United States, pp. 809–846, 1995.
- Robertson, D.M., Saad, D.A., Christiansen, D.E., and Lorenz, D.J.: Simulated impacts of climate change on phosphorus loading to Lake Michigan, *J. Great Lakes Res.*, 42, 536–548, 2016.
- Rumelhart, D. and McClelland, J.: *Parallel distributed processing*, MIT Press, Cambridge, Massachusetts, the United States, 567 pp., 1986.
- Rutherford, J.C., Dumnov, S.M., and Ross, A.H.: Predictions of phosphorus in Lake Rotorua following load reductions, *New Zeal. J. Mar. Fresh.*, 30, 383–396, 1996.
- Saleh, A., and Du, B.: Evaluation of SWAT and HSPF within BASINS program for the upper north Bosque river watershed in central Texas, *T. ASAE.*, 47, 1039–1049, 2004.
- Schneiderman, E., Järvinen, M., Jennings, E., May, L., Moore, K., Naden, P.S., and Pierson, D.: Modeling the effects of climate change on catchment hydrology with the GWLF model, in: *the impact of climate change on European Lakes*, edited by: George, G., Springer, Dordrecht, Netherlands, pp. 33–50, 2010.
- Shaw, B., Mechenich, C., and Klessig, L.: *Understanding lake data*, G3582, University of Wisconsin-Stevens Point, Wisconsin, the United States, 20 pp., 2004.
- Smith, R.A., Schwarz, G.E., and Alexander, R.B.: Regional interpretation of water-quality monitoring data, *Water Resour. Res.*, 33, 2781–2798, 1997.
- Tarboton, G.D.: *Rainfall–runoff processes, a workbook to accompany the Rainfall-Runoff Processes Web module*, Utah State University, Logan, UT, the United States, 159 pp., 2003.

- USDA–SCS: Chapter 9: Hydrologic Soil–Cover Complexes, In National Engineering Handbook, part 630: hydrology, Natural Resources Conservation Service and Agricultural Research Service, United States Department of Agriculture, Washington D.C., 20 pp., 2004.
- van Liew, M.W., and Garbrecht, J.: Hydrologic simulation of the little Wachita river experimental watershed using SWAT, *J. Am. Water Resour. As.*, 39, 413–426, 2003.
- Vollenweider, R.A.: Input–output models with special reference to the phosphorus loading concept in limnology, *Schweiz. Z. Hydrol.*, 37, 53–84, 1975.
- Wetzel, R.G.: *Limnology: lake and river ecosystems*, 3<sup>rd</sup> ed, Academic Press, San Diego, CA, the United States, 1009 pp., 2001.
- White, M.J., Storm, D.E., Busted, P.R., Stoodley, S.H., and Phillips. S.J.: Evaluating nonpoint source critical source area contributions at the watershed scale, *J. Environ. Qual.*, 38, 1654–1663, 2009.
- Whitehead, P.G., Wilby, R.L., Battarbee, R., Kernan, M., and Wade, A.: A review of the potential impacts of climate change on surface water quality, *Hydrol. Sci. J.*, 54, 101–123, 2009.
- Williams, J.R.: Sediment routing for agricultural watersheds, *Water Resour. Bull.*, 11, 965–974, 1975.
- Winter, T.C., Harvey, J.W., Franke, O.L., and Alley, W.M.: *Ground water and surface water—a single resource*, U.S. Geological Survey Circular 1139, U.S. Geological Survey, Denver, Colorado, 87 pp., 1998.
- Xie, H., and Lian, Y.: Uncertainty-based evaluation and comparison of SWAT and HSPF applications to the Illinois River Basin, *J. Hydrol.*, 481, 119–131, 2013.
- Yang, Y.S., and Wang, L.: A review of modelling tools for implementation of the EU water framework directive in handling diffuse water pollution, *Water Resour. Manag.*, 24, 1819–1843, 2010.

## **2 Effects of hydrologic conditions on SWAT model performance and parameter sensitivity for a small, mixed land use catchment in New Zealand**

### **2.1 Abstract**

The Soil Water Assessment Tool (SWAT, version rev488) was configured for the Puarenga Stream catchment (77 km<sup>2</sup>), Rotorua, New Zealand. The configuration was used to quantify model performance and parameter sensitivity during different hydrologic conditions. A Sequential Uncertainty Fitting (SUFI-2) procedure was used to auto-calibrate unknown parameter values in the SWAT2009 model for years 2004–2008. Model validation was performed using: 1) monthly instantaneous measurements of suspended sediment (SS), total phosphorus (TP) and total nitrogen (TN) concentrations (1994–1997); and 2) daily discharge-weighted mean concentrations calculated from high-frequency event-based samples for concentrations of SS (nine events), TP and TN (both 14 events) at 1–2 h frequency (2010–2012). Model error associated with quick-flow was underestimated (44% bias for SS, 70% bias for TP) compared with monthly measurements derived predominantly from base flow measurements (< 1% bias for SS, 24% bias for TP). The use of low-frequency base flow measurements for model calibration provided poor simulation results for “flashy” lower-order streams. The model results highlight the importance of using high-frequency, event-based monitoring data for calibration, to alleviate the potential for underestimation of storm-driven fluxes. A manual procedure (one-at-a-time sensitivity analysis) was used to quantify parameter sensitivity for the two hydrologically-separated regimes. Parameters relating to tuning of main channel processes (e.g., lateral flow slope length and travel time) were more sensitive for base flow estimates (particularly discharge and SS), while those relating to overland processes (e.g., Manning’s n value for overland flow) were more sensitive for the quick flow estimates. Separating discharge and loads of sediments and nutrients into a base flow and a quick flow component provided important insights into uncertainties in parameter values. This research has important implications for performance of hydrological models applied to catchments with large fluctuations in stream flow, and in cases where models are used to examine scenarios that involve substantial changes to the

existing flow regime. Antecedent hydrologic conditions should be considered in calibration of parameters and application of hydrologic models.

## **2.2 Introduction**

Catchment models are valuable tools for understanding natural processes occurring at basin scales and for simulating the effects of different management regimes on soil and water resources (e.g., Cao et al., 2006). Model applications may have uncertainties as a result of errors associated with the forcing variables, measurements used for calibration, and conceptualisation of the model itself (Lindenschmidt et al., 2007). The ability of catchment models to simulate hydrological processes and pollutant loads can be assessed through analysis of uncertainty or errors during a calibration process that is specific to the application domain (White and Chaubey, 2005).

The SWAT model is increasingly used to predict discharge, sediment and nutrient loads on a temporally resolved basis, and to quantify material fluxes from a catchment to the downstream receiving environment such as a lake (e.g., Nielsen et al., 2013). The SWAT model can provide distributed descriptions of hydrologic processes at sub-basin scale (Arnold et al., 1998). It is physically-based if the Green-Ampt infiltration method (Green and Ampt, 1911) is used for the calculation of surface runoff (Neitsch et al., 2011). It has numerous parameters but not all are physically-based, i.e., some can be fixed on the basis of pre-existing catchment data (e.g., soil maps) or knowledge gained in other studies. However, values for other parameters need to be assigned during a calibration process as a result of complex spatial and temporal variations that are not readily captured either through measurements or within the model algorithms themselves (Boyle et al., 2000). Such parameter values assigned during calibration are therefore lumped, i.e., they integrate variations in space and/or time and thus provide an approximation for real values which often vary widely within a study catchment. Model calibration is an iterative process whereby parameters are adjusted to the system of interest by refining model predictions to fit closely with observations under a given set of conditions (Moriassi et al., 2007). Manual calibration depends on knowledge of the catchment or the system used for model application, the experience in using the model, and knowledge of the model algorithms. It tends to be subjective and time-

consuming. By contrast, auto-calibration provides a less labour-intensive approach by using optimisation algorithms (Eckhardt and Arnold, 2001). The SUFI-2 procedure (with a fitting function) has previously been applied to auto-calibrate discharge parameters in a SWAT application for the Thur River, Switzerland (Abbaspour et al., 2007), as well as for groundwater recharge, evapotranspiration and soil storage water considerations in West Africa (Schuol et al., 2008). Model validation is subsequently performed using measured data that are independent of those used for calibration.

Values for hydrological parameter values in the SWAT model can vary temporally. Cijin et al. (2010) found that the optimum calibrated values for hydrological parameters varied with different flow regimes (low, medium and high), thus suggesting that SWAT model performance can be optimised by assigning parameter values based on hydrological regimes. Other work has similarly demonstrated benefits from assigning separate parameter values to low, medium, and high discharge periods (Yilmaz et al., 2008), or based on whether a catchment is in a dry, drying, wet or wetting state (Choi and Beven, 2007). Such temporal dependence of model parameterisation on hydrologic conditions has implications for model performance. Krause et al. (2005) compared different statistical metrics of hydrological model performance separately for base flow periods and storm events to evaluate the performance. The authors found that the logarithmic form of the Nash-Sutcliffe efficiency (NSE) value provided more information on the sensitivity of model performance for discharge simulations during storm events, while another modified form of NSE based on relative deviations was better for base flow periods. Similarly, Guse et al. (2014) investigated sensitivity of SWAT hydrological parameters using Fourier amplitude sensitivity test (Reusser et al., 2011) and examined temporal dynamics of model performance using cluster analysis (Reusser et al., 2009). Guse et al. (2014) found that three groundwater parameters were highly sensitive during quick flow, while one evaporation parameter was most sensitive during base flow, and model performance was also found to vary significantly for the two flow regimes. Zhang et al. (2011) calibrated SWAT hydrological parameters for periods separated on the basis of six climatic indexes. Model performance improved when different values were assigned to parameters based on six hydroclimatic periods. Similarly, Pfannerstill et al. (2014) found that assessment of model performance was improved by considering an

additional performance statistic for very low–flow simulations amongst five hydrologically–separated regimes.

To date, analysis of temporal dynamics of SWAT parameters has predominantly focused on simulations of discharge rather than water quality constituents. This partly reflects the paucity of comprehensive water quality data for many catchments; near–continuous discharge data can readily be collected but this is not the case for water quality parameters such as suspended sediment or nutrient concentrations. Data collected in monitoring programmes that involve sampling at regular time intervals (e.g., monthly) are often used to calibrate water quality models, but these are unlikely to fully represent the range of hydrologic conditions in a catchment (Bieroza et al., 2014). In particular, water quality data collected during storm flow periods are rarely available in lower–order catchments (e.g., Chiwa et al., 2010; Abell et al., 2013), thus prohibiting opportunities to calibrate SWAT parameters and investigate how parameter sensitivity varies under conditions which can contribute disproportionately to nutrient or sediment transport. Failure to fully consider storm flow processes could therefore result in an unsatisfactory model performance. Thus, further research is required to examine how water quality parameters vary during different flow regimes and to understand how model uncertainty may vary under future climatic conditions that affect flow regimes (Brigode et al., 2013).

In this study, the SWAT model was configured to a relatively small, mixed land use catchment in New Zealand that has been the subject of an intensive water quality sampling programme designed to target a wide range of hydrologic conditions. A catchment–wide set of parameters was calibrated using the SUFI–2 procedure which is integrated into the SWAT Calibration and Uncertainty Program (SWAT–CUP). The objectives of this study were to: (1) quantify the performance of the model in simulating discharge and fluxes of suspended sediments and nutrients at the catchment outlet; (2) rigorously evaluate model performance by comparing daily simulation output with monitoring water quality data collected under a range of hydrologic conditions; and (3) quantify whether parameter sensitivity varies between base flow and quick flow conditions.

## 2.3 Methods

### 2.3.1 Study area

The Puarenga Stream is the second-largest surface inflow to Lake Rotorua (Bay of Plenty, New Zealand) and drains a catchment of 77 km<sup>2</sup>. The catchment is situated in the central North Island of New Zealand, which has a warm temperate climate. Annual mean temperature at Rotorua Airport (Fig. 2.1a) is 15±4 °C and annual mean evapotranspiration is 714 mm yr<sup>-1</sup> (1993–2012; National Climatic Database; available at <http://cliflo.niwa.co.nz/>). Annual mean precipitation at Kaituna rain gauge (Fig. 2.1a) is 1500 mm yr<sup>-1</sup> (1993–2012; Bay of Plenty Regional Council; BoPRC). The catchment is relatively steep (mean slope = 9%; derived from the digital elevation model; BoPRC), resulting in substantial sub-surface lateral flow contributions to stream channels. The dominant soil type is pumice that has high macroporosity and infiltration rates (New Zealand Land Resource Inventory & digital soil map; available at <http://smap.landcareresearch.co.nz/>). Two cold-water springs (Waipa Spring and Hemo Spring) and one geothermal spring (Fig. 2.1b) are located in the catchment area. The two cold-water springs have annual mean discharge of ~0.19 m<sup>3</sup> s<sup>-1</sup> (Rotorua District Council) and the geothermal spring has annual mean discharge of ~0.12 m<sup>3</sup> s<sup>-1</sup> (White et al., 2004).

The dominant land use (47%) is exotic forest (*Pinus radiata*). Approximately 26% is managed pastoral farmland, 11% mixed scrub and 9% indigenous forest (New Zealand Land Cover Database Version 2; BoPRC). Since 1991, treated wastewater (10 mm d<sup>-1</sup>) has been pumped from the Rotorua Wastewater Treatment Plant and spray-irrigated over 16 blocks of total area of 1.93 km<sup>2</sup> in the Whakarewarewa Forest (Fig. 2.1a). Groundwater level increased by 0.11 m after four years of irrigation (Tomer et al., 1999) and elevated nitrate concentrations (c. 0.44 mg L<sup>-1</sup>) were also found in the receiving waters of the Puarenga Stream (Paku, 2001). Prior to 2002, the irrigation schedule entailed applying wastewater to two blocks per day so that each block was irrigated approximately weekly. Since 2002, 10 to 14 blocks have been irrigated simultaneously at a frequency of 2 h d<sup>-1</sup> with irrigation rate of 5 mm hr<sup>-1</sup> (Lowe et al., 2007). Over the entire period of irrigation, nutrient concentrations in the irrigated water have gradually decreased as improvements in treatment of the wastewater have been made (Lowe et al., 2007).

Measurements from the Forest Research Institute (FRI) stream–gauge (1.7 km upstream of Lake Rotorua; Fig. 2.1b) were considered representative of the downstream/outlet conditions of the Puarenga Stream. The FRI stream–gauge was discontinued in mid 1997, then restarted late in 2004 (Environment Bay of Plenty, 2007). Annual mean discharge at this site is  $2.0 \text{ m}^3 \text{ s}^{-1}$  (1994–1997 and 2004–2008; BoPRC). The Puarenga Stream receives a high proportion of flow from groundwater and has only moderate seasonality in discharge. On average, the lowest mean daily discharge is during summer (December to February;  $1.7 \text{ m}^3 \text{ s}^{-1}$ ) and the highest mean daily discharge is during winter (June to August;  $2.4 \text{ m}^3 \text{ s}^{-1}$ ). Discharge records during 1998–2004 were intermittent and this precluded a detailed comparison of measured and simulated discharge during that period. In July 2010, the gauge was repositioned 720 m downstream to the State Highway 30 (SH 30) bridge (Fig. 2.1b).

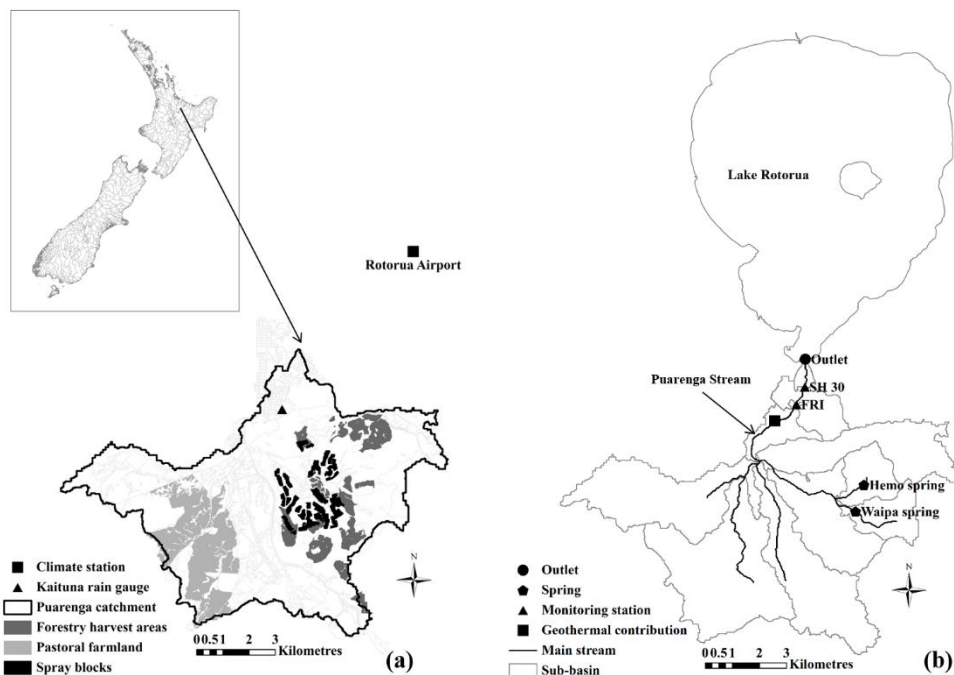


**Figure 2.1** (a) Location of Puarenga Stream surface catchment in New Zealand, Kaituna rain gauge, climate station and managed land areas for which management schedules were prescribed in SWAT, and (b) location of the Puarenga Stream, major tributaries, monitoring stream–gauges, two cold–water springs and the Whakarewarewa geothermal contribution. Measurement data (Table 2.3) used to calibrate the SWAT model were from the Forest Research Institute (FRI) stream–gauge and were considered representative of the downstream/outlet conditions of the Puarenga Stream.

### 2.3.2 Model configuration

SWAT input data requirements included a digital elevation model (DEM), meteorological records, records of springs and water abstractions, soil characteristics, land use classification, and management schedules for key land uses (pastoral farming, wastewater irrigation, and timber harvesting). The SWAT model (version SWAT2009\_rev488) was run on an hourly time step, but daily mean simulation outputs were used for this study.

The DEM was used to delineate boundaries of the whole catchment and individual sub-catchments, with a stream map used to “burn-in” channel locations to create accurate flow routings. Hourly rainfall estimates were used as hydrologic forcing data. The Penman–Monteith method (Monteith, 1965) was used to calculate evapotranspiration (ET) and potential ET. The Green and Ampt (1911) method was used to calculate infiltration and the hourly rainfall/Green & Ampt infiltration/hourly routing method was chosen to simulate surface runoff, soil erosion and in-stream sediment transport (Neitsch et al., 2011). Ten sub-catchments were represented in the Puarenga Stream catchment, each comprising numerous Hydrologic Response Units (HRUs). Each HRU aggregates cells with the same combination of land cover, soil, and slope. A total of 404 HRUs was defined in the model. Runoff and nutrient transport were predicted separately within SWAT for each HRU, with predictions summed to obtain the total for each sub-catchment.

Descriptions and sources of the data used to configure the SWAT model are given in Table 2.1. There were a total of 197 model parameters. Values of SWAT parameters were assigned based on: i) measured data (e.g., some of the soil parameters; Table 2.1); ii) literature values from published studies of similar catchments (e.g., parameters for dominant land uses; Table 2.2); or iii) by calibration where parameters were not otherwise prescribed. Initial parameter values required for model configuration were based on the monitoring data that was measured around the start date of the simulation period.

**Table 2.1** Description of data used to configure the SWAT model.

Data	Application	Data description and configuration details	Source
Digital elevation model (DEM) & digitised stream network	Sub-basin delineation (Fig. 2.1b)	25 m resolution. Used to define five slope classes: 0–4%, 4–10%, 10–17%, 17–26% and > 26%.	Bay of Plenty Regional Council (BoPRC)
Spring discharge and nutrient loads	Point source (Fig. 2.1b)	Constant daily discharge and nutrient concentrations assigned to two cold-water springs (Waipa Spring and Hemo Spring) and one geothermal spring.	White et al., 2004; Proffit, 2009 (Unpublished Site Visit Report); Paku, 2001; Mahon, 1985; Glover, 1993; Rotorua District Council (pers. comm.)
Water abstraction volumes	Water use	Monthly water abstraction assigned to two cold-water springs.	Kusabs and Shaw, 2008; Jowett, 2008
Land use	HRU definition	25 m resolution, 10 basic land-cover categories derived from New Zealand Land Cover Database (version 2). Some specific land-cover parameters were prior-estimated (Table 2.2).	BoPRC
Soil characteristics	HRU definition	22 soil types. Properties were quantified based on measurements (if available) or estimated using regression analysis to estimate properties for unmeasured functional horizons.	New Zealand Land Resource Inventory & digital soil map (available at <a href="http://smap.landcareresearch.co.nz">http://smap.landcareresearch.co.nz</a> )
Meteorological data	Meteorological forcing	Daily maximum and minimum temperature, daily mean relative humidity, daily global solar radiation, daily (9 am) surface wind speed, derived from Rotorua Airport Automatic Weather Station (Fig. 2.1a).	National Climate Database (available at <a href="http://cliflo.niwa.co.nz/">http://cliflo.niwa.co.nz/</a> )
		Hourly precipitation derived from Kaituna rain gauge (Fig. 2.1a).	BoPRC

**Table 2.1** (continued) Description of data used to configure the SWAT model. Note that some of the agricultural management data obtained in certain years was assumed constant or interpolated for the whole simulation period.

Data	Application	Data description and configuration details	Source
Agricultural management practices	Agricultural management schedules	Stock density	Statistics New Zealand, 2006; Ledgard and Thorrold, 1998
		Applications of urea and di-ammonium phosphate	Statistics New Zealand, 2006; Fert Research, 2009
		Applications of manure-associated nutrients	Dairying Research Corporation, 1999
Nutrient loading by wastewater application	Nonpoint-source from land treatment irrigation	Wastewater application rates and effluent composition (TN and TP concentration) for 16 spray blocks from 1996–2012. Each spray block was assigned an individual management schedule specifying daily application rates.	Rotorua District Council, 2006
Forest stand map and harvest dates	Forestry planting and harvesting operations	Planting and harvesting data for 472 ha forestry stands. Prior to 2007 we assumed stands were cleared one-year prior to the establishment year. Post 2007, harvesting date was assigned to the first day of harvesting month.	Timberlands Limited, Rotorua, New Zealand (pers. comm.)

**Table 2.2** Prior-estimated parameter values for three dominant types of land-cover in the Puarenga Stream catchment. Values of other land use parameters were based on the default values in the SWAT database.

Land-cover type	Parameter	Definition	Value	Source
PINE ( <i>Pinus radiata</i> )	HVSTI	Percentage of biomass harvested	0.65	(Ximenes et al., 2008)
	T_OPT (°C)	Optimal temperature for plant growth	15	(Kirschbaum and Watt 2011)
	T_BASE (°C)	Minimum temperature for plant growth	4	(Kirschbaum and Watt 2011)
	MAT_YRS	Number of years to reach full development	30	(Kirschbaum and Watt 2011)
	BMX_TREES (tonnes ha <sup>-1</sup> )	Maximum biomass for a forest	400	(Bi et al., 2010)
	GSI (m s <sup>-1</sup> )	Maximum stomatal conductance	0.00198	(Whitehead et al., 1994)
	BLAI (m <sup>2</sup> m <sup>-2</sup> )	Maximum leaf area index	5.2	(Watt et al., 2008)
	BP3	Proportion of phosphorus in biomass at maturity	0.000163	(Hopmans and Elms 2009)
	BN3	Proportion of nitrogen in biomass at maturity	0.00139	(Hopmans and Elms 2009)
FRSE (Evergreen forest)	HVSTI	Percentage of biomass harvested	0	–
	BMX_TREES (tonnes ha <sup>-1</sup> )	Maximum biomass for a forest	372	(Hall et al., 2001)
	MAT_YRS (years)	Number of years for tree to reach full development	100	–
PAST (Pastoral farm)	T_OPT (°C)	Optimal temperature for plant growth	25	(McKenzie et al., 1999)
	T_BASE (°C)	Minimum temperature for plant growth	5	(McKenzie et al., 1999)

SWAT simulates hydrological pathways including direct runoff, lateral flow, shallow aquifer and deep aquifer recharge. These components contribute to streamflow that is then used to compare with measurements taken at the in-stream monitoring station. Detailed descriptions of the various model components are given in Neitsch et al. (2011). Sediment yield was estimated using the modified universal soil loss equation (MUSLE; Williams, 1975) in SWAT.

SWAT simulates loads of “mineral phosphorus” (MINP) and “organic phosphorus” (ORGP) of which the sum is TP. The MINP fraction represents soluble P either in mineral or in organic form, while ORGP refers to particulate P bound either by algae or by sediment (White et al., 2014). Soluble P may be taken up during algae growth, or released from benthic sediment. This fraction can be transformed to particulate P contained in algae or sediment.

SWAT simulates loads of nitrate–nitrogen ( $\text{NO}_3\text{-N}$ ), ammonium–nitrogen ( $\text{NH}_4\text{-N}$ ) and organic nitrogen (ORGN), the sum of which is TN. Nitrogen parameters were auto-calibrated for each N fraction. The SWAT model does not account for the initial nitrate concentration in shallow aquifers, as also noted by Conan et al. (2003). Ekanayake and Davie (2005) indicated that SWAT underestimated N loading from groundwater and suggested a modification by adding a background concentration of nitrate in streamflow to represent groundwater nitrate contributions. Over the period of the first four years (1991–1994) of wastewater irrigation, nitrate concentrations in shallow groundwater draining the Waipa Stream sub-catchment were estimated to have increased by c.  $0.44 \text{ mg L}^{-1}$  (Paku, 2001). SWAT has no capability to dynamically adjust the groundwater concentration during a simulation run. Therefore, we added  $0.44 \text{ mg N L}^{-1}$  to all model simulations of TN concentration and assumed that groundwater concentrations had equilibrated with the applied wastewater nitrogen since 1994.

### **2.3.3 Model calibration and validation**

Daily mean discharge was first calibrated based on daily mean values of 15-minute measurements (Table 2.3). Water quality variables were then calibrated in the sequence: SS, TP and TN. Modelled daily mean concentrations were compared with concentrations measured during monthly grab sampling, with monthly instantaneous measurements assumed equal to concentrations on the corresponding

day (Table 2.3). The first year (1993) was used for model warm-up to a steady state for the subsequent simulated period of interest. The calibration period was from 2004 to 2008 and the validation period was from 1994 to 1997. A validation period that pre-dated the calibration period was chosen because discharge records were available for two separate periods (1994–1997 and post 2004). In addition, the operational regime for the wastewater irrigation has varied since operations began in 1991, with a marked change occurring in 2002 when operations switched from applying the wastewater load to two blocks (rotated daily for a total of 14 blocks in a week; i.e., each block irrigated weekly), to 10–14 blocks each irrigated daily. This operational regime continues today and we therefore decided to assign the most recent (post 2002) period (2004–2008) to calibration to ensure that the model was configured to reflect current operations.

Parameter values that were not derived from measurements or the literature were assigned based on either automated or manual calibration (Table 2.4). Manual calibration was undertaken for 11 parameters related to TP, while a Sequential Uncertainty Fitting (SUFI-2) procedure was applied to auto-calibrate 21 parameters for discharge simulations, nine parameters for SS simulations, and 17 parameters related to TN. The SUFI-2 procedure has been integrated into the SWAT Calibration and Uncertainty Program (SWAT-CUP). SUFI-2 is a procedure that efficiently quantifies and constrains parameter uncertainties/ranges from default ranges with the fewest number of iterations (Abbaspour et al., 2004), and has been shown to provide optimal results relative to the use of alternative algorithms (Wu and Chen, 2015). SUFI-2 involves Latin hypercube sampling (LHS), which is a method that generates a sample of plausible parameter values from a multidimensional distribution and ensures that samples cover the entire parameter space, therefore ensuring that the optimum solution is not a local minimum (Marino et al., 2008).

**Table 2.3** Description of data used to calibrate the SWAT model. Data were measured at the Forest Research Institute (FRI) stream–gauge and were considered representative of the downstream/outlet conditions of the Puarenga Stream.

Data	Application	Measurement data details	Source
Stream discharge measurements	Calibration (2004–2008)	15–min stream discharge data were measured at FRI stream–gauge (Fig. 2.1b) within the catchment and aggregated as daily mean values (1994–1997; 2004–2008).	BoPRC; Abell et al., 2013
	Validation (1994–1997)		
Stream water quality measurements	Calibration (2004–2008)	Monthly grab samples for determination of suspended sediment (SS), total phosphorus (TP) and total nitrogen (TN) concentrations (1994–1997; 2004–2008), and high–frequency event–based samples for concentrations of SS (nine events), TP and TN (both 14 events) at 1–2 h frequency (2010–2012), were also measured at FRI stream–gauge (Fig. 2.1b) within the catchment.	BoPRC; Abell et al., 2013
	Validation <sup>1</sup> (1994–1997; 2010–2012)		

<sup>1</sup> Model validation was undertaken using two different datasets. The monthly measurements (1994–1997) were predominantly collected when base flow was the dominant contributor to stream discharge. Data from high–frequency sampling during rain events (2010–2012) were also used to validate model performance during periods when quick flow was high.

The SUFI-2 procedure analyses relative sensitivities of parameters by randomly generating combinations of values for model parameters (Abbaspour et al., 2014). A sample size of 1000 was chosen for each iteration of LHS, resulting in 1000 combinations of parameters and 1000 simulations. Model performance was quantified for each simulation based on the Nash–Sutcliffe efficiency (NSE). An objective function was defined as a linear regression of a combination of parameter values generated by each LHS against the NSE value calculated from each simulation. Each compartment was not given weight to formulate the objective function because only one variable was specifically focused on at each time. A parameter sensitivity matrix was then computed based on the changes in the objective function after 1000 simulations. Parameter sensitivity was quantified based on the  $p$  value from a Student's  $t$ -test, which was used to compare the mean of simulated values with the mean value of measurements (Rice, 2006). A parameter was deemed sensitive if  $p \leq 0.05$  after 1000 simulations (one iteration). Numerous iterations of LHS were conducted. Values of  $p$  from numerous iterations were averaged for each parameter, and the frequency of iterations where a parameter was deemed sensitive was summed. Rankings of relative sensitivities of parameters were developed based on how frequently the sensitive parameter was identified and the averaged value of  $p$  calculated from several iterations. The most sensitive parameter was determined based on the frequency that the parameter was deemed sensitive, and the smallest average  $p$ -value from all iterations.

SUFI-2 considers two criteria to constrain uncertainty in each iteration. One is the P-factor, the percentage of measured data bracketed by 95% prediction uncertainty (95PPU). Another is the R-factor, the average thickness of the 95PPU band divided by the standard deviation of measured data. A range was first defined for each parameter based on a synthesis of ranges from similar studies or from the SWAT default range. Parameter ranges were updated after each iteration based on the computation of upper and lower 95% confidence limits. The 95% confidence interval and the standard deviation of a parameter value were derived from the diagonal elements of the covariance matrix, which was calculated from the sensitivity matrix and the variance of the objective function. Steps and equations used in the SUFI-2 procedure to constrain parameter ranges are outlined by Abbaspour et al. (2004).

The total numbers of iterations performed for each simulated variable (Q, SS, MINP, ORGN, NH<sub>4</sub>-N and NO<sub>3</sub>-N) reflected the numbers required to ensure that > 90% of measured data were bracketed by simulated output and the R-factor was close to one. The “optimal” parameter value was obtained when the Nash–Sutcliffe efficiency (NSE) criterion was satisfied (NSE > 0.5; Moriasi et al., 2007). Auto-calibrated parameters for simulations of Q, SS, and TN were changed by absolute values within the given ranges. Some of those given ranges were restricted based on the optimum values calibrated in similar studies. Parameter values for TP simulations were manually-calibrated based on the relative percent deviation from the predetermined values of those auto-calibrated parameters for MINP simulations, given by the objective functions (e.g., NSE). Parameters related to the physical characteristics of the catchment were not changed because their values were considered to be representative of the catchment characteristics. In addition, high-frequency (1–2 h) water quality sampling was undertaken at the FRI stream-gauge during 2010–2012 (Abell et al., 2013; Table 2.3) to derive estimates of daily mean contaminant loads during storm events. Samples were analysed for SS (nine events), TP and TN (both 14 events) over sampling periods of 24–73 h. The sampling programme was designed to encompass pre-event base flow, storm generated quick flow and post-event base flow. These data permitted calculation of daily discharge-weighted (Q-weighted) mean concentrations to compare with modelled daily mean estimates. We did not use the high-frequency observations to calibrate the model, because of the limited number of high-frequency (1–2 h) samples (nine events for SS and 14 events for TP and TN in 2010–2012). The use of the high-frequency observations for model validation allowed us to examine how the model performed during short (1–3 day) high flow periods. The Q-weighted mean concentrations  $C_{QWM}$  were calculated as:

$$C_{QWM} = \frac{\sum_{i=1}^n C_i Q_i}{\sum_{i=1}^n Q_i} \quad (1)$$

where n is the number of samples,  $C_i$  is the contaminant concentration measured at time i, and  $Q_i$  is the discharge measured at time i.

**Table 2.4** Summary of calibrated SWAT parameters. Discharge (Q), suspended sediment (SS) and total nitrogen (TN) parameter values were assigned using auto-calibration, while total phosphorus (TP) parameters were manually calibrated. SWAT default ranges and input file extensions are shown for each parameter. Parameters are unitless unless otherwise specified. “revap” indicates water movement into the overlying unsaturated layers.

Parameter	Definition	Unit	Default range	Calibrated value
Q				
EVRCH.bsn	Reach evaporation adjustment factor		0.5–1	0.9
SURLAG.bsn	Surface runoff lag coefficient		0.05–24	15
ALPHA_BF.gw	Base flow alpha factor (0–1)		0.0071–0.0161	0.01
GW_DELAY.gw	Groundwater delay	d	0–500	500
GW_REVAP.gw	Groundwater “revap” coefficient		0.02–0.2	0.08
GW_SPYLD.gw	Special yield of the shallow aquifer	m <sup>3</sup> m <sup>-3</sup>	0–0.4	0.13
GWHT.gw	Initial groundwater height	m	0–25	14
GWQMN.gw	Threshold depth of water in the shallow aquifer required for return flow to occur	mm	0–5000	372
RCHRG_DP.gw	Deep aquifer percolation fraction		0–1	0.87
REVAPMN.gw	Threshold depth of water in the shallow aquifer required for “revap” to occur	mm	0–500	260
CANMX.hru	Maximum canopy storage	mm	0–100	0.6
EPCO.hru	Plant uptake compensation factor		0–1	0.34
ESCO.hru	Soil evaporation compensation factor		0–1	0.9
HRU_SLP.hru	Average slope steepness	m m <sup>-1</sup>	0–0.6	0.5
LAT_TTIME.hru	Lateral flow travel time	d	0–180	3
RSDIN.hru	Initial residue cover	kg ha <sup>-1</sup>	0–10000	1
SLSOIL.hru	Slope length for lateral subsurface flow	m	0–150	40
CH_K2.rte	Effective hydraulic conductivity in the main channel alluvium	mm h <sup>-1</sup>	0–500	20
CH_N2.rte	Manning’s n value for the main channel		0–0.3	0.16
CH_K1.sub	Effective hydraulic conductivity in the tributary channel alluvium	mm h <sup>-1</sup>	0–300	100
CH_N1.sub	Manning’s n value for the tributary channel		0.01–30	20

Parameter	Definition	Unit	Default range	Calibrated value
SS				
USLE_P.mgt	USLE equation support practice factor		0–1	0.5
PRF.bsn	Peak rate adjustment factor for sediment routing in the main channel		0–2	1.9
SPCON.bsn	Linear parameter for calculating the maximum amount of sediment that can be re-entrained during channel sediment routing		0.0001–0.01	0.001
SPEXP.bsn	Exponent parameter for calculating sediment re-entrained in channel sediment routing		1–1.5	1.26
LAT_SED.hru	Sediment concentration in lateral flow and groundwater flow	mg L <sup>-1</sup>	0–5000	5.7
OV_N.hru	Manning's n value for overland flow		0.01–30	28
SLSUBBSN.hru	Average slope length	m	10–150	92
CH_COV1.rte	Channel erodibility factor		0–0.6	0.17
CH_COV2.rte	Channel cover factor		0–1	0.6
TP				
P_UPDIS.bsn	Phosphorus uptake distribution parameter		0–100	0.5
PHOSKD.bsn	Phosphorus soil partitioning coefficient		100–200	174
PPERCO.bsn	Phosphorus percolation coefficient		10–17.5	14
PSP.bsn	Phosphorus sorption coefficient		0.01–0.7	0.5
GWSOLP.gw	Soluble phosphorus concentration in groundwater loading	mg P L <sup>-1</sup>	0–1000	0.063
LAT_ORGP.gw	Organic phosphorus in the base flow	mg P L <sup>-1</sup>	0–200	10
ERORGP.hru	Organic phosphorus enrichment ratio		0–5	2.5
CH_OPCO.rte	Organic phosphorus concentration in the channel	mg P L <sup>-1</sup>	0–100	0.02
BC4.swq	Rate constant for mineralisation of organic phosphorus to dissolved phosphorus in the reach at 20 °C	d <sup>-1</sup>	0.01–0.7	0.3
RS2.swq	Benthic (sediment) source rate for dissolved phosphorus in the reach at 20 °C	mg m <sup>-2</sup> d <sup>-1</sup>	0.001–0.1	0.02
RS5.swq	Organic phosphorus settling rate in the reach at 20 °C	d <sup>-1</sup>	0.001–0.1	0.05

Parameter	Definition	Unit	Default range	Calibrated value
TN				
RSDCO.bsn	Residue decomposition coefficient		0.02–0.1	0.09
CDN.bsn	Denitrification exponential rate coefficient		0–3	0.3
CMN.bsn	Rate factor for humus mineralisation of active organic nitrogen		0.001–0.003	0.002
N_UPDIS.bsn	Nitrogen uptake distribution parameter		0–100	0.5
NPERCO.bsn	Nitrogen percolation coefficient		0–1	0.0003
RCN.bsn	Concentration of nitrogen in rainfall	mg N L <sup>-1</sup>	0–15	0.34
SDNCO.bsn	Denitrification threshold water content		0–1	0.02
HLIFE_NGW.gw	Half-life of nitrate–nitrogen in the shallow aquifer	d	0–200	195
LAT_ORGN.gw	Organic nitrogen in the base flow	mg N L <sup>-1</sup>	0–200	55
SHALLST_N.gw	Nitrate–nitrogen concentration in the shallow aquifer	mg N L <sup>-1</sup>	0–1000	1
ERORGN.hru	Organic nitrogen enrichment ratio		0–5	3
CH_ONCO.rte	Organic nitrogen concentration in the channel	mg N L <sup>-1</sup>	0–100	0.01
BC1.swq	Rate constant for biological oxidation of ammonium–nitrogen to nitrite–nitrogen in the reach at 20 °C	d <sup>-1</sup>	0.1–1	1
BC2.swq	Rate constant for biological oxidation of nitrite–nitrogen to nitrate–nitrogen in the reach at 20 °C	d <sup>-1</sup>	0.2–2	0.7
BC3.swq	Rate constant for hydrolysis of organic nitrogen to ammonium–nitrogen in the reach at 20 °C	d <sup>-1</sup>	0.2–0.4	0.4
RS3.swq	Benthic (sediment) source rate for ammonium–nitrogen in the reach at 20 °C	mg m <sup>-2</sup> d <sup>-1</sup>	0–1	0.2
RS4.swq	Rate coefficient for organic nitrogen settling in the reach at 20 °C	d <sup>-1</sup>	0.001–0.1	0.05

### 2.3.4 Hydrograph and contaminant load separation

The Web-based Hydrograph Analysis Tool (Lim et al., 2005) was applied to partition measured and simulated discharges into base flow ( $Q_b$ ) and quick flow ( $Q_q$ ). Two default parameters values required by the Hydrograph Analysis Tool: an Eckhardt filter parameter of 0.98 and ratio of base flow to total discharge of 0.8 (cf. Lim et al., 2005). There was a total of 60 days without quick flow during the calibration period (2004–2008) and 1379 days for which hydrograph separation was used to define base flow and quick flow. For those 60 days without quick flow, base flow recession was the only contributor to the discharge. For those 1379 days with both base flow and quick flow, direct runoff during extensive rainfall and base flow recession due to the preceding rainfall were both taken into account for discharge estimations.

Contaminant (SS, TP and TN) concentrations ( $C_{sep}$ ) were partitioned into base flow ( $C_b'$ ) and quick flow components ( $C_q'$ ; cf. Rimmer and Hartmann, 2014) to separately examine the sensitivity of water quality parameters during base flow and quick flow:

$$C_{sep} = \frac{Q_q \times C_q' + Q_b \times C_b'}{Q_q + Q_b} \quad (2)$$

$C_b'$  for each contaminant was estimated as the average concentration for the 60 days with no quick flow.  $C_q'$  for each contaminant was calculated by rearranging Eq. (2).

To ensure that  $C_q'$  is positive,  $C_b'$  is constrained to be the minimum of  $\bar{C}_{sep}$  and  $C_{sep}$ . Measured and simulated base flow and quick flow contaminant loads were then calculated.

A one-at-a-time (OAT) routine proposed by Morris (1991) was applied to investigate how parameter sensitivity varied between the two flow regimes (base flow and quick flow), based on the ranking of relative sensitivities of parameters that were identified by randomly generating combinations of values for model parameters for each individual variable using the SUFI-2 procedure. OAT sensitivity analysis was then employed by varying the parameter of interest among ten equidistant values within the default range. The natural logarithm was used by Krause et al. (2005) and therefore the standard deviation (STD) of the ln-

transformed NSE was used to indicate parameter sensitivity for the two flow regimes.

Parameters were ranked from most to least sensitive on the basis of the sensitivity metric (STD of ln-transformed NSE), using a value of 0.2 as a threshold above which parameters were deemed particularly “sensitive”. The threshold value of 0.2 was chosen in this study, based on the median value derived from the calculations of the STD of ln-transformed NSE. Methods used to separate the two flow constituents and to quantify parameter sensitivity are illustrated in Fig. 2.2.

### **2.3.5 Model evaluation**

Model goodness-of-fit was assessed graphically and quantified using Pearson product moment correlation coefficient ( $r$ ), Nash-Sutcliffe efficiency (NSE) and percent bias (PBIAS; Table 2.5). Values of  $r$  (range -1 to 1) indicate the degree of linear relationship between simulated and measured data. Values of  $r$  were deemed statistically significant for values of  $p < 0.05$  (Bewick et al., 2003). Value of NSE (range  $-\infty$  to 1) is commonly used to evaluate SWAT model performance (Gassman et al., 2007). PBIAS value indicates the average tendency of simulated outputs to be larger or smaller than observations (Gupta et al., 1999).

Model uncertainty was evaluated with two criteria: R-factor and P-factor (see Section 2.3.3). They were used to constrain parameter ranges during the calibration using measured Q and loads of SS, MINP, ORGN, NH<sub>4</sub>-N and NO<sub>3</sub>-N in the SUFI-2 procedure. The R software (R Development Core Team, 1997) was used to graphically show the 95% confidence and prediction intervals for measurement data (Neyman, 1937) and model prediction intervals (Seymour, 1993) for Q and concentrations of SS, TP and TN during the calibration period (2004–2008).

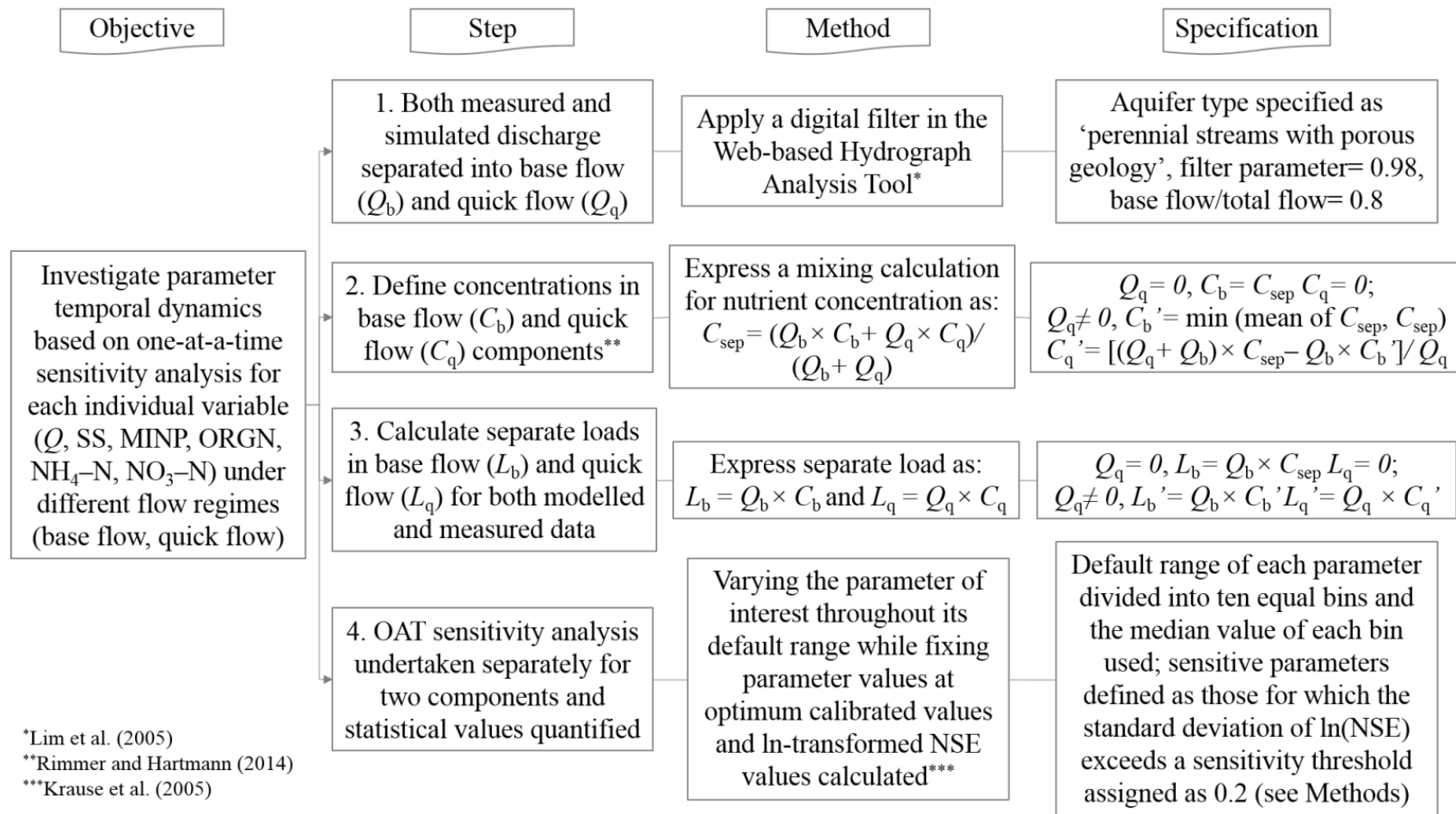


**Figure 2.2** Flow chart of methods used to separate hydrograph and contaminant loads and to quantify parameter sensitivities for:  $Q$  (discharge), SS (suspended sediment), MINP (mineral phosphorus), ORGN (organic nitrogen),  $\text{NH}_4\text{-N}$  (ammonium–nitrogen), and  $\text{NO}_3\text{-N}$  (nitrate–nitrogen). NSE: Nash–Sutcliffe efficiency.

**Table 2.5** Criteria for model performance. Note:  $o_n$  is the  $n^{\text{th}}$  observed datum,  $s_n$  is the  $n^{\text{th}}$  simulated datum,  $\bar{o}$  is the observed mean value,  $\bar{s}$  is the simulated daily mean value, and  $N$  is the total number of observed data. Performance rating criteria are based on Moriasi et al. (2007) for Q: discharge, SS: suspended sediment, TP: total phosphorus and TN: total nitrogen. Moriasi et al. (2007) derived these criteria based on extensive literature review and analysing the reported performance ratings for recommended model evaluation statistics.  $r$ : Pearson product moment correlation coefficient; NSE: Nash–Sutcliffe efficiency; PBIAS: percent bias.

Statistic equation	Constituent	Performance ratings			
		Unsatisfactory	Satisfactory	Good	Very good
$r = \frac{\sum_{n=1}^N [(o_n - \bar{o})(s_n - \bar{s})]}{\sqrt{\sum_{n=1}^N (o_n - \bar{o})^2 \times \sum_{n=1}^N (s_n - \bar{s})^2}} \quad (3)$	All	–	–	–	–
$\text{NSE} = 1 - \frac{\sum_{n=1}^N (o_n - s_n)^i}{\sum_{n=1}^N (o_n - \bar{o})^i} \quad i = 2 \quad (4)$	All	< 0.5	0.5 – 0.65	0.65 – 0.75	0.75 – 1
	Q	> 25	15 – 25	10 – 15	< 10
$\text{PBIAS}\% = \frac{\sum_{n=1}^N (o_n - s_n)}{\sum_{n=1}^N o_n} \times 100\% \quad (5)$	SS	> 55	30 – 55	15 – 30	< 15
	TP, TN	> 70	40 – 70	25 – 40	< 25

## 2.4 Results

### 2.4.1 Model performance and uncertainty

Numerous rounds (each comprising 1000 iterations) of LHS were conducted for each simulated variable until the performance criteria were satisfied. The total number of rounds of LHS for each simulated variable was as follows (number in parentheses): Q (7), SS (7), MINP (11), ORGN (10), NH<sub>4</sub>-N (4) and NO<sub>3</sub>-N (4). The parameters that provided the best statistical outcomes (i.e., best match to observed data) are given in Table 2.4. Two criteria (R-factor and P-factor) were used to show model uncertainties for simulations of discharge and contaminant loads, with values as follows: Q (0.97, 0.43), SS (0.48, 0.19), MINP (2.64, 0.14), ORGN (0.47, 0.17), NH<sub>4</sub>-N (1.16, 0.56) and NO<sub>3</sub>-N (1.2, 0.29). Model uncertainties for simulations of Q and SS, TP and TN concentrations are shown in Fig. 2.3.

Modelled and measured base flow showed high correspondence, although measured daily mean discharge during storm peaks was often underestimated (Fig. 2.4a, e). Annual mean percentages of lateral flow recharge, shallow aquifer recharge and deep aquifer recharge to total water yield were predicted by SWAT as 30%, 10%, 58%, respectively. Modelled SS concentrations overestimated measurements of monthly grab samples by an average of 18.3% during calibration and 0.32% during validation (Fig. 2.4b, f). Measured TP concentrations in monthly grab samples were underestimated by 23.8% during calibration (Fig. 2.4c) and 24.5% during validation (Fig. 2.4g). Similarly, measured TP loads were underestimated by 34.5% and 38.4%, during calibration and validation, respectively. Modelled and measured TN concentrations were generally better aligned during base flow (Fig. 2.4d), apart from a mismatch prior to 1996 when monthly measured TN concentrations were substantially lower than model predictions, although the concentrations gradually increased (Fig. 2.4h) during the validation period (1994–1997). The average measured TN load increased from 134 kg N d<sup>-1</sup> prior to 1996, to 190 kg N d<sup>-1</sup> post 1996. The comparable increase in modelled TN load was 167 kg N d<sup>-1</sup> to 205 kg N d<sup>-1</sup>, respectively.

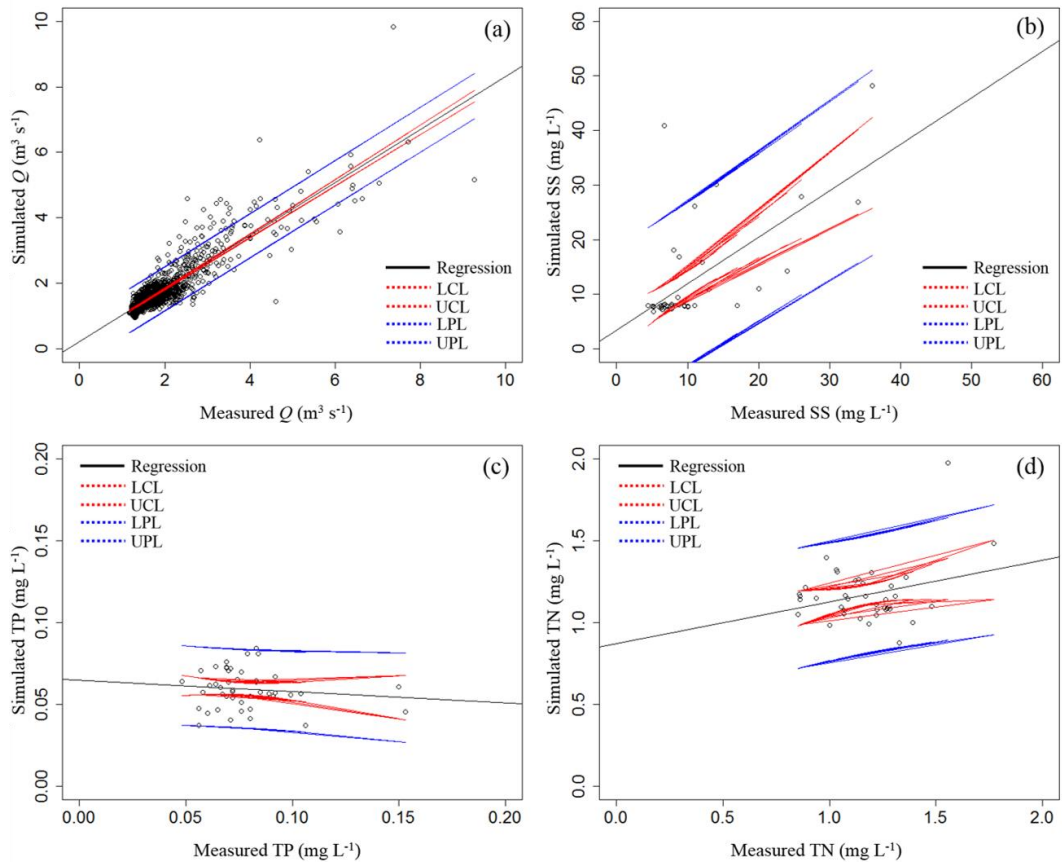


**Figure 2.3** Regression of measured and simulated (a) discharge ( $Q$ ), concentrations of (b) suspended sediment (SS), (c) total phosphorus (TP), and (d) total nitrogen (TN) including lower and upper 95% confidence limits (LCL and UCL) and lower and upper 95% prediction limits (LPL and UPL). Note that the “choppy” shape of confidence limits shown in figures b–d resulted from the few data points ( $< 50$ ) in the regressions of measured and simulated SS, TP and TN concentrations.

Statistical evaluations of goodness-of-fit are shown in Table 2.6. The  $r$  values for daily mean discharge were 0.88 for calibration ( $p < 0.001$ ) and 0.83 for validation ( $p < 0.001$ ). The NSE values for daily mean discharge were 0.73 for calibration and 0.62 for validation, corresponding to model performance ratings (cf. Moriasi et al., 2007) of “good” and “satisfactory” (Table 2.5). Positive PBIAS (7.8% for calibration and 8.8% for validation) indicated a tendency for underestimation of daily mean discharge, however, the low magnitude of PBIAS values corresponded to a performance rating of “very good”. The  $r$  values for SS were 0.65 for calibration ( $p < 0.001$ ) and 0.90 for validation ( $p < 0.001$ ). The NSE values for SS were -0.08 (unsatisfactory) for calibration and 0.76 (very good) for validation. The model did not simulate trends well for monthly measured TP and TN concentrations. The  $r$  values for TP and TN were both  $< 0.3$  ( $p > 0.05$ ) during calibration and

validation and NSE values were both  $< 0$  (unsatisfactory). Values of PBIAS corresponded to “good” or “very good” performance ratings for TP and TN.

Observed Q-weighted daily mean concentrations derived from hourly measurements and simulated daily mean concentrations of SS, TP and TN during an example two-day storm event are shown in Fig. 2.5a–c. The simulations of SS and TN concentrations were somewhat better than for TP. Comparisons of Q-weighted daily mean concentrations ( $C_{QWM}$ ) during storm events from 2010 to 2012 are shown in Fig. 2.5d–f for SS (nine events), TP and TN (both 14 events). The  $C_{QWM}$  of TP exceeded the simulated daily mean by between 0.02 and 0.2 mg P L<sup>-1</sup>, and on average, the model underestimated measurements by 69.4% (Fig. 2.5e). Although NSE value for  $C_{QWM}$  of TN was unsatisfactory (Table 2.6), it was close to the threshold for satisfactory performance (0.5), and the  $r$  value was 0.68 ( $p < 0.05$ ). For  $C_{QWM}$  of SS and TP, NSE values indicated that the model performance was unsatisfactory and negative  $r$  value for TP, although the  $r$  value was 0.61 ( $p < 0.05$ ) for SS. The PBIAS value of -0.87 for  $C_{QWM}$  of TN corresponded to model performance ratings of “very good”, while the PBIAS values for  $C_{QWM}$  of SS and TP were 43.9 and 69.4, respectively, indicating satisfactory model performance.

Measured and simulated discharge and contaminant loads separated for the two flow regimes (base flow and quick flow) are shown in Fig. 2.6. Model performance statistics differed between the two flow regimes (Table 2.7). Simulations of discharge and constituent loads under quick flow were more closely related to the measurements (i.e., higher values of  $r$  and NSE) than simulations under base flow. Base flow TN load simulations during the validation period showed better model performance than simulations under quick flow. Additionally, measurements under quick flow were better reproduced by the model than the measurements for the whole simulation period. Simulations of contaminant loads matched measurements much better than for contaminant concentrations, as indicated by statistical values for model performance given in Table 2.6 and 2.7.

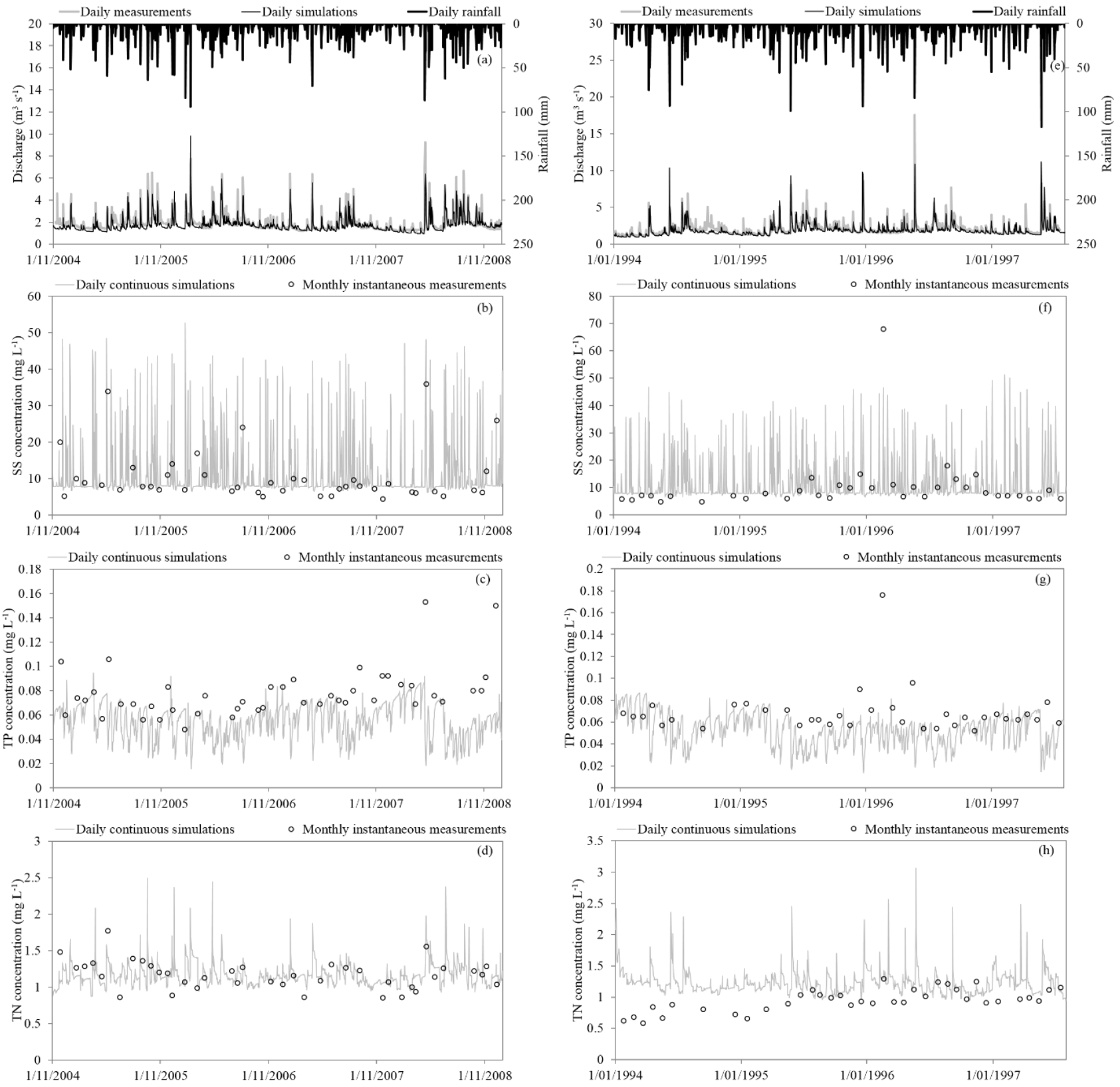


**Figure 2.4** Measurements and daily mean simulated values of discharge, suspended sediment (SS), total phosphorus (TP) and total nitrogen (TN) during calibration (a–d) and validation (e–h). Measured daily mean discharge was calculated from 15-min observations and measured concentrations of SS, TP and TN correspond to monthly grab samples.

**Table 2.6** Model performance ratings for simulations of discharge (Q), concentrations of suspended sediment (SS), total phosphorus (TP) and total nitrogen (TN). n indicates the number of measurements. Q-weighted mean concentrations were calculated using Eq. (1). *r*: Pearson product moment correlation coefficient; NSE: Nash–Sutcliffe efficiency; PBIAS: percent bias. The significance of correlations between simulations and measurements was quantified based on the *p* value (see Section 2.3.5). \**p* < 0.05; \*\**p* < 0.01; \*\*\**p* < 0.001.

Model performance	Statistics	Q	SS	TP	TN
Calibration with instantaneous measurements (2004–2008)		n = 1439	n = 43	n = 45	n = 39
	<i>r</i>	0.88***	0.65***	-0.12	0.28
	NSE	0.73 (Good)	-0.08 (Unsatisfactory)	-1.31 (Unsatisfactory)	-0.30 (Unsatisfactory)
	±PBIAS%	7.8 (Very good)	-18.3 (Very good)	23.8 (Very good)	-0.05 (Very good)
Validation with instantaneous measurements (1994–1997)		n = 1294	n = 37	n = 37	n = 36
	<i>r</i>	0.83***	0.90***	0.10	-0.09
	NSE	0.62 (Satisfactory)	0.76 (Very good)	-0.97 (Unsatisfactory)	-2.67 (Unsatisfactory)
	±PBIAS%	8.8 (Very good)	-0.32 (Very good)	24.5 (Very good)	-26.7 (Good)
Validation with Q-weighted mean measurements (2010–2012)		–	n = 12	n = 18	n = 18
	<i>r</i>	–	0.61*	-0.24	0.68*
	NSE	–	-0.03 (Unsatisfactory)	-4.88 (Unsatisfactory)	0.42 (Unsatisfactory)
	±PBIAS%	–	43.9 (Satisfactory)	69.4 (Satisfactory)	-0.87 (Very good)

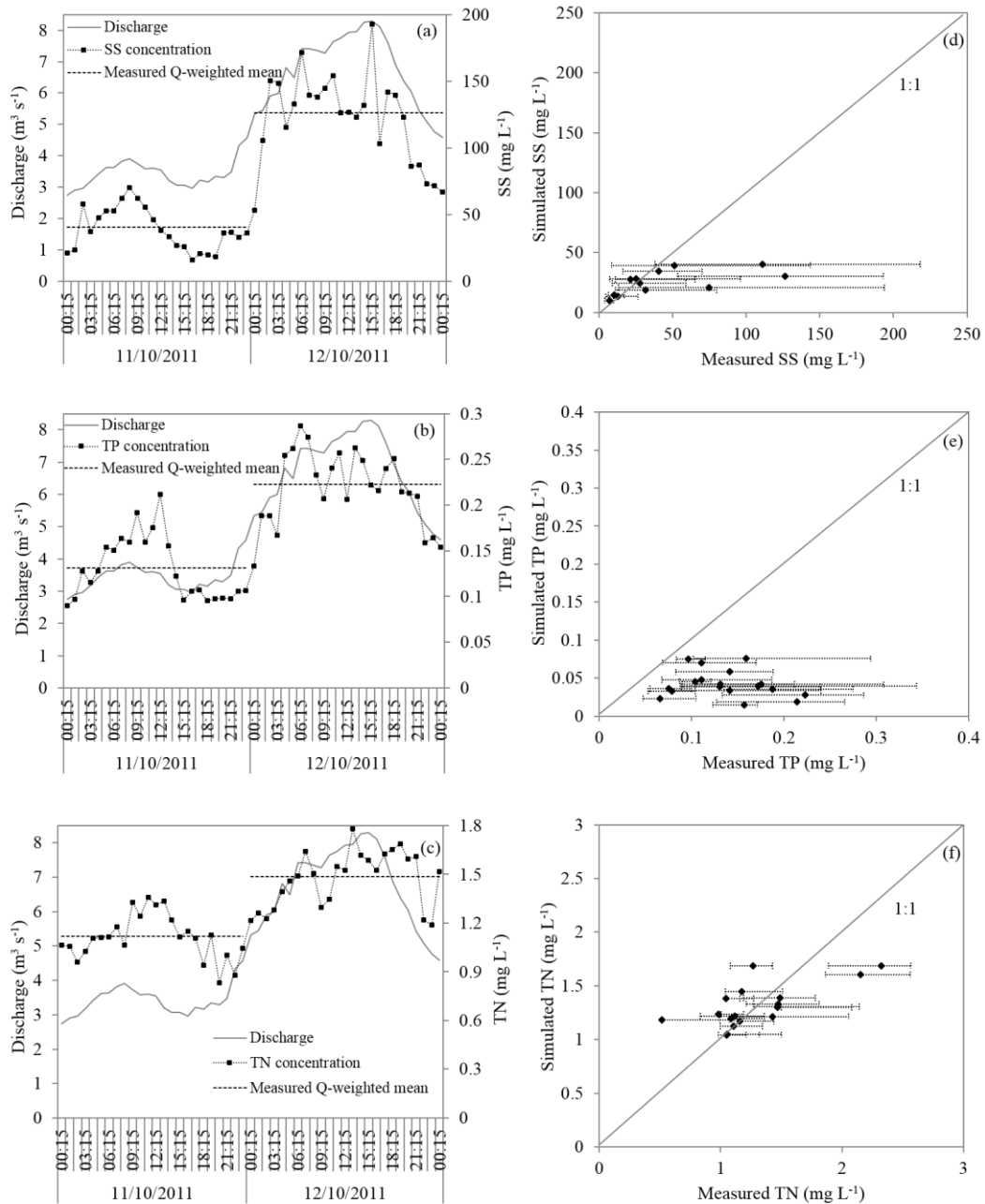


**Figure 2.5** Example of a storm event showing derivation of discharge (Q)-weighted daily mean concentrations (dashed horizontal line) based on hourly measured concentrations (black dots) of suspended sediment (SS), total phosphorus (TP) and total nitrogen (TN) over two days (a–c). Comparisons of Q-weighted daily mean concentrations with simulated daily mean estimates of SS, TP and TN (scatter plot, d–f). The horizontal bars show the ranges in hourly measurements during each storm event in 2010–2012.

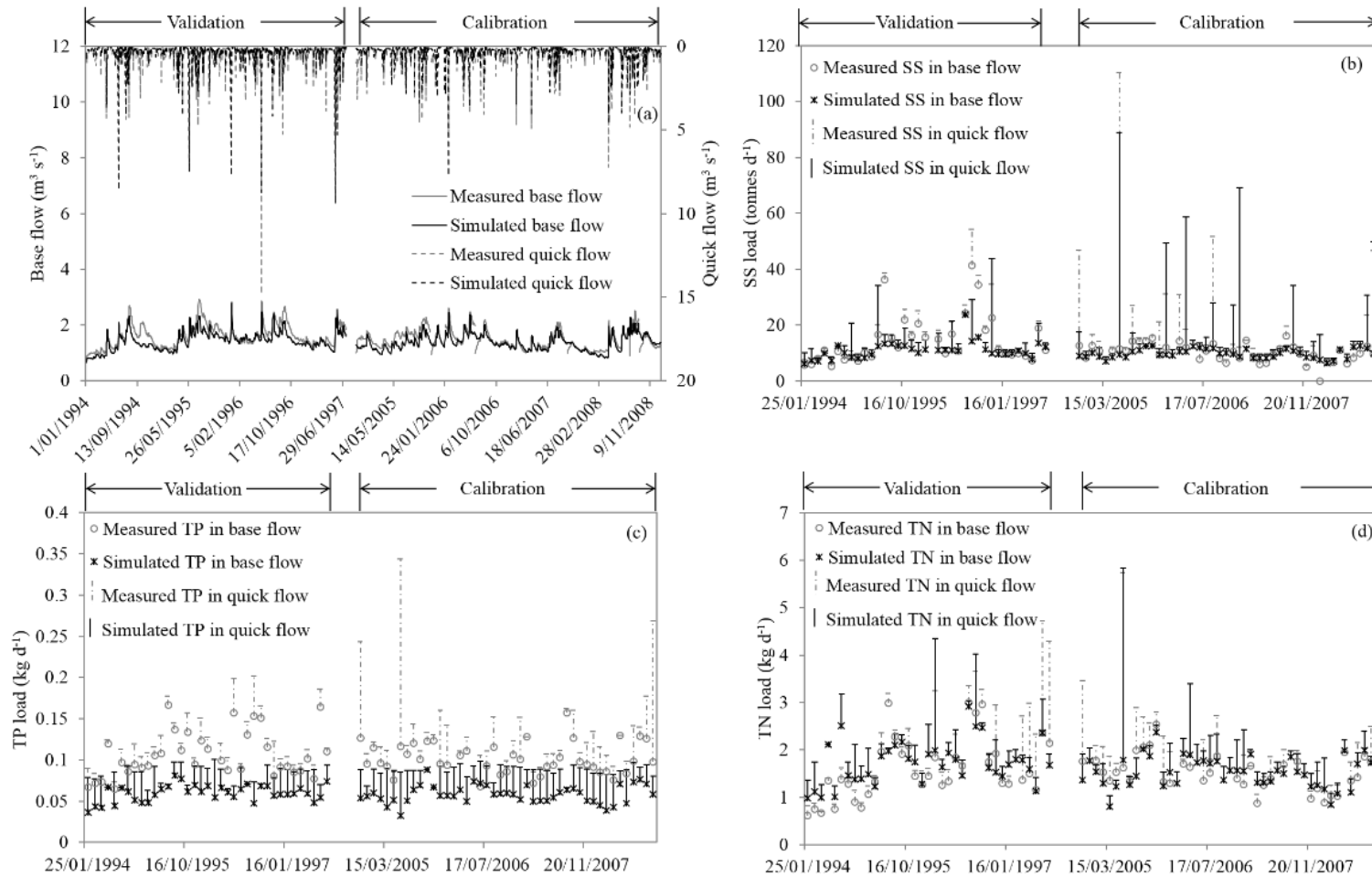


**Figure 2.6** Measurements and simulations derived using the calibrated set of parameter values. Data are shown separately for base flow and quick flow. (a) Daily mean base flow and quick flow; (b) suspended sediment (SS) load; (c) total phosphorus (TP) load; (d) total nitrogen (TN) load. Vertical lines in b–d show the contaminant load in quick flow. Time series relate to calibration (2004–2008) and validation (1994–1997) periods (note time discontinuity). Measured instantaneous loads of SS, TP, and TN correspond to monthly grab samples.

**Table 2.7** Model performance statistics for simulations of discharge (Q), and loads of suspended sediment (SS), total phosphorus (TP) and total nitrogen (TN). Statistics were calculated for both overall and separated simulations.  $Q_{all}$  and  $L_{all}$  indicate the overall simulations;  $Q_b$  and  $L_b$  indicate the base flow simulations;  $Q_q$  and  $L_q$  indicate the quick flow simulations.  $r$ : Pearson product moment correlation coefficient; NSE: Nash–Sutcliffe efficiency; PBIAS: percent bias. The significance of correlations between simulations and measurements was quantified based on the  $p$  value (see Section 2.3.5). \* $p < 0.05$ ; \*\* $p < 0.01$ ; \*\*\* $p < 0.001$ .

Model performance	Statistics	Q			SS			TP			TN		
		$Q_b$	$Q_q$	$Q_{all}$	$L_b$	$L_q$	$L_{all}$	$L_b$	$L_q$	$L_{all}$	$L_b$	$L_q$	$L_{all}$
Calibration (2004– 2008)	$r$	0.84***	0.84***	0.88***	0.66***	0.68***	0.61***	0.24	0.65***	0.39**	0.72***	0.97***	0.95***
	NSE	0.6	0.71	0.73	0.33	0.33	0.27	-6.2	0.09	-0.17	0.5	0.89	0.85
	$\pm$ PBIAS%	7.5	8.7	7.8	7.57	-23.4	-3.6	45.4	40.1	43.6	0.8	6.6	2.7
Validation (1994– 1997)	$r$	0.87***	0.81***	0.83***	0.36*	0.98***	0.95***	0.27	0.27	0.06	0.79***	0.33*	0.58***
	NSE	0.56	0.62	0.62	-0.03	0.43	0.85	-1.9	0.04	-0.64	0.58	-0.07	0.33
	$\pm$ PBIAS%	11.3	-1.2	8.8	34.5	-79.7	11.1	45.8	-9.3	37	-7.6	14.3	-2.5

## 2.4.2 Separated parameter sensitivity

Based on the ranking of relative sensitivities of hydrological and water quality parameters derived from the SUFI-2 procedure (see Table 2.8), the OAT sensitivity analysis undertaken separately for base flow and quick flow identified three parameters that most influenced the quick flow estimates, and five parameters that most influenced the base flow estimates (parameters above the dashed line in Fig. 2.7a). Channel hydraulic conductivity (CH\_K2) is used to estimate the peak runoff rate (Lane, 1983). Lateral flow slope length (SLSOIL) and lateral flow travel time (LAT\_TIME) have an important controlling effect on the amount of lateral flow entering the stream reach during quick flow. Both slope (HRU\_SLP) and soil available water content (SOL\_AWC) were particularly sensitive for the base flow simulation because they affect lateral flow within the kinematic storage model in SWAT (Sloan and Moore, 1984). The aquifer percolation coefficient (RCHRG\_DP) and the base flow alpha factor (ALPHA\_BF) strongly influenced base flow calculations (Sangrey et al., 1984), as did the channel Manning's n value (CH\_N2) which is used to estimate channel flow (Chow, 2008).

For SS loads, 12 and four parameters, respectively, were identified as sensitive in relation to the simulations of base flow and quick flow (parameters above the dashed line in Fig. 2.7b). Parameters that control main channel processes (e.g., CH\_K2 and CH\_N2) and subsurface water transport processes (e.g., LAT\_TIME and SLSOIL) were found to be much more sensitive for base flow SS load estimations. Exclusive parameters for SS estimations, such as SPCON (linear parameter), PRF (peak rate adjustment factor), SPEXP (exponent parameter), CH\_COV1 (channel erodibility factor), and CH\_COV2 (channel cover factor) were found to be much more sensitive in base flow SS load, while LAT\_SED (SS concentration in lateral flow and groundwater flow) was more sensitive in quick flow SS load. Parameters that control overland processes, e.g., CN2 (the curve number), OV\_N (overland flow Manning's n value) and SLSUBBSN (sub-basin slope length), were found to be much more sensitive for quick flow SS load estimations.

Of the sensitive parameters, BC4 (ORGP mineralisation rate) was particularly sensitive for the simulation of base flow MINP load (Fig. 2.7c). RCN (nitrogen concentration in rainfall) related specifically to the dynamics of the base flow NO<sub>3</sub>-N load and NPERCO (nitrogen percolation coefficient) significantly affected quick flow NO<sub>3</sub>-N load (Fig. 2.7d). Parameter CH\_ONCO (channel ORGN concentration) similarly affected both flow components of ORGN load (Fig. 2.7e) and SOL\_CBN (organic carbon content) was most sensitive for the simulations of quick flow ORGN and NH<sub>4</sub>-N loads. Parameter BC1 (nitrification rate in reach) was particularly sensitive for the simulation of base flow NH<sub>4</sub>-N load (Fig. 2.7f).

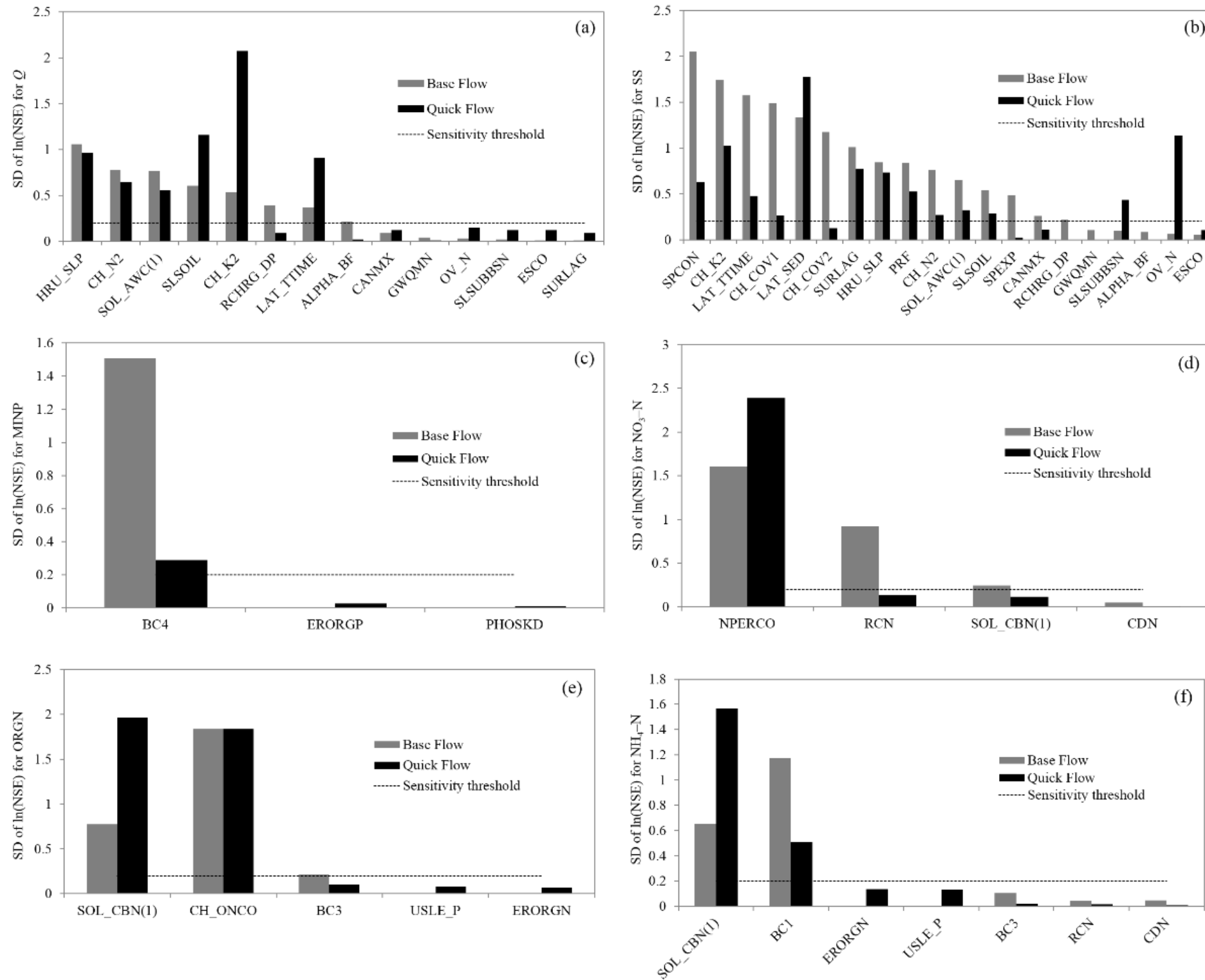


**Figure 2.7** The standard deviation (STD) of the ln-transformed Nash-Sutcliffe efficiency (NSE) used to indicate parameter sensitivity based on one-at-a-time (OAT) sensitivity analysis for separate base and quick flow components: (a) Q (discharge); (b) SS (suspended sediment); (c) MINP (mineral phosphorus); (d) NO<sub>3</sub>-N (nitrate-nitrogen); (e) ORGN (organic nitrogen); (f) NH<sub>4</sub>-N (ammonium-nitrogen). A median value (0.2) derived from the STD of ln-transformed NSE was chosen as a threshold above which parameters were deemed to be “sensitive”. Definitions of each parameter are shown in Table 2.4.

**Table 2.8** Rankings of relative sensitivities of parameters (from most to least) for variables (header row) of Q (discharge), SS (suspended sediment), MINP (mineral phosphorus), ORGN (organic nitrogen), NH<sub>4</sub>-N (ammonium–nitrogen), and NO<sub>3</sub>-N (nitrate–nitrogen). Relative sensitivities were identified by randomly generating combinations of values for model parameters and comparing modelled and measured data with a Student’s t test ( $p \leq 0.05$ ). Bold text denotes that a parameter was deemed sensitive relative to more than one simulated variable. Shaded text denotes that parameter deemed insensitive to any of the two flow components (base and quick flow; see Figure 2.7) using one–at–a–time sensitivity analysis. Definitions and units for each parameter are shown in Table 2.4.

Q	SS	MINP	ORGN	NH <sub>4</sub> -N	NO <sub>3</sub> -N
<b>SLSOIL</b>	LAT_SED	<b>CH_OPCO</b>	<b>CH_ONCO</b>	<b>CH_ONCO</b>	NPERCO
<b>CH_K2</b>	CH_N2	BC4	BC3	BC1	<b>CDN</b>
HRU_SLP	SLSUBBSN	<b>RS5</b>	SOL_CBN(1)	<b>CDN</b>	<b>ERORGN</b>
<b>LAT_TTIME</b>	SPCON	ERORGP	<b>RS4</b>	<b>RS3</b>	<b>CMN</b>
<b>SOL_AWC(1)</b>	ESCO	<b>PPERCO</b>	<b>RCN</b>	<b>RCN</b>	<b>RCN</b>
RCHRG_DP	OV_N	<b>RS2</b>	<b>N_UPDIS</b>		<b>RSDCO</b>
GWQMN	<b>SLSOIL</b>	PHOSKD	USLE_P		
<b>GW_REVAP</b>	<b>LAT_TTIME</b>	<b>GWSOLP</b>	<b>SDNCO</b>		
<b>GW_DELAY</b>	<b>SOL_AWC(1)</b>	<b>LAT_ORGP</b>	<b>SOL_NO3(1)</b>		
<b>CH_COV1</b>	<b>EPCO</b>		<b>CMN</b>		
<b>CH_COV2</b>	<b>CANMX</b>		<b>HLIFE_NGW</b>		
<b>EPCO</b>	<b>CH_K2</b>		<b>RSDCO</b>		
<b>SPEXP</b>	<b>GW_DELAY</b>		<b>USLE_K(1)</b>		
<b>CANMX</b>	ALPHA_BF				
<b>CH_N1</b>	<b>GW_REVAP</b>				
<b>PRF</b>	<b>CH_COV1</b>				
SURLAG					

## **2.5 Discussion**

This study examined temporal dynamics of model performance and parameter sensitivity in a SWAT model application that was configured for a small, relatively steep and lower order stream catchment in New Zealand. This country faces increasing pressures on freshwater resources (Parliamentary Commissioner for the Environment, 2013) and models such as SWAT potentially offer valuable tools to inform management of water resources although, to date, the SWAT model has received limited consideration in New Zealand (Cao et al., 2006). Model evaluation on the basis of the data collected during an extended monitoring programme enabled a detailed examination of how model performance varied during different flow regimes. It also permitted error in daily mean estimates of contaminant loads to be quantified with relative precision, allowing assessment of the ability of the SWAT model to simulate contaminant loads during storm events when lower-order streams typically exhibit considerable sub-daily variability in both discharge and contaminant concentrations (Zhang et al., 2010). Separating discharge and loads of sediments and nutrients into those associated with base flow and quick flow for separate OAT sensitivity analyses provided important insights into the varying dependency of parameter sensitivity on hydrologic conditions.

### **2.5.1 Temporal dynamics of model performance**

The modelled estimates of deep aquifer recharge (58%) and combined lateral flow and shallow aquifer recharge (40%) were comparable with estimates derived by Rutherford et al. (2011), who used an alternative catchment model to derive respective estimates of 30% and 70% for these two fluxes. Our decision to deliberately select a validation period (1994–1997) during which the boundary conditions of the system (specifically anthropogenic nutrient loading) differed considerably from the calibration period allowed us to rigorously assess the capability of SWAT to accurately predict water quality under an altered management scenario (i.e., the purpose of most SWAT applications).

Overestimation of TN concentrations prior to 1996 reflects higher  $\text{NO}_3\text{-N}$  concentrations in groundwater during the calibration period (2004–2008) due to the wastewater irrigation operation. Nitrate concentrations appeared to reach a new quasi-steady state as wastewater loads and in-stream attenuation came into balance.

SWAT may not adequately represent the dynamics of groundwater nutrient concentrations (Bain et al., 2012) particularly in the presence of changes in catchment inputs (e.g., with start-up of wastewater irrigation). The groundwater delay parameter was set to five years (cf. Rotorua District Council, 2006), but this did not appear to capture adequately the lag in response to increases in stream nitrate concentrations following wastewater irrigation from 1991.

The poor fit between simulated daily mean TP concentrations and monthly instantaneous measurements may partly reflect a mismatch between the dominant processes affecting phosphorus cycling in the stream and those represented in SWAT. The ORGP fraction that is simulated in SWAT includes both organic and inorganic forms of particulate phosphorus, however, the representation of particulate phosphorus cycling only focusses on organic phosphorus cycling, with limited consideration of interactions between inorganic streambed sediments and dissolved reactive phosphorus in the overlying water (White et al., 2014). This contrasts with phosphorus cycling in the study stream where it has been shown that dynamic sorption processes between the dissolved and particulate inorganic phosphorus pools exert major control on phosphorus cycling (Abell and Hamilton, 2013).

Our finding that measured Q-weighted mean concentrations ( $C_{QWM}$ ) of TP and SS during storm events (2010–2012) were greatly underestimated relative to simulated daily mean TP and SS concentrations has important implications for studies that examine effects of altered flow regimes on contaminant transport. For example, studies which simulate scenarios comprising more frequent large rainfall events (associated with climate change predictions for many regions; IPCC, 2013) may considerably underestimate projected future loads of SS and associated particulate nutrients if only base flow water quality measurements (i.e., those predominantly collected during “state of environment” monitoring) are used for calibration/validation (see Radcliffe et al., 2009 for a discussion of this issue in relation to phosphorus). This is also reflected by the model performance statistics relating to validation of modelled SS concentrations using monthly grab samples (predominantly base flow; “very good”) and  $C_{QWM}$  estimated during storm sampling (“unsatisfactory”) based on NSE values.

### 2.5.2 Key uncertainties

Model uncertainty in this study may arise from four main factors: 1) model parameters; 2) forcing data; 3) measurements used for evaluation of model fit, and; 4) model structure or algorithms that represent the catchment (Lindenschmidt et al., 2007). The values of most parameters assigned for model calibration, although specific to different soil types (e.g., soil parameters), were lumped across land uses and slopes in this study. They integrated spatial and temporal variations, thus neglecting any variability throughout the study catchment during a study period. Furthermore, the “assumed” steady state after the one-year model warm-up might not have been reached. In terms of forcing data, the assumption of constant values of spring discharge rate and nutrient concentrations may inadequately reflect the temporal variability and therefore increase model uncertainty, although this should contribute little to the model error term.

Most water quality data used for model calibration comprised monthly instantaneous samples taken during base flow conditions. The use of those measurements for model calibration would likely lead to considerable underestimation of constituent concentrations (notably SS and TP) due to failure to account for short-duration high flow events. The disparity in goodness-of-fit statistics between discharge (typically “good” or “very good”) and nutrient variables (often “unsatisfactory”) highlights the potential for catchment models which inadequately represent contaminant cycling processes (manifest in unsatisfactory concentration estimates) to nevertheless produce satisfactorily load predictions (e.g., compare model performance statistics for prediction of nutrient concentrations in Table 2.6 with statistics for prediction of loads in Table 2.7). This highlights the potential for model uncertainty to be underestimated in studies which aim to predict the effects of scenarios associated with changes in contaminant cycling, such as increases in fertiliser application rates.

Inadequate representation of groundwater processes in the model structure is another key factor that is likely to affect model uncertainty, particularly for nitrogen simulations. The analysis of model performance based on datasets separated into base flow and quick flow constituents enabled uncertainties in the structure of hydrological models to be identified, denoted by different model performance between these two flow constituents.

### 2.5.3 Temporal dynamics of parameter sensitivity

To date, studies of temporal variability in parameters have focused on hydrological parameters, rather than on water quality parameters. The characteristics of concentration–discharge relationships for SS and TP are different to that for TN (Abell et al., 2013). In quick flow, there is a positive relationship between Q and concentrations of SS and TP, reflecting mobilisation of sediments and associated particulate P. Total nitrogen concentrations declined slightly in quick flow, reflecting the dilution of nitrate from surface runoff. Defining separate contaminant concentrations in base flow and quick flow enabled us to examine how the sensitivity of water quality parameters varied depending on hydrologic conditions.

In a study of a lowland catchment (481 km<sup>2</sup>), Guse et al. (2014) found that three groundwater parameters, RCHRG\_DP (aquifer percolation coefficient), GW\_DELAY (groundwater delay) and ALPHA\_BF (base flow alpha factor) were highly sensitive in relation to simulating discharge during quick flow, while ESCO (soil evaporation compensation factor) was most sensitive during base flow. This is counter to the findings of this study for which the base–flow discharge simulation was sensitive to RCHRG\_DP and ALPHA\_BF. This result may reflect that, relative to our study catchment, the catchment studied by Guse et al. (2014) had moderate precipitation (884 mm yr<sup>-1</sup>) with less forest cover and flatter topography. Although the GW\_DELAY parameter reflects the time lag that it takes water in the soil water to enter the shallow aquifers, its lack of sensitivity under both base flow and quick flow conditions in this study is a reflection of higher water infiltration rates and steeper slopes. The ESCO parameter controls the upwards movement of water from lower soil layers to meet evaporative demand (Neitsch et al., 2011). Its lack of sensitivity in our study may reflect relatively high and seasonally–consistent rainfall (1500 mm yr<sup>-1</sup>), in addition to extensive forest cover in the Puarenga Stream catchment, which reduces soil evaporative demand by shading. Soil texture is also likely a contributor to this result. The predominant soil horizon type in the Puarenga Stream catchment was “A” (referring to “topsoil”), indicating high macroporosity which promotes high water infiltration rate and inhibits upward transport of water by capillary action (Neitsch et al., 2011). The variability in the sensitivity of the parameter SURLAG (surface runoff lag coefficient) between this study (relatively insensitive) and that of Cibin et al. (2010; relatively sensitive) likely reflects

differences in catchment size. The Puarenga Stream catchment (77 km<sup>2</sup>) is much smaller than the study catchment (St Joseph River; 2800 km<sup>2</sup>) of Cibin et al. (2010) and, consequently, distances to the main channel are much shorter, with less potential for attenuation of surface runoff in off-channel storage sites. The curve number (CN2) parameter was found to be insensitive in both this study and Shen et al. (2012), because surface runoff was simulated based on the Green and Ampt method (1911) requiring the hourly rainfall inputs, rather than the curve number equation which is an empirical model. By contrast, the most sensitive parameters in our study are those that determine the extent of lateral flow, an important contributor to streamflow in the catchment, due to a general lack of ground cover under plantation trees and formation of gully networks on steep terrain.

Parameters that control surface water transport processes (e.g., LAT\_TIME and SLSOIL) were found to be much more sensitive for base flow SS load estimation than parameters that control groundwater processes (e.g., ALPHA\_BF and RCHRG\_DP), reflecting the importance of surface flow processes for sediment transport. Sensitive parameters for quick flow SS load estimation related to overland flow processes (e.g., OV\_N and SLSUBBSN), thus reflecting the fact that sediment transport is largely dependent on rainfall-driven processes, as is typical of steep and lower-order catchments. Modelled base flow NO<sub>3</sub>-N loads were most sensitive to the nitrogen concentration in rainfall (RCN) because of rainfall as a predominant contributor to recharging base flow. The nitrogen percolation coefficient (NPERCO) was more influential for quick flow NO<sub>3</sub>-N load estimation, probably indicating that the quick flow NO<sub>3</sub>-N load is more influenced by the mobilisation of concentrated nitrogen sources associated with agriculture or treated wastewater distribution. High sensitivity of the organic carbon content (SOL\_CBN) for quick flow ORGN load estimates likely reflects mobilisation of N associated with organic material following rainfall. The finding that base flow NH<sub>4</sub>-N load was more sensitive to nitrification rate in reach (BC1) likely reflects that base flow provides more favourable conditions to complete this oxidation reaction, as NH<sub>4</sub>-N is less readily leached and transported. Similarly, the ORGP mineralisation rate (BC4) strongly influenced base flow MINP load estimation, reflecting that base flow phosphorus transport is relatively more influenced by cycling from channel bed stores, whereas quick flow phosphorus transport predominantly reflects the transport of phosphorus that originated from sources distant from the channel.

## 2.6 References

- Abbaspour, K.C.: Swat–Cup4: SWAT Calibration and Uncertainty Programs Manual Version 4, Department of Systems Analysis, Integrated Assessment and Modelling (SIAM), Eawag, Swiss Federal Institute of Aquatic Science and Technology, Duebendorf, Switzerland, 106 pp., 2014.
- Abbaspour, K.C., Johnson, C.A., and van Genuchten, M.T.H.: Estimating uncertain flow and transport parameters using a sequential uncertainty fitting procedure, *Vadose Zone J.*, 3, 1340–1352, 2004.
- Abbaspour, K.C., Yang, J., Maximov, I., Siber, R., Bogner, K., Mieleitner, J., Zobrist, J., and Srinivasan, R.: Modelling hydrology and water quality in the pre–alpine/alpine Thur watershed using SWAT, *J. Hydrol.*, 333, 413–430, 2007.
- Abell, J.M. and Hamilton, D.P.: Bioavailability of phosphorus transported during storm flow to a eutrophic polymictic lake, *New Zeal. J. Mar. Fresh.*, 47, 481–489, 2013.
- Abell, J.M., Hamilton, D.P., and Rutherford, J.C.: Quantifying temporal and spatial variations in sediment, nitrogen and phosphorus transport in stream inflows to a large eutrophic lake, *Environ. Sci.: Processes Impacts*, 15, 1137–1152, 2013.
- Arnold, J.G., Srinivasan, R., Muttiah, R.S., and Williams, J.R.: Large area hydrologic modeling and assessment Part I: Model development, *J. Am. Water Resour. As.*, 34, 73–89, 1998.
- Bain, D.J., Green, M.B., Campbell, J.L., Chamblee, J.F., Chaoka, S., Fraterrigo, J.M., Kaushal, S.S., Martin, S.L., Jordan, T.E., and Parolari, A.J.: Legacy effects in material flux: structural catchment changes predate long–term studies, *BioScience*, 62, 575–584, 2012.
- Bewick, V., Cheek, L., and Ball, J.: Statistics review 7: correlation and regression, *Crit. Care*, 7, 451–459, 2003.
- Bi, H.Q., Long, Y.S., Turner, J., Lei, Y.C., Snowdon, P., Li, Y., Harper, R., Zerihun, A., and Ximenes, F.: Additive prediction of aboveground biomass for *Pinus radiata* (D. Don) plantations, *Forest Ecol. Manag.*, 259, 2301–2314, 2010.
- Bieroza, M.Z., Heathwaite, A.L., Mullinger, N.J., and Keenan, P.O.: Understanding nutrient biogeochemistry in agricultural catchments: the challenge of appropriate monitoring frequencies, *Environ. Sci.: Processes Impacts*, 16, 1676–1691, 2014.
- Boyle, D.P., Gupta, H.V., and Sorooshian, S.: Toward improved calibration of hydrologic models: Combining the strengths of manual and automatic methods, *Water Resour. Res.*, 36, 3663–3674, 2000.
- Brigode, P., Oudin, L., and Perrin, C.: Hydrological model parameter instability: A source of additional uncertainty in estimating the hydrological impacts of climate change?, *J. Hydrol.*, 476, 410–425, 2013.

- Cao, W., Bowden, W.B., Davie, T., and Fenemor, A.: Multi-variable and multi-site calibration and validation of SWAT in a large mountainous catchment with high spatial variability, *Hydrol. Process.*, 20, 1057–1073, 2006.
- Chiwa, M., Ide, J., Maruno, R., Higashi, N., and Otsuki, K.: Effects of storm flow samplings on the evaluation of inorganic nitrogen and sulfate budgets in a small forested watershed, *Hydrol. Process.*, 24, 631–640, 2010.
- Choi, H.T. and Beven, K.J.: Multi-period and multi-criteria model conditioning to reduce prediction uncertainty in an application of TOPMODEL within the GLUE framework, *J. Hydrol. (NZ)*, 332, 316–336, 2007.
- Chow, V.T.: *Open-channel hydraulics*, Blackburn Press, Caldwell, New Jersey, 728 pp., 2008.
- Cibin, R., Sudheer, K.P., and Chaubey, I.: Sensitivity and identifiability of stream flow generation parameters of the SWAT model, *Hydrol. Process.*, 24, 1133–1148, 2010.
- Conan, C., Bouraoui, F., Turpin, N., de Marsily, G., and Bidoglio, G.: Modelling flow and nitrate fate at catchment scale in Brittany (France), *J. Environ. Qual.*, 32, 2026–2032, 2003.
- Dairying Research Corporation, AgResearch, Fert Research: Fertiliser use on New Zealand Dairy Farms, In *New Zealand Fertiliser Manufacturers' Research Association*, Roberts, A.H.C. and Morton, J.D. (eds), Auckland, New Zealand, 36 pp., 1999.
- Eckhardt, K. and Arnold, J.G.: Automatic calibration of a distributed catchment model, *J. Hydrol.*, 251, 103–109, 2001.
- Ekanayake, J. and Davie, T.: The SWAT model applied to simulating nitrogen fluxes in the Motueka River catchment, *Landcare Research ICM Report 2004–05/04*, Landcare Research, Lincoln, New Zealand, 18 pp., 2005.
- Environment Bay of Plenty: Historical data summary, Report prepared for Bay of Plenty Regional Council, New Zealand, 522 pp., 2007.
- Fert Research: Fertiliser Use on New Zealand Sheep and Beef Farms, In *New Zealand Fertiliser Manufacturers' Research Association*, Balance, J.M. and Ravensdown, A.R. (eds), Newmarket, Auckland, New Zealand, 52 pp., 2009.
- Gassman, P.W., Reyes, M.R., Green, C.H., and Arnold, J.G.: The Soil and Water Assessment Tool: Historical development, applications, and future research directions, *T. ASABE*, 50, 1211–1250, 2007.
- Glover, R.B.: Rotorua Chemical Monitoring to June 1993, GNS Client Report prepared for Bay of Plenty Regional Council, #722305.14, Bay of Plenty Regional Council, New Zealand, 38 pp., 1993.
- Green, W.H. and Ampt, G.A.: Studies on soil physics, part I – the flow of air and water through soils, *J. Agr. Sci.*, 4, 1–24, 1911.

- Gupta, H.V., Sorooshian, S., and Yapo, P.O.: Status of automatic calibration for hydrologic models: Comparison with multilevel expert calibration, *J. Hydrol. Eng.*, 4, 135–143, 1999.
- Guse, B., Reusser, D.E., and Fohrer, N.: How to improve the representation of hydrological processes in SWAT for a lowland catchment–temporal analysis of parameter sensitivity and model performance, *Hydrol. Process.*, 28, 2651–2670, 2014.
- Hall, G.M.J., Wiser, S.K., Allen, R.B., Beets, P.N., and Goulding, C.J.: Strategies to estimate national forest carbon stocks from inventory data: the 1990 New Zealand baseline, *Glob. Change Biol.*, 7, 389–403, 2001.
- Hopmans, P. and Elms, S.R.: Changes in total carbon and nutrients in soil profiles and accumulation in biomass after a 30–year rotation of *Pinus radiata* on podzolised sands: Impacts of intensive harvesting on soil resources, *Forest Ecol. Manag.*, 258, 2183–2193, 2009.
- IPCC: Climate Change 2013: The Physical Science Basis. Contribution of Working Group I to the Fifth Assessment Report of the Intergovernmental Panel on Climate Change. Stocker, T.F., Qin, D., Plattner, G.K., Tignor, M., Allen, S.K., Boschung, J., Nauels, A., Xia, Y., Bex, V., and Midgley, P.M. (eds), Cambridge University Press, Cambridge, United Kingdom and New York, NY, USA, 1535 pp., 2013.
- Jowett, I.: Instream habitat and minimum flow requirements for the Waipa Stream, Ian Jowett Consulting Client report: IJ0703, Report prepared for Rotorua District Council, Rotorua, New Zealand, 31 pp., 2008.
- Kirschbaum, M.U.F. and Watt, M.S.: Use of a process–based model to describe spatial variation in *Pinus radiata* productivity in New Zealand, *Forest Ecol. Manag.*, 262, 1008–1019, 2011.
- Krause, P., Boyle, D.P., and Bäse, F.: Comparison of different efficiency criteria for hydrological model assessment, *Advances in Geosciences*, 5, 89–97, 2005.
- Kusabs, I. and Shaw, W.: An ecological overview of the Puarenga Stream with particular emphasis on cultural values: prepared for Rotorua District Council and Environment Bay of Plenty, Rotorua, New Zealand, 42 pp., 2008.
- Lane, L.J.: Chapter 19: Transmission Losses, In Soil Conservation Service, National engineering handbook, section 4: hydrology, U.S. Government Printing Office, Washington, D.C., 19-1–19-21, 1983.
- Ledgard, S. and Thorrold, B.: Nitrogen Fertiliser Use on Waikato Dairy Farms, AgResearch and Dexcel, New Zealand, 5 pp., 1998.
- Lim, K.J., Engel, B.A., Tang, Z., Choi, J., Kim, K., Muthukrishnan, S., and Tripathy, D.: Automated Web GIS–based Hydrograph Analysis Tool, WHAT, *J. Am. Water Resour. As.*, 41, 1407–1416, 2005.
- Lindenschmidt, K., Fleischbein, K., and Baborowski, M.: Structural uncertainty in a river water quality modelling system, *Ecol. Model.*, 204, 289–300, 2007.

- Lowe, A., Gielen, G., Bainbridge, A., and Jones, K.: The Rotorua Land Treatment Systems after 16 years, In *New Zealand Land Treatment Collective–Proceedings for 2007 Annual Conference*, Rotorua, 14–16 March 2007, pp. 66–73, 2007.
- Mahon, W.A.J.: The Rotorua geothermal field: technical report of the Geothermal Monitoring Programme, 1982–1985, Ministry of Energy, Oil and Gas Division, Wellington, New Zealand, 522 pp., 1985.
- Marino, S., Hogue, I.B., Ray, C.J., and Kirschner, D.E.: A methodology for performing global uncertainty and sensitivity analysis in systems biology, *J. Theor. Biol.*, 254, 178–196, 2008.
- McKenzie, B.A., Kemp, P.D., Moot, D.J., Matthew, C., and Lucas, R.J.: Environmental effects on plant growth and development, In *New Zealand Pasture and Crop Science*, White, J.G.H. and Hodgson, J. (eds), Oxford University Press: Auckland, New Zealand, pp. 29–44, 1999.
- Monteith, J.L.: Evaporation and the environment. In the state and movement of water in living organisms, 19<sup>th</sup> Symposia of the Society for Experimental Biology, Cambridge Univ. Press, London, U.K., pp. 205–234, 1965.
- Moriasi, D.N., Arnold, J.G., Van Liew, M.W., Bingner, R.L., Harmel, R.D., and Veith, T.L.: Model evaluation guidelines for systematic quantification of accuracy in watershed simulations, *T. ASAE*, 50, 885–900, 2007.
- Morris, M.D.: Factorial sampling plans for preliminary computational experiments, *Technometrics*, 33, 161–174, 1991.
- Neitsch, S.L., Arnold, J.G., Kiniry, J.R., and Williams, J.R.: Soil and Water Assessment Tool Theoretical Documentation Version 2009, Texas Water Resources Institute Technical Report No. 406, Texas A&M University System, College Station, Texas, 647 pp., 2011.
- Neyman, J.: Outline of a Theory of Statistical Estimation Based on the Classical Theory of Probability, *Phil. Trans. R. Soc. A*, 236, 333–380, 1937.
- Nielsen, A., Trolle, D., Me, W., Luo, L.C., Han, B.P., Liu, Z.W., Olesen, J.E., and Jeppesen, E.: Assessing ways to combat eutrophication in a Chinese drinking water reservoir using SWAT, *Mar. Freshwater Res.*, 64, 475–492, 2013.
- Paku, L.K.: The use of carbon-13 to trace the migration of treated wastewater and the chemical composition in a forest environment, Master Thesis, Science in Chemistry, the University of Waikato, Hamilton, New Zealand, 92 pp., 2001.
- Parliamentary Commissioner for the Environment: *Water Quality in New Zealand: Land Use and Nutrient Pollution*, New Zealand, 82 pp., 2013.
- Pfannerstill, M., Guse, B., and Fohrer, N.: Smart low flow signature metrics for an improved overall performance evaluation of hydrological models, *J. Hydrol.*, 510, 447–458, 2014.
- Radcliffe, D.E., Lin, Z., Risse, L.M., Romeis, J.J., and Jackson, C.R.: Modeling phosphorus in the Lake Allatoona watershed using SWAT: I. Developing phosphorus parameter values, *J. Environ. Qual.*, 38, 111–120, 2009.

- Reusser, D.E., Blume, T., Schaefli, B., and Zehe, E.: Analysing the temporal dynamics of model performance for hydrological models, *Hydrol. Earth Syst. Sc.*, 13, 999–1018, 2009.
- Reusser, D.E. and Zehe, E.: Inferring model structural deficits by analysing temporal dynamics of model performance and parameter sensitivity, *Water Resour. Res.*, 47, W07550, 15 pp., 2011.
- Rice, J.A.: *Mathematical statistics and data analysis*, Boston, MA, Cengage Learning, 688 pp., 2006.
- Rimmer, A. and Hartmann, A.: Optimal hydrograph separation filter to evaluate transport routines of hydrological models, *J. Hydrol.*, 514, 249–257, 2014.
- Rotorua District Council, Rotorua Wastewater Treatment Plant, Rotorua, New Zealand, 22 pp., 2006.
- Rutherford, K., Palliser, C., and Wadhwa, S.: Prediction of nitrogen loads to Lake Rotorua using the ROTAN model, Report prepared for Bay of Plenty Regional Council, New Zealand, 183 pp., 2011.
- Sangrey, D.A., Harrop–Williams, K.O., and Klaiber, J.A.: Predicting ground–water response to precipitation, *J. Geotech. Eng.*, 110, 957–975, 1984.
- Schuol, J., Abbaspour, K.C., Yang, H., and Srinivasan, R.: Modeling blue and green water availability in Africa, *Water Resour. Res.*, 44, W07406, 18 pp, 2008.
- Seymour, G.: *Predictive Inference: An Introduction*, Chapman & Hall, New York, 280 pp., 1993.
- Shen, Z.Y., Chen, L., and Chen, T.: Analysis of parameter uncertainty in hydrological and sediment modeling using GLUE method: a case study of SWAT model applied to Three Gorges Reservoir Region, China, *Hydrol. Earth Syst. Sc.*, 16, 121–132, 2012.
- Sloan, P.G. and Moore, I.D.: Modelling subsurface stormflow on steeply sloping forested watersheds, *Water Resour. Res.*, 20, 1815–1822, 1984.
- Statistics New Zealand: *Fertiliser use in New Zealand*, Statistics New Zealand, New Zealand, 13 pp., 2006.
- Tomer, M.D., Knowles, S.F., Fenton, J.A., Bardsley, W.E., and Oliver, G.R.: Soil water, ground water, and wetland seepage within an effluent–irrigated hillslope, *J. Hydrol. (NZ)*, 38, 97–120, 1999.
- Watt, M.S., Clinton, P.W., Coker, G., Davis, M.R., Simcock, R., Parfitt, R.L., and Dando, J.: Modelling the influence of environment and stand characteristics on basic density and modulus of elasticity for young *Pinus radiata* and *Cupressus lusitanica*, *Forest Ecol. Manag.*, 255, 1023–1033, 2008.
- White, K.L. and Chaubey, I.: Sensitivity analysis, calibration, and validations for a multisite and multivariable SWAT model, *J. Am. Water Resour. As.*, 41, 1077–1089, 2005.

- White, M.J., Storm, D.E., Mittelstet, A., Busted, P.R., Haggard, B.E., and Rossi, C.: Development and testing of an in-stream phosphorus cycling model for the Soil and Water Assessment Tool, *J. Environ. Qual.*, 43, 215–223, 2014.
- White, P.A., Cameron, S.G., Kilgour, G., Mroczek, E., Bignall, G., Daughney, C., and Reeves, R.R.: Review of groundwater in Lake Rotorua catchment, Prepared for Environment Bay of Plenty, Institute of Geological & Nuclear Sciences Client Report 2004/130, Whakatane, New Zealand, 245 pp., 2004.
- Whitehead, D., Kelliher, F.M., Lane, P.M., and Pollock, D.S.: Seasonal partitioning of evaporation between trees and understorey in a widely spaced *Pinus radiata* stand, *J. Appl. Ecol.*, 31, 528–542, 1994.
- Williams, J.R.: Sediment routing for agricultural watersheds, *Water Resour. Bull.*, 11, 965–974, 1975.
- Wu, H., and Chen, B.: Evaluating uncertainty estimates in distributed hydrological modeling for the Wenjing River watershed in China by GLUE, SUFI-2, and ParaSol methods. *Ecological Engineering* 76, 110–121, 2015.
- Ximenes, F.A., Gardner, W.D., and Kathuria, A.: Proportion of above-ground biomass in commercial logs and residues following the harvest of five commercial forest species in Australia, *Forest Ecol. Manag.*, 256, 335–346, 2008.
- Yilmaz, K.K., Gupta, H.V., and Wagener, T.: A process-based diagnostic approach to model evaluation: Application to the NWS distributed hydrologic model, *Water Resour. Res.*, 44, W09417, 18 pp, 2008.
- Zhang, H., Huang, G.H., Wang, D.L., and Zhang, X.D.: Multi-period calibration of a semi-distributed hydrological model based on hydroclimatic clustering, *Adv. Water Resour.*, 34, 1292–1303, 2011.
- Zhang, Z., Tao, F., Shi, P., Xu, W., Sun, Y., Fukushima, T., and Onda, Y.: Characterizing the flush of stream chemical runoff from forested watersheds, *Hydrol. Process.*, 24, 2960–2970, 2010.

### **3 Water quality effects of treated municipal wastewater application to a temperate forested catchment: Insights from SWAT modelling**

#### **3.1 Abstract**

Spray irrigation of treated wastewater ( $10 \text{ mm d}^{-1}$ ) in plots in the Whakarewarewa Forest (193 ha), Rotorua, New Zealand, was envisaged as a solution to address eutrophication of Lake Rotorua. We investigated the impacts of wastewater irrigation on discharge and water quality of the Waipa Stream, which drains the irrigated area. Our objective was to simulate the effects of irrigation of the sub-catchment and examine alternatives for managing the wastewater. A modified version of Soil and Water Assessment Tool (SWAT2012 rev629) with hourly routing algorithms was adapted to the sub-catchment, which drains the wider Puarenga catchment. The SWAT2012 model was run at an hourly time step for a 10-year (2003–2012) period and validated by comparing weekly average predictions with measurements of the stream discharge and water quality using a range of statistical metrics. The model performed well for simulating discharge ( $r = 0.83$ ;  $p < 0.001$ ) and total nitrogen (TN) load ( $r = 0.82$ ;  $p < 0.001$ ). Performance was satisfactory but generally lower (e.g.,  $r \geq 0.54$ ;  $p < 0.001$ ) for simulating suspended sediment (SS) and total phosphorus (TP) loads. Hourly load predictions had high temporal variability ( $SS > TP > TN$ ), consistent with the pattern observed in field measurements downstream. A range of scenarios was simulated that included ceasing irrigation and changing the area and frequency of irrigation, while keeping the annual irrigation volume constant. Increasing the irrigation area decreased simulated TP and TN loads. The impact of changing irrigation frequency from daily to one day each week was small for annual TP load simulations but annual TN load increased considerably under weekly irrigation, reflecting increased N leaching rate. Compared with low-frequency, high-volume wastewater applications (once every seven days), the current strategy of daily wastewater irrigation minimises TN leaching and reduces saturation of the subsurface layer. Our improvements to the SWAT2012 model and the use of hourly routing to capture high-frequency (daily and hourly) variability of nutrient discharges under different land management regimes can assist with developing strategies to manage

the effects of nutrient and sediment pollution from the irrigated area by refining the area, timing and frequency of irrigation.

### **3.2 Introduction**

Across the world, inland cities have sought ways to treat their municipal wastewater effectively and avoid direct disposal of treated effluent into sensitive receiving waters (Raschid–Sally and Jayakody, 2008). As treatment technology has improved, attention has increasingly been focused on the management of nitrogen and phosphorus, nutrients that can promote excessive growth of algae and result in eutrophication of receiving waters. For example, diverting municipal wastewater discharge away from Lake Washington (Seattle, USA) in the early 1970s resulted in reduced levels of phosphorus (by 83%) in the lake (Krebs, 2008). Similarly, there has been marked decrease in total phosphorus concentrations in Lake Constance (Germany) following wastewater diversion out of the lake catchment in the late 1970s, coupled with greater use of phosphate–free detergents since c. 1980 (OECD, 2001). An alternate approach to diversion of wastewater from sensitive ecosystems is to implement tertiary treatment to remove nutrients to levels so that the wastewater can still be discharged within the catchment of the affected water body without significantly impairing water quality. The use of agricultural crops and forestry areas for wastewater irrigation has increasingly been adopted for this purpose in India, resulting in 25–50% reduction of N and P fertiliser use and 15–27% increase in crop productivity (Kaur et al., 2012). Despite the benefits associated with controlled wastewater irrigation, there are potential disadvantages related to soil waterlogging and enrichment, which could increase nutrient leaching (Farahat and Linderholm, 2015). Forest harvesting can also aggravate erosion and nutrient losses from soils in irrigated areas (Carpenter et al., 1998). For land–based treatment to be sustainable, it is necessary to balance the amount of wastewater applied with uptake rates from trees and losses from processes such as denitrification (Mussely and Goodwin, 2012), so that losses to runoff and leaching are minimised.

The evaluation of the long–term effectiveness of wastewater irrigation is also very important. Because field experiments are not often feasible, modelling is generally used to predict potential impacts from a range of irrigation management

strategies (Behera and Panda, 2006). Models that combine hydrological and biogeochemical components of a system, and which capture the dominant temporal and spatial variability, may be a valuable tool for this purpose. Vieritz et al. (2003) for example, applied the MEDLI model (Model for Effluent Disposal using Land Irrigation) to investigate the sustainability of irrigating a grass crop (Monto Vetiver grass) with effluent in Queensland, Australia, with focus on capturing the dynamics of grass growth, nutrient uptake and hydrogeology. Another model used for this purpose is SPASMO (Soil Plant Atmosphere System), which simulates water and solute movement through soil profiles (Green et al., 2003). This model was applied to simulate effects of varying irrigation rates of effluent applied on pine trees in Rotorua, New Zealand (Vogeler et al., 2004). These two case studies did not examine the broader implications of the wastewater irrigation, including nutrient losses through surface runoff or to groundwater, which are not simulated by these two models.

The SWAT model simulates hydrological and biogeochemical processes in both terrestrial and in-stream phases (Arnold et al., 1998). It integrates a large amount of spatially distributed information into a GIS (Geographic Information System) platform, providing a tool to estimate the contribution of nutrient sources distributed throughout a catchment to loading of receiving waters (e.g., Dabrowski, 2014). The SWAT model has been used to evaluate impacts of treated wastewater irrigation from agricultural areas on catchment hydrology (Cau and Paniconi, 2007) and nitrogen transport (e.g., Pisinaras et al., 2010; Aouissi et al., 2014). Dechmi et al. (2012) adapted SWAT2005 code to estimate return flow from irrigated wastewater originating from a water source outside of the catchment. The adapted code (termed SWAT-IRRIG) was used to evaluate impacts of management practices on the water balance and phosphorus yield for a small (~ 19 km<sup>2</sup>) catchment in Spain (Dechmi and Skhiri, 2013). These adjustments have since been incorporated in both SWAT2009 and SWAT2012 code for agriculture and forestry area simulations. However, the SWAT2009 model used in Me et al. (2015) was found not to be able to simulate the detail of a complex irrigation operation, as evidenced by poor statistical fit of simulations for P. Therefore, the SWAT2012 model, along with the relevant modified code, was used in this study to extend the study of Me et al. (2015) and evaluate the impacts of treated wastewater irrigation on the forestry area.

The SWAT2012 code encompasses two sets of flow routing algorithms (hourly and daily). The use of each set of algorithms is dependent on the temporal resolution (daily and hourly) of hydrological forcing data. For example, hourly hydrological forcing data require the Green and Ampt infiltration method (Green and Ampt, 1911) to be used to simulate flow routing at hourly time step. Alternatively, hourly rainfall data could also be converted to the daily data in SWAT using daily routing algorithms to simulate surface runoff (Arnold et al., 2013). Yang et al. (2016) applied SWAT2012 code and evaluated the impacts of different temporal resolution (daily and hourly) of hydrological forcing data on SWAT2012 model performance for daily streamflow simulations. The authors found that the hourly time step version (i.e., hourly routing algorithms) of SWAT2012 model driven with the hourly rainfall data performed better for daily predictions, in particular, during high rainfall–runoff events. Yang et al. (2015) optimised parameter values separately for both the hourly and daily models, which suggests time–step dependence. Ideally, parameter values should be identical between hourly routing and daily routing algorithms. Time–step independence of parameter values may reflect parameter uncertainties, potentially being associated with an issue of equifinality where it is difficult to validate model parameters through measurements (Shen et al., 2012).

Jeong et al. (2010) developed hourly rainfall–runoff algorithms in SWAT2005 and applied these to water infiltration, surface runoff and hydrological lags for in–stream flow routing in a small catchment (1.9 km<sup>2</sup>) near Riesel, Texas. Although evapotranspiration, soil water movement, base flow and lateral flow routings were still simulated on a daily basis, the hourly model improved simulations at high discharge during intensive rainfall. Jeong et al. (2011) modified hourly routing algorithms for soil erosion and in–stream sediment transport based on the hourly rainfall–runoff algorithms developed in SWAT2005. They found that the hourly model (aggregated to daily output) predicted annual sediment yield better than the daily model (daily output). Although nutrient biogeochemical processes in soils were still simulated at daily interval, forcing data (e.g., rainfall) at hourly resolution may better allow the model to represent the dynamics of nutrients transported in steep areas of small catchments (Jeong et al., 2011).

The study site is a wastewater–irrigated forestry area in Rotorua, New Zealand. It is steep (max slope = 26%; derived from the digital elevation model;

BoPRC) and the discharge responds rapidly to rainfall events. Hourly routing algorithms in the SWAT2012 code (rev629) were applied to simulate discharge and both dissolved and total nutrient species fluxes. Modelled results are presented at two time scales; hourly and weekly mean (aggregated from a simulations at daily time scale). Using a single parameter set, the model performance was compared between hourly and daily routing algorithms. The effect of hourly routing on the variability of each simulated variable was also examined during the course of a day. The objectives of the study were to: (1) increase the model capability to simulate complex irrigation operations; (2) simulate the hourly variability of downstream discharge and nutrient fluxes during treated wastewater application to the Rotorua Land Treatment System, and; (3) quantify differences in daily simulations of total annual nutrient loads in the receiving stream under four possible management scenarios. A key task was to modify the SWAT2012 code to simulate the effects of irrigation and rainfall on the variability of contaminant loads using the hourly routing algorithms.

### **3.3 Methods**

#### **3.3.1 Study catchment**

The Waipa Stream catchment (16 km<sup>2</sup>) is 4.5 km southeast of the Rotorua City and is comprised of 80% exotic pine forest (*Pinus radiata*). The soil of the catchment is mainly allophanic, sandy and well drained, with 85–95% P retention capacity (Beets et al., 2013). The Waipa Stream flows into the Puarenga Stream, which is a major inflow to Lake Rotorua (surface area 80 km<sup>2</sup>; Fig. 3.1). Lake Rotorua is a nationally–iconic water body and minimizing eutrophication is a priority for lake managers. Municipal wastewater (10 mm d<sup>-1</sup>) from Rotorua City is treated by the Rotorua Wastewater Treatment Plant to secondary level. The treated municipal wastewater contained up to 28 tonnes yr<sup>-1</sup> TP and 51 tonnes yr<sup>-1</sup> TN which were discharged directly to Lake Rotorua until 1991 (Lowe et al., 2007). The treated wastewater has since been irrigated in the land treatment system (LTS) in the Whakarewarewa Forest, located in the southern part of the lake catchment and drained by the Waipa Stream. The LTS covers an area of 193 ha and consists of 14 spray–irrigated blocks. Prior to 2002, the irrigation schedule entailed applying wastewater to two blocks per day so that each block was irrigated approximately

weekly. Since 2002, 10 to 14 blocks have been irrigated simultaneously at for duration of 2 h d<sup>-1</sup> at an irrigation rate of 5 mm hr<sup>-1</sup> (Lowe et al., 2007). Over recent years of irrigation, nutrient concentrations in the irrigated water have gradually decreased as improvements have been made in treatment of the wastewater (Lowe et al., 2007). The LTS was designed to reduce the mass load of nitrogen in irrigated wastewater using plant uptake or microbial denitrification, and for most of the wastewater phosphorus the majority would be retained in the soil by adsorption (Hu et al., 2007). Nutrients not removed by these processes would leach into the Waipa Stream, which flows into Lake Rotorua via the Puarenga Stream (Fig. 3.1). Resource consent limits exist in the Puarenga Stream for the contributions of wastewater; 3 tonnes yr<sup>-1</sup> for TP and 30 tonnes yr<sup>-1</sup> for TN (Park and Holst, 2009).

### **3.3.2 Sampling measurements**

Monthly instantaneous discharge was measured at the Waipa D/S hydrometric station (Fig. 3.1) at the catchment outlet. Weekly mean discharge (Q) and weekly flow-proportional concentrations of the following analytes were also measured at the same location by Bay of Plenty Regional Council: SS, dissolved reactive phosphorus (DRP), TP, nitrate-nitrogen (NO<sub>3</sub>-N), ammonium-nitrogen (NH<sub>4</sub>-N), total Kjeldahl nitrogen (TKN; NH<sub>4</sub>-N + organic N), and TN. A weekly flow-proportional sampling programme is carried out by Rotorua Lakes Council using an automatic sampler to collect a single weekly composite sample. For Waipa D/S hydrometric station, the weekly composite sample was typically comprised of ~200 sub-samples and each sub-sample was collected every 1800 m<sup>3</sup> of discharge. Weekly contaminant loads were calculated based on weekly flow-proportional concentrations multiplied by weekly mean discharge, and the product was then used to compare against measurements, for model evaluation purposes.

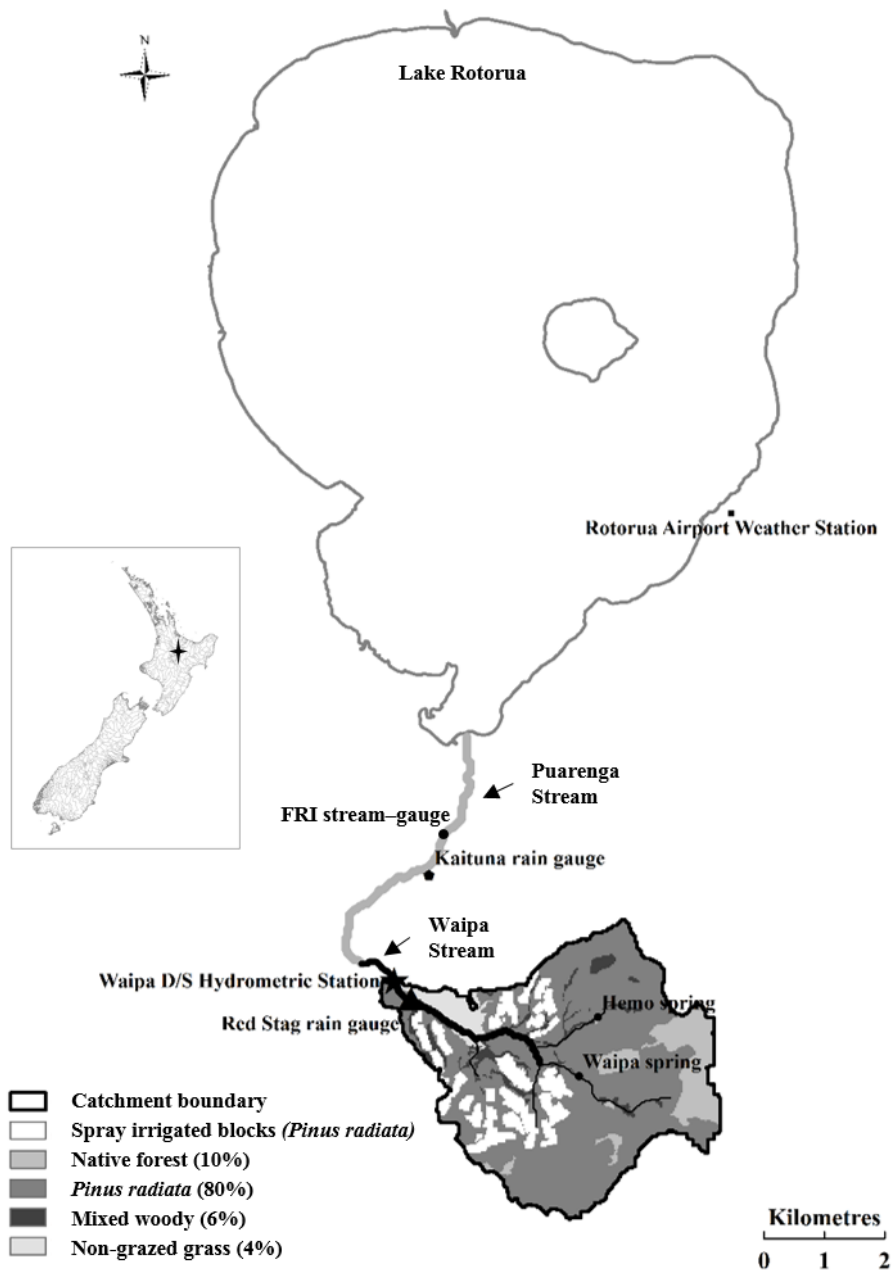


**Figure 3.1** Study catchment drained by the Waipa Stream, Rotorua, New Zealand. Treated wastewater is spray-irrigated onto 14 blocks within the Whakarewarewa Forest, upstream of Lake Rotorua.

### 3.3.3 Model configuration and code modification

The details used for model configuration and parameterisation are given in Me et al. (2015). Briefly, key SWAT input data requirements include: a digital elevation model (DEM; 25 m horizontal resolution); meteorological records (obtained from National Climatic Database; available at <http://cliflo.niwa.co.nz/>); records of spring locations, discharge and water abstraction; a stream map (obtained from Bay of

Plenty Regional Council, BoPRC); physical soil characteristics derived from S-map (developed by Landcare Research; available at <http://smap.landcareresearch.co.nz/home>); land use classifications (obtained from New Zealand Land Cover Database Version 2, BoPRC), and; management schedules (obtained from BoPRC) for key land uses (i.e., wastewater irrigation and timber harvesting).

Initial parameter values required for model configuration were based on the monitoring data that were measured close to the start date of the simulation period. Parameter values related to plant growth and nutrient uptake were taken from Me et al. (2015) for the dominant land use category (PINE, representing *Pinus radiata*) identified in this study. Soil chemical properties were derived from Beets et al. (2013) who measured N and P at six permanent soil sampling sites inside the study catchment in 2012.

The DEM was used to delineate boundaries for the whole catchment and individual sub-catchments, with a stream map used to “burn-in” channel locations to create accurate flow routings. The Waipa D/S hydrometric station (Fig. 3.1; downstream of the LTS, 537 m upstream of the confluence with the Puarenga Stream), was specified as the most downstream location in the model. Twenty-one sub-catchments were represented in the Waipa Stream catchment, each comprising numerous Hydrologic Response Units (HRUs). Each HRU aggregates cells with the same combination of land cover, soil, and slope. A total of 441 HRUs was defined in the model.

Weekly total precipitation (hereafter “rainfall”) data were obtained from the Red Stag rain gauge (Fig. 3.1) located within the study catchment. These data were used together with hourly rainfall measured at the Kaituna rain gauge (Fig. 3.1; ~2 km to the north of the Waipa Stream catchment) to derive an hourly distribution of rainfall for the Red Stag rain gauge. Hourly rainfall estimates were used as hydrologic forcing data and the hourly rainfall/Green & Ampt infiltration/hourly routing method (Arnold et al., 2013) was used to simulate upland and in-stream hydrological processes and nutrient transport for each HRU, with hourly or daily predictions summed to obtain the total for each sub-catchment.

### **3.3.3.1 Sediment erosion**

Estimation of sediment routing and channel erosion in SWAT was based on the simplified Bagnold Equation (Bagnold, 1977). The original SWAT2012 code was not functional for SS load simulations when the hourly routing algorithms were used. Therefore, adjustments were made in four FORTRAN files (“rthsed.f”, “rtout.f”, “route.f”, “ysed.f”) to permit: 1) hourly initialisation of peak runoff rate in each reach; 2) hourly simulations of SS loads in each reach; 3) summation of modelled reach SS loads at hourly intervals; and 4) daily predictions of SS loss caused by erosion.

### **3.3.3.2 Management schedules**

The forested blocks where wastewater is spray-irrigated were manually digitised based on maps provided by the LTS operators. Daily management schedules used as input to SWAT, including wastewater irrigation and forestry operations, were configured for each block. Wastewater irrigation was represented in SWAT by defining separate irrigation and fertilisation management schedules as part of the input of water and nutrients, respectively, to the model. The source of irrigation was specified in the model as outside of the catchment. The required daily irrigation depths were based on daily irrigation volumes for each block. The fraction of daily surface runoff from the irrigated wastewater draining from the sprayed block was estimated based on a digital filter method (Eckhardt filter) and using the Hydrograph Analysis Tool (Lim et al., 2005). This tool has been used to separate daily streamflow into base flow and surface runoff, and was also used in this study for the separation of daily irrigated wastewater (plus daily rainfall) into surface runoff and subsurface infiltration. The fraction of the separated daily surface runoff was then estimated (multi-year daily mean = 0.6), which meant the remaining irrigated-wastewater was assumed to have infiltrated the soil. In addition to daily excess rainfall, daily excess irrigation depths have also been added to account for daily water percolation below the bottom of the soil profile in the SWAT2012 code, as done in Dechmi et al. (2012).

Nutrients in the irrigated wastewater were represented in SWAT as fertiliser inputs, with a daily composition configured from monthly mean concentrations measured in 7-day composite samples of the irrigated-wastewater. The daily irrigated fertiliser was input in  $\text{kg ha}^{-1} \text{d}^{-1}$  where the area unit represents the irrigated

block. The deficiencies of the original SWAT2012 code were 1) omission of the area of each irrigated block, 2) applied organic N in wastewater was added in both fresh and active organic N pools, and 3) omission of the summations of  $\text{NH}_4\text{-N}$  load in the soil. Adjustments were therefore made in the FORTRAN files “sched\_mgt.f”, “fert.f” and “soil\_write.f” to address these deficiencies.

Configuration of forest harvest operations was based on annual harvesting data provided by forestry managers. Each block was deemed mature at the start of the modelling period. Harvesting of each block was a clear-fell operation and was assigned in the model as taking one year to complete, during which time no irrigation was carried out. A total of 14 blocks was configured on daily intervals for the three operations (irrigation, fertiliser application and tree harvesting) over the modelling period of 10 years. An additional variable “iopera” was added in the FORTRAN file “allocate\_parms.f” of the SWAT2012 source code to indicate the management schedule. A dimension of 12,000 ( $\sim 10 \text{ years} \times 365 \text{ days} \times 3 \text{ operations}$ ) was assigned to this variable.

### **3.3.3.3 Nutrient simulations**

The QUAL2E model (Brown and Barnwell, 1987) linked with SWAT was used to simulate the in-stream nitrogen and phosphorus dynamics. SWAT simulates loads of  $\text{NO}_3\text{-N}$ ,  $\text{NH}_4\text{-N}$  and organic N (ORGN), the sum of which is TN load (nitrite is assumed negligible), and loads of mineral P (MINP) and organic P (ORGP), the sum of which is TP load. The MINP fraction represents soluble P in mineral and organic form. Due to the small proportion of soluble organic P observed at the Waipa D/S hydrometric station, the MINP fraction was presumed to be directly comparable to DRP measured in stream water samples. The ORGP represents particulate organic P (e.g., P in phytoplankton) and inorganic P bound to sediments adsorbed to sediments (White et al., 2014).

Adjustments were also made in the source code files “orgn.f” (unit corrections), “nminrl.f” (constants corrected) and “nitvol.f” (nitrification and volatilisation calculations) to permit 1) the calculation of ORGN load lost from the soil in surface runoff; 2) the calculation of N mineralisation and immobilisation; and 3) the calculation of rates of N nitrification and volatilisation. Adjustments made in “soil\_chem.f”, “psed.f”, “enrsb.f”, and “solp.f” (unit corrections) to permit 1) the initialisation of soil chemical properties; 2) the calculation of MINP and

ORGP loads in surface runoff; 3) calculation of the “enrichment ratio”, which is the ratio of the phosphorus concentration associated with fine suspended sediments to the concentration in surface soil; and 4) the calculation of MINP load lost from the soil in either surface runoff or leaching to groundwater.

A diagrammatic representation of all the required modifications of SWAT2012 code is shown in Fig. 3.2, followed by detailed descriptions of these modifications in Appendix 1.

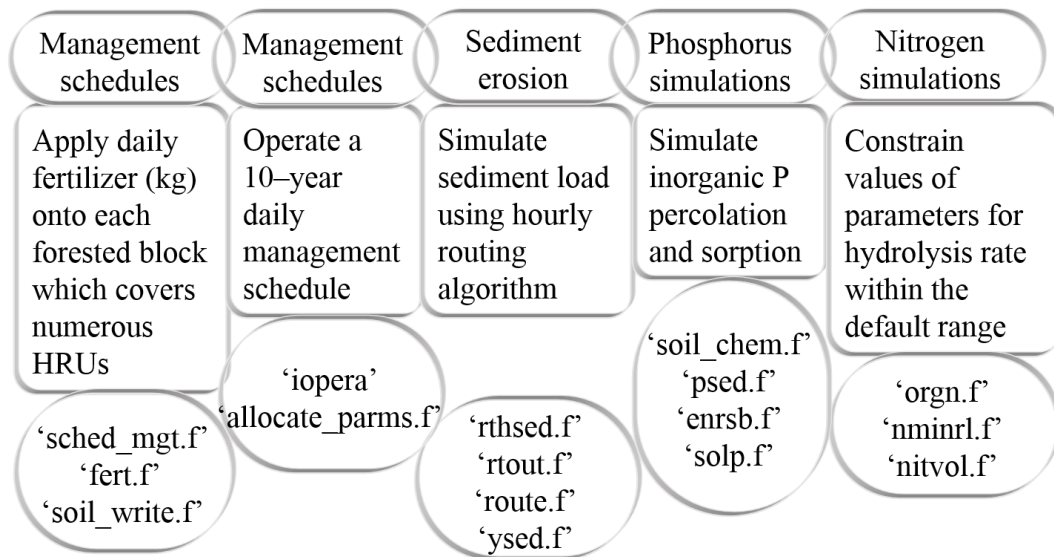


**Figure 3.2** Diagram of the modification of SWAT2012 code required for the Waipa irrigated forestry catchment. Components in the first row indicate the processes for which code modifications were required. Components in the second row describe each process. Components in the third row indicate the specific FORTRAN files where the SWAT2012 code was modified (see Appendix 1).

### 3.3.4 Parameter sensitivity and calibration

Values of SWAT parameters were assigned based on (i) measured data (e.g., soil parameters), (ii) literature values from published studies of similar catchments (e.g., land use parameters), or (iii) manual adjustment where parameters were not otherwise prescribed. Hydrological parameters were calibrated manually based on the weekly mean measurements of discharge. Water quality parameters for simulations of SS, ORGP, MINP, ORGN, NH<sub>4</sub>-N, and NO<sub>3</sub>-N loads were also manually calibrated using weekly flow-proportional sampling loads.

The SWAT2012 model was run from 2002 to 2012, i.e., for the period following a change from daily to weekly irrigation of each block (see Section 3.3.1).

The first year (2002) was used for model “warm-up”. The calibration period was from 2003 to 2010 and the validation period was from 2011 to 2012. A one-at-a-time (OAT) routine proposed by Morris (1991) was applied to examine parameter sensitivity for each simulated variable (Q, SS, ORGP, MINP, ORGN, NH<sub>4</sub>-N, and NO<sub>3</sub>-N).

### 3.3.5 Model evaluation

Hourly routing and daily routing model performances were evaluated in this study using a common parameter set. Model evaluation was based on the comparisons between weekly mean simulations and measurements for discharge, SS, ORGP, MINP, TP, ORGN, NH<sub>4</sub>-N, NO<sub>3</sub>-N, and TN loads. Weekly means were aggregated for the daily output using both the hourly and daily routing models. Model goodness-of-fit between simulated outputs and observations was initially assessed graphically and then quantified using four commonly-used model evaluation statistics (Moriassi et al., 2007): Pearson product moment correlation coefficient ( $r$ ), root mean square error (RMSE), mean absolute error (MAE), and percent bias (PBIAS). Values of  $r$  indicate the degree of linear relationship between simulated and measured data. Values of  $r$  were deemed statistically significant for values of  $p < 0.05$  (Bewick et al., 2003). Values of RMSE and MAE reflect the model error in units of the variables of interest. PBIAS indicates the average tendency for model predictions to be larger or smaller than observations. Definitions and statistical inferences are shown in Table 3.1.

Hourly simulations of discharge, SS, TP and TN loads were also used for model evaluation during short (1–3 day) high rainfall days (i.e., storm events). The period 10–12 October 2011 was chosen to include the pre, during and post storm event (max. rainfall 7.67 mm h<sup>-1</sup>). This period also corresponded to the sampling period given in Abell et al. (2013), where high-frequency (1–2 h) water quality sampling was undertaken (nine events for SS and 14 events for TP and TN) during 2010–2012 at the downstream FRI stream-gauge (FRI; Fig. 3.1). The use of hourly simulations for model evaluation in this study allowed examination of the range of variation in each simulated variable over the course of one day.

**Table 3.1** Statistics used to evaluate model performance. Note:  $o_n$  is the  $n^{\text{th}}$  observed datum,  $s_n$  is the  $n^{\text{th}}$  simulated datum,  $\bar{o}$  is the observed mean value,  $\bar{s}$  is the simulated daily mean value, and  $N$  is the total number of observed data.

Statistic	Definition	Features
Pearson product moment correlation coefficient	$r = \frac{\sum_{n=1}^N [(o_n - \bar{o})(s_n - \bar{s})]}{\sqrt{\sum_{n=1}^N (o_n - \bar{o})^2 \times \sum_{n=1}^N (s_n - \bar{s})^2}}$	Range from -1 to 1. The value of 0 indicates no linear relationship, while the value of 1 or -1 indicates a perfect positive or negative linear relationship between simulated and measured data.
Root mean square error	$\text{RMSE} = \sqrt{\frac{\sum_{n=1}^N (s_n - o_n)^2}{N}}$	A value of 0 indicates a perfect fit. This measure is disproportionately affected by large errors.
Mean absolute error	$\text{MAE} = \frac{\sum_{n=1}^N  s_n - o_n }{N}$	A value of 0 indicates a perfect fit. A measure of the average of all model errors.
Percent bias Statistic	$\text{PBIAS}\% = \frac{\sum_{n=1}^N (o_n - s_n)}{\sum_{n=1}^N o_n} \times 100\%$	A value of 0 indicates a perfect fit. Positive values indicate model underestimates and negative values indicate model overestimates.

### 3.3.6 Irrigation scenarios

Five different treated municipal wastewater irrigation scenarios were simulated using the hourly routing to evaluate impacts of 10–14 blocks irrigated daily (actual irrigation scenario; S0), decreasing the irrigated area (eight, four or two blocks irrigated while keeping the total irrigation volume unchanged; S1), reassigning the same amount of irrigated wastewater from high rainfall days ( $\geq 20 \text{ mm d}^{-1}$ ) to low rainfall days ( $< 20 \text{ mm d}^{-1}$ ; S2), reducing irrigation frequency (e.g., total weekly irrigation applied on one day each week; S3), and no irrigation (S4). Specifications for each of these scenarios are given in Table 3.2. Fertilisation schedules were also varied accordingly. The effects of different treated municipal wastewater irrigation scenarios on nutrient yields from the Waipa Stream catchment were analysed using the percentage change of a multi-year mean of annual nutrient loads aggregated from SWAT2012 daily outputs, compared with the simulations under scenario S0 (the current irrigation regime).

**Table 3.2** Descriptions and specifications of treated municipal wastewater irrigation scenarios used for SWAT2012 simulations.

Scenario	Purpose	Specification
S0: 10–14 blocks irrigated daily	Evaluate effects of the actual irrigation scenario.	Wastewater applied to 10 blocks or 14 blocks on different soil types within the land treatment system in 2003–2012.
S1: Decreased irrigated area	Evaluate effects of decreasing the size of the irrigated area.	Wastewater applied to eight blocks (122 ha), four blocks (61 ha) or two blocks (26 ha) on the same soil type (“Haparangi 1 and 2”) in 2003–2012. To allow upland and in–stream nutrient cycling and transport processes, wastewater was applied only to the blocks that were furthest upstream of the Waipa Stream. The total volume of wastewater applied was unchanged for each simulation.
S2: Irrigation on low rainfall days	Evaluate interactions between irrigation and rainfall.	Irrigation during high rainfall days ( $\geq 20 \text{ mm d}^{-1}$ ) in 2003–2012 reassigned to the first subsequent low rainfall day ( $< 20 \text{ mm d}^{-1}$ ). For periods with multiple consecutive high rainfall days (maximum = three days), the combined total irrigation was reassigned from high rainfall days to the first subsequent low rainfall day. The total volume of wastewater applied within three days was unchanged.
S3: Weekly irrigation	Evaluate effect of reducing irrigation frequency.	A weekly irrigation frequency was applied in 2003–2012, i.e., total weekly wastewater was irrigated on the first day of a week and no irrigation was undertaken on the remaining days in that week. The total volume of wastewater applied within a week was unchanged.
S4: No irrigation	Examine effect of no irrigation.	No irrigation for the period 2003–2012.

## 3.4 Results

### 3.4.1 Sensitive and optimised parameters

The optimised values of the most sensitive parameters, based on (i) measured data (e.g., soil parameters), ii) fixed values from the literature of similar catchments, or iii) auto-calibration followed by manual adjustment, are shown in Table 3.3 for the following variables: Q, SS, ORGP, MINP, ORGN, NH<sub>4</sub>-N, and NO<sub>3</sub>-N. Some nutrient parameters with file extension of “bsn” can only be given one value for the whole catchment (Arnold et al., 2013). Values for the remaining parameters were also assigned for the whole catchment in this study.

The value of the parameter channel erodibility factor (CH\_COV1) was optimised for the hourly routing to estimate the net amount of sediment re-entrained by deposition and degradation in the channel. The optimised value was relatively high (0.15; Table 3.3). The soil P parameter values used in this study were mainly derived from data in Beets et al. (2013), who measured P storage through soil depths at six sampling sites within the Waipa Stream catchment. They found mean measured P retention rates at 0–20 cm soil depth of 70% for the control (unirrigated) sites and 45% for irrigated sites. In SWAT, the soil P adsorption coefficient (PSP; P retention rate or P availability index) was not spatially distributed or dependent on soil depth (Arnold et al., 2013). It was therefore assigned as the average of 70% and 45% for the whole catchment (PSP; ~0.6; Table 3.3).

The optimised parameter values generally fall within the SWAT default ranges except for two parameters related to MINP load simulations; PHOSKD (phosphorus soil partitioning coefficient) and PPERCO (phosphorus percolation coefficient), and one parameter for NH<sub>4</sub>-N load simulations; RS3 (benthic sediment source rate for NH<sub>4</sub>-N in a reach at 20 °C). Parameter PHOSKD is the ratio of soluble P concentration in topsoil (10 mm) to that dissolved in discharge through surface runoff. The SWAT default range is 100 to 200 m<sup>3</sup> t<sup>-1</sup> (Neitsch et al., 2011). A larger value of 400 optimised for PHOSKD in this study may relate to large proportions of soluble P retained in topsoil as opposed to being discharged through surface runoff (Beets et al., 2013). Parameter PPERCO assigns the ratio of soluble P concentration in topsoil (10 mm) to that infiltrated into the subsurface soil layers. The SWAT default range is 100 to 175 m<sup>3</sup> t<sup>-1</sup> (Neitsch et al., 2011). A unit

conversion for PPERCO was taken out in code modifications, to be consistent with the equations in the manual documentation, so the adjusted default range is between 0.01 and 0.0175. The lower value of 0.01 optimised for PPERCO in this study indicated higher soluble P in infiltration than that in the topsoil (10 mm).

The optimised value for the parameter stream benthic (sediment) flux of  $\text{NH}_4\text{-N}$  (RS3) of  $10 \text{ mg m}^{-2} \text{ d}^{-1}$  exceeded the SWAT default range from 0 to  $1 \text{ mg m}^{-2} \text{ d}^{-1}$ . The high value of this optimised parameter was nevertheless less than the value from Gabriele et al. (2013) who investigated headwater streams from an Austrian agricultural catchment and the authors found RS3 values between 24 and  $48 \text{ mg m}^{-2} \text{ d}^{-1}$ .

### **3.4.2 Model performance**

Hourly routing of discharge averaged to weekly time scale showed larger fluctuations than daily routing simulations (Fig. 3.2a, b). Both model simulations provided strong correlations with weekly mean discharge measurements ( $r > 0.8$ ;  $p < 0.001$ ; Table 3.4). Weekly mean discharge peaks corresponding to high rainfall (weekly mean  $\geq 20 \text{ mm d}^{-1}$ ) tended to be overestimated by the hourly routing model (see PBIAS in Table 3.4).

Hourly routing underestimated several peaks of weekly mean SS load during high rainfall events. The underestimates were found either during or after a large number of blocks had been harvested (Fig. 3.3c). Both routings gave positive correlations with the measured weekly mean SS load ( $r > 0.4$ ;  $p < 0.001$ ; Table 3.4). However, daily routing of SS load averaged to weekly time scale was considerably higher than the hourly routing simulations (Fig. 3.3d; PBIAS in Table 3.4).

**Table 3.3** Optimised values and default ranges for the most sensitive parameters for discharge (Q), suspended sediment (SS), organic phosphorus (ORGP), mineral phosphorus (MINP), organic nitrogen (ORGN), ammonium–nitrogen (NH<sub>4</sub>–N), and nitrate–nitrogen (NO<sub>3</sub>–N) load simulations using a modified SWAT2012 code. The parameters marked with an asterisk have an optimised value outside of the SWAT default range. Parameters are unitless unless otherwise specified.

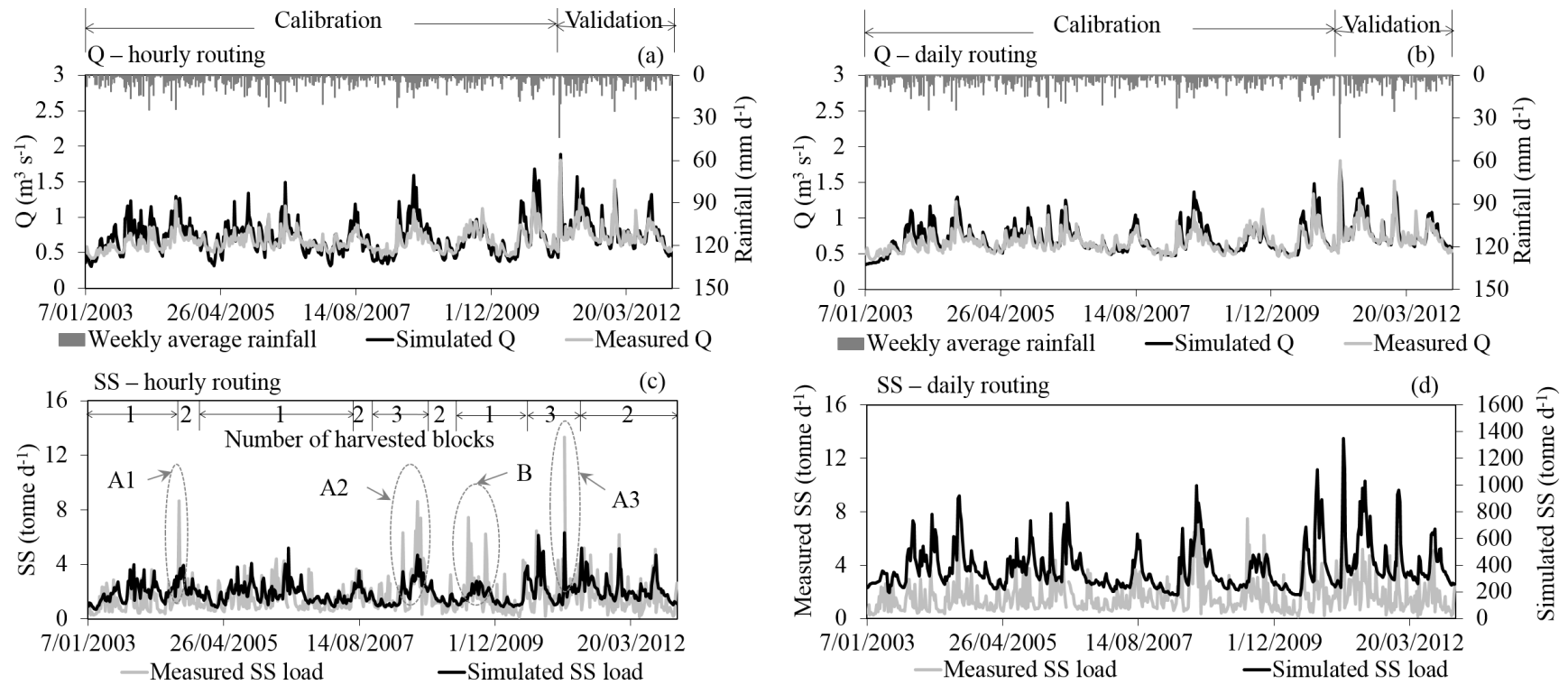
Parameter	Optimum	Min	Max	Definition	Unit
Q					
SLSOIL.hru	15	0	150	Slope length for lateral subsurface flow	m
CH_K2.rte	250	0	500	Effective hydraulic conductivity in the main channel alluvium	mm h <sup>-1</sup>
CH_N2.rte	0.01	0	0.3	Manning's N value for the main channel	
HRU_SLP.hru	0.6	0	1	Average slope steepness	m m <sup>-1</sup>
LAT_TTIME.hru	14	0	180	Lateral flow travel time	d
GWQMN.gw	400	0	5000	Threshold depth of water in the shallow aquifer required for return flow to occur	mm
RCHRG_DP.gw	0.65	0	1	Deep aquifer percolation fraction	
ALPHA_BF.gw	0.01	0	1	Base flow alpha factor	
SS					
CH_COV1.rte	0.15	0	0.6	Channel erodibility factor	
CH_COV2.rte	0.15	0	1	Channel cover factor	
LAT_SED.hru	5	0	5000	Sediment concentration in lateral flow and groundwater flow	mg L <sup>-1</sup>
PRF.bsn	2	0	2	Peak rate adjustment factor for sediment routing in the main channel	
SPCON.bsn	0.003	0.0001	0.01	Linear parameter for calculating the maximum amount of sediment that can be re–entrained during channel sediment routing	
SPEXP.bsn	2	1	2	Exponent for calculating sediment re–entrained in channel sediment routing	
OV_N.hru	20	0.01	30	Manning's N value for overland flow	
SLSUBBSN.hru	83	10	150	Average slope length	m

Parameter	Optimum	Min	Max	Definition	Unit
ORGP					
LAT_ORGP.gw	10	0	200	Organic P in base flow	mg P L <sup>-1</sup>
BC4.swq	0.7	0.01	0.7	Rate constant for mineralisation of organic phosphorus to dissolved phosphorus in the reach at 20 °C	d <sup>-1</sup>
RS4.swq	0.001	0.001	0.1	Organic phosphorus settling rate in the reach at 20 °C	d <sup>-1</sup>
MINP					
PSP.bsn	0.6	0.01	0.7	Phosphorus availability index	
*PHOSKD.bsn	400	100	500	Phosphorus soil partitioning coefficient	m <sup>3</sup> t <sup>-1</sup>
*PPERCO.bsn	0.01	0.01	0.0175	Phosphorus percolation coefficient	m <sup>3</sup> t <sup>-1</sup>
ORGN & NH <sub>4</sub> -N					
SURLAG.bsn	1	0.05	24	Surface runoff lag coefficient	
LAT_ORGN.gw	55	0	200	Organic nitrogen in the base flow	mg N L <sup>-1</sup>
BC3.swq	0.4	0.2	0.4	Rate constant for hydrolysis of organic nitrogen to ammonium–nitrogen in the reach at 20 °C	d <sup>-1</sup>
RS4.swq	0.001	0.001	0.1	Rate constant for organic nitrogen settling in the reach at 20 °C	d <sup>-1</sup>
NH <sub>4</sub> -N					
BC1.swq	0.1	0.1	1	Rate constant for biological oxidation of ammonium–nitrogen to nitrite–nitrogen in the reach at 20 °C	d <sup>-1</sup>
*RS3.swq	10	0	50	Benthic (sediment) source rate for ammonium–nitrogen in the reach at 20 °C	mg m <sup>-2</sup> d <sup>-1</sup>
NO <sub>3</sub> -N					
CDN.bsn	0.01	0	3	Denitrification exponential rate coefficient	
CMN.bsn	0.001	0.001	0.003	Rate factor for humus mineralisation of active organic nitrogen	
NPERCO.bsn	0.001	0	1	Nitrogen percolation coefficient	
SDNCO.bsn	0.95	0	1	Denitrification threshold water content	
HLIFE_NGW.gw	500	0	5000	Half–life of nitrate in the shallow aquifer	d

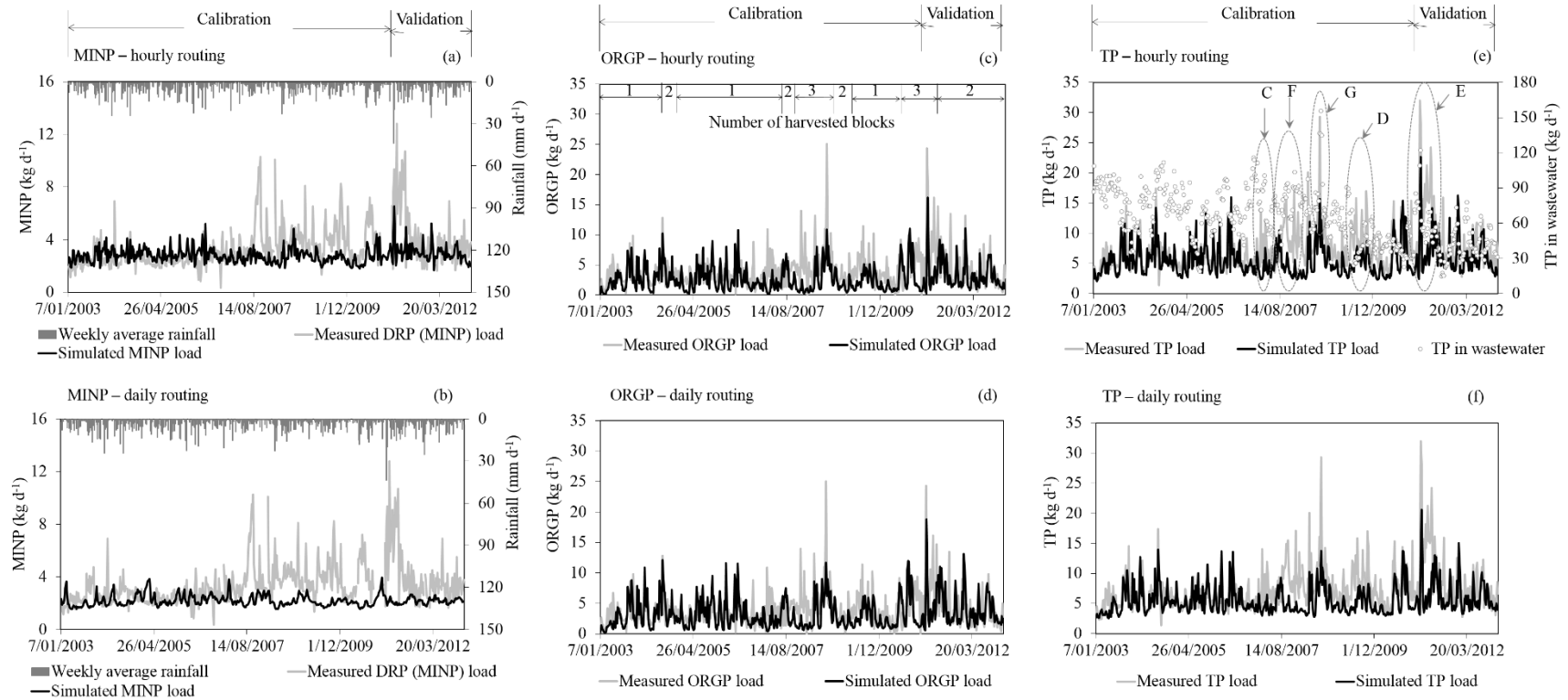
Fig. 3.4a–f shows that simulated loads of P species averaged to weekly time scale using hourly routing aligned well with the measurements prior to 2007, however the hourly model underestimated the weekly mean measurements after 2007. Underestimates of weekly mean MINP and ORGP peaks appeared to be related to extreme rainfall (weekly mean  $\geq 40 \text{ mm d}^{-1}$ ) and harvesting operations (i.e.,  $\geq$  three forestry blocks harvested). Underestimates of weekly mean TP peaks appeared to be a lagged response to high rainfall, high TP in wastewater or several blocks harvested concurrently. Hourly routing simulations of MINP load averaged to weekly values showed positive correlation with measurements during calibration and validation ( $r > 0$ ;  $p < 0.05$ ), while daily routing gave negative correlations (Table 3.4). Hourly routing gave underestimates of weekly mean MINP load by 13.9% during calibration and 27.3% during validation, while these underestimates increased for the daily routing simulations. By contrast, weekly mean ORGP load was underestimated using hourly routing compared with the daily routing simulation output of this variable (see PBIAS in Table 3.4). However, daily simulations of TP load averaged to weekly values were identical using hourly and daily routing models (Fig. 3.4e–f).

Fig. 3.5a–d indicates that for hourly routing averaged to weekly time scale, fluctuations in ORGN and  $\text{NH}_4\text{-N}$  loads were related to high rainfall. Most peaks in hourly routing of  $\text{NO}_3\text{-N}$  and TN loads averaged to weekly time scale also corresponded to high rainfall as well as to high TN loads in wastewater (Fig. 3.6a–d). Hourly routing of  $\text{NH}_4\text{-N}$  load averaged to weekly time scale showed high correlations with the measured values ( $r = 0.53$ ;  $p < 0.001$ ), while daily routing simulations were less accurate ( $r = 0.34$ ;  $p < 0.001$ ) and tended to underestimate measurements (see PBIAS in Table 3.4). By contrast, weekly mean ORGN load was underestimated using the hourly routing compared with the daily routing simulation. As for  $\text{NO}_3\text{-N}$  and TN loads, daily simulations averaged to weekly values using both hourly and daily routings were strongly correlated ( $r > 0.5$ ;  $p < 0.001$ ) with measurements during calibration and validation (Table 3.4).

The hourly routing model yielded better statistical fit to the measurements at weekly time scale and was therefore used in for further simulations. Fig. 3.7 shows an example of hourly simulations of discharge, SS, TP and TN loads for 10–12 October 2011. Fluctuations in simulated discharge and SS, TP and TN loads at hourly time scale are closely related to variations in rainfall (Fig. 3.7). Monthly mean discharge, SS, TP and TN loads aggregated from hourly simulations are shown in Table 3.5. The standard deviation (Std.Dev.) for hourly simulations of each variable is mostly larger than the mean (Table 3.5), indicating high variability at hourly time scale.



**Figure 3.3** Weekly mean values derived from simulated daily outputs for (a–b) discharge (Q) and (c–d) suspended sediment (SS) load, compared with weekly flow-proportional measurements at the Waipa D/S hydrometric station. The comparisons were undertaken by using a modified SWAT2012 code based on hourly routing (left) and daily routing (right). The calibration period was from 2003 to 2010 and the validation period was from 2011 to 2012. The model underestimated SS peaks when high rainfall occurred either during (A1–A3) or after (B) harvest of multiple blocks, as indicated by the number of harvested blocks in the upper panel of (c).



**Figure 3.4** Weekly mean values derived from simulated daily outputs for loads of (a–b) mineral phosphorus (MINP), (c–d) organic phosphorus (ORGP), and (e–f) total phosphorus (TP), compared with weekly flow–proportional measurements at the Waipa D/S hydrometric station. The comparisons were undertaken by using a modified SWAT2012 code based on hourly routing (left) and daily routing (right). Calibration was from 2003 to 2010 and validation from 2011 to 2012. Underestimates of TP peaks were related to a lagged response to high rainfall only (C), high rainfall following (D) or during (E) harvest of more blocks, only during harvest of more blocks without high rainfall (F), and high TP in wastewater during harvest of multiple blocks at once (G), as indicated by the number of harvested blocks in the upper panel of (c).

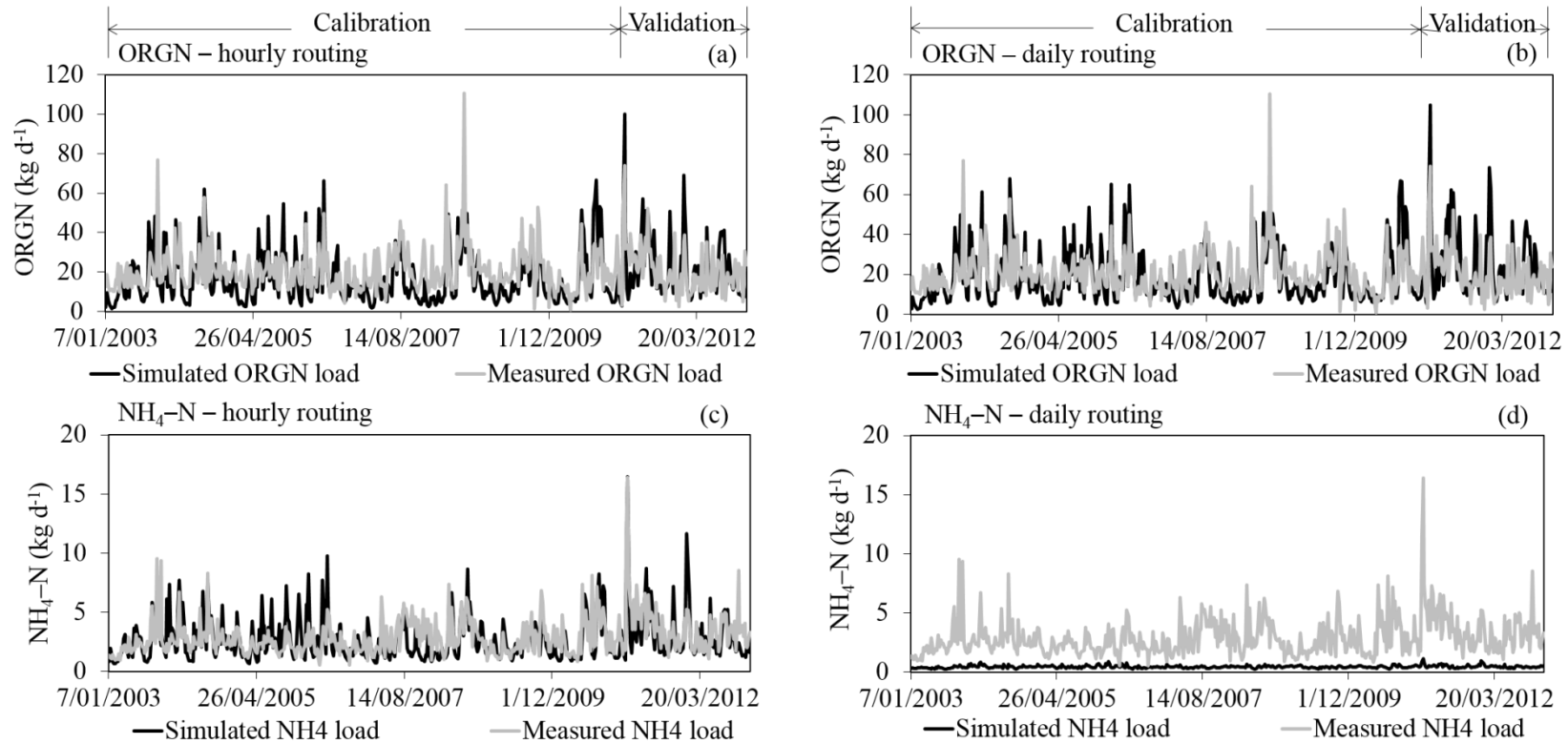


**Figure 3.5** Weekly mean values derived from simulated daily outputs for loads of (a–b) organic nitrogen (ORGN) and (c–d) ammonium–nitrogen (NH<sub>4</sub>-N), compared with weekly flow–proportional measurements at the Waipa D/S hydrometric station. The comparisons were undertaken by using a modified SWAT2012 code based on hourly routing (left) and daily routing (right). The calibration period was from 2003 to 2010 and the validation period was from 2011 to 2012.

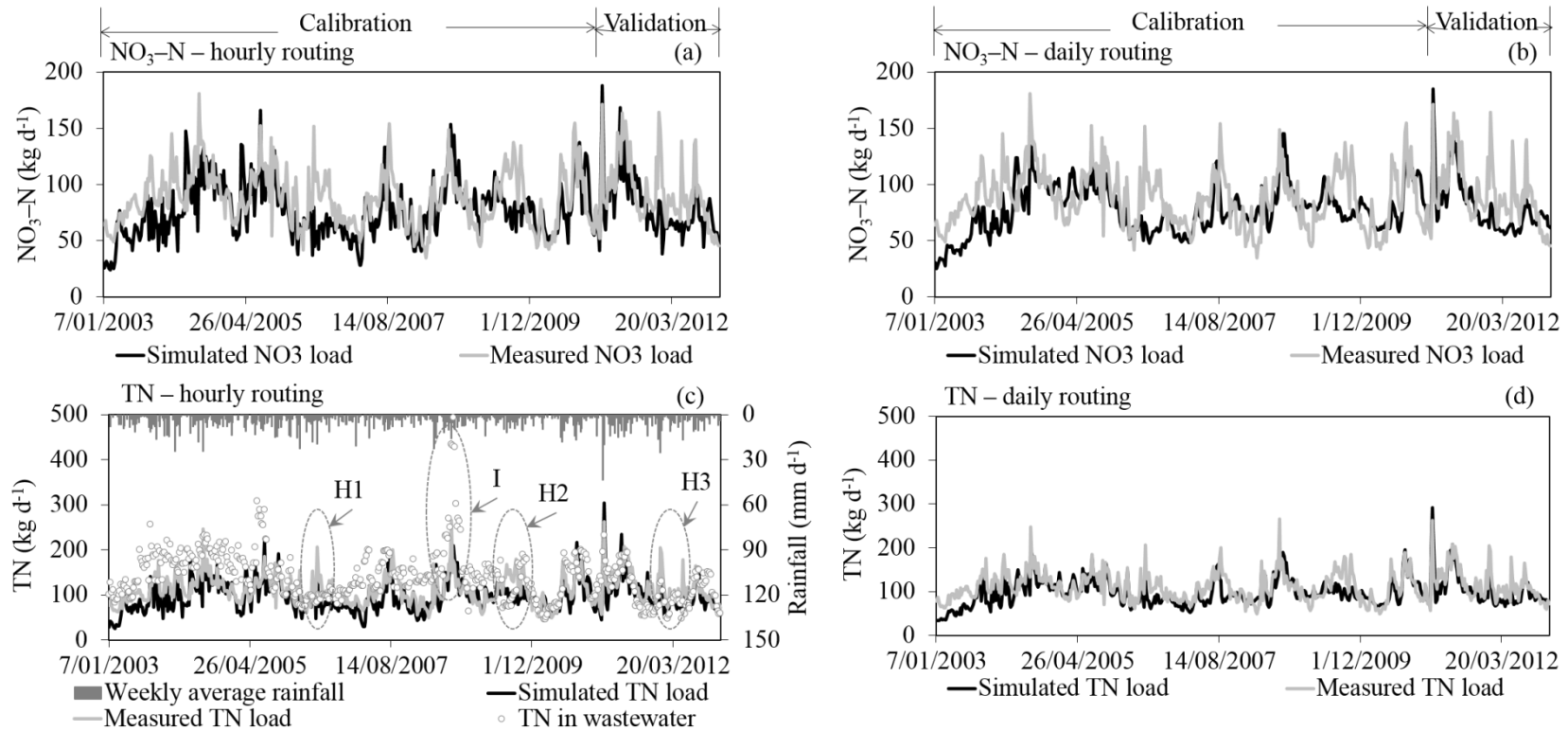


**Figure 3.6** Weekly average values derived from simulated daily outputs for loads of (a–b) nitrate–nitrogen (NO<sub>3</sub>-N) and (c–d) total nitrogen (TN), compared with weekly flow–proportional measurements at the Waipa D/S hydrometric station. The comparisons were undertaken by using a modified SWAT2012 code based on hourly routing (left) and daily routing (right). The calibration period was from 2003 to 2010 and the validation period was from 2011 to 2012. Several underestimates of peaks in TN load were related to consecutive wet days (H1–H3) and high TN in wastewater (I).

**Table 3.4** Statistical values of Pearson product moment correlation coefficient ( $r$ ), root mean square error (RMSE), mean absolute error (MAE), and percent bias (PBIAS), used to indicate the SWAT model performance for daily simulations averaged to weekly time scale of discharge (Q), loads of suspended sediment (SS), mineral phosphorus (MINP), organic phosphorus (ORGP), total phosphorus (TP), organic nitrogen (ORGN), ammonium–nitrogen (NH<sub>4</sub>–N), nitrate–nitrogen (NO<sub>3</sub>–N) and total nitrogen (TN). The statistical values were calculated using a modified SWAT2012 code based on (I) hourly routing and (II) daily routing. The significance of correlation is asterisked where  $p < 0.05$ , otherwise  $p < 0.001$ . Units are relevant to RMSE and MAE values.

Simulation period	Statistics	Processes calculation	Q (m <sup>3</sup> s <sup>-1</sup> )	SS (tonne d <sup>-1</sup> )	MINP (kg d <sup>-1</sup> )	ORGP (kg d <sup>-1</sup> )	TP (kg d <sup>-1</sup> )	ORGN (kg d <sup>-1</sup> )	NH <sub>4</sub> –N (kg d <sup>-1</sup> )	NO <sub>3</sub> –N (kg d <sup>-1</sup> )	TN (kg d <sup>-1</sup> )	
Calibration (2003–2010)	$r$	I	0.81	0.43	0.11*	0.42	0.45	0.61	0.53	0.57	0.73	
		II	0.84	0.45	-0.14*	0.40	0.45	0.60	0.34	0.48	0.70	
	RMSE	I	0.16	1.2	1.5	2.8	3.4	11.2	1.5	25.0	28.2	
		II	0.12	393.2	1.9	2.8	3.3	11.1	2.6	25.4	27.5	
	MAE	I	0.12	0.9	1.0	2.0	2.4	8.5	1.1	19.7	22.3	
		II	0.08	361.8	1.3	2.0	2.3	8.3	2.3	20.9	21.8	
	PBIAS%	I	-7.4	-17.9	13.9	31.8	22.5	17.8	5.5	11.3	12.4	
		II	-6.2	-22,682	32.1	17.6	22.9	8.4	83.7	10.4	11.8	
	Validation (2011–2012)	$r$	I	0.83	0.54	0.24*	0.6	0.54	0.63	0.71	0.63	0.82
			II	0.83	0.54	-0.22*	0.59	0.54	0.64	0.67	0.66	0.85
RMSE		I	0.15	1.5	2.4	3.4	4.9	12.5	1.8	26.4	26.3	
		II	0.10	499.9	2.9	3.3	4.9	13.8	3.8	25.2	23.7	
MAE		I	0.10	1.1	1.5	2.2	3.3	9.0	1.3	20.2	20.9	
		II	0.10	452.6	2.0	2.2	3.2	10.3	3.2	20	18.8	
PBIAS%		I	-5.2	-21.7	27.3	29.4	26.9	-3.3	11.3	13.1	10.1	
		II	-4.8	-24,860	46.9	12.4	27.0	-17.5	86.8	13.2	10.1	

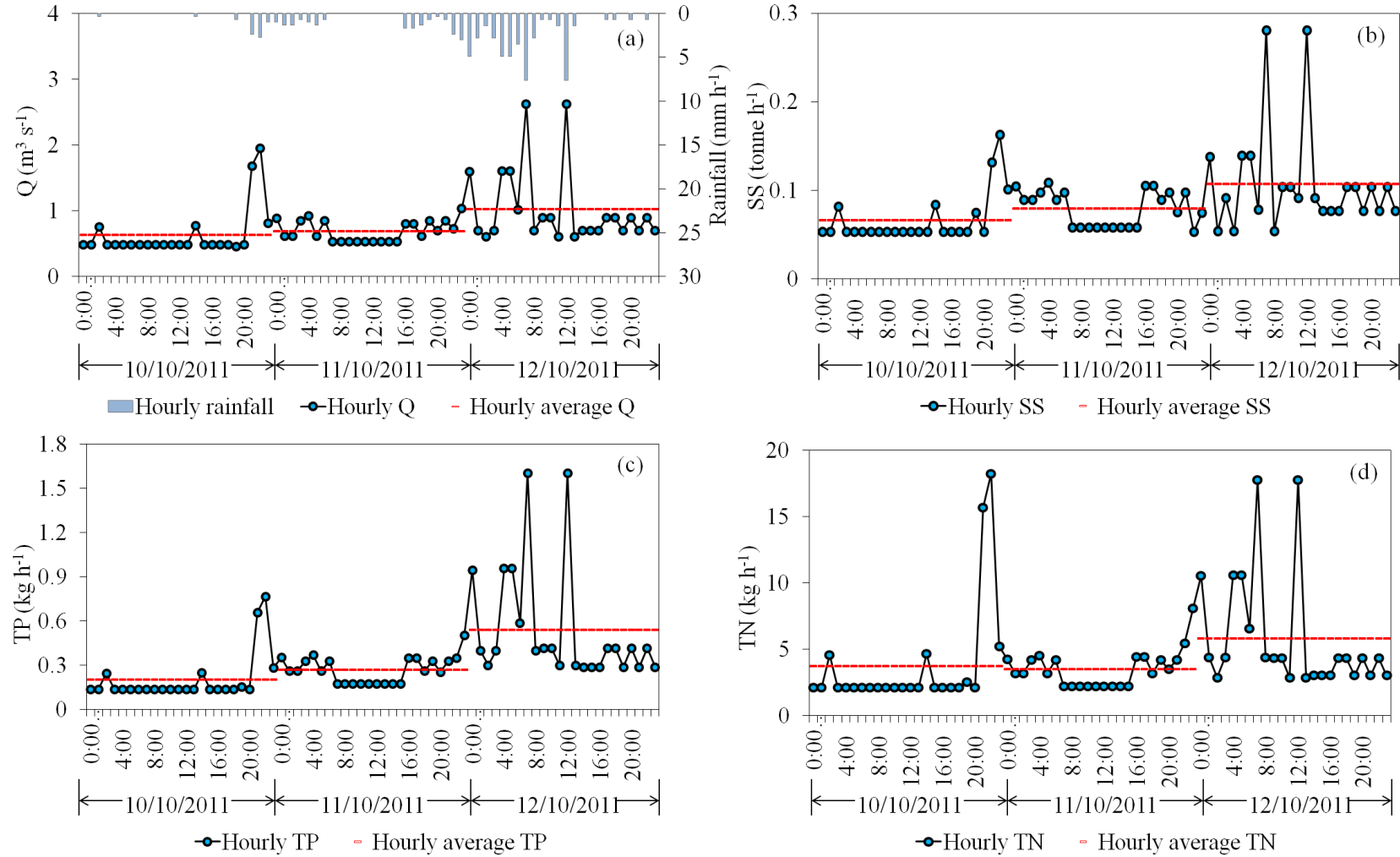


**Figure 3.7** Example of a storm event for the period 10–12 October 2011 showing variability of hourly SWAT2012 simulations of (a) discharge ( $Q$ ), (b) suspended sediment (SS), (c) total phosphorus (TP) and (d) total nitrogen (TN) loads over three days. The horizontal red lines show daily mean values. Rainfall (inverted scale) is shown in (a).

**Table 3.5** Multi-year monthly mean aggregated from SWAT2012 hourly simulations for discharge (Q), suspended sediment (SS), total phosphorus (TP) and total nitrogen (TN) loads. Std.Dev. is standard deviation.

Month	Q (m <sup>3</sup> s <sup>-1</sup> )		SS (tonne d <sup>-1</sup> )		TP (kg d <sup>-1</sup> )		TN (kg d <sup>-1</sup> )	
	Mean	Std.Dev.	Mean	Std.Dev.	Mean	Std.Dev.	Mean	Std.Dev.
Jan	0.63	0.83	1.7	5.3	4.9	10.1	78.9	133.9
Feb	0.62	0.64	1.6	2.8	4.7	7.2	75.5	112.2
Mar	0.59	0.42	1.6	1.6	4.3	4.7	80.9	100.5
Apr	0.60	0.48	1.6	2.2	4.6	6.2	90.5	110.1
May	0.79	1.04	2.3	5.6	6.6	11.5	110.5	188.1
Jun	0.84	1.05	2.4	5.4	6.5	10.2	105.7	171.7
Jul	0.87	1.10	2.6	5.8	6.8	10.8	113.3	199.2
Aug	0.94	1.34	2.9	7.7	7.2	12.7	123.4	221.2
Sep	0.81	0.92	2.3	4.7	5.8	8.8	110.3	165.4
Oct	0.80	0.97	2.3	5.2	6.2	10.1	109.8	176.5
Nov	0.64	0.47	1.7	2.0	4.3	4.5	89.1	89.7
Dec	0.61	0.59	1.6	2.8	4.8	7.0	85.7	115.3

### 3.4.3 Irrigation scenarios simulations

Irrigation scenarios are presented in Fig. 3.8 as multi-year (2003–2012) means of annual nutrient loads aggregated from SWAT2012 daily outputs using hourly routing algorithms. Under the actual irrigation scenario (S0: 10–14 blocks irrigated daily), simulated multi-year mean TP load was 2 t yr<sup>-1</sup> and TN load was 35.8 t yr<sup>-1</sup> in the Waipa Stream (Fig. 3.8). Compared with the measurements in the Waipa Stream, annual TP load was underestimated by 26% and annual TN load was underestimated by 12%.

The highest simulated nutrient loads occurred with decreasing the irrigated area from 10–14 blocks to two blocks (Fig. 3.8). Compared with the simulations under scenario S0, irrigation applied on two upstream blocks accounted for the largest increase in the annual nutrient load, i.e., annual TP load increased by 20% and annual TN load increased by 88%. The smallest increase in scenario S0 occurred for the wastewater application on eight blocks.

Simulations of annual mean nutrient loads under scenario S2, i.e., irrigation reassigned from high rainfall days ( $\geq 20$  mm d<sup>-1</sup>) to low rainfall days ( $< 20$  mm d<sup>-1</sup>) showed an unexpected small increase compared with the scenario S0. For example, annual TP load increased by 5% and annual TN load by 2.5% (Table 3.6).

Simulations of multiyear mean nutrient loads under scenario S3, i.e., reducing irrigation frequency to weekly on one day each week, increased TN load by 2.5% from the simulations under scenario S0, while almost no change was found in TP load (Fig. 3.8). Interannual variability in TP load simulations was relatively small, while large increases in annual TN load were found under scenario S3 (Table 3.6).

Simulations of multiyear mean nutrient loads under scenario S4 of no irrigation gave a major decrease in TN load (66%) and less so for TP load (10%), compared with the scenario S0 (Fig. 3.8). A visual inspection of Fig. 3.9 shows that it took around nine months for NO<sub>3</sub>-N load to decrease to within about 20% of its pre-irrigation values after irrigation ceased. Interannual variability in nutrient loads was relatively small (Table 3.6).

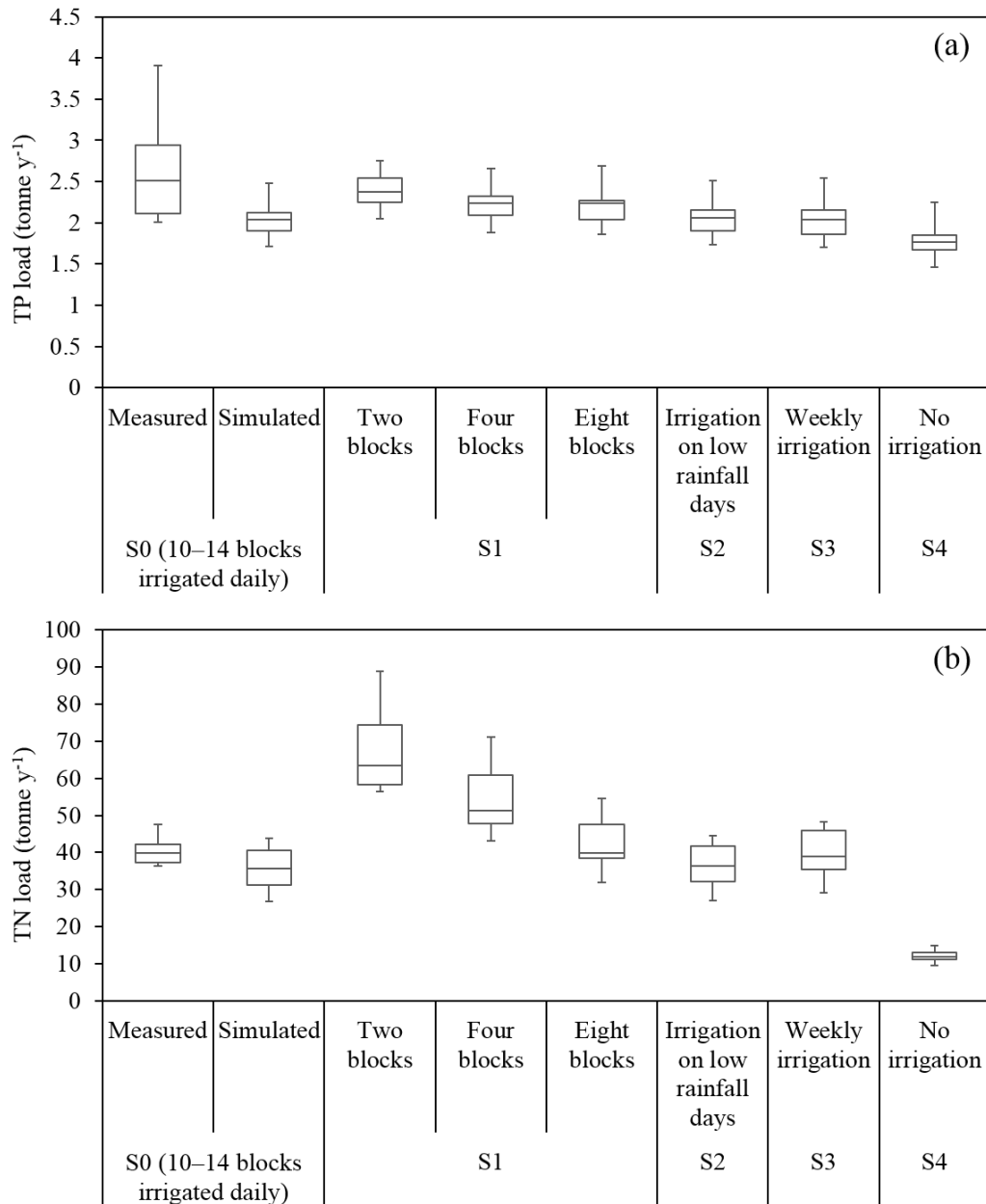


**Figure 3.8** Multiyear (2003–2012) mean of total annual measured and simulated (a) total phosphorus (TP) and (b) total nitrogen (TN). S0 is 10–14 blocks irrigated daily, S1 is decreased irrigated area, S2 is reassigned irrigation from high rainfall ( $\geq 20 \text{ mm d}^{-1}$ ) days to low rainfall days, S3 is reduced irrigation frequency to one day per week and S4 is no irrigation. Boxes denote interquartile ranges (i.e., 25% and 75%); whiskers denote minimum and maximum values; horizontal lines denote median values.

**Table 3.6** Change of annual total phosphorus (TP) and total nitrogen (TN) loads under four different irrigation scenarios from the simulations under the actual irrigation scenario (S0: 10–14 blocks irrigated daily) during 2003–2012.

Scenario	Description	Change in annual TP load (%)									
		2003	2004	2005	2006	2007	2008	2009	2010	2011	2012
S1	Two blocks	26.3	17.8	16.8	16.6	26.2	22.8	18.2	10.3	10.9	13.4
	Four blocks	11.6	11.6	9.8	10.7	13.3	11.0	8.4	4.9	7.0	6.6
	Eight blocks	7.7	10.1	9.5	11.0	11.0	7.7	6.9	5.5	8.5	6.3
S2	Irrigation on low rainfall days	0.2	1.1	1.2	1.6	1.0	1.6	1.3	1.0	1.1	1.3
S3	Weekly irrigation	-3.2	0.6	-0.4	0.0	-0.9	-1.4	0.8	1.2	2.4	2.5
S4	No irrigation	-10.9	-9.7	-13.2	-13.1	-14.8	-12.9	-16.2	-15	-9.2	-13.2
		Change in annual TN load (%)									
		2003	2004	2005	2006	2007	2008	2009	2010	2011	2012
S1	Two blocks	109.9	109.8	98.0	94.4	95.7	73.4	83.7	72.0	74.3	79.0
	Four blocks	60.6	68.0	60.9	60.9	59.0	42.1	46.8	40.4	42.8	47.2
	Eight blocks	18.7	28.6	26.3	30.4	24.4	9.5	12.8	11.1	12.2	18.1
S2	Irrigation on low rainfall days	1.0	3.8	3.1	4.6	3.2	2.9	2.2	1.5	1.8	2.3
S3	Weekly irrigation	9.2	13.6	16.2	14.2	16.7	7.8	8.2	9.7	7.3	8.7
S4	No irrigation	-49.2	-70.2	-72.1	-61.9	-69.2	-68.5	-71.4	-68.0	-65.8	-60.0

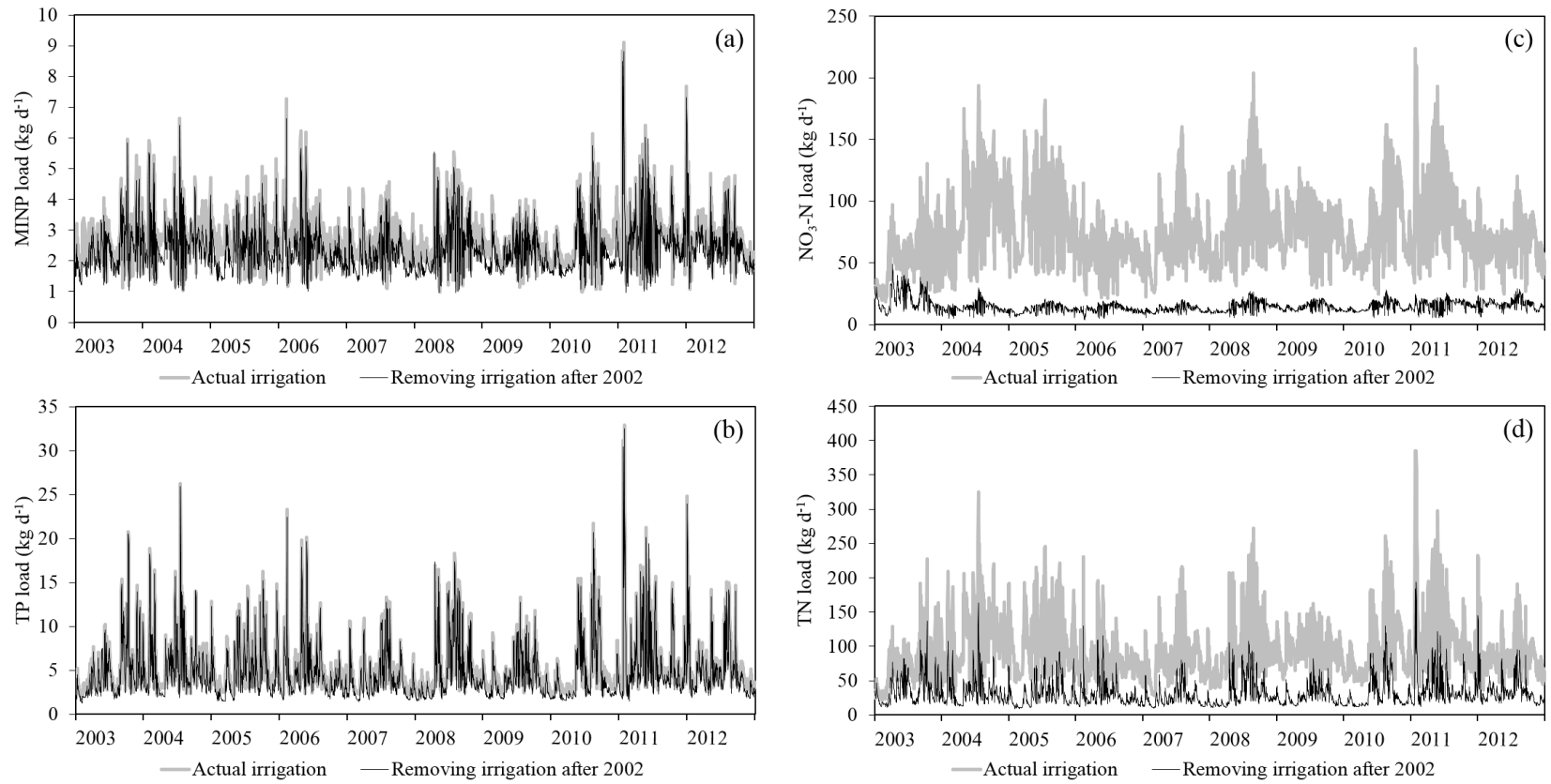


**Figure 3.9** Daily mean load simulations of (a) mineral phosphorus (MINP), (b) total phosphorus (TP), (c) nitrate–nitrogen (NO<sub>3</sub>-N), and (d) total nitrogen (TN) under actual irrigation and no irrigation.

### **3.5 Discussion**

The reuse of treated wastewater for forest irrigation has become commonplace around the world (Braatz and Kandiah, 1996), however, there are few modelling evaluations of its downstream environmental impacts (e.g., Pisinaras et al., 2010; Aouissi et al., 2014). Variability in stream discharge and nutrients will be impacted by the relative area of irrigation. Abell et al. (2013) showed high-frequency variability of discharge and nutrient concentrations in the Puarenga Stream downstream of the Waipa Stream that drains the wastewater-irrigated forest area (193 ha) which was the subject of this study. The hourly routing algorithms in the SWAT2012 model used in this study to model the Waipa Stream catchment were required to capture this variability (see Jeong et al., 2011). The SWAT2012 code was also modified to simulate a complex irrigation operation involving different spatial and temporal irrigation regimes. Simulated and measured weekly mean discharge, SS, TP and TN loads were in reasonable agreement and improved upon the statistical fit of the hourly routing algorithms, enabling the SWAT2012 model to be utilised with confidence to evaluate impacts of alternate management regimes for wastewater irrigation.

#### **3.5.1 Effectiveness and uncertainties of modified SWAT2012 code**

In this study parameters were optimised at Waipa downstream hydrometric station using hourly routing and an identical set of parameters was then used for daily routing. The hourly model, with output aggregated to weekly, overestimated observed peaks of discharge more than the daily model but tended to underestimate base flow. Overestimates of surface runoff and underestimates of base flow were also found in SWAT2005 model application by Jeong et al. (2010). Based on the same set of parameters tuned for the hourly algorithms in SWAT2005, Jeong et al. (2011) predicted annual SS yield of  $1.46 \text{ t ha}^{-1} \text{ yr}^{-1}$  for a small catchment ( $1.9 \text{ km}^2$ ), which was about one-half of that predicted using daily routing ( $2.89 \text{ t ha}^{-1} \text{ yr}^{-1}$ ). They excluded hourly routings in calculations of soil water movement, base flow and lateral flow. A similar outcome in our study suggests that parameter values may vary between daily and hourly routings (Jeong et al., 2011). Higher standard deviations in the hourly routing model appear to be related to capturing the high variability of SS in small catchments that may tend to be “flashy” (Abell et al., 2013).

The hourly routing improved simulations of MINP loads and gave high temporal variability of TP load compared with the daily routing. This may also suggest that the hourly routing is able to capture the mobilisation of TP during high flows, giving a positive relationship between discharge and TP concentrations during high flows (Abell et al., 2013). Both hourly and daily routing underestimated observed loads of P species in the stream after 2007. Harvesting operations have been widely varied amongst different harvest blocks since that time. Neither the hourly or daily routing models captured the observed increases in stream TP loads during or following harvest of several forest blocks concurrently. This suggests that algorithms for overland erosion processes that mobilise P may need to be developed or refined for this purpose, i.e., in response to temporal and spatial variance in episodic events. Wastewater application decreased after 2008, however, measured TP load in the stream increased. Both the hourly or daily routing models underestimated TP load in the stream post 2008, suggesting the algorithms may not represent certain processes associated with extended periods of wastewater irrigation, e.g., the build-up of P in the soil, the potential leaching of P into the groundwater system, and ultimately into the stream receiving waters (Beets et al., 2013). Some phosphorus parameters, e.g., PSP (soil P adsorption rate or P retention rate), PHOSKD (the ratio of P in topsoil to that discharged through surface runoff) and PPERCO (the ratio of P in topsoil to that infiltrated into subsurface soils), can be only given one value in a SWAT model applicable over the whole catchment (Arnold et al., 2013). Fixed parameter values are not temporally and spatially varied to reflect the rapid “flushing” of P from soils in response to shifting harvest areas and the legacy of soil P which builds up and may ultimately enter groundwater in long-term wastewater applications.

Despite optimisation of parameters for the hourly routing model, it would likely still be expected to perform better than the daily routing model because of ability to replicate rapid “flushing” of  $\text{NH}_4\text{-N}$  from soils in response to high rainfall events (Abell et al., 2013). The optimised value of the parameter for  $\text{NH}_4\text{-N}$  release rate from stream sediments (RS3;  $10 \text{ mg N m}^{-2} \text{ d}^{-1}$ ) was found to increase  $\text{NH}_4\text{-N}$  loads to levels comparable to those of the observations. However, this optimised value exceeded the SWAT default range ( $0\text{--}1 \text{ mg N m}^{-2} \text{ d}^{-1}$ ; see Section 3.4.1). Other model parameters affecting  $\text{NH}_4\text{-N}$  loads, e.g., mineralisation, nitrification and volatilisation rates in both terrestrial and channel processes, were constrained

within their theoretical limits in this study. Taking a parameter value beyond its default range could mean, for example, that 1) some nutrient sources in the catchment might not be accounted for (e.g.,  $\text{NH}_4$ -enriched geothermal springs; Abell et al., 2013), or 2) the model is missing some key processes related to unconsumed  $\text{NH}_4\text{-N}$  (e.g., ammonia movement in groundwater, Böhlke et al., 2006) or  $\text{NH}_4\text{-N}$  losses (e.g., ANAMMOX; anaerobic ammonia oxidation, Sliemers et al., 2003). The hourly routing also gave high temporal variability of  $\text{NO}_3\text{-N}$  and TN loads compared with the daily routing, although lower than the variability of SS and TP loads, suggesting that the hourly routing captured high-flow flushing of sediment and nutrients, i.e., in terms of variability:  $\text{SS} > \text{TP} > \text{TN}$ . This revealed different mass export mechanisms operating in the catchment between base flow and high rainfall-runoff events (Zhang et al., 2016).

### **3.5.2 Impacts of temporal and spatial variations in management practices**

In terms of model scenarios, the greatest increase in nutrient loads occurred with decreasing the irrigated area from 10–14 blocks to two blocks. Using the reverse argument, increasing the irrigation area could be expected to decrease nutrient loads. In the SWAT model the value of parameter PSP (soil P adsorption rate or P retention rate) is not distributed through soil profiles (Arnold et al., 2013), i.e., it likely had little effect on soil P adsorption rate. It is not unexpected that there was little change in P percolation and leaching into the stream for annual TP load simulations with changing irrigation frequency from daily to one day each week. By contrast, hydraulic conductivity varied through the soil profile in SWAT (Arnold et al., 2013) and therefore P leaching can be expected to increase with weekly irrigation and saturation of surface soils, resulting in increases in stream TP load. Results of reassigning irrigation during high rainfall days (maximum = three days) to the first subsequent low rainfall day produced results similar to the scenario of low-frequency and/or high-rate wastewater application. Surface soil layers become saturated at higher application rates, leading to increased P percolation and leaching into the stream, producing small increases in annual TP load.

Annual TN load increased considerably under weekly irrigation due to rapid leaching of  $\text{NO}_3\text{-N}$  through the soil profile. Compared with low-frequency, high-volume applications (once every seven days), the current strategy of daily

wastewater irrigation minimises leaching and reduces saturation of the subsurface layer. Magesan et al. (1998) investigated nitrate leaching through volcanic and allophanic soil in the study catchment (the wastewater irrigated forestry area) during 1992–1996, when the irrigation frequency was weekly. They estimated about one-half of the  $\text{NO}_3\text{-N}$  load was leached and the rest was adsorbed by the allophanic soils which have a net positive charge. In this study, during the modelling period of 2003–2012 when wastewater was irrigated daily on the forestry area, downstream measurements showed that about 30% of N load from wastewater was lost to the stream. This is a lower amount than recorded in measurements by Magesan et al. (1998) but comparable to SWAT2012 simulations (35% lost to the stream). The differences between in-stream nitrogen measurements undertaken during two irrigation regimes (weekly vs. daily) are consistent with modelling, showing decreased in-stream TN loads under daily irrigation. Decreases in stream TN load could also be contributed by increasing irrigated area and facilitating losses to plant uptake and denitrification.

Me et al. (2015) applied the SWAT2009 parameter set optimised for nutrient simulations under daily irrigation, to the period of weekly irrigation (1994–1997). They overestimated in-stream TN concentrations. They suggested that the SWAT2009 model may not adequately represent the dynamics of groundwater nutrient concentrations, particularly in the presence of changes in catchment inputs (e.g., with start-up of wastewater irrigation). Under the present regime of daily irrigation of treated wastewater, soil sorption capacity and plant uptake rates of N may ultimately reach some quasi equilibrium, with minimal adsorption and high rates of N percolation to the groundwater. Therefore, an embedded groundwater module could be used to simulate the temporal dynamics of N leaching to groundwater and to give opportunities to explicitly account for the dynamics of the subsurface zone.

Rotorua District Council consent conditions restrict nutrient inputs into the Waipa Stream (TN: 30 tonnes  $\text{yr}^{-1}$ ; TP: 3 tonnes  $\text{yr}^{-1}$ ; Park and Holst, 2009). Non-compliance with the nutrient limits in the study catchment has been increasing because of the irrigated wastewater application and increasing volumes of wastewater coming into the treatment plant as sewage reticulation of widely dispersed settlements has expanded. Removing irrigation completely was modelled in this study as the most effective strategy reduce nutrient loads. The simulation

result showed that it took around nine months for NO<sub>3</sub>-N load to decrease to within about 20% of its pre-irrigation values after irrigation ceased. The Rotorua District Council has made a decision to cease irrigation to the Whakarewarewa Forest by 2019 although there has been no decision on an alternate method of disposal of wastewater. Thus the no-irrigation scenario will be directly relevant to the situation in 2019. Observations following irrigation removal can be expected to provide a robust test of model performance, particularly with respect to the duration on which NO<sub>3</sub>-N concentrations can be expected to decrease in the Waipa Stream.

### 3.6 References

- Abell, J.M., Hamilton, D.P., and Rutherford, J.C.: Quantifying temporal and spatial variations in sediment, nitrogen and phosphorus transport in stream inflows to a large eutrophic lake, *Environ. Sci.: Processes Impacts*, 15, 1137–1152, 2013.
- Aouissi, J., Benabdallah, S., Chabaâne, Z.L., and Cudennec, C.: Modeling water quality to improve agricultural practices and land management in a Tunisian catchment using the Soil and Water Assessment Tool, *J. Environ. Qual.*, 43, 18–25, 2014.
- Arnold, J., Kiniry, J., Srinivasan, R., Williams, J., Haney, E., and Neitsch, S.: Soil & Water Assessment Tool Input/output documentation version 2012, Technical Report No 439, Texas Water Resources Institute, College Station, TX, the United States, 651 pp., 2013.
- Arnold, J.G., Srinivasan, R., Muttiah, R.S., and Williams, J.R.: Large area hydrologic modeling and assessment Part I: Model development, *J. Am. Water Resour. As.*, 34, 73–89, 1998.
- Bagnold, R.A.: Bed load transport by natural rivers, *Water Resour. Res.*, 13, 303–312, 1977.
- Beets, P.N., Gielen, G., Oliver, G.R., Pearce, S.H., and Graham, J.D.: Determination of the level of soil N and P storage and soil health at the Rotorua Land Treatment site, Scion Report 50659, New Zealand Forest Research Institute Limited, Rotorua, New Zealand, 39 pp., 2013.
- Behera, S.K., and Panda, R.K.: Evaluation of management alternatives for an agricultural watershed in a sub-humid subtropical region using a physical process based model, *Agr. Ecosyst. Environ.*, 113, 62–72, 2006.
- Bewick, V., Cheek, L., and Ball, J.: Statistics review 7: correlation and regression, *Crit. Care*, 7, 451–459, 2003.

- Böhlke, J., Smith, R.L., and Miller, D.N.: Ammonium transport and reaction in contaminated groundwater: application of isotope tracers and isotope fractionation studies, *Water Resour. Res.*, 42, W05411, 2006.
- Braatz, S., and Kandiah, A.: The use of municipal waste water for forest and tree irrigation, *Unasylva*, 47, 45–51, 1996.
- Brown, L.C., and Barnwell, Jr. T.O.: The enhanced water quality models QUAL2E and QUAL2E-UNCAS: documentation and user manual, EPA document EPA/600/3-87/007, Environmental Research Laboratory Office of Research and Development, U.S. Environmental Protection Agency, Athens, Georgia, the United States, 204 pp., 1987.
- Carpenter, S.R., Caraco, N.F., Correll, D.L., Howarth, R.W., Sharpley, A.N., and Smith, V.H.: Nonpoint pollution of surface waters with phosphorus and nitrogen, *Ecol. Appl.*, 8, 559–568, 1998.
- Cau, P., and Paniconi, C.: Assessment of alternative land management practices using hydrological simulation and a decision support tool: Arborea agricultural region, Sardinia, *Hydrol. Earth Syst. Sc.*, 11, 1811–1823, 2007.
- Dabrowski, J.M.: Applying SWAT to predict ortho-phosphate loads and trophic status in four reservoirs in the upper Olifants catchment, South Africa, *Hydrol. Earth Syst. Sc.*, 18, 2629–2643, 2014.
- Dechmi, F., Burguete, J., and Skhiri, A.: SWAT application in intensive irrigation systems: Model modification, calibration and validation, *J. Hydrol.*, 470–471, 227–238, 2012.
- Dechmi, F., and Skhiri, A.: Evaluation of best management practices under intensive irrigation using SWAT model, *Agr. Water Manage.*, 123, 55–64, 2013.
- Farahat, E., and Linderholm, H.W.: The effect of long-term wastewater irrigation on accumulation and transfer of heavy metals in *Cupressus sempervirens* leaves and adjacent soils, *Sci. Total Environ.*, 512–513, 1–7, 2015.
- Gabriele, W., Welte, N., and Hein, T.: Limitations of stream restoration for nitrogen retention in agricultural headwater streams, *Ecol. Eng.*, 60, 224–234, 2013.
- Green, S.R., Snow, V.O., and Clothier, B.E.: Modelling the nitrogen dynamics under pasture irrigated with dairy factory effluent, HortResearch Client Report No. 2003/6115, HortResearch, Palmerston North, New Zealand, 54 pp., 2003.
- Green, W.H. and Ampt, G.A.: Studies on soil physics, part I – the flow of air and water through soils, *J. Agr. Sci.*, 4, 1–24, 1911.
- Hu, H.R., Wang, H.L., Beecroft, K., Kimberley, M., Magesan, G., and Bolan, N.: Movement of phosphorus in soil at the Rotorua land treatment system, New Zealand Land Treatment Collective: Proceedings of the 2007 Annual Conference, Rotorua, New Zealand, pp. 74–81, 2007.

- Jeong, J., Kannan, N., Arnold, J., Glick, R., Gosselink, L., and Srinivasan, R.: Development and integration of sub-hourly rainfall-runoff modeling capability within a watershed model, *Water Resour. Manag.*, 24, 4505–4527, 2010.
- Jeong, J., Kannan, N., Arnold, J.G., Glick, R., Gosselink, L., Srinivasan, R., and Harmel, R.D.: Development of sub-daily erosion and sediment transport algorithms for SWAT, *T. ASABE.*, 54, 1685–1691, 2011.
- Kaur, R., Wani, S.P., Singh, A.K., and Lal, K.: Wastewater production, treatment and use in India, Presented at the Second Regional Workshop of the Project ‘Safe Use of Wastewater in Agriculture’, New Delhi, India, 13 pp., 2012.
- Krebs, C.J.: Restoration ecology applies ecological knowledge to repair damaged communities, in: *The ecological world view*, edited by: Krebs, C.J., University of California Press, Berkeley and Los Angeles, California, the United States, 300 pp., 2008.
- Lim, K.J., Engel, B.A., Tang, Z., Choi, J., Kim, K., Muthukrishnan, S., and Tripathy, D.: Automated Web GIS-based Hydrograph Analysis Tool, WHAT, *J. Am. Water Resour. As.*, 41, 1407–1416, 2005.
- Lowe, A., Gielen, G., Bainbridge, A., and Jones, K.: The Rotorua Land Treatment Systems after 16 years, in: *New Zealand Land Treatment Collective – Proceedings for the 2007 Annual Conference*, Rotorua, New Zealand, pp. 66–73, 2007.
- Magesan, G.N., McLay, C.D.A., and Lal, V.V.: Nitrate leaching from a free-draining volcanic soil irrigated with municipal sewage effluent in New Zealand, *Agr. Ecosyst. Environ.*, 70, 181–187, 1998.
- Me, W., Abell, J.M., and Hamilton, D.P.: Effects of hydrologic conditions on SWAT model performance and parameter sensitivity for a small, mixed land use catchment in New Zealand, *Hydrol. Earth Syst. Sc.*, 19, 4127–4147, 2015.
- Moriasi, D.N., Arnold, J.G., Van Liew, M.W., Bingner, R.L., Harmel, R.D., and Veith, T.L.: Model evaluation guidelines for systematic quantification of accuracy in watershed simulations, *T. ASAE*, 50, 885–900, 2007.
- Morris, M.D.: Factorial sampling plans for preliminary computational experiments, *Technometrics*, 33, 161–174, 1991.
- Mussely, H., and Goodwin, E.: Feasibility of land-based aquaculture in New Zealand, Cawthron Report No. 2094, Cawthron Institute, Nelson, New Zealand, 20 pp., 2012.
- Neitsch, S.L., Arnold, J.G., Kiniry, J.R., and Williams, J.R.: Soil and Water Assessment Tool theoretical documentation version 2009, Texas Water Resources Institute Technical Report No. 406, Texas A&M University System, College Station, Texas, the United States, 647 pp., 2011.

- OECD (Organisation for Economic Co-operation and Development): Environmental performance reviews: Germany, Environmental Performance, Paris, France, 236 pp., 2001.
- Park, S., and Holst, J.: Rotorua District Council Spray Irrigation Compliance Report, Environmental Publication 2009/13, Environment Bay of Plenty, Whakatane, New Zealand, 50 pp., 2009.
- Pisinaras, V., Petalas, C., Gikas, G.D., Gemitzi, A., and Tsihrintzis, V.A.: Hydrological and water quality modeling in medium-sized basin using the Soil and Water Assessment Tool (SWAT), *Desalination*, 250, 274–286, 2010.
- Raschid-Sally, L., and Jayakody, P.: Drivers and characteristics of wastewater agriculture in developing countries: results from a global assessment, International Water Management Institute Research Report 127, Colombo, Sri Lanka, 35 pp., 2008.
- Shen, Z.Y., Chen, L., and Chen, T.: Analysis of parameter uncertainty in hydrological and sediment modeling using GLUE method: a case study of SWAT model applied to three gorges reservoir region, China, *Hydrol. Earth Syst. Sc.*, 16, 121–132, 2012.
- Sliemers, A.O., Third, K.A., Abma, W., Kuenen, J.G., and Jetten, M.S.M.: Canon and Anammox in a gas-lift reactor, *FEMS Microbiol. Lett.*, 218, 339–344, 2003.
- Vieritz, A.M., Truong, P., Gardner, T., and Smeal, C.: Modelling *Monto vetiver* growth and nutrient uptake for effluent irrigation schemes, Proceedings for the Third International Conference on Vetiver, Guangzhou, China, 13 pp., 2003.
- Vogeler, I., Green, S., Magesan, G., and Clothier, B.: Measuring and modelling water dynamics under effluent irrigated pine trees, SuperSoil 2004: Proceedings of the 3rd Australian New Zealand Soils Conference, University of Sydney, Australia, 6 pp., 2004.
- White, M.J., Storm, D.E., Mittelstet, A., Busteed, P.R., Haggard, B.E., and Rossi, C.: Development and testing of an in-stream phosphorus cycling model for the Soil and Water Assessment Tool, *J. Environ. Qual.*, 43, 215–223, 2014.
- Yang, X., Liu, Q., He, Y., Luo, X., and Zhang, X.: Comparison of daily and sub-daily SWAT models for daily streamflow simulation in the Upper Huai River Basin of China, *Stoch. Env. Res. Risk A.*, 30, 959–972, 2016.
- Zhang, Q., Ball, W.P., and Moyer, D.L.: Decadal-scale export of nitrogen, phosphorus, and sediment from the Susquehanna River basin, USA: analysis and synthesis of temporal and spatial patterns, *Sci. Total Environ.*, 563, 1016–1029, 2016.

## **4 Simulating variations in discharge and nutrient loads from a mixed land use catchment to a eutrophic lake: Effects of nutrient reductions and future climate**

### **4.1 Abstract**

Understanding anthropogenic changes to catchment nutrient transport and climate-induced changes in lake processes is critical for eutrophication assessment and sustainable management of lakes. The objective of this study was to combine the catchment model Soil and Water Assessment Tool (SWAT2012 rev629) with the one-dimensional lake water quality model DYRESM-CAEDYM (DYnamic REservoir Simulation Model – Computational Aquatic Ecosystem DYnamics Model version 4.0) to simulate the trophic state of Lake Rotorua, in response to nutrient load reductions from wastewater-irrigated forest and farmland in a major sub-catchment (the Puarenga Stream) under present and future climates. A range of statistical metrics indicated that the SWAT2012 model performed well ( $r \geq 0.88$ ,  $p < 0.001$ ) with respect to daily catchment discharge, and monthly total nitrogen (TN) and total phosphorus (TP) loads for the 4-year (2006–2010) simulation period. The model simulated TN concentrations ( $r = 0.78$ ,  $p < 0.01$ ) better than TP concentrations ( $r = 0.17$ ,  $p > 0.5$ ). SWAT2012 model simulations were used for the Puarenga Stream input to the DYRESM-CAEDYM model of Lake Rotorua while other inflows used measured data. Considering the 1.5-year lake residence time for Lake Rotorua, the DYRESM-CAEDYM model was validated using monthly data collected at two sites during 2008–2010. The performance of the lake model was satisfactory ( $r \geq 0.63$ ;  $p < 0.01$ ) for surface water TP and TN concentrations in both the calibration and validation periods, providing confidence that the key processes that affect trophic status variables were adequately represented, but the performance was not as good for bottom-water nutrient concentrations. Effects of changes to land management in one sub-catchment were then examined by using three scenarios of nutrient loading reduction relating to cessation of current wastewater irrigation and/or cessation of pastoral fertilisation. Simulating removal of both pastoral and irrigation nutrient sources yielded nutrient load reductions of 39.5% for TP and 75.2% for TN in the Puarenga Stream but these had little effect on nutrient concentrations in the lake, with reductions of 3.5% for TP, 5.7% for TN,

and 4.1% for chlorophyll *a* (Chl *a*) in surface waters. To simulate effects due to projected climate change, downscaled climate projections for 2090 were derived from 22 general circulation models and used as input to SWAT2012 and DYRESM–CAEDYM. For the projected future climate of 2090, annual mean precipitation and solar radiation increase by 2.8% and 1.4%, respectively, humidity decreases by 0.6%, and air temperature increases by 2.7 °C. Simulations using a projected climate for 2090 had moderate impact on catchment nutrient loads (6% increase for TP, 7.6% decrease for TN) but large impacts on lake surface water quality, with predicted increases of 45.9% for TP, 44.5% for TN, and 44.9% for Chl *a* concentrations from 2010 to 2090. This suggests that future climate change would exacerbate eutrophication, primarily due to effects on in-lake processes rather than catchment processes. Increased water temperatures would cause more frequent and prolonged periods of thermal stratification in polymictic lakes such as Lake Rotorua, which would likely result in greater depletion of dissolved oxygen and potential for anoxia of bottom waters. This overarching effect of climate change is likely to be through a physical response of the lake in the form of increased stratification and greater levels of internal nutrient loading. The combined climate–catchment–lake modelling results suggest that increased internal loads and higher rates of phytoplankton growth may increase eutrophication more than changes in external loading, but the two effects will act synergistically to increase the potential for eutrophication of lake ecosystems.

## **4.2 Introduction**

Increased nutrient loads from agricultural and municipal wastewater sources have dramatically reduced the ecological quality of receiving waterbodies in many lake catchments (Foote et al., 2015; Hussain et al., 2002). In many catchments, actions are underway to address point and diffuse sources of nutrient pollution, as mandated by environmental regulation and community concerns regarding water quality (Scavia et al., 2014; Hamilton et al., 2016). Examples of such actions include the diversion of wastewater discharges (OECD, 2001; Krebs, 2008), changes to farming practices and agricultural land use (Abell et al., 2011), or the use of a range of geo-engineering techniques (e.g., Spears et al., 2013), including the application of alum (aluminium sulphate) to lake inflows (Smith et al., 2016).

In addition to the management changes described above, changes in climate are predicted to affect the hydrological cycle and thus also modify nutrient transformation and transport processes in terrestrial and aquatic environments. For example, an increase in total phosphorus (TP) loads of 3.3% to 16.5% in Danish streams in the next century was predicted by Jeppesen et al. (2009), mostly in response to increased precipitation in winter. A climate-induced increase in the loss of total nitrogen (TN) from a small Mediterranean catchment (30 km<sup>2</sup>) in Slovenia was predicted by Glavan et al. (2015), who applied six climate scenarios for three future periods (2030s, 2060s, 2090s). Their modelled changes in TN loads (2061–2090) ranged from 5.3% to 80.2%, mostly in response to increasing precipitation. On the contrary, other studies have indicated that nutrient loading for the catchment may actually go down with climate warming primarily because warmer air temperatures increase evaporation, resulting in less runoff. Robertson et al. (2016) projected decreases in total annual streamflow (-1.8% average, ranging from -21.2% to +8.9%) and TP loads (-3.1% average, ranging from -21.2% to +8.9%) for the Lake Michigan Basin by 2045–2065, in consideration of the projected variability in total annual precipitation (+5.1% average, ranging from -5.1% to +16.7%) and average annual air temperature (+2.6 °C average, ranging from +2.1 to +4.0 °C).

Climate change also directly influences lake water temperature and stratification, which may in turn modify in-lake nutrient dynamics (Arnell et al., 2015). A modelling study of three New Zealand lakes (Trolle et al., 2011) showed that the effect on water quality of a mid-range climate warming projection for 2100 would equate to increasing external nutrient loads by 25–50%. Similarly, Hamilton et al. (2012) showed negative effects of future climate on lake water quality, including increased trophic state and frequency of cyanobacteria blooms. Climate change could also affect the transport and processing of nutrients in lake catchments, as well as processes within receiving waters. Some of these processes may be synergistic whereby increased catchment nutrient loads interact with higher water temperatures to stimulate growth of bloom-forming cyanobacteria (Hamilton et al., 2016).

Few studies have connected climate, catchment and lake models to provide ecosystem-scale assessments of hydrological and water quality responses to climate and land use changes. General circulation models (GCMs), downscaled by pattern scaling methods (Santer et al., 1990) provide future climate scenarios at a

regional scale (Tebaldi and Arblaster, 2014; Herger et al., 2015) and have been applied to examine impacts on freshwater resources (Todd et al., 2011) and terrestrial processes (Huntingford et al., 2010). The main assumption underlying the pattern scaling method is that the local response of a climate variable is linearly related to the global mean temperature change (Mitchell, 2003). This theory has some limitations in projecting future extreme events (Lustenberger et al., 2014) and the spatial variability of climate data (Tebaldi and Arblaster, 2014). To overcome these limitations, ensemble simulations using multiple GCMs is recommended for the assessment of climate change impacts (Murphy et al., 2007; Lopez et al., 2014).

To assess temporal responses of receiving environments to catchment inputs, studies have been undertaken that link outputs from a catchment model (e.g., SWAT: Soil Water and Assessment Tool) to a water quality model (e.g., CEQUAL-W2; Debele et al., 2008, WASP; Narasimhan et al., 2010, or DYRESM-CAEDYM; Copetti et al., 2006). The process-based catchment model SWAT provides the ability to simulate time-varying land management practices in catchments (Neitsch et al., 2011), and has been applied to a small number of New Zealand catchments (e.g., Cao et al., 2006; Morcom, 2013; Me et al., 2015). DYRESM-CAEDYM, a process-based, one-dimensional hydrodynamic-biogeochemical aquatic ecosystem model, can be used to simulate in-lake processing of nutrients and biological responses (Hamilton and Schladow, 1997). It has been applied to lakes across the globe (Bruce et al., 2006; Trolle et al., 2008) and to several New Zealand lakes to predict water quality and trophic state (Rutherford et al., 1996; Burger et al., 2008; Trolle et al., 2011). DYRESM-CAEDYM has been supplied with inflow data from simulations using the SWAT model for a catchment in North Italy (Copetti et al., 2006) to examine seasonal trends in lake surface water temperature, water column thermal gradients and dynamics of phosphorus and phytoplankton.

Lake Rotorua, located in the Bay of Plenty Region of the North Island of New Zealand, is a nationally-*iconic* water body and plays a significant role in recreation and tourism at national scale (Hamilton et al., 2012). However, pastoral land has been progressively developed throughout the lake catchment over recent decades, and eutrophication has increased due to the resulting intensification of catchment land use (e.g., Mueller et al., 2015). Urban wastewater was discharged to the lake until 1991 after which time forest blocks in one lake sub-catchment

(Puarenga) have been irrigated with treated municipal wastewater. Resource consent conditions for wastewater disposal to the forest blocks restrict TN and TP wastewater losses to the receiving stream to 30 t yr<sup>-1</sup> and 3 t yr<sup>-1</sup>, respectively. Previous assessments of nutrient losses have indicated some non-compliance with the TN consent limit and there is some indication of an increase in TP loading to the receiving stream since 2002 (Me et al., 2017). These increases may be caused by a number of factors including the application rate of wastewater, increases in the nutrient load from non-irrigated areas within the catchment, forest operations not associated with wastewater irrigation and altered rainfall patterns. The SWAT2012 model was used in this study to simulate discharge and nutrient loads from the Puarenga Stream to the lake under current land use practices and climate, to provide a “reference” condition. An essential task was to assess how a suite of scenarios of nutrient reductions and climate change might affect nutrient loads in the Puarenga Stream (using SWAT2012 rev629) and water quality in Lake Rotorua (using DYRESM-CAEDYM version 4.0). Coupling of these two models (i.e., output from SWAT2012 as input for DYRESM-CAEDYM to simulate common variables) was used in this study to better understand the potential for synergistic or antagonistic interactions between climate and land use in Lake Rotorua.

## **4.3 Methods**

### **4.3.1 Study area and measured data**

Lake Rotorua is located in the North Island of New Zealand (Fig. 4.1) and is subjected to a warm temperate climate. Annual mean precipitation of 1252 mm, air temperature 12.6 °C, relative humidity 81%, short-wave radiation 170 W m<sup>-2</sup> and wind speed 3.6 m s<sup>-1</sup> (at 10 m above the water surface) for Lake Rotorua were calculated for the period July 2006 – June 2010 (Fig. 4.1; National Climatic Database; available at <http://cliflo.niwa.co.nz/>).

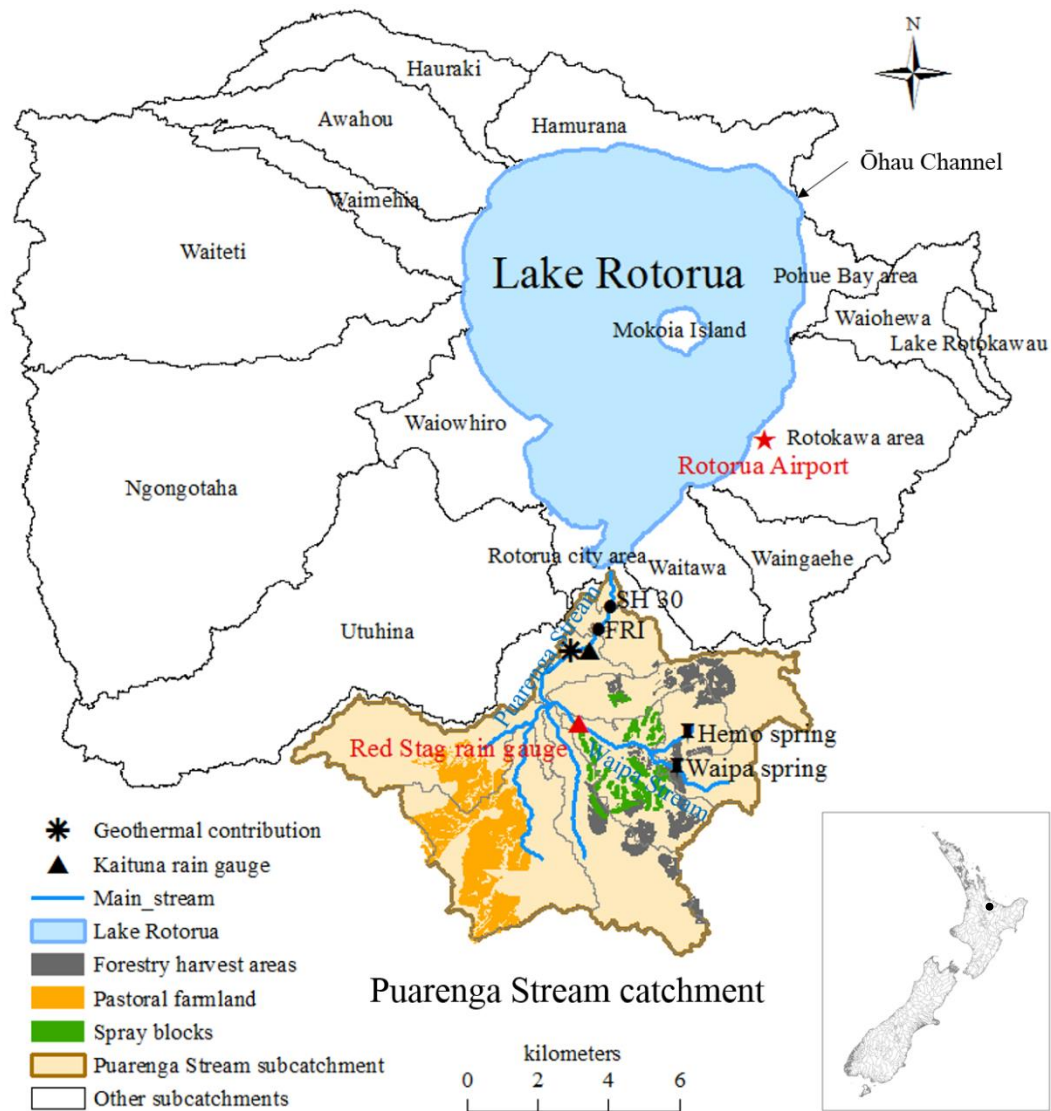


**Figure 4.1** Lake Rotorua surface topographic catchment showing the major sub-catchments. The Puarenga Stream catchment modelled in this study is located in the south. The only outlet from Lake Rotorua is the Ōhau Channel. Inset: Map of New Zealand showing location of Rotorua.

Lake Rotorua (surface area 80.8 km<sup>2</sup>, mean depth 10.8 m) is a polymictic, temperate lake which receives inflow from nine major surface streams and nine smaller surface streams (Fig. 4.1; Hoare, 1980). The only surface outflow (mean annual discharge 18.5 m<sup>3</sup> s<sup>-1</sup>) is the Ōhau Channel (Fig. 4.1; Hoare, 1980). The residence time of Lake Rotorua is 1.5 years. Surface water temperature at 0.5 m in Lake Rotorua ranges from 10 °C to 22 °C for 2006–2010 (Abell et al., 2015). The regional management authority, Bay of Plenty Regional Council (BoPRC), has assigned a target Trophic Level Index (TLI) for Lake Rotorua of 4.2. The TLI is commonly used in New Zealand to quantify trophic state and integrates annual

mean values of four variables: Secchi disc depth (a measure of transparency) and concentrations of Chl *a*, TP, and TN (Burns et al., 1999). The target value of 4.2 for Lake Rotorua corresponds to a eutrophic status (i.e., between 4 and 5) and is based on historical data for around 1970, when the lake was deemed to have acceptable water quality (Scholes 2011). Alum dosing of two inflows has been used to reduce TP in Lake Rotorua and correspondingly, the TLI (Smith et al., 2016). The first dosing station commenced operation in the Utuhina Stream in June 2006 and the second dosing commenced in the Puarenga Stream in January 2010 (Fig. 4.1). Measured data for Lake Rotorua during January 2008 – June 2010 were used for DYRESM–CAEDYM baseline simulations. Concentrations of phosphate (PO<sub>4</sub>–P), ammonium–nitrogen (NH<sub>4</sub>–N), nitrate–nitrogen (NO<sub>3</sub>–N), TP, TN and Chl *a* are monitored monthly at two depths (integrated 0–6 m and 19 m) in Lake Rotorua by BoPRC.

The Puarenga Stream is the second largest surface inflow to Lake Rotorua and drains a catchment of 77 km<sup>2</sup> (Fig. 4.1). The Puarenga Stream catchment is moderately steep (mean slope = 9%; equal to 5.7 degrees slope) and the predominant land uses are exotic *Pinus radiata* forest (47%) and pastoral farmland (26%; New Zealand Land Cover Database Version 2, BoPRC). There are two cold–water springs (Waipa Spring and Hemo Spring) and one geothermal spring within the catchment area (Fig. 4.1). Cold–water springs in the Puarenga catchment originate from aquifers in the underlying volcanic geology (Morgenstern et al., 2015) and contribute a high TP load (8.75 t P yr<sup>-1</sup>) to the Puarenga Stream (Kim Lockie; Rotorua Lakes Council; personal communication). Fertiliser (~40 t yr<sup>-1</sup> of P and 127 t yr<sup>-1</sup> of N) has been applied to 8 km<sup>2</sup> of pastoral farmland (Fig. 4.1) in the Puarenga Stream catchment since about 1950 (Anastasiadis et al., 2011). Urea is typically applied twice, in winter and spring, and four times during summer and autumn, at a total rate of ~200 kg ha<sup>-1</sup> yr<sup>-1</sup> of N; di–ammonium phosphate is applied once or twice, in spring and autumn, at a total rate equivalent to ~50 kg ha<sup>-1</sup> yr<sup>-1</sup> of P (Alastair McCormick; BoPRC; personal communication). Treated municipal wastewater has been applied to up to 16 forestry blocks (~2 km<sup>2</sup> in total; Fig. 4.1) since 1991, at a rate of ~19,000 m<sup>3</sup> d<sup>-1</sup>, which equates to approximately 25 t yr<sup>-1</sup> of P and 53 t yr<sup>-1</sup> of N. The initial irrigation schedule involved applying wastewater to two blocks with a daily rotation (i.e., a total of 14 blocks were irrigated weekly). Since 2002, wastewater has been irrigated daily on 10–14 blocks (Lowe et al., 2007).

The irrigated land treatment area has allophanic soils which retain 85–95% of the irrigated P (Beets et al., 2013), and the unirrigated area has mostly pumice soils that have moderate (50–60%) soil sorption capacity for P (Saunders, 1965; Fertiliser & Lime Research Centre, 2014).

Puarenga Stream water samples were collected at the Forest Research Institute (FRI) stream–gauge (1.7 km upstream of Lake Rotorua; Fig. 4.1) by BoPRC. Measurements at the FRI stream–gauge were considered representative of the contribution of the Puarenga Stream catchment to Lake Rotorua. Discharge data were collected by BoPRC at 15–minute intervals for the period 2005 through 2010 (annual mean  $2.2 \text{ m}^3 \text{ s}^{-1}$ ). Discharge records of the Puarenga Stream during 1998–2004 were intermittent because the FRI stream–gauge was closed in mid–1997 and reopened late in 2004 (Environment Bay of Plenty, 2007). Measured data for the Puarenga Stream before June 2010 were used for the SWAT2012 model baseline simulation as the FRI stream–gauge was thereafter repositioned 720 m downstream to the State Highway 30 (SH 30) (Fig. 4.1). Concentrations of suspended sediment (SS), dissolved reactive phosphorus (DRP), organic phosphorus (ORGP),  $\text{NH}_4\text{-N}$ ,  $\text{NO}_3\text{-N}$ , organic nitrogen (ORGN), TP and TN were measured monthly in the Puarenga Stream (Scholes, 2011). Daily surface inflow and nutrient concentrations of eight other major inflows of Lake Rotorua were measured and nine minor inflows were estimated by Abell et al. (2015; see Table 4.1) for the same period as the Puarenga Stream. Based on these data the Puarenga Stream contributes 16.5% of total inflow volume, 15.6% of TP load, and 16.2% of TN load to Lake Rotorua (Table 4.1). The locations of contributing catchments are shown in Fig. 4.1.

#### **4.3.2 Model configuration**

Key SWAT input data requirements included: a digital elevation model (DEM; 25 m horizontal resolution); meteorological records obtained from Rotorua Airport Weather Station; rainfall data from the Kaituna and Red Stag rain gauges; records of two cold–water springs and one geothermal spring, water abstraction and nutrient concentrations in spring discharges; a stream digital map obtained from BoPRC; soil characteristics obtained from S–map (developed by Landcare Research; see <http://smap.landcareresearch.co.nz/home>); land use classifications (obtained from New Zealand Land Cover Database Version 2, BoPRC); and management schedules (obtained from BoPRC) for key land uses (i.e., pasture fertilisation,

wastewater irrigation and timber harvesting). The delineation of the Puarenga Stream catchment (Me et al., 2015) included ten sub-catchments (Fig. 4.1) and 622 hydrological response units (HRUs). The SWAT2012\_rev629 code was used which includes modifications to hourly simulations of SS loads in-stream, nutrient applications in management practice, and some unit corrections in soil nutrient cycling calculations. Further details of code modifications are outlined in Appendix 1.

The SWAT2012 model was not set up for eight other major catchments or nine minor catchments because the information required for model setup was limited and a key objective of the study was to examine the effects of treated wastewater irrigation (specific to the Puarenga Stream) on lake water quality. Instead, other inflow input data used either measurements or values derived from other studies.

The DYRESM-CAEDYM model (version 4.0) was used to simulate hydrodynamic and biogeochemical processes in Lake Rotorua. Key forcing data were climate, bathymetry, inflow volume and nutrient concentrations, and outflow volume. The nine major inflows were classified into surface water-dominated or groundwater-dominated based on the variability of daily inflow water temperature. Catchments where mainstream water temperatures ranged  $> \pm 25\%$  of their multi-year daily mean water temperature were defined as surface water-dominated and the remainder as groundwater-dominated (see Table 4.1). The remaining nine minor streams were represented as a single inflow representing the residual term of the lake water balance used in DYRESM-CAEDYM. A lake water balance to estimate additional residual inflow was calculated after the method described in Hamilton et al. (2012). The inflow from minor streams was assumed to be predominantly surface waters. Outflow via the Ōhau Channel represented in the lake model was based on daily mean discharge measurements provided by Abell et al. (2015).

**Table 4.1** Inflows to Lake Rotorua represented in the model. Six inflows were classified as surface (S) water–dominated catchments and four as groundwater (G)–dominated catchments (see Section 4.3.2). Mean annual inflow water temperature ( $T_{inf}$ ), discharge, concentrations of total phosphorus (TP) and total nitrogen (TN), and percentage of inflow volume, TP and TN load contributions were derived from Abell et al. (2015) for July 2006 to June 2010.

Stream name	Water source	Catchment area (km <sup>2</sup> )	$T_{inf}$ (°C)	Discharge (m <sup>3</sup> s <sup>-1</sup> )	Inflow volume (%)	TP (mg L <sup>-1</sup> )	TP load (%)	TN (mg L <sup>-1</sup> )	TN load (%)
Awahou	G	19.9	15.4	1.9	14.3	0.065	14.6	1.38	17.3
Hamarana	G	16.0	12.4	2.6	19.6	0.077	23.7	0.77	13.2
Ngongotaha	S	77.4	11.0	2.0	15.0	0.043	10.2	0.98	12.9
Puarenga	S	77.0	14.5	2.2	16.5	0.060	15.6	1.12	16.2
Utuhina	S	61.0	12.8	1.8	13.5	0.057	12.1	0.95	11.3
Waingaehe	G	11.0	15.4	0.3	2.3	0.106	3.8	1.60	3.2
Waiohewa	S	11.7	13.4	0.4	3.0	0.067	3.2	2.56	6.8
Waiowhiro	S	13.6	12.7	0.3	2.3	0.057	2.0	0.95	1.9
Waiteti	G	61.9	11.8	1.4	10.5	0.052	8.6	1.41	13.0
Minor streams	S	61.1	16.0	0.4	3.0	0.130	6.2	1.61	4.2

### 4.3.3 Model calibration and validation

Simulation results were generated at daily interval from SWAT2012 for the four-hydrological-year baseline period from July 2006 to June 2010. The calibration period was July 2006 to June 2009, and the validation period was July 2009 to June 2010. This period coincided with when alum dosing started in June 2006 (Smith et al., 2016) and the stream gauge repositioning in July 2010. One year was for the SWAT2012 model warm-up and its simulations from July 2006 were used to drive DYRESM-CAEDYM. The lake model warm-up was from June 2006 to December 2007, corresponding to the 1.5-year lake residence time and a transition period of water quality first responding to alum dosing. The calibration period for the DYRESM-CAEDYM model was January 2008 to June 2009, and the validation period was July 2009 to June 2010.

Initial parameter values required for the setup of both models were based on observed monitoring data that were measured close to the start date of the simulation period. Parameter values for the lake model (DYRESM-CAEDYM) were based on previous applications of the model for Lake Rotorua with subsequent adjustments of parameters for nutrient release rates from the bottom sediment (Burger et al., 2008) and particulate organic matter size and density (to increase sedimentation rates) to account for the in-lake effects of alum dosing (Hamilton et al., 2012; Abell et al., 2015). Minor adjustments were made based on one-at-a-time (OAT) calibration (Morris, 1991) using the mean values of measurements collected at the two lake sampling sites (see Section 4.3.1). For the SWAT2012 model, the OAT routine was also applied to manually calibrate the parameter values for each simulated variable (Q, SS, ORGP, DRP, ORGN, NH<sub>4</sub>-N, and NO<sub>3</sub>-N) based on measurements collected at the FRI stream-gauge (Fig. 4.1). One parameter set was used for the whole Puarenga Stream catchment for the SWAT2012 application.

Daily mean values of 15-min discharge measurements (see Section 4.3.1) were used to calibrate SWAT parameters to simulate daily mean discharge in the Puarenga Stream. Measured nutrient and SS concentrations from monthly samples were converted to loads based on total discharge volume on the corresponding day. The measured monthly loads were then used to calibrate parameters by comparing with the simulations of nutrient loads from SWAT2012 on that sampling day.

Daily mean simulated discharge and nutrient concentrations for Puarenga Stream were used to evaluate the catchment model performance and then provide inputs to the lake model (DYRESM–CAEDYM). Inflow volume and nutrient concentrations for eight other major inflows and nine minor inflows of Lake Rotorua used in DYRESM–CAEDYM were based on the measured or estimated hydrologic and water quality data in Abell et al. (2015). Daily simulated concentrations from DYRESM–CAEDYM were compared with monthly mean values measured in the lake on that sampling day, and then used to evaluate the lake model performance. A modified “TLI3” (a three–variable TLI that excludes Secchi depth) is compared with model output because Secchi depth is not explicitly estimated by DYRESM–CAEDYM. The TLI target of 4.2 for Lake Rotorua is equivalent to a TLI3 value of 4.32 (Hamilton et al. 2015).

For both the catchment model (SWAT2012) and lake model (DYRESM–CAEDYM), model outputs from the “warm–up” period were not further considered for model evaluation. Model goodness–of–fit between simulated outputs and observations was initially assessed graphically and then quantified using four commonly–used model evaluation statistics (Moriassi et al., 2007): Pearson product moment correlation coefficient ( $r$ ), root mean square error (RMSE), mean absolute error (MAE), and percent bias (PBIAS) (Table 4.2).

#### **4.3.4 Model scenarios**

##### **4.3.4.1 Nutrient applications**

Nutrient inputs to the Puarenga Stream catchment from treated municipal wastewater irrigation (Irr) and fertiliser applied on pastoral land (Pas) were assigned separately in the SWAT2012 model (see Section 4.3.1). Four nutrient scenarios were compared: 1) the current (“reference”) scenario, with both nutrient sources (S1–Irr1Pas1), 2) pasture fertilisation only (S2–Irr0Pas1), 3) wastewater irrigation only (S3–Irr1Pas0), and 4) no nutrient applications (S4–Irr0Pas0). Nutrient loadings from other catchments remained unchanged, i.e., simulations of different nutrient application scenarios were only undertaken for the Puarenga Stream catchment. The effects of nutrient reduction scenarios (S2–S4) on loads from the Puarenga Stream catchment and the water quality of Lake Rotorua (both surface and bottom waters) were analysed by calculating the percentage change relative to the reference scenario (S1) simulation.

**Table 4.2** Statistics used to evaluate model performance. Note:  $o_n$  is the  $n^{\text{th}}$  observed datum,  $s_n$  is the  $n^{\text{th}}$  simulated datum,  $\bar{o}$  is the observed mean value,  $\bar{s}$  is the simulated daily mean value, and  $N$  is the total number of observed data.

Statistic	Definition	Features
Pearson product moment correlation coefficient	$r = \frac{\sum_{n=1}^N [(o_n - \bar{o})(s_n - \bar{s})]}{\sqrt{\sum_{n=1}^N (o_n - \bar{o})^2 \times \sum_{n=1}^N (s_n - \bar{s})^2}}$	Range from -1 to 1. A value of 0 indicates no linear relationship and 1 or -1 indicates a perfect positive or negative linear relationship. Significance of relationship commonly judged by $p$ value ( $< 0.05$ ; Bewick et al., 2003).
Root mean square error	$\text{RMSE} = \sqrt{\frac{\sum_{n=1}^N (s_n - o_n)^2}{N}}$	A value of 0 indicates a perfect fit. This measure is disproportionately affected by large errors.
Mean absolute error	$\text{MAE} = \frac{\sum_{n=1}^N  s_n - o_n }{N}$	A value of 0 indicates a perfect fit. A measure of the mean of the model error.
Percent bias	$\text{PBIAS}\% = \frac{\sum_{n=1}^N (o_n - s_n)}{\sum_{n=1}^N o_n} \times 100\%$	A value of 0 indicates a perfect fit. Positive values indicate model underestimates and negative values indicate model overestimates.

#### 4.3.4.2 Future climate projection

Future climate projections were determined with SimCLIM, a software package used for generating regional scenarios of future climate (Yin et al., 2013). The scenarios are based on the Intergovernmental Panel on Climate Change Fifth Assessment report (IPCC, 2013). The RCP8.5 scenario was chosen, which corresponds to climate change equivalent to a short-wave radiation increase of  $8.5 \text{ W m}^{-2}$  in 2100 due to increased levels of anthropogenic greenhouse gas emissions (Van Vuuren et al., 2011). Amongst the 40 GCMs presented in SimCLIM, 22 simulate all of the climate variables (Yin et al., 2013) required as input by SWAT and DYRESM-CAEDYM (Table 4.3).

A pattern scaling method (Santer et al., 1990) in SimCLIM produces regional change factors that were used in this study according to the SimCLIM 2013 Data Manual (Yin et al., 2013). Climate change perturbations were downscaled to

regional scale using linear functions of the global annual mean temperature change using a method described in Mitchell (2003). Monthly median change factors (Touma et al., 2015) derived from the downscaled climate projections (Fig. 4.2) were used in the present climate data by adding to air temperature or by applying as a multiplicative factor to the other climate variables. Future changes in wind speed were not considered in this study because there is high uncertainty about relative change based on GCMs.

The current climate (hereafter CC0) was represented by the period from July 2005 to June 2010. SWAT baseline simulations used a subset of this period from July 2006 to June 2010 and DYRESM–CAEDYM used January 2008 to June 2010. Regional projections of global mean temperature change were derived for the period 2090–2099. The projected future climate of 2090 shows that precipitation will be higher from January to August (mid–summer to late winter) and lower from September to December (early spring to early summer), with annual mean air temperature increases of 2.7 °C (see Fig. 4.2).

Downscaled 2090 climate data were input to the SWAT2012 model to predict future (hereafter CC1) nutrient loadings from the Puarenga Stream catchment under the four scenarios of nutrient application (S1–S4). The future 2090 climate responses of Puarenga Stream to the lake examined the changes relative to reference scenario S1–Irr1Pas1 simulations. For other streams, scenario S2–Irr0Pas1, with no wastewater irrigation, was applied for the future climate impact on the lake (hereafter CC2). Climate change interactions with S2–Irr0Pas1 were considered because 1) other streams catchments did not have treated wastewater application; and 2) the Rotorua District Council has made a decision to cease irrigation to the Whakarewarewa Forest by 2019. For surface water–dominated sub–catchments (see Section 4.3.2), the temperatures of major stream inflows were increased based on the increases predicted for the Puarenga Stream. For groundwater–dominated catchments, stream water temperatures were increased by adding 88% of the projected increase in air temperature, based on Kurylyk et al. (2013).

**Table 4.3** The 22 general circulation models (GCMs) used in this study and the country where each GCM originated. See IPCC (2013).

No.	GCM	Country	No.	GCM	Country
1	ACCESS1-0	Australia	12	HADCM3	UK
2	ACCESS1-3	Australia	13	HADGEM2-CC	UK
3	CANESM2	Canada	14	HADGEM2-ES	UK
4	CSIRO-MK3-6-0	Australia	15	INMCM4	Russia
5	GFDL-CM3	USA	16	IPSL-CM5A-LR	France
6	GFDL-ESM2G	USA	17	IPSL-CM5A-MR	France
7	GFDL-ESM2M	USA	18	IPSL-CM5B-LR	France
8	GISS-E2-H	USA	19	MIROC-ESM	Japan
9	GISS-E2-H-CC	USA	20	MIROC-ESM-CHEM	Japan
10	GISS-E2-R	USA	21	MIROC5	Japan
11	GISS-E2-R-CC	USA	22	MRI-CGCM3	Japan

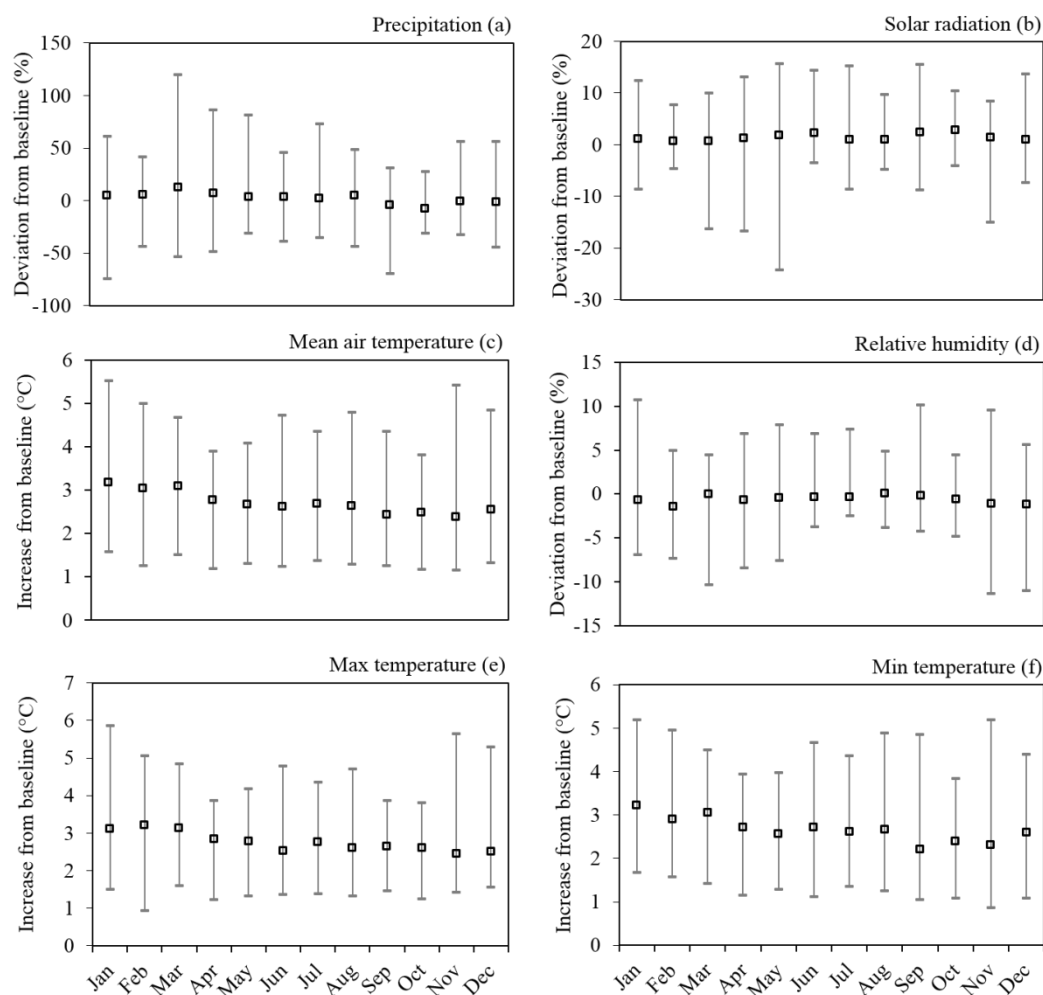


**Figure 4.2** Monthly median change factors (square marker) applied in 22 general circulation models (GCMs) that were used to generate 2090 regional climate data for modelling the Puarenga Stream catchment and Lake Rotorua. (a) precipitation; (b) solar radiation; (c) mean air temperature; (d) relative humidity; (e) maximum temperature; and (f) minimum temperature. Error bars indicate the range of monthly changes derived from the 22 GCMs.

## 4.4 Results

### 4.4.1 Calibration and model performance

#### 4.4.1.1 SWAT2012 model of the Puarenga Stream catchment

Optimised parameter values for the SWAT2012 model are presented in Table 4.4 for the whole Puarenga Stream catchment. Differences in some parameter values from previous SWAT2009 model runs in Me et al. (2015) reflected the modified SWAT2012 source code used in this study. Three parameter values were adjusted beyond the SWAT default range (Table 4.4): (1) the number of days for groundwater delay (GW\_DELAY), (2) the phosphorus percolation coefficient (PPERCO), and (3) benthic (sediment) release rate for  $\text{NH}_4\text{-N}$  in the stream reach at 20 °C (RS3).

The parameter GW\_DELAY (groundwater delay days) was set to 1825 days (five years) for the Waipa Stream sub-catchment, which was the value of mean groundwater residence time reported in Rutherford et al. (2009). This value was set as five years because in-stream nitrate concentrations appeared to reach a new equilibrium five years after treated wastewater was spray-irrigated within the Waipa Stream sub-catchment in 1991, which would be consistent with nitrate transport times in shallow groundwater (Rutherford et al., 2009). Recently, Morgenstern et al. (2015) re-examined the mean groundwater residence times for the wider Puarenga Stream catchment which has a more complex groundwater system, and reported a mean value of c. 40 years.

The parameter PPERCO (phosphorus percolation coefficient) was adjusted because the Puarenga Stream catchment outside of the irrigation area has pumice soils with moderate levels of P adsorption capacity (50–60%) and the wastewater spray blocks drained by the Waipa Stream have allophanic soil with high P adsorption capacity (85–95%) (see Section 4.3.1). The parameter value for RS3 (sediment release rate for in-stream  $\text{NH}_4\text{-N}$ ,  $50 \text{ mg m}^{-2} \text{ d}^{-1}$ ) was based on Gabriele et al. (2013) who investigated headwater streams from an Austrian catchment where there is intensive agriculture and the stream channel is rich in organic material. Gabriele et al. (2013) estimated RS3 in the range 24 to  $48 \text{ mg m}^{-2} \text{ d}^{-1}$ , so our value reflected high  $\text{NH}_4\text{-N}$  inputs and may have been reflective of some geothermal source inputs to the Puarenga Stream.

Simulations of discharge from the Puarenga Stream catchment showed high correspondence with measured values (Fig. 4.3a). Discharge peaks during high rainfall events were reasonably well simulated by the SWAT2012 model, although a few peaks were underestimated. Discharge after high rainfall events was overestimated, in particular during winter. Overall, the SWAT2012 model overestimated discharge by 3.9% during calibration (July 2006 – June 2009) and 14.4% during validation (July 2009 – June 2010) but with high values of  $r$  ( $> 0.8$ ,  $p < 0.001$ ; Table 4.5).

The range of concentrations of SS simulated by SWAT2012 was smaller than that of measured data from the Puarenga Stream catchment (Fig. 4.3b). Simulated and measured SS concentrations were positively correlated during calibration ( $r = 0.45$ ,  $p < 0.05$ ) but negative during validation ( $r = -0.23$ ,  $p > 0.05$ ; Table 4.5). Base flow SS concentrations were generally overestimated, and several peaks of SS concentrations were underestimated, contributing to an underestimate of SS concentrations of 4.3% during calibration and an overestimate of 5.3% during validation. The correlations between simulated and measured SS load were positive during calibration ( $r = 0.52$ ,  $p < 0.01$ ) and validation ( $r = 0.30$ ,  $p > 0.05$ ), with an underestimate of 3.9% during calibration and an overestimate of 17.2% during validation (Table 4.5).

Concentrations of P species were generally not simulated accurately for the Puarenga Stream catchment (Fig. 4.3c–e). The correlations were weak for both ORGP and DRP during calibration ( $r \leq 0.25$ ,  $p > 0.05$ ; Table 4.5) but were stronger during validation ( $r = 0.70$ ,  $p < 0.05$  for ORGP;  $r = 0.68$ ,  $p < 0.05$  for DRP). Concentrations of ORGP were overestimated by 27.9% and concentrations of DRP were underestimated by 9.8% during calibration, while during validation ORGP concentrations were underestimated by 23% and DRP concentrations were overestimated by 37.2% (Table 4.5). Concentrations of TP were overestimated by 11.3% during calibration and 0.3% during validation, with poor correlation statistics ( $r = 0.05$ ,  $p > 0.05$  for calibration;  $r = 0.17$ ,  $p > 0.05$  for validation; Table 4.5). However, simulated and measured ORGP and TP loads were positively correlated during calibration ( $r = 0.48$ ,  $p < 0.05$  for ORGP;  $r = 0.59$ ,  $p < 0.001$  for TP) and validation ( $r = 0.89$ ,  $p < 0.001$  for both; Table 4.5), reflecting the major impact of discharge on loads. Correlations between simulated and measured DRP loads were weak during calibration ( $r = 0.12$ ,  $p > 0.05$ ) and validation ( $r = 0.22$ ,  $p > 0.05$ ; Table 4.5).

**Table 4.4** Optimised parameter values with input file extensions for the whole Puarenga Stream catchment for discharge (Q), suspended sediment (SS), total phosphorus (TP), and total nitrogen (TN) concentration simulations. The asterisked values were adjusted beyond the SWAT default range (see text). Input file extensions are shown for each parameter. Parameters are unitless unless otherwise specified. “revap” indicates water movement into the overlying unsaturated layers.

Parameter	Definition	Unit	Default range	Optimal value
Q				
EVRCH.bsn	Reach evaporation adjustment factor		0.5–1	0.7
CH_K2.rte	Effective hydraulic conductivity in the main channel alluvium	mm h <sup>-1</sup>	0–500	20
CH_N2.rte	Manning’s n value for the main channel		0–0.3	0.01
CH_K1.sub	Effective hydraulic conductivity in the tributary channel alluvium	mm h <sup>-1</sup>	0–300	62
CH_N1.sub	Manning’s n value for the tributary channel		0.01–30	12.5
ALPHA_BF.gw	Base flow alpha factor (0–1)		0–1	0.01
GW_DELAY.gw	Groundwater delay	d	0–500	1825*
GW_REVAP.gw	Groundwater “revap” coefficient		0.02–0.2	0.07
GW_SPYLD.gw	Special yield of the shallow aquifer	m <sup>3</sup> m <sup>-3</sup>	0–0.4	0.2
GWHT.gw	Initial groundwater height	m	0–25	12
GWQMN.gw	Threshold depth of water in the shallow aquifer required for return flow to occur	mm	0–5000	400
RCHRG_DP.gw	Deep aquifer percolation fraction		0–1	0.1
REVAPMN.gw	Threshold depth of water in the shallow aquifer required for “revap” to occur	mm	0–500	344
CANMX.hru	Maximum canopy storage	mm	0–100	0.6
EPCO.hru	Plant uptake compensation factor		0–1	0.34
ESCO.hru	Soil evaporation compensation factor		0–1	0.5
HRU_SLP.hru	Average slope steepness	m m <sup>-1</sup>	0–0.6	0.1
LAT_TTIME.hru	Lateral flow travel time	d	0–180	3
RSDIN.hru	Initial residue cover	kg ha <sup>-1</sup>	0–10000	1

Parameter	Definition	Unit	Default range	Optimal value
SS				
SLSOIL.hru	Slope length for lateral subsurface flow	m	0–150	15
CH_COV1.rte	Channel erodibility factor		0–0.6	0.1
CH_COV2.rte	Channel cover factor		0–1	0.1
LAT_SED.hru	Sediment concentration in lateral flow and groundwater flow	mg L <sup>-1</sup>	0–5000	5
OV_N.hru	Manning's n value for overland flow		0.01–30	20
SLSUBBSN.hru	Average slope length	m	10–150	83
SURLAG.bsn	Surface runoff lag coefficient		0.05–24	1
SPCON.bsn	Linear parameter for calculating the maximum amount of sediment that can be re-entrained during channel sediment routing		0.0001–0.01	0.003
SPEXP.bsn	Exponent parameter for calculating sediment re-entrained in channel sediment routing		1–2	1.8
TP				
P_UPDIS.bsn	Phosphorus uptake distribution parameter		0–100	0.5
PHOSKD.bsn	Phosphorus soil partitioning coefficient	m <sup>3</sup> t <sup>-1</sup>	100–500	100
PPERCO.bsn	Phosphorus percolation coefficient	m <sup>3</sup> t <sup>-1</sup>	0.01–0.0175	0.005*
PSP.bsn	Phosphorus availability index		0.01–0.7	0.6
GWSOLP.gw	Soluble phosphorus concentration in groundwater loading	mg P L <sup>-1</sup>	0–1000	0.03
LAT_ORGP.gw	Organic phosphorus in the base flow	mg P L <sup>-1</sup>	0–200	5
ERORGP.hru	Organic phosphorus enrichment ratio		0–5	0.1
CH_OPCO.rte	Organic phosphorus concentration in the channel	mg P L <sup>-1</sup>	0–100	0.066
BC4.swq	Rate constant for mineralisation of organic phosphorus to dissolved phosphorus in the reach at 20 °C	d <sup>-1</sup>	0.01–0.7	0.3
RS2.swq	Benthic (sediment) source rate for dissolved phosphorus in the reach at 20 °C	mg m <sup>-2</sup> d <sup>-1</sup>	0.001–0.1	0.02
RS5.swq	Organic phosphorus settling rate in the reach at 20 °C	d <sup>-1</sup>	0.001–0.1	0.05
USLE_P.mgt	Universal Soil Loss Equation (USLE) support practice factor		0–1	0.5

Parameter	Definition	Unit	Default range	Optimal value
TN				
RSDCO.bsn	Residue decomposition coefficient		0.02–0.1	0.1
CDN.bsn	Denitrification exponential rate coefficient		0–3	0.09
CMN.bsn	Rate factor for humus mineralisation of active organic nitrogen		0.001–0.003	0.001
N_UPDIS.bsn	Nitrogen uptake distribution parameter		0–100	0.5
NPERCO.bsn	Nitrogen percolation coefficient		0–1	0.05
RCN.bsn	Concentration of nitrogen in rainfall	mg N L <sup>-1</sup>	0–15	0.34
SDNCO.bsn	Denitrification threshold water content		0–1	0.05
HLIFE_NGW.gw	Half-life of nitrate–nitrogen in the shallow aquifer	d	0–200	200
LAT_ORGN.gw	Organic nitrogen in the base flow	mg N L <sup>-1</sup>	0–200	25
SHALLST_N.gw	Nitrate–nitrogen concentration in the shallow aquifer	mg N L <sup>-1</sup>	0–1000	1
ERORGN.hru	Organic nitrogen enrichment ratio		0–5	0.1
CH_ONCO.rte	Organic nitrogen concentration in the channel	mg N L <sup>-1</sup>	0–100	0.34
BC1.swq	Rate constant for biological oxidation of ammonium–nitrogen to nitrite–nitrogen in the reach at 20 °C	d <sup>-1</sup>	0.1–1	0.55
BC2.swq	Rate constant for biological oxidation of nitrite–nitrogen to nitrate–nitrogen in the reach at 20 °C	d <sup>-1</sup>	0.2–2	1.1
BC3.swq	Rate constant for hydrolysis of organic nitrogen to ammonium–nitrogen in the reach at 20 °C	d <sup>-1</sup>	0.2–0.4	0.21
RS3.swq	Benthic (sediment) source rate for ammonium–nitrogen in the reach at 20 °C	mg m <sup>-2</sup> d <sup>-1</sup>	0–1	50*
RS4.swq	Rate coefficient for organic nitrogen settling in the reach at 20 °C	d <sup>-1</sup>	0.001–0.1	0.05

The simulated concentrations of N species from the Puarenga Stream catchment showed high seasonal variability (Fig. 4.3f–i), with concentrations typically higher during the drier periods of summer and autumn, and lower during the wetter periods of winter and spring. Simulations of ORGN concentrations were generally within the range of measured data (Fig. 4.3f), although several measured peaks were underestimated during calibration (PBIAS = 0.5%), while base flow concentrations were overestimated during validation (PBIAS = -19.8%; Table 4.5). The correlations between simulated and measured ORGN concentrations were positive during calibration ( $r = 0.47$ ,  $p < 0.05$ ) and validation ( $r = 0.75$ ,  $p < 0.01$ ; Table 4.5). By contrast, correlations between simulated and measured  $\text{NH}_4\text{-N}$  concentrations were negative, with underestimates of 12.8% during calibration ( $r = -0.47$ ,  $p < 0.05$ ) and 15% during validation ( $r = -0.31$ ,  $p > 0.05$ ; Table 4.5). Simulations of  $\text{NO}_3\text{-N}$  and TN concentrations were strongly correlated with measurements during calibration ( $r \geq 0.40$ ,  $p < 0.05$ ) and validation ( $r \geq 0.67$ ,  $p < 0.05$ ), although  $\text{NO}_3\text{-N}$  and TN concentrations were underestimated by ~10% (see PBIAS in Table 4.5). Catchment loads of  $\text{NO}_3\text{-N}$  and TN were generally underestimated during calibration (9.3% for  $\text{NO}_3\text{-N}$ , 9.1% for TN) and overestimated during validation (4.9% for  $\text{NO}_3\text{-N}$ , 7.6% for TN; Table 4.5). Higher  $r$  values for simulations of  $\text{NO}_3\text{-N}$  and TN loads during calibration ( $r \geq 0.52$ ,  $p < 0.01$ ) and validation ( $r \geq 0.93$ ,  $p < 0.001$ ) were again indicative of the importance of discharge.

#### **4.4.1.2 DYRESM–CAEDYM model of Lake Rotorua**

Most DYRESM–CAEDYM parameter values used in this study were taken from the latest modelling study of Lake Rotorua in Abell et al. (2015) but two were adjusted to better fit observed data. The adjusted parameters included the maximum denitrification rate coefficient, altered from 0.8 to 0.5  $\text{d}^{-1}$ , and release rate of  $\text{NH}_4\text{-N}$  from the sediment, altered from 0.2 to 0.3  $\text{g m}^{-2} \text{d}^{-1}$ . A summary of key parameter values that were optimised by manual calibration in both Abell et al. (2015) and this study is shown in Table 4.6.

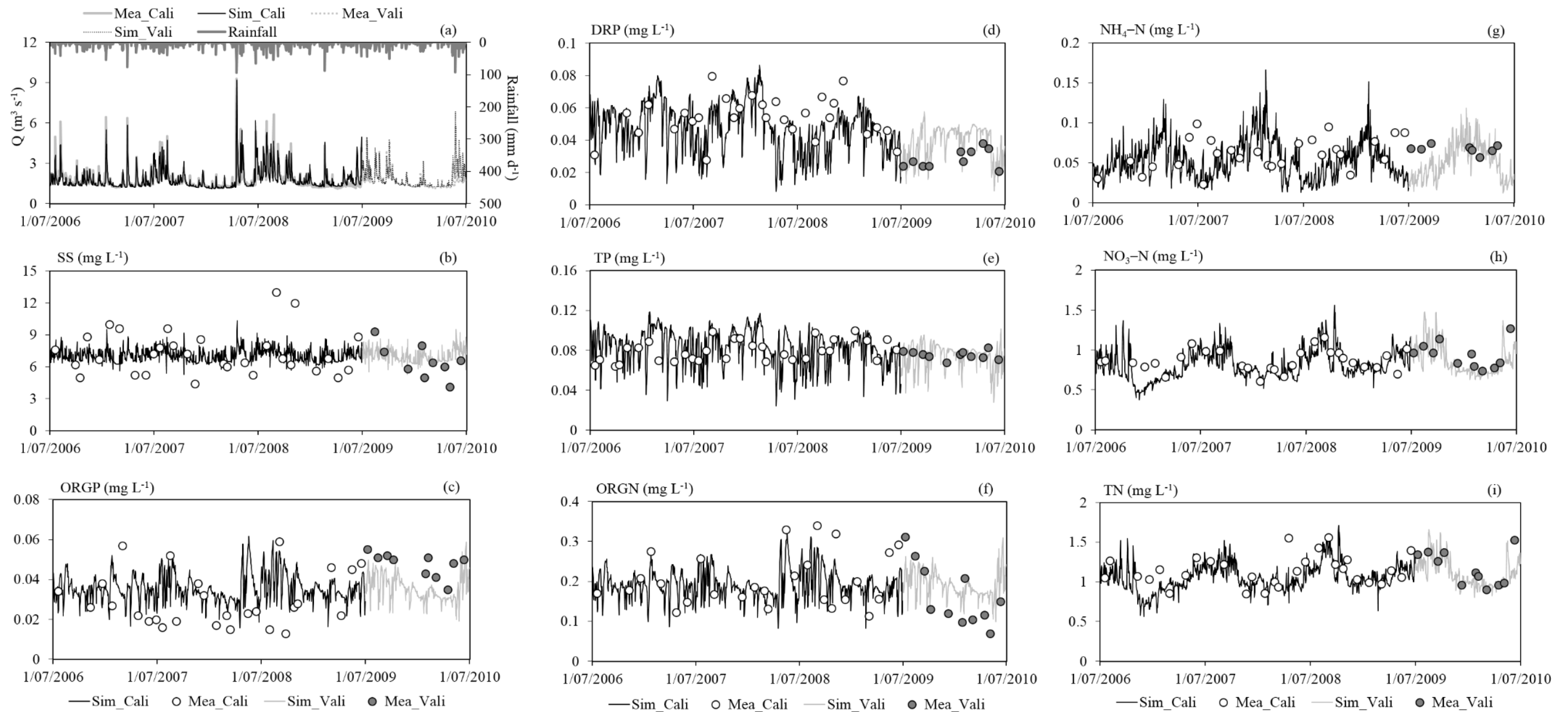


**Figure 4.3** Comparison of measurements taken at the FRI stream-gauge and SWAT2012 model outputs of (a) discharge (Q), concentrations of (b) suspended sediment (SS), (c) organic phosphorus (ORGP), (d) dissolved reactive phosphorus (DRP), (e) total phosphorus (TP), (f) organic nitrogen (ORGN), (g) ammonium-nitrogen ( $\text{NH}_4\text{-N}$ ), (h) nitrate-nitrogen ( $\text{NO}_3\text{-N}$ ) and (i) total nitrogen (TN) during calibration (July 2006 to June 2009) and validation (July 2009 to June 2010) periods.

**Table 4.5** Statistical values of Pearson product moment correlation coefficient ( $r$ ), root mean square error (RMSE), mean absolute error (MAE), and percent bias (PBIAS), used to assess SWAT2012 model performance for daily mean simulations of discharge (Q), loads and concentrations of suspended sediment (SS), organic phosphorus (ORGP), dissolved reactive phosphorus (DRP), total phosphorus (TP), organic nitrogen (ORGN), ammonium–nitrogen (NH<sub>4</sub>–N), nitrate–nitrogen (NO<sub>3</sub>–N) and total nitrogen (TN) from the Puarenga Stream catchment. The significance of correlations between simulations and measurements was quantified based on the  $p$  value (see Section 4.3.2). \* $p < 0.05$ ; \*\* $p < 0.01$ ; \*\*\* $p < 0.001$ . Units are relevant to RMSE and MAE values only.

Modelling period	Statistics	Q	SS	ORGP	DRP	TP	ORGN	NH <sub>4</sub> –N	NO <sub>3</sub> –N	TN	
Calibration (July 2006 – June 2009)		(m <sup>3</sup> s <sup>-1</sup> )	Concentration (mg L <sup>-1</sup> )								
	$r$	0.81***	0.45*	0.00	0.25	0.05	0.47*	-0.47*	0.40*	0.66***	
	RMSE	0.476	1.883	0.018	0.016	0.018	0.058	0.032	0.174	0.176	
	MAE	0.254	1.419	0.015	0.013	0.016	0.046	0.027	0.139	0.149	
	PBIAS%	-3.9	4.3	-27.9	9.8	-11.3	0.5	12.8	9.3	9.1	
			Load (t d <sup>-1</sup> )	Load (kg d <sup>-1</sup> )							
	$r$		0.52**	0.48*	0.12	0.59***	0.71***	-0.44*	0.52**	0.62***	
	RMSE		0.4	2.4	2.2	2.3	9.0	4.2	39.5	42.9	
	MAE		0.3	1.9	1.8	2.0	6.4	3.5	29.4	33.1	
	PBIAS%		3.9	-30.2	9.4	-10.4	2.5	15.1	9.2	7.6	
Validation (July 2009 – June 2010)		(m <sup>3</sup> s <sup>-1</sup> )	Concentration (mg L <sup>-1</sup> )								
	$r$	0.88***	-0.23	0.70*	0.68*	0.17	0.75**	-0.31	0.67*	0.78**	
	RMSE	0.479	1.656	0.012	0.012	0.008	0.065	0.025	0.159	0.156	
	MAE	0.278	1.372	0.011	0.011	0.007	0.060	0.021	0.109	0.097	
	PBIAS%	-14.4	-5.3	23.0	-37.2	-0.3	-19.8	15.0	10.8	7.4	
			Load (t d <sup>-1</sup> )	Load (kg d <sup>-1</sup> )							
	$r$		0.30	0.89***	0.22	0.89***	0.63*	-0.36	0.93***	0.94***	
	RMSE		0.3	1.2	2.1	1.9	12.8	3.1	28.5	30.9	
	MAE		0.3	1.1	2.0	1.5	9.9	2.7	18.8	20.6	
	PBIAS%		-17.2	8.9	-54.9	-14.5	-37.4	10.9	-4.9	-7.6	

In surface waters of Lake Rotorua (0–6 m deep), variations in nutrient concentrations were generally well reproduced by DYRESM–CAEDYM, including increases in winter and decreases in summer for PO<sub>4</sub>–P (identical to the variable DRP simulated by SWAT), NH<sub>4</sub>–N and NO<sub>3</sub>–N (Fig. 4.4a, e and g). Simulations of PO<sub>4</sub>–P and NH<sub>4</sub>–N showed low or negative *r* values during calibration (January 2008 – June 2009) and validation (July 2009 – June 2010) and tended to be overestimated (PBIAS ≤ -38.1%) during validation (Table 4.7). However, the modelled TP concentrations showed reasonable agreement with the observations during calibration (*r* = 0.63; *p* < 0.01) and validation (*r* = 0.79; *p* < 0.01), although concentrations were slightly underestimated, by 12.1% during calibration and 16.5% during validation (Table 4.7). A highly positive correlation (*r* = 0.74; *p* < 0.01) between simulated and observed concentrations of NO<sub>3</sub>–N was found during validation, although values were overestimated (PBIAS = -72.3%; Table 4.7). Simulated TN concentrations also showed good agreement with observations during both calibration (*r* = 0.73; *p* < 0.01) and validation (*r* = 0.81; *p* < 0.01), with low bias (+6.1% and -2.4%, respectively, Table 4.7).

Model performance for lake surface Chl *a* concentrations (Fig. 4.4k) was poor, showing low *r* values during calibration (*r* = 0.09, *p* > 0.05) and validation (*r* = 0.38, *p* > 0.05) and tended to underestimate during calibration (PBIAS = 24.1%) and validation (PBIAS = 10.8%; Table 4.7). The mean TLI3 value was 4.54 for July 2009 to June 2010 based on the measured concentrations of Chl *a*, TP and TN in surface waters of Lake Rotorua, compared to 4.47 based on the DYRESM–CAEDYM simulation under baseline conditions of both wastewater irrigation and pasture fertilisation (Table 4.8).

At 19 m depth (“bottom”), simulated nutrient concentrations showed large variations, with peaks corresponding either to periods of hypoxia in the hypolimnion during stratified periods, or intervening isothermal periods, depending on the analyte (Fig. 4.4). However, the DYRESM–CAEDYM model simulations showed only modest statistical performance with most of the measured nutrient concentrations (range in *r* values of -0.38 to 0.37 during calibration and validation; Table 4.7). Simulated concentrations of PO<sub>4</sub>–P and NH<sub>4</sub>–N in bottom waters were highest during summer thermal stratification (Fig. 4.4b, f), which coincided with the period of occasional hypolimnetic anoxia. A positive correlation (*r* = 0.37; *p* > 0.05) between simulated and observed concentrations of NO<sub>3</sub>–N

(PBIAS = 3.4%) was found during validation (Table 4.7). The highest simulated concentrations of NO<sub>3</sub>-N occurred in winter when the water column was continuously well mixed (Fig. 4.4h). When the water column was stratified for periods of up to several days, both modelled and observed TP at 19 m depth predominantly comprised PO<sub>4</sub>-P (Fig. 4.4b, d) and TN predominantly comprised NH<sub>4</sub>-N (Fig. 4.4f, j). Modelled TP concentrations showed poor agreement with the observations ( $r = 0.19$ ;  $p > 0.05$ ) during calibration and were underestimated by 29.0% (Table 4.7).

Measurements at monthly intervals and simulated concentrations on corresponding days in the surface and bottom waters of Lake Rotorua under the current climate (CC0) during calibration (January 2008 – June 2009) and validation (July 2009 – June 2010) are also compared in Fig. 4.5, showing larger variances in the measured data than the simulated results.

**Table 4.6** Sensitive DYRESM–CAEDYM parameter values that were adjusted from Abell et al. (2015).

Parameter	Unit	Calibrated value
<i>Dissolved organic nutrients</i>		
Max. rate of mineralisation of labile dissolved organic phosphorus (DOPL) to phosphate (PO <sub>4</sub> -P)	d <sup>-1</sup>	0.01
Max. rate of mineralisation of labile dissolved organic nitrogen (DONL) to ammonium (NH <sub>4</sub> -N)	d <sup>-1</sup>	0.01
<i>Dissolved inorganic nutrients</i>		
Denitrification rate coefficient	d <sup>-1</sup>	0.50
Nitrification rate coefficient	d <sup>-1</sup>	0.10
<i>Nutrient fluxes in sediment</i>		
Release rate of PO <sub>4</sub> -P	g m <sup>-2</sup> d <sup>-1</sup>	0.02
Release rate of NH <sub>4</sub> -N	g m <sup>-2</sup> d <sup>-1</sup>	0.30
Release rate of nitrate (NO <sub>3</sub> -N)	g m <sup>-2</sup> d <sup>-1</sup>	-0.10

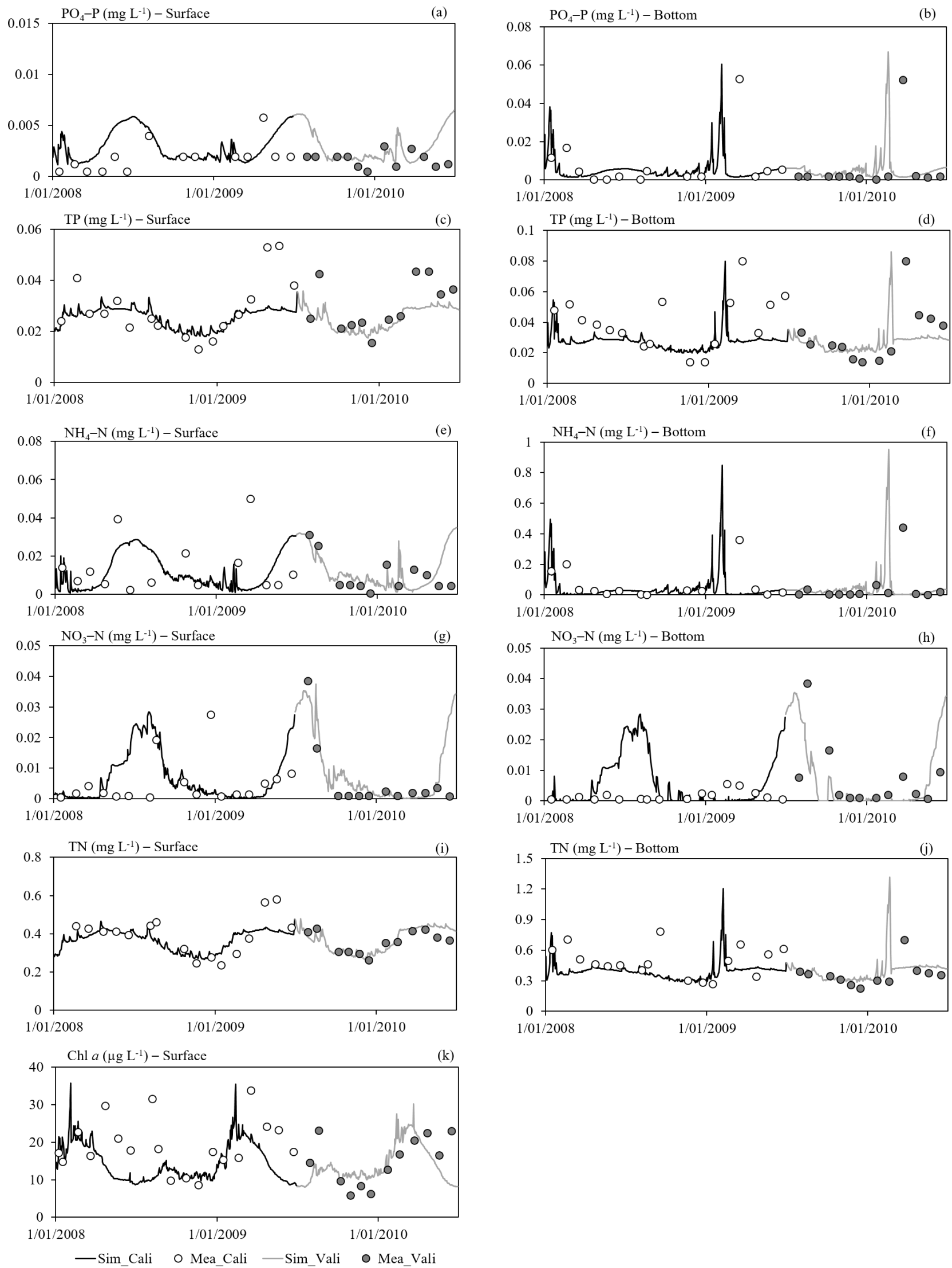


**Figure 4.4** Comparisons of concentrations simulated with DYRESM-CAEDYM of (a–b) phosphate (PO<sub>4</sub>-P), (c–d) total phosphorus (TP), (e–f) ammonium-nitrogen (NH<sub>4</sub>-N), (g–h) nitrate-nitrogen (NO<sub>3</sub>-N), (i–j) total nitrogen (TN), and (k) chlorophyll *a* (Chl *a*) with the measurements taken at the surface (0–6 m) and the bottom (19 m) water of Lake Rotorua, during calibration (January 2008 to June 2009) and validation (July 2009 to June 2010) period.

**Table 4.7** Model performance of DYRESM–CAEDYM for daily mean concentrations of phosphate (PO<sub>4</sub>–P), total phosphorus (TP), ammonium–nitrogen (NH<sub>4</sub>–N), nitrate–nitrogen (NO<sub>3</sub>–N) and total nitrogen (TN) for surface (0–6 m) and bottom (19 m) waters of Lake Rotorua and surface water chlorophyll *a* (Chl *a*) during calibration (January 2008 to June 2009) and validation (July 2009 to June 2010). Values of Pearson product moment correlation coefficient (*r*), level of significance (*p*), root mean square error (RMSE), mean absolute error (MAE), and percent bias (PBIAS) were used to indicate model performance. \*\**p* < 0.01. Units are relevant to RMSE and MAE values only.

Model performance	Statistics	Lake surface waters (0–6 m)						Lake bottom waters (19 m)				
		PO <sub>4</sub> –P	TP	NH <sub>4</sub> –N	NO <sub>3</sub> –N	TN	Chl <i>a</i>	PO <sub>4</sub> –P	TP	NH <sub>4</sub> –N	NO <sub>3</sub> –N	TN
		mg L <sup>-1</sup>						μg L <sup>-1</sup>	mg L <sup>-1</sup>			
Calibration	<i>r</i>	0.10	0.63**	-0.15	0.14	0.73**	0.09	0.00	0.19	0.20	-0.38	0.16
(January	RMSE	0.002	0.010	0.018	0.011	0.074	9.280	0.016	0.020	0.138	0.011	0.136
2008 –	MAE	0.002	0.007	0.014	0.006	0.057	7.425	0.008	0.015	0.075	0.007	0.136
June 2009)	PBIAS%	-63.0	12.1	13.8	-40.1	6.1	24.1	25.3	29.0	25.0	-312.7	17.0
Validation	<i>r</i>	-0.24	0.79**	0.28	0.74**	0.81**	0.38	-0.16	-0.10	-0.12	0.37	-0.07
(July	RMSE	0.002	0.008	0.012	0.009	0.035	6.338	0.023	0.024	0.273	0.012	0.281
2009 –	MAE	0.002	0.006	0.009	0.006	0.029	5.054	0.012	0.017	0.132	0.008	0.150
June 2010)	PBIAS%	-76.1	16.5	-38.1	-72.3	-2.4	10.8	-60.2	0.9	-109.6	3.4	-26.5

#### 4.4.2 Catchment and lake scenarios: current climate

Under the reference scenario (S1–Irr1Pas1) corresponding to current climate, 65 t yr<sup>-1</sup> of P was applied to the Puarenga catchment from July 2006 to June 2010; 61.5% (40 t yr<sup>-1</sup>) as pastoral fertiliser and 38.5% (25 t yr<sup>-1</sup>) as irrigated wastewater (Table 4.9). As part of these applications, 180 t yr<sup>-1</sup> of N was also applied; 70.6% (127 t yr<sup>-1</sup>) as pastoral fertiliser and 29.4% (53 t yr<sup>-1</sup>) as irrigated wastewater (Table 4.9).

Mean TP and TN loads at the FRI stream–gauge for the four years of the SWAT simulation (July 2006 – June 2010; baseline period) varied among the four nutrient application scenarios relative to the current climate condition (CC0). For S1–Irr1Pas1, the TP load at the FRI stream–gauge was 4.3 t yr<sup>-1</sup> (Table 4.9), indicating that 93.4% of the 65 t yr<sup>-1</sup> applied to land from wastewater irrigation and pasture fertilisation was attenuated and therefore not exported downstream during that period. The application of pastoral fertiliser alone (S2–Irr0Pas1) resulted in an in–stream TP load of 3.7 t yr<sup>-1</sup> (Table 4.9), a reduction of 14.0% from the simulations under S1–Irr1Pas1. The scenario comprising only wastewater irrigation (S3–Irr1Pas0) resulted in an annual TP load of 2.9 t yr<sup>-1</sup> (Table 4.9), a 32.6% reduction from simulations of TP under S1–Irr1Pas1. Simulations with no nutrient application (S4–Irr0Pas0) reduced the in–stream annual TP load by 39.5% (2.6 t yr<sup>-1</sup>; Table 4.9) from the load under S1–Irr1Pas1.

The mean simulated in–stream TN load at the FRI stream–gauge over the four–year simulation for S1–Irr1Pas1 was 62.9 t yr<sup>-1</sup> (Table 4.9), representing an attenuation of 65.1% of the TN load applied from wastewater irrigation and pasture fertilisation (S1–Irr1Pas1; 53 and 127 t yr<sup>-1</sup>, respectively). The applications of S2–Irr0Pas1, S3–Irr1Pas0, S4–Irr0Pas0 resulted in a four–year annual mean in–stream TN load of 46.7, 31.8 and 15.6 t yr<sup>-1</sup>, respectively (Table 4.9). These three scenarios represent respective reductions of 25.8%, 49.4%, and 75.2% (Table 4.9) relative to simulations under the reference scenario S1–Irr1Pas1.

**Table 4.8** Measured sampling days and corresponding simulation days with changes in surface and bottom water temperature ( $\Delta T$ ) > 0.5 °C, with bottom water dissolved oxygen (DO) concentrations < 2 mg L<sup>-1</sup>, and with surface water chlorophyll *a* (Chl *a*) concentrations > 15 µg L<sup>-1</sup>, and TLI3 values under the current climate during calibration (2008–2009) and validation (2009–2010); daily simulated number of days with  $\Delta T$  > 0.5 °C, DO < 2 mg L<sup>-1</sup>, Chl *a* > 15 µg L<sup>-1</sup>, and mean TLI3 values under current climate (CC0) relative to four nutrient load scenarios (S1–S4) during baseline period (2008–2010), and under 2090 climate changes to catchment only (CC1) and changes to both catchment and lake (CC2). Nutrient load scenarios are described in the Methods. The TLI3 is a three–variable Trophic Level Index function derived from concentrations of total nitrogen, total phosphorus and Chl *a*, which is used to indicate the lake trophic state (Burns et al., 1999).

	CC0: S1–Irr1Pas1 (monthly values)				CC0: S1–S4 (daily values)				CC1: catchment only (daily values)	CC2: catchment & lake (daily values)
	Calibration: 2008–2009		Validation: 2009–2010		Baseline: 2008–2010				Future: 2090	Future: 2090
	Measured	Simulated	Measured	Simulated	S1–Irr1Pas1	S2–Irr0Pas1	S3–Irr1Pas0	S4–Irr0Pas0	S2–Irr0Pas1	S2–Irr0Pas1
	Number of days (d)		Number of days (d)		Number of days (d)				Number of days (d)	Number of days (d)
$\Delta T > 0.5$ °C	5	3	1	2	316	294	308	291	303	345
Bottom DO < 2 mg L <sup>-1</sup>	1	1	1	1	75	58	62	53	70	141
Surface Chl <i>a</i> > 15 µg L <sup>-1</sup>	10	4	4	1	306	291	296	291	301	446
mean TLI3	4.68	4.5	4.54	4.47	4.49	4.46	4.46	4.44	4.46	4.88



For the DYRESM–CAEDYM simulations of 2.5 years (January 2008 – June 2010; baseline period), annual mean concentrations of TP and TN in the surface and bottom waters and Chl *a* in surface waters are similar for the different nutrient application scenarios (S1–S4) under current climate (CC0) (see Fig. 4.5), as well as the mean TLI3 value (see Table 4.8).

Annual mean TP concentrations at the lake surface under the catchment scenarios of S2–Irr0Pas1, S3–Irr1Pas0, and S4–Irr0Pas0 were slightly reduced, by 2.4%, 2.4%, and 3.5% (Table 4.9), respectively, compared with the annual mean (0.0254 mg L<sup>-1</sup>) under S1–Irr1Pas1 (Table 4.9). Annual mean TP concentration at the lake bottom under the catchment scenarios of S2–Irr0Pas1, S3–Irr1Pas0, and S4–Irr0Pas0 declined slightly, by 4.7%, 4.4%, and 6.9% (Table 4.9), respectively, compared with the value of 0.0275 mg L<sup>-1</sup> at the lake bottom under S1–Irr1Pas1 (Table 4.9).

Annual mean TN concentrations at the lake surface under the catchment scenarios of S2–Irr0Pas1, S3–Irr1Pas0, and S4–Irr0Pas0 declined slightly, by 2.7%, 4.1%, and 5.7% (Table 4.9), respectively, compared with 0.0368 mg L<sup>-1</sup> at the lake surface under S1–Irr1Pas1 (Table 4.9). Annual mean TN concentrations at the lake bottom under the catchment scenarios of S2–Irr0Pas1, S3–Irr1Pas0, and S4–Irr0Pas0 also declined slightly, by 5.3%, 6.3%, and 9.4% (Table 4.9), respectively, compared with 0.0394 mg L<sup>-1</sup> at the lake bottom under S1–Irr1Pas1 (Table 4.9).

Annual mean Chl *a* concentration at the lake surface under the catchment scenarios of S2–Irr0Pas1, S3–Irr1Pas0, and S4–Irr0Pas0 declined slightly, by 3.2%, 2.8%, and 4.1% (Table 4.9), respectively, compared with 14.178 µg L<sup>-1</sup> at the lake surface under S1–Irr1Pas1 (Table 4.9).

Decreases in nutrient loads in the Puarenga Stream under scenario S4–Irr0Pas0 gave reductions in total external loads from the whole Rotorua catchment of only 6.2% for TP and 11.3% for TN. Given that the changes were only made to 15.6% of TP load and 16.2% of TN load contributing to Lake Rotorua, large changes in water quality of the whole lake would not be expected, i.e., ~84% of the TP and TN input remained unchanged.

**Table 4.9** Model results under current climate (CC0) for four nutrient load scenarios comprising changes to total phosphorus (TP) and total nitrogen (TN) loads from the Puarenga Stream catchment and in-stream TP and TN loads during baseline period (July 2006 to June 2010); changes to TP and TN concentrations in surface and bottom waters, and surface water chlorophyll *a* (Chl *a*) concentrations of Lake Rotorua during the baseline period (January 2008 to June 2010). Percentage change denotes changes to the simulations under scenarios S2–S4 relative to the simulations under the “reference” scenario S1. Nutrient load scenarios (S1–S4) are described in the Methods. S1–Irr1Pas1: both nutrient applications, S2–Irr0Pas1: pasture fertilisation only, S3–Irr1Pas0: wastewater irrigation only, S4–Irr0Pas0: no nutrient applications.

Scenarios	TP				TN				Chl <i>a</i>
	Applied to catchment (t yr <sup>-1</sup> )	In-stream load to lake (t yr <sup>-1</sup> )	Surface of lake (mg L <sup>-1</sup> )	Bottom of lake (mg L <sup>-1</sup> )	Applied to catchment (t yr <sup>-1</sup> )	In-stream load to lake (t yr <sup>-1</sup> )	Surface of lake (mg L <sup>-1</sup> )	Bottom of lake (mg L <sup>-1</sup> )	Surface of lake (µg L <sup>-1</sup> )
S1–Irr1Pas1	65	4.3	0.0254	0.0275	180	62.9	0.368	0.394	14.178
S2–Irr0Pas1	40	3.7	0.0248	0.0262	127	46.7	0.358	0.373	13.731
S3–Irr1Pas0	25	2.9	0.0248	0.0263	53	31.8	0.353	0.369	13.775
S4–Irr0Pas0	0	2.6	0.0245	0.0256	0	15.6	0.347	0.357	13.597
	% change				% change				% change
S1–Irr1Pas1 vs. S2–Irr0Pas1	-38.5	-14.0	-2.4	-4.7	-29.4	-25.8	-2.7	-5.3	-3.2
S1–Irr1Pas1 vs. S3–Irr1Pas0	-61.5	-32.6	-2.4	-4.4	-70.6	-49.4	-4.1	-6.3	-2.8
S1–Irr1Pas1 vs. S4–Irr0Pas0	-100.0	-39.5	-3.5	-6.9	-100.0	-75.2	-5.7	-9.4	-4.1

### **4.4.3 Catchment and lake scenarios: 2090 climate**

Two climate change scenarios were simulated to predict changes to lake trophic state in response to a projected future climate of 2090. The first considered the effects of 2090 climate forcing on discharge and nutrient loadings from the catchment but simulated the lake with meteorological input data from a current (2006–10) climate. The second used 2090 climate data as input to both the catchment and the lake models. This study design was intended to isolate the impact on lake water quality of projected future climate effects on catchment processes (e.g., altered discharge and nutrient fluxes) from projected future climate effects directly on the lake (e.g., increased phytoplankton growth rates due to elevated temperature). For the 2090 climate impact on the catchment only (CC1) and on both catchment and lake (CC2), scenario S2–Irr0Pas1 was applied for other streams and on the lake (see details in Section 4.3.4.2).

#### **4.4.3.1 Effects of climate change on catchment discharge, suspended solids and nutrient loads**

For the projected future climate of 2090 (IPCC, 2013), annual mean precipitation and solar radiation are projected to increase by 2.8% and 1.4%, respectively, humidity to decrease by 0.6%, and air temperature to increase by 2.7 °C. For precipitation, the largest increase will be in the month of March and the largest decrease will be in October, although total annual precipitation is predicted to change negligibly.

Relative to the scenario S2–Irr0Pas1, for each sub-catchment discharge and SS loads increased by 4.6% and 3.8%, respectively, under the 2090 climate scenario (Table 4.10). Nutrient loads increased with the exception of NO<sub>3</sub>-N and TN. The largest load increases were 14.4% for NH<sub>4</sub>-N load, followed by 6% for DRP, ORGP, TP and 5.8% for ORGN. The largest load decrease was 13.4% for NO<sub>3</sub>-N, which was mostly responsible for a load decrease in TN by 7.6%. A 2090 climate generally resulted in large increases in discharge, suspended solids and nutrients from January to April, and small increases from May to September (Table 4.10). Increases were greatest in March; 11.1% for discharge, 11.5% for SS load, 15.3% for ORGP, 10.4% for TP, and 14.3% for ORGN. For dissolved nutrient species loads, decreases of NO<sub>3</sub>-N were greatest in September (28%), and increases of DRP (7.5%) and NH<sub>4</sub>-N (15.7%) were greatest in July.



Relative to the scenario S2–Irr0Pas1, the 2090 climate scenario (i.e., 2090 climate applied to the catchment model but current climate applied to the lake model; CC1) was predicted by DYRESM–CAEDYM to cause relatively minor changes in Lake Rotorua water quality (see Table 4.8 and 4.10). Periods of lake thermal stratification indicated by the number of days with changes in surface and bottom water temperatures ( $\Delta T$ ) greater than 0.5 °C (Losordo and Piedrahita, 1991) under current climate (CC0) were similar to the periods of thermal stratification under 2090 climate applied only to the catchment (CC1) (see Table 4.8). Minimal changes were also found to the number of days with dissolved oxygen (DO) concentrations in bottom waters  $< 2 \text{ mg L}^{-1}$  (i.e., a threshold for depletion of DO; Stuber et al., 1982) and the number of days with Chl *a* concentrations in surface waters  $> 15 \text{ } \mu\text{g L}^{-1}$  (i.e., a threshold for cold water fisheries; McGhee, 1983) under CC0 and CC1 for the catchment (Table 4.8).

Under the 2090 climate scenario (CC1), annual mean TN concentration decreased by 3.0% in lake surface waters and 2.3% in bottom waters (Table 4.10), with the largest monthly decrease in surface waters in September (5.6%) and in bottom waters in January (6.3%). Small increases were predicted in annual mean TP concentrations in the lake surface (0.2%) and bottom (0.9%) waters. Small increases (1.9%) were predicted in annual mean Chl *a* concentrations in the lake surface by 2090 (Table 4.10). Relative to the scenario S2–Irr0Pas1, applying the climate change scenario (CC1) to the catchment model (but not the lake model) yielded a negligible change in the mean TLI3 value (Table 4.8).

#### **4.4.3.2 Effects of climate change on catchment and lake water quality**

Under the projected future climate of 2090, annual mean evaporation is predicted by the lake model to increase by 10.6% (Table 4.11). For the surface water catchment, annual mean inflow water temperature simulated by the SWAT2012 model increases by 2 °C. For the groundwater recharge catchment, inflow water temperature increases by 2.4 °C (quantified by 88% of the projected increase in air temperature; Kurylyk et al., 2013). Generally, largest increases in water temperatures for surface water and groundwater were found from January to April (Table 4.11).

Relative to the scenario S2–Irr0Pas1, more frequent and longer periods of thermal stratification were simulated by DYRESM–CAEDYM for Lake Rotorua in 2090 (see Table 4.8), indicated by the number of days with  $\Delta T > 0.5$  °C increasing from 294 (under CC0) to 345 (under CC2). The number of days with DO concentrations in bottom waters  $< 2$  mg L<sup>-1</sup> was predicted to increase 2.4–fold from 58 (under CC0) to 141 (under CC2), while the number of days with Chl *a* concentrations in surface waters  $> 15$  µg L<sup>-1</sup> was predicted to increase 1.5–fold from 291 (under CC0) to 446 (under CC2).

Applying the combined catchment–lake model simulations using forcing data for a projected 2090 climate gave an increase in annual mean TP, TN and Chl *a* concentrations in lake surface waters of 45.9%, 44.5% and 44.9%, respectively (Table 4.11), compared with concentrations under the current climate (CC0). The largest increase was in March for TP (57.5%) and February for TN (56.9%) in lake surface waters. For Chl *a* in surface waters, the largest increase was in January (109%) and the smallest increase was in July (4.2%). For bottom waters TP and TN concentrations increased by 56.4% and 56.8%, respectively (Table 4.11). The largest increase occurred in February for TP (141.1%) and TN (152.0%) in bottom waters.

The 2090 climate scenario applied to the catchment and the lake model gave a substantial increase in the mean TLI3 value from 4.46 (current climate) to 4.88 (Table 4.8). Figure 4.5 shows the major changes in annual mean concentrations of TP and TN in the surface and bottom waters and Chl *a* in surface waters of Lake Rotorua between the 2090 climate on the catchment only (CC1) and on both the catchment and lake (CC2).

**Table 4.11** Precipitation (PCP), solar radiation (SLR), air temperature ( $T_a$ ), humidity (HMD), evaporation ( $E_a$ ), water temperatures of inflows from groundwater discharge sub-catchments ( $T_{gw}$ ) and from surface water sub-catchments ( $T_{sw}$ ), and changes in nutrient concentrations in Lake Rotorua in response to a projected 2090 climate, for both Lake Rotorua catchment and lake. The increase in  $T_{gw}$  was 88% of the increase in  $T_a$  while the increase in  $T_{sw}$  was from the SWAT output. The TLI3 is a three-variable Trophic Level Index function derived from concentrations of total nitrogen (TN), total phosphorus (TP) and chlorophyll *a* (Chl *a*), which used to indicate the lake trophic state (Burns et al., 1999). The colour scale was specified for each variable in each column and indicates the range of % change.

Month	Absolute changes in inflow water temperature (°C)		Changes for water balance calculations (%)					Changes of concentrations (%)					
	* $T_{gw}$	* $T_{sw}$	* $T_a$	SLR	HMD	$E_a$	PCP	Lake surface			Lake bottom		TLI3
								TP	TN	Chl <i>a</i>	TP	TN	
Jan	2.8	2.4	3.2	1.1	-0.7	8.6	5.0	48.0	46.3	109.9	56.0	58.7	
Feb	2.6	2.3	3.0	0.7	-1.4	7.7	6.0	56.9	56.9	98.7	141.1	152.0	
Mar	2.7	2.3	3.1	0.7	0.0	10.0	12.7	57.5	56.3	52.2	61.1	60.1	
Apr	2.5	2.1	2.8	1.2	-0.7	20.4	6.9	51.7	52.8	28.1	52.6	53.7	
May	2.4	2.0	2.7	1.8	-0.4	21.5	3.4	48.4	49.8	17.5	48.4	49.9	
Jun	2.3	1.9	2.6	2.2	-0.3	20.9	3.6	45.6	46.3	9.0	45.6	46.3	
Jul	2.4	2.0	2.7	0.9	-0.3	12.2	2.2	39.7	38.5	4.2	39.7	38.5	
Aug	2.4	2.0	2.7	1.0	0.0	12.8	4.9	36.9	32.2	16.6	36.8	32.8	
Sep	2.1	1.8	2.4	2.4	-0.1	9.6	-4.1	34.5	28.7	9.4	32.9	28.8	
Oct	2.2	1.9	2.5	2.8	-0.6	5.9	-7.8	34.2	28.1	6.2	35.5	30.4	
Nov	2.1	1.8	2.4	1.4	-1.1	8.1	-0.5	33.2	29.0	15.8	37.7	32.3	
Dec	2.3	1.9	2.6	1.0	-1.2	7.1	-1.7	38.2	35.1	42.6	45.1	42.0	
<b>Annual</b>	<b>2.4</b>	<b>2.0</b>	<b>2.7</b>	<b>1.4</b>	<b>-0.6</b>	<b>10.6</b>	<b>2.8</b>	<b>45.9</b>	<b>44.5</b>	<b>44.9</b>	<b>56.4</b>	<b>56.8</b>	<b>4.88</b>



## 4.5 Discussion

This study integrated catchment discharge and nutrient concentrations from the SWAT2012 model with lake water quality modelled by DYRESM–CAEDYM, yielding a quantitative assessment of the effects of land management practices and future climate change on trophic state of a nationally iconic lake in New Zealand. Simulation of a range of nutrient load and climate scenarios using a factorial study design allowed the relative effects of land management and projected climate change to be examined. Further, the effects of projected climate change on lake water quality were then examined to isolate the effects due to catchment processes, from those due to in-lake processes. The results show that the effects on lake water quality due to major changes to nutrient loading in one sub-catchment are minor relative to the effects due to changes to in-lake processes associated with projected climate change.

### 4.5.1 Model performance and sensitivity

Concentrations of TN and TP in the Puarenga Stream simulated with the improved SWAT2012 model were better than those using SWAT2009 (see Me et al., 2015). For the validation period, discharge and TP and TN loads from the Puarenga Stream catchment simulated using the SWAT2012 model generally showed positive correlations ( $r \geq 0.88$ ,  $p < 0.001$ ) with the measured data, but less so for in-stream concentrations of TN ( $r = 0.78$ ,  $p < 0.01$ ) and TP ( $r = 0.17$ ,  $p > 0.05$ ). Overestimates of discharge in Puarenga Stream during high rainfall in winter could be due to overestimates of lateral flow contributions (Cartwright et al., 2014). The relatively high value of parameter slope steepness (HRU\_SLP), assigned as 0.1 (equal to 5.7 degrees slope) and integrated over the entire catchment in this study, may have resulted in overestimates of lateral flow contributions from shallow aquifers to stream channels (Ward et al., 2012).

Periods of elevated discharge are also important because they correspond to increased nutrient mobilisation and erosive processes operating at the landscape scale (Abell et al., 2013). Poor model performance for simulations of DRP and TP concentrations could be partly related to the SWAT2012 soil P parameters, which are lumped for the catchment, such as PSP (P availability index), PHOSKD (soil P partitioning coefficient) and PPERCO (soil P percolation coefficient) (Arnold et al.,

2013). Ideally, parameter values should also be optimised with regard to episodic events (Zhang et al., 2015) and for dry and wet periods or different upland irrigation regimes such as in the forestry-harvested area in this study. It is possible therefore, that the values of these parameters do not accurately represent P transport on the landscape following rainfall.

Seasonal variations in concentrations of N species from the Puarenga Stream catchment were well simulated by SWAT2012. Higher simulated concentrations of  $\text{NH}_4\text{-N}$  occurred in summer, likely due to the increased temperature in this season, which enhances rates of organic mineralisation processes (Hien et al., 2016). The underestimation of  $\text{NH}_4\text{-N}$  concentrations in winter could have also resulted from overestimates of discharge in Puarenga Stream during high rainfall in winter. Higher concentrations of  $\text{NO}_3\text{-N}$  simulated in winter were probably caused by the higher leaching rates of  $\text{NO}_3\text{-N}$  when the soils become saturated in winter during high rainfall, resulting in high rates of lateral flow to the stream. Simulated  $\text{NO}_3\text{-N}$  concentrations were lower than observed values in summer, probably because of the inability of SWAT to adequately replicate the relative increase in groundwater, with elevated  $\text{NO}_3\text{-N}$  concentrations, contributing to the stream discharge (Bain et al., 2012). This highlights the importance of enhancing SWAT predictions by simulating interactions between the groundwater aquifer and river channel, which represents a critical area for nutrient dynamics (Guzman et al., 2015).

The lake model (DYRESM-CAEDYM) predictions for surface waters showed strong seasonality that was similar to the measured data, with high positive correlations for measured and simulated TP and TN concentrations. Small increases in TP and TN concentrations observed in lake surface waters in spring were well reproduced by DYRESM-CAEDYM, and this was associated with bottom nutrients being transported to surface waters during mixing (Shaw et al., 2004). Polymictic, temperate lakes mix intermittently during the summer stratified period in response to wind (Kourzeneva et al., 2012) and this was both observed and simulated in this study. Brief spikes of  $\text{PO}_4\text{-P}$  and  $\text{NH}_4\text{-N}$  concentrations observed in lake surface waters in summer were also well simulated due to the ability of the model to capture wind-driven lake-turnover events. The accumulated nutrients and increased temperature during this period concurrently accelerated phytoplankton growth, resulting concentrations of Chl *a* (as a proxy for phytoplankton biomass)

in lake surface waters were simulated high in summer. However, poor model performance for Chl *a* concentrations could be attributed that changes to phytoplankton assemblages (e.g., the proportion of cyanobacteria) responding differently to nutrient enrichment and temperature were not considered in this study. In general, DYRESM–CAEDYM reproduces well the temporary stratification and deoxygenation events that lead to release of PO<sub>4</sub>–P and NH<sub>4</sub>–N from the bottom sediments (Hamilton et al., 2004; Burger et al. 2007a). The annual maximum of PO<sub>4</sub>–P, NO<sub>3</sub>–N and NH<sub>4</sub>–N concentrations in surface waters was both observed and simulated during winter, which could be attributed to higher rainfall during this season, transporting more nutrients into the lake (Abell et al., 2013), as well as lower nutrient uptake rates associated with lower temperature and reduced light availability.

#### **4.5.2 Reducing nutrient loads to the Puarenga Stream catchment**

Nutrient loads to the Puarenga Stream decreased as expected under the different nutrient load reduction scenarios. Under the scenario of wastewater removal (S2–Irr0Pas1), the reduction (38.5%) in the applied TP load was larger than the reduction (14.0%) in in–stream TP load. This finding could be explained by the high soil P adsorption rate (PSP was set to 0.6; mean value derived from Beets et al., 2013). Loads of TN in the farmland–applied fertiliser were 2.4 times higher than those associated with the applied wastewater, and consequently simulations of in–stream annual TN loads under the scenario S2–Irr0Pas1 were 1.5 times higher than those under the scenario of farmland–applied fertiliser removal (S3–Irr1Pas0). The difference indicates there is also some loss of N between the stream and where it is applied, which may be attributed to processes such as plant uptake and export of N in production, as well as denitrification. Without any anthropogenic nutrient loadings (S4–Irr0Pas0), there was a moderate reduction of in–stream annual TP load (39.5%) and a large reduction of in–stream annual TN load (75.2%). The difference between N and P may be attributed to the high soil P adsorption rate (PSP; 0.6), resulting in a legacy of P (see Sharpley et al., 2014) being retained in the catchment soils. By contrast, the relatively rapid leaching of N reflects the mobile nature of this nutrient (Zogg et al., 2000) with high N percolation rate assigned in the SWAT model (NPERCO; 0.05).

The scenario without any anthropogenic nutrient loadings from the Puarenga Stream catchment (i.e., S4-Irr0Pas0) was predicted to cause minimal improvement to lake water quality. Simulated nutrient reductions in the Puarenga Stream catchment are a minor fraction of total catchment nutrient load to Lake Rotorua and TP and TN loads remain largely unchanged. In the short term, the benefits from external nutrient load reductions may be difficult to decipher unless they are large in magnitude relative to internal loading. For shallow, polymictic Lake Rotorua, periods of thermal stratification, of sufficient duration to generate hypoxia, lead to large nutrient releases to bottom waters (Burger et al., 2007a) and are interspersed with mixing events that make these nutrients available to support phytoplankton production in euphotic waters.

### **4.5.3 Climate change impacts on catchment and lake**

Predictions from the combined climate–catchment model indicate that there would be increases in discharge, and loads of SS, and especially particulate N and P, mostly from January to April for a 2090 climate. This could be explained by the elevated rates of soil erosion and mobilisation of particulate P and N associated with increased frequency of intense rainfall events which generate quick flow. Decreases in simulated discharge during October reflect small projected declines in precipitation during the Austral spring. The finding that discharge goes up by 4.6% when precipitation only increases by 2.8% could be explained by the fact that the Puarenga Stream catchment is covered extensively by forest (47%) and reflects relatively high and seasonally–consistent rainfall (1252 mm yr<sup>-1</sup>), which reduces soil evaporative demand through tree shading.

Elevated soil temperature and in–stream water temperature in 2090 would increase decomposition and mineralisation of organic matter, which would then increase DRP and NH<sub>4</sub>–N loads. Hien et al. (2016) predicted that NH<sub>4</sub>–N loads would increase in almost all months of the year in response to projected future climate warming, an effect that they attributed to organic mineralisation processes. Large decreases in NO<sub>3</sub>–N load exported from the Puarenga Stream catchment occurred in September and October under projected climate change compared with current climate, which corresponded to a period of decreased precipitation in these months. Loads of NO<sub>3</sub>–N also decreased from January to August 2090 during a period of increased precipitation, revealing that elevated soil temperature due to

warming would increase plant uptake and denitrification processes, causing a decrease in  $\text{NO}_3\text{-N}$  losses and leaching from the catchment. This is consistent with N simulation results in Arheimer et al. (2012), who modeled climate change impacts on riverine nutrient loads to the Baltic Sea. They similarly predicted decreased  $\text{NO}_3\text{-N}$  losses associated with climate change, which they attributed to plant uptake and denitrification processes.

Donnelly et al. (2011) predicted that TN load from the Vistula River catchment (Poland; 325 km<sup>2</sup>; 63% agricultural land use) would decrease by 4% under increased temperature due to global warming. In the Puarenga Stream catchment, 47% of the land use is exotic *Pinus radiata* forest, and therefore plant uptake could play the primary role in reducing TN loads from the catchment; TN loads decreased 7.6% under the 2090 climate in our study. For 10 catchments (areas 4.36 to 41.91 km<sup>2</sup>) in the north of Denmark with similar rainfall to our study area, predicted increases in TP loads ranged from 3.3% to 16.5% by 2100 (Jeppesen et al., 2009). Increases in TP load (6%) predicted for the Puarenga Stream catchment in 2090 were small compared to values given by Jeppesen et al (2009), and may reflect high soil P adsorption in soils of this catchment (Beets et al., 2013) and correspondingly high P adsorption rate (0.6) in the model. The contrasting response of catchment TN and TP loads to projected climate change likely reflects the relatively rapid mobilisation of N through leaching, while P is mostly retained in the soils. Under the 2090 climate applied to the catchment only, there was a decrease (3.0%) in annual mean TN concentration in lake surface waters but an increase (1.9%) in annual mean Chl *a* concentrations, highlighting the potential that redox dynamics of N in the bottom waters could be changed by the decreased external  $\text{NO}_3\text{-N}$  load (Burger et al., 2008).

For shallow, polymictic Lake Rotorua, increased water temperatures in 2090, with frequent and longer periods of summer thermal stratification and bottom water deoxygenation, are consistent with previous models of this lake (Özkundakci et al., 2012) and lakes elsewhere (e.g., Wilhelm and Adrian, 2008). The stratification–deoxygenation effect was well predicted by DYRESM–CAEDYM under base conditions. An increase in temperature will also enhance the mineralisation of organic matter as well as causing higher rates of sediment nutrient release (e.g.,  $\text{NH}_4\text{-N}$  and  $\text{PO}_4\text{-P}$ ) from bottom sediments (Adrian et al., 2009). These two inorganic nutrient species ( $\text{NH}_4\text{-N}$  and  $\text{PO}_4\text{-P}$ ) have been found by

Burger et al. (2008) to be the dominant source of increases in N and P concentrations in surface waters of Lake Rotorua when there are mixing events following extended stratification periods during summer. Burger et al. (2008) also found that nutrients released from the bottom sediments contributed a major proportion of nutrients inputs to the lake compared with external loadings. Increasing water temperature in 2090 and more stratification produced simulations with higher concentrations of TP and TN from January to April in particular, in the climate warming scenarios. Following the release from bottom sediments, nutrients, i.e.,  $\text{NH}_4\text{-N}$  and  $\text{PO}_4\text{-P}$  forms readily assimilated by phytoplankton (Burger et al., 2008), accumulate in bottom waters and accelerate phytoplankton growth when subsequently mixed through the water column (Hamilton et al., 2012). Concurrently, increased temperature directly stimulates growth of phytoplankton, which explained that concentrations of Chl *a* (as a proxy for phytoplankton biomass) in lake surface waters were simulated to increase from January to March with increased temperature under a 2090 climate, compared with the baseline climate. Catchment TN loadings (dominated by  $\text{NO}_3\text{-N}$ ) decreased by 7.6% while lake surface TN concentrations (dominated by  $\text{NH}_4\text{-N}$ ) increased by 44.5% under a 2090 climate, highlighting that careful consideration of the different forms of nitrogen is required to better understand responses to climate change.

Increases in external nutrient loads and increasing temperature in a future climate are likely to act synergistically to negatively impact on lake water quality (e.g., Komatsu et al., 2007). Although external nitrogen load was predicted in this study to decline moderately, by 7.6% with future climate warming of 2090, TN concentrations were much higher for the lake (> 40%), implying that direct effects of climate change dominate in this eutrophic polymictic lake. Although changes to phytoplankton assemblages (e.g., the proportion of cyanobacteria) were not considered in this study, potential for changes in species composition have also been noted in many studies (e.g., Carey et al., 2012). Trolle et al. (2011) modelled mean Chl *a* concentrations dominated by chlorophytes and diatoms in a shallow and eutrophic lake (Lake Ellesmere, Canterbury, South Island) using DYRESM-CAEDYM and found that chlorophytes increasingly dominated diatoms with water temperature increases. In eutrophic Lake Rotoehu (maximum depth ~ 13 m) in the Bay of Plenty Region near Lake Rotorua, Trolle et al. (2011) found that cyanophytes increased substantially in summer months under a warmer climate.

Lower diatom biomass was also predicted during future winter climates by Mooij et al. (2007), who examined the impacts of increasing water temperature on a shallow lake in Europe using the PCLake model. These studies indicate that different groups of phytoplankton will respond differently to N and P enrichment, as well as climate change. Variations in internal nutrient loads may also influence the succession of phytoplankton, as noted by Burger et al. (2007b).

The predictions of water quality in lake surface waters with climate change may have some degree of uncertainty because future changes in wind speed were not considered in this study. Water column stratification is highly sensitive to this variable (Adrian et al., 2009). Furthermore, long-term variability of bottom-sediment composition was not considered in DYRESM-CAEDYM simulations in this study. Rather, fixed sediment release rate parameters were input to the model, with rates adjusted within model simulations according to overlying water temperature and DO. Özkundakci et al. (2012) provide an empirical attempt to modify sediment composition of Lake Rotorua according to lake trophic status but more information would ideally be required to apply this in our study. Nutrient releases will continue to be highly important for lake management but the model simulations have clearly identified that there is potential for major increases in trophic state in Lake Rotorua without adoption of more stringent nutrient control measures for the catchment.

In summary, simulations using the lake model (DYRESM-CAEDYM) showed that lake water quality effects caused by large reductions to nutrient loads in the Puarenga Stream were relatively small as the stream contributes only ~16% of total nutrient loads to Lake Rotorua. Lake water quality effects caused by climate change arise primarily from changes in internal nutrient loads as a result of changes in thermal stratification. For shallow, polymictic Lake Rotorua, by 2090 there are likely to be more extended periods of thermal stratification in summer. In the short term (i.e., months to a few years) internal lake nutrient dynamics (i.e., sediment-water exchanges) affect water quality considerably more than external nutrient loadings from the catchment.

## 4.6 References

- Abell, J.M., Hamilton, D.P., and Paterson, J.: Reducing the external environmental costs of pastoral farming in New Zealand: experiences from the Te Arawa lakes, Rotorua, *Australasian J. Environ. Manage.*, 18, 139–154, 2011.
- Abell, J.M., Hamilton, D.P., and Rutherford J.C.: Quantifying temporal and spatial variations in sediment, nitrogen and phosphorus transport in stream inflows to a large eutrophic lake, *Environ. Sci. Processes Impacts*, 15, 1137–1152, 2013.
- Abell, J.M., McBride, C.M., and Hamilton, D.P.: Lake Rotorua wastewater discharge: environmental effects study, ERI Report No. 80, Client report prepared for Rotorua Lakes Council, Environmental Research Institute, Faculty of Science and Engineering, the University of Waikato, Hamilton, New Zealand, 122 pp., 2015.
- Adrian, R., O'Reilly, C.M., Zagarese, H., Baines, S.B., Hessen, D.O., Keller, W., Livingstone, D.M., Sommaruga, R., Straile, D., Van Donk, E., Weyhenmeyer, G.A., and Winder, M.: Lakes as sentinels of climate change, *Limnol. Oceanogr.*, 54, 2283–2297, 2009.
- Anastasiadis, S., Nauleau, M-L., Kerr, S., Cox, T., and Rutherford K.: Water quality management in Lake Rotorua: a comparison of regulatory approaches using the NManager Model, Proceedings of the 52<sup>nd</sup> Annual Conference of the New Zealand Association of Economists, Wellington, New Zealand, 46 pp., 2011.
- Arheimer, B., Dahné, J., and Donnelly, C.: Climate change impact on riverine nutrient load and land-based remedial measures of the Baltic Sea Action Plan, *Ambio*, 41, 600–612, 2012.
- Arnell, N.W., Halliday, S.J., Battarbee, R.W., Skeffington, R.A., and Wade, A.J.: The implications of climate change for the water environment in England, *Prog. Phys. Geog.*, 39, 93–120, 2015.
- Arnold, J., Kiniry, J., Srinivasan, R., Williams, J., Haney, E., and Neitsch, S.: Soil & Water Assessment Tool Input/output documentation version 2012, Technical Report No 439, Texas Water Resources Institute, College Station, TX, the United States, 651 pp., 2013.
- Bain, D.J., Green, M.B., Campbell, J.L., Chamblee, J.F., Chaoka, S., Fraterrigo, J.M., Kaushal, S.S., Martin, S.L., Jordan, T.E., and Parolari, A.J.: Legacy effects in material flux: structural catchment changes predate long-term studies, *BioScience*, 62, 575–584, 2012.
- Beets, P.N., Gielen, G., Oliver, G.R., Pearce, S.H., and Graham, J.D.: Determination of the level of soil N and P storage and soil health at the Rotorua Land Treatment site, Scion Report 50659, New Zealand Forest Research Institute Limited, Rotorua, New Zealand, 39 pp., 2013.
- Bewick, V., Cheek, L., and Ball, J.: Statistics review 7: correlation and regression, *Crit. Care*, 7, 451–459, 2003.

- Bruce, L.C., Hamilton, D.P., Imberger, J., Gal, G., Gophen, M., Zohary, T., and Hambright, K.D.: A numerical simulation of the role of zooplankton in C, N and P cycling in Lake Kinneret, Israel. *Ecol. Model.*, 193, 412–436, 2006.
- Burger, D.F., Hamilton, D.P., Pilditch, C.A., and Gibbs, M.M.: Benthic nutrient fluxes in a eutrophic, polymictic lake, *Hydrobiologia*, 584, 13–25, 2007a.
- Burger, D.F., Hamilton, D.P., Hall, J.A., and Ryan, E.F.: Phytoplankton nutrient limitation in a polymictic eutrophic lake: community versus species-specific responses, *Fund. Appl. Limnol.*, 169, 57–68, 2007b.
- Burger, D.F., Hamilton, D.P., and Pilditch, C.A.: Modelling the relative importance of internal and external nutrient loads on water column nutrient concentrations and phytoplankton biomass in a shallow polymictic lake, *Ecol. Model.*, 21, 411–423, 2008.
- Burns, N.M., Rutherford, J.C., and Clayton, J.S.: A monitoring and classification system for New Zealand lakes and reservoirs, *Lake Reserv. Manage.*, 15, 255–271, 1999.
- Cao, W., Bowden, W.B., Davie, T., and Fenemor, A.: Multi-variable and multi-site calibration and validation of SWAT in a large mountainous catchment with high spatial variability, *Hydrol. Process.*, 20, 1057–1073, 2006.
- Carey, C.C., Ibelings, B.W., Hoffman, E.P., Hamilton, D.P., and Brookes J.D.: Eco-physiological adaptations that favour freshwater cyanobacteria in a changing climate, *Water Res.*, 46, 1394–1407, 2012.
- Cartwright, I., Gilfedder, B., and Hofmann, H.: Contrasts between estimates of baseflow help discern multiple sources of water contributing to rivers, *Hydrol. Earth Syst. Sc.*, 18, 15–30, 2014.
- Copetti, D., Tartari, G., Morabito, G., Oggioni, A., Legnani, E., and Imberger, J.: A bio-geochemical model of Lake Pusiano (North Italy) and its use in the predictability of phytoplankton blooms: first preliminary results, *J. Limnol.*, 65, 59–64, 2006.
- Debele, B., Srinivasan, R., and Parlange, J.Y.: Coupling upland watershed and downstream water body hydrodynamic and water quality models (SWAT and CE-QUAL-W2) for better water resources management in complex river basins, *Environ. Model. Assess.*, 13, 135–153, 2008.
- Donnelly, C., Strömqvist, J., and Arheimer, B.: Modelling climate change effects on nutrient discharges from the Baltic Sea Catchment, in: *Water Quality: Current Trends and Expected Climate Change Impacts*, Proceedings of symposium H04 held during IUGG2011, Melbourne Australia, IAHS Publ., 348, 145–150, 2011.
- Environment Bay of Plenty: Historical data summary, Report prepared for Bay of Plenty Regional Council, Rotorua, New Zealand, 522 pp., 2007.
- Fertiliser & Lime Research Centre: Sustainable nutrient management in New Zealand agriculture: Introductory notes and mastery test, Institute of Agriculture & Environment, Massey University, Palmerston North, New Zealand, 94 pp., 2014.

- Foote, K.J., Joy, M.K., and Death, R.G.: New Zealand dairy farming: Milking our environment for all its worth, *Environ. Manage.*, 56, 709–720, 2015.
- Gabriele, W., Welti, N., and Hein, T.: Limitations of stream restoration for nitrogen retention in agricultural headwater streams, *Ecol. Eng.*, 60, 224–234, 2013.
- Glavan, M., Ceglar, A., and Pintar, M.: Assessing the impacts of climate change on water quantity and quality modelling in small Slovenian Mediterranean catchment – lesson for policy and decision makers, *Hydrol. Process.*, 29, 3124–3144, 2015.
- Guzman, J.A., Moriasi, D.N., Gowda, P.H., Steiner, J.L., Starks, P.J., Arnold, J.G., Srinivasan, R.: A model integration framework for linking SWAT and MODFLOW, *Environ. Model. Softw.*, 73, 103–116, 2015.
- Hamilton, D.P., Alexander, W., and Burger, D.: Nutrient budget for Lakes Rotoiti and Rotorua Part 1: Internal nutrient loads, Centre for Biodiversity and Ecology Research, the University of Waikato, Hamilton, New Zealand, 49 pp., 2004.
- Hamilton, D.P., McBride, C.G., and Jones, H.F.E.: Assessing the effects of alum dosing of two inflows to Lake Rotorua against external nutrient load reductions: Model simulations for 2001-2012, Report 49, Environmental Research Institute, University of Waikato, Hamilton, New Zealand, 56 pp., 2015.
- Hamilton, D.P., Özkundakci, D., McBride, C.G., Ye, W., Luo, L., Silvester, W., and White, P.: Predicting the effects of nutrient loads, management regimes and climate change on water quality of Lake Rotorua, University of Waikato Report 005, Environmental Research Institute, University of Waikato, Hamilton, New Zealand, 73 pp., 2012.
- Hamilton, D.P., and Schladow, S.G.: Prediction of water quality in lakes and reservoirs. Part I – Model description, *Ecol. Model.*, 96, 91–110, 1997.
- Hamilton, D.P., Salmaso, N., and Paerl, H.W.: Mitigating harmful cyanobacterial blooms: strategies for control of nitrogen and phosphorus loads, *Aquat. Ecol.*, 50, 351–366, 2016.
- Herger, N., Sanderson, B.M, and Knutti, R.: Improved pattern scaling approaches for the use in climate impact studies, *Geophys. Res. Lett.*, 42, 3486–3494, 2015.
- Hien, H.N., Hoang, B.H., Huong, T.T., Than, T.T., Ha, P.T.T., Toan, T.D., and Son, N.M.: Study of the climate change impacts on water quality in the upstream portion of the Cau River Basin, Vietnam, *Environ. Model Assess.*, 21, 261–277, 2016.
- Hoare, R.A.: Inflows to Lake Rotorua, *Journal of Hydrology (NZ)*, 19, 49–59, 1980.
- Huntingford, C., Booth, B., Sitch, S., Gedney, N., Lowe, J., Liddicoat, S., Mercado, L., Best, M., Weedon, G., Fisher, R.A., Good, P., Zelazowski, P., Spessa, A.C., and Jones, D.C.: IMOGEN: an intermediate complexity model to evaluate terrestrial impacts of a changing climate, *Geosci Model Dev.*, 3, 679–687, 2010.

- Hussain, I., Raschid, L., Hanjra, M.A., Marikar, F., and van der Hoek, W.: Wastewater use in agriculture: Review of impacts and methodological issues in valuing impacts, Working Paper 37, International Water Management Institute, Colombo, Sri Lanka, 62 pp., 2002.
- IPCC: Climate Change 2013: The physical science basis, in: Contribution of Working Group I to the Fifth Assessment Report of the Intergovernmental Panel on Climate Change, edited by: Stocker, T.F., Qin, D., Plattner, G.-K., Tignor, M.M.B., Allen, S.K., Boschung, J., Nauels, A., Xia, Y., Bex, V., and Midgley, P.M., Cambridge University Press, Cambridge, New York, the United States, 1535 pp., 2013.
- Jeppesen, E., Kronvang, B., Meerhoff, M., Søndergaard, M., Hansen, K.M., Andersen, H.E., Lauridsen, T.L., Beklioglu, M., Ozen, A., and Olesen, J.E.: Climate change effects on runoff, catchment phosphorus loading and lake ecological state, and potential adaptations, *J. Environ. Qual.*, 38, 1930–1941, 2009.
- Komatsu, E., Fukushima, T., and Harasawa, H.: A modeling approach to forecast the effect of long-term climate change on lake water quality, *Ecol. Model.*, 209, 351–366, 2007.
- Kourzeneva, E., Martin, E., Batrak, Y., and Le Moigne, P.: Climate data for parameterisation of lakes in numerical weather prediction models, *Tellus A*, 64, 1–17, 2012.
- Krebs, C.J.: Restoration ecology applies ecological knowledge to repair damaged communities, in: *The ecological world view*, edited by: Krebs, C.J., University of California Press, Berkeley and Los Angeles, California, the United States, 300 pp., 2008.
- Kurylyk, B.L., Bourque, C.P.-A., and MacQuarrie, K.T.B.: Potential surface temperature and shallow groundwater temperature response to climate change: an example from a small forested catchment in east-central New Brunswick (Canada), *Hydrol. Earth Syst. Sc.*, 17, 2701–2716, 2013.
- Lopez, A., Suckling, E.B., and Smith, L.A.: Robustness of pattern scaled climate change scenarios for adaptation decision support, *Clim. Chang.*, 122, 555–566, 2014.
- Losordo, T.M., and Piedrahita, R.H.: Modelling temperature variation and thermal stratification in shallow aquaculture ponds, *Ecol. Model.*, 54, 189–226, 1991.
- Lowe, A., Gielen, G., Bainbridge, A., and Jones, K.: The Rotorua land treatment systems after 16 years, in: *New Zealand Land Treatment Collective – Proceedings for the 2007 Annual Conference, 14–16 March 2007, Rotorua, New Zealand*, pp. 66–73, 2007.
- Lustenberger, A., Knutti, R., and Fischer, E.M.: The potential of pattern scaling for projecting temperature-related extreme indices, *Int. J. Climatol.*, 34, 18–26, 2014.
- McGhee, R.F.: Experiences in developing a chlorophyll *a* standard in the Southeast to protect lakes, reservoirs and estuaries, in: *Lake Restoration Protection and Management, Proc. 2<sup>nd</sup> Annu. Conf., N. Am. Lake Manage.*

- Soc., EPA 440/5-83-001, U.S. Environ. Prot. Agency, Washington, D.C., pp. 163-165, 1983.
- Me, W., Abell, J.M., and Hamilton, D.P.: Effects of hydrologic conditions on SWAT model performance and parameter sensitivity for a small, mixed land use catchment in New Zealand, *Hydrol. Earth Syst. Sc.*, 19, 4127-4147, 2015.
- Me, W., Hamilton, D.P., and Abell, J.M.: Simulating discharge and contaminant loads from the Waipa Stream catchment under different irrigation scenarios using the SWAT model, Client report prepared for Rotorua Lakes Council, ERI Report No. 98, Faculty of Science and Engineering, University of Waikato, Hamilton, New Zealand, 32 pp., 2017.
- Mitchell, T.D.: Pattern scaling: An examination of the accuracy of the technique for describing future climates, *Clim. Chang.*, 60, 217-242, 2003.
- Mooij, W.M., Janse, J.H., De Senerpont Domis, L.N., Hülsmann, S., and Ibelings, B.W.: Predicting the effect of climate change on temperate shallow lakes with the ecosystem model PCLake, *Hydrobiologia*, 584, 443-454, 2007.
- Morcom, C.P.: Nitrogen yields into the Tauranga Harbour based on sub-catchment land use, Master thesis, Master of Science, the University of Waikato, Hamilton, New Zealand, 132 pp., 2013.
- Morgenstern, U., Daughney, C., Leonard, G., Gordon, D., Donath, F., and Reeves, R.: Using groundwater age and hydrochemistry to understand sources and dynamics of nutrient contamination through the catchment into Lake Rotorua, New Zealand, *Hydrol. Earth Syst. Sc.*, 19, 803-822, 2015.
- Moriasi, D. N., Arnold, J. G., Van Liew, M. W., Bingner, R. L., Harmel, R. D., and Veith, T. L.: Model evaluation guidelines for systematic quantification of accuracy in watershed simulations, *T. ASAE*, 50, 885-900, 2007.
- Morris, M.D.: Factorial sampling plans for preliminary computational experiments, *Technometrics*, 33, 161-174, 1991.
- Mueller, H., Hamilton, D.P., and Doole, G.J.: Response lags and environmental dynamics of restoration efforts for Lake Rotorua, New Zealand, *Environ. Res. Lett.*, 10, 2015.
- Murphy, J.M., Booth, B.B.B., Collins, M., Harris, G.R., Sexton, D.M.H., and Webb, M.J.: A methodology for probabilistic predictions of regional climate change from perturbed physics ensembles, *Phil. Trans. R. Soc. A.*, 365, 1993-2028, 2007.
- Narasimhan, B., Srinivasan, R., Bednarz, S.T., Ernst, M.R., and Allen, P.M.: A comprehensive modeling approach for reservoir water quality assessment and management due to point and nonpoint source pollution, *T. ASABE.*, 53, 1605-1617, 2010.
- Neitsch, S.L., Arnold, J.G., Kiniry, J.R., and Williams, J.R.: Soil and Water Assessment Tool theoretical documentation version 2009, Texas Water Resources Institute Technical Report No. 406, Texas A&M University System, College Station, Texas, 647 pp., 2011.

- OECD (Organisation for Economic Co-operation and Development): Environmental performance reviews: Germany, Environmental Performance, Paris, France, 236 pp., 2001.
- Özkundakci, D., McBride, C.G., and Hamilton, D.P.: Parameterisation of sediment geochemistry for simulating water quality responses to long-term catchment and climate Changes in Polymictic, eutrophic Lake Rotorua, New Zealand, *Water Pollut. XI*, 171–182, 2012.
- Robertson, D.M., Saad, D.A., Christiansen, D.E., and Lorenz, D.J.: Simulated impacts of climate change on phosphorus loading to Lake Michigan, *J. Great Lakes Res.*, 42, 536–548, 2016.
- Rutherford, J.C., Dumnov, S.M., and Ross, A.H.: Predictions of phosphorus in Lake Rotorua following load reductions, *New Zeal. J. Mar. Fresh.*, 30, 383–396, 1996.
- Rutherford, J.C., Palliser, C., and Wadhwa, S.: Nitrogen exports from the Lake Rotorua catchment – calibration of the ROTAN model, NIWA client report: HAM2009-019, National Institute of Water & Atmospheric Research Ltd, Hamilton, New Zealand, 66 pp., 2009.
- Santer, B.D., Wigley, T.M.L., Schlesinger, M.E., and Mitchell, J.F.B.: Developing climate scenarios from equilibrium GCM results, Report No. 47, Max-Planck-Institute, Fuer Meteorologie, Hamburg, Germany, 31 pp., 1990.
- Saunders, W.M.H.: Phosphate retention by New Zealand soils and its relationship to free sesquioxides, organic matter, and other soil properties, *New Zealand Journal of Agricultural Research*, 8, 30–57, 1965.
- Scholes, P.: 2010/2011 Rotorua Lakes Trophic Level Index Update, Bay of Plenty Regional Council Environmental Publication 2011/17, Whakatane, New Zealand, 37 pp., 2011.
- Scavia, D., Allan, J.D., Arend, K.K., Bartell, S., Beletsky, D., Bosch, N.S., Brandt, S.B., Briland, R.D., Daloğlu, I., DePinto, J.V., Dolan, D.M., Evans, M.A., Farmer, T.M., Goto, D., Han, H., Höök, T.O., Knight, R., Ludsin, S.A., Mason, D., Michalak, A.M., Richards, R.P., Roberts, J.J., Rucinski, D.K., Rutherford, E., Schwab, D.J., Sesterhenn, T.M., Zhang, H., Zhou, Y.: Assessing and addressing the re-eutrophication of Lake Erie: Central basin hypoxia, *J. Great Lakes Res.*, 40, 226–246, 2014.
- Sharpley, A., Jarvie, H.P., Buda, A., May, L., Spears, B., and Kleinman, P.: Phosphorus legacy: Overcoming the effects of past management practices to mitigate future water quality impairment, *J. Environ. Qual.*, 42, 1308–1326, 2014.
- Shaw, B., Mechenich, C., and Klessig, L.: Understanding lake data, G3582, University of Wisconsin-Stevens Point, Wisconsin, the United States, 20 pp., 2004.
- Smith, V.H., Wood, S.A., McBride, C.G., Atalah, J., Hamilton, D.P., and Abell, J.: Phosphorus and nitrogen loading restraints are essential for successful eutrophication control of Lake Rotorua, New Zealand, *Inland Waters*, 6, 273–283, 2016.

- Spears, B.M., Dudley, B., Reitzel, K., and Rydin E.: Geo-Engineering in Lakes-A Call for Consensus, *Environ. Sci. Technol.*, 47, 3953–3954, 2013.
- Stuber, R.J., Gebhart, G., and Maughan, O.E.: Habitat suitability index models: Largemouth bass, FWS/OBS–82/10.16, Fish Wildl. Serv., U.S. Dept. Int., Washington, D.C., 32 pp., 1982.
- Tebaldi, C., and Arblaster, J.M.: Pattern-scaling: Its strengths and limitations, and an update on the latest model simulations, *Clim Chang.*, 122, 459–471, 2014.
- Todd, M.C., Taylor, R.G., Osborn, T.J., Kingston, D.G., Arnell, N.W., and Gosling, S.N.: Uncertainty in climate change impacts on basin-scale freshwater resources - preface to the special issue: the QUEST-GSI methodology and synthesis of results, *Hydrol. Earth Syst. Sc.*, 15, 1035–1046, 2011.
- Touma, D., Ashfaq, M., Nayak, M.A., Kao, S.C., and Diffenbaugh, N.S.: A multi-model and multi-index evaluation of drought characteristics in the 21<sup>st</sup> century, *J. Hydrol.*, 526, 196–207, 2015.
- Trolle, D., Skovgaard, H., and Jeppesen, E.: The Water Framework Directive: setting the phosphorus loading target for a deep lake in Denmark using the 1D lake ecosystem model DYRESMeCAEDYM, *Ecol. Model.*, 219, 138–152, 2008.
- Trolle, D., Hamilton, D.P., Pilditch, C.A., Duggan, I.C., and Jeppesen, E.: Predicting the effects of climate change on trophic state of three morphologically varying lakes: Implications for lake restoration and management, *Environ. Modell. Softw.*, 26, 354–370, 2011.
- Van Vuuren, D.P., Edmonds, J., Kainuma, M.L.T., Riahi, K., Thomson, A., Matsui, T., Hurtt, G., Lamarque, J-F., Meinshausen, M., Smith, S., Grainer, C., Rose, S., Hibbard, K.A., Nakicenovic, N., Krey, V., and Kram, T.: The representative concentration pathways: An overview, *Clim. Chang.*, 109, 5–31, 2011.
- Ward, A.S., Gooseff, M.N., Fitzgerald, M., Voltz, T.J., Binley, A.M., and Singha, K.: Hydrologic and geomorphic controls on hyporheic exchange during base flow recession in a headwater mountain stream, *Water Resour. Res.*, 48, W04513, 2012.
- Wilhelm, S., and Adrian, R.: Impact of summer warming on the thermal characteristics of a polymictic lake and consequences for oxygen, nutrients and phytoplankton, *Freshw. Biol.*, 53, 226–237, 2008.
- Yin, C., Li, Y., and Urich, P.: SimCLIM2013 Data Manual, CLIMsystems, Hamilton, New Zealand, 35 pp., 2013.
- Zhang, D., Chen, X., Yao, H., and Lin, B.: Improved calibration scheme of SWAT by separating wet and dry seasons, *Ecol. Model.*, 301, 54–61, 2015.
- Zogg, G.P., Zak, D.R., Pregitzer, K.S., and Burton, A.J.: Microbial immobilization and the retention of anthropogenic nitrate in a northern hardwood forest, *Ecology*, 81, 1858–1866, 2000.

## **5 Concluding discussion and synthesis**

### **5.1 Overview**

This thesis firstly described the applicability of a process-based catchment model (SWAT) to a small, mixed land use catchment of Lake Rotorua, New Zealand. The effects were examined of different hydrologic conditions on model performance and parameter sensitivity. By using the hourly routing algorithms and modifying relevant model code to simulate complex catchment irrigation operations, the SWAT2012 model performance was improved, as indicated by better predictions of high-frequency variations in SS, TP and TN loadings in the major catchment drainage stream. Finally, the modified SWAT2012 model was combined with the lake model (DYRESM-CAEDYM) to predict the effects on lake nutrient concentrations and trophic states of different land management scenarios, including removal of wastewater irrigation, under present and future climate projections. The objectives of this chapter are to bring together the key findings of each research chapter, to examine any deficiencies and to make suggestions for future research.

### **5.2 Key findings and recommendations**

The objective of Chapter 2 was to examine the SWAT2009 model (version rev488) applicability to a small, mixed land use catchment (the Puarenga catchment) of Lake Rotorua under different hydrologic conditions, and also to test model parameter sensitivity. Monthly instantaneous TP and TN concentrations were generally not reproduced well, indicating that the use of low-frequency base flow measurements for model calibration can lead to poor predictions of composition for “flashy” lower-order streams. Model error increased during periods of quick-flow for discharge-weighted mean concentrations of TP and SS. Use of high-frequency, event-based monitoring data for model calibration can help to alleviate the potential for underestimating storm-driven fluxes. Model error also arises parameter values that are lumped (i.e., assigned one value) across the whole catchment in the calibration process (Lindenschmidt et al., 2007), but values may vary spatially or temporally depending on the model configuration and the parameter concerned (Niraula et al., 2012).

Inadequate representation of groundwater processes in the SWAT2009 model structure is another factor explaining some of the deviation of simulated output from measurements (Rostamian et al., 2008). Variability in N applications to the catchment likely contributes to a non-steady state condition (Bain et al., 2012) and this was reflected most in NO<sub>3</sub>-N and TN due to preferential leaching of NO<sub>3</sub>-N compared with other dissolved nutrient species. Improvements in groundwater processes in the SWAT2009 model structure (e.g., an embedded groundwater module MODFLOW) would likely capture the leaching process (Guzman et al., 2015), some of the attenuation of NO<sub>3</sub>-N and the lag times associated with movement through the unsaturated zone to the groundwater aquifer (Schmalz et al., 2008).

The relative input of groundwater flow to stream discharge tends to be greater under base flow conditions (Neitsch et al., 2011), and therefore parameters relating to tuning of the stream channel processes (e.g., average slope steepness) also tend to be more sensitive under base flow conditions. Surface runoff is determined mostly by overland processes, and therefore parameters controlling overland flow (e.g., Manning's n value for overland flow) are more sensitive under quick flow conditions. Several SWAT parameters have no degree of temporal variability because model algorithms fail to adjust them with environmental conditions (Guse et al., 2014). Modification of model algorithms or opportunities to vary SWAT parameters may help to better capture some of the temporal dynamics of "flashy" streams such as Puarenga.

The objective of Chapter 3 was to improve the SWAT2012 model (version rev629) applicability for capturing high-frequency (daily and hourly) variability of water and nutrient discharges and for simulating the effects of long-term wastewater irrigation in the forested sub-catchment of Chapter 2. Comparing daily and hourly routing models, and a fixed parameter set for each case, the hourly routing model performed better in reproducing the dynamics of stormflows which contributed to the inherent variability in the weekly aggregated measurements. Jeong et al. (2010) noted that the hourly routing model in SWAT2012 applies hourly algorithms for calculations of infiltration, surface runoff and channel routings, but daily algorithms for soil water movement, base flow and lateral flow. Therefore, variability caused by stormflows cannot be expected to be captured with these daily algorithms. Higher variability of SS and TP loads than TN loads was

found in the hourly routing model because SS and TP are predominantly mobilized in storm flows (Abell et al., 2013), while the denitrification and volatilisation processes which facilitate N losses have less flow dependence (Zhang et al., 2016).

The increases in TP load observed during or following forest block harvesting were underestimated by both hourly and daily routing models. Parameters relevant to soil enrichment by P determine the amount of both organic and mineral P which is attached to sediments that are eroded and enter the stream channel. This erosion will vary temporally and spatially, particularly in response to environmental drivers such as forest harvesting. The constant value of the soil erodibility factor used to simulate SS losses through surface runoff may not be adequate in representing these complex harvesting operations. This suggests that algorithms for overland erosion processes that mobilise P may need to be developed or refined for this purpose, i.e., in response to temporal and spatial variance in episodic events.

The optimised value of parameter for ammonium release rate from stream sediments (RS3;  $10 \text{ mg N m}^{-2} \text{ d}^{-1}$ ) was beyond the SWAT default range ( $0\text{--}1 \text{ mg N m}^{-2} \text{ d}^{-1}$ ). This value of RS3 is nevertheless lower than the values of 24 to  $48 \text{ mg m}^{-2} \text{ d}^{-1}$  given in Gabriele et al. (2013) who investigated headwater streams from an Austrian agricultural catchment. Sources of  $\text{NH}_4$  input to the Puarenga Stream (receiving nutrient discharges from the Waipa stream) may be related to enriched geothermal springs; Abell et al., 2013), which may help to explain why RS3 was high in this study. Alternately, or in addition, some key processes might not have been accounted for, such as  $\text{NH}_4\text{--N}$  movement through the aquifer and recharge to the stream. Böhlke et al., (2006) stated that anaerobic degradation of organic matter and organic waste disposal resulted in the presence of  $\text{NH}_4^+$  in groundwater that exceeded  $\text{NH}_4^+$  sorption and nitrification processes. It should be noted, however, that in the Waipa Stream  $\text{NH}_4\text{--N}$  makes up only a small proportion of TN, compared with  $\text{NO}_3\text{--N}$  as the dominant N source.

Alternatives for managing and optimising the wastewater irrigation were examined in Chapter 3, with respect to reducing nutrient losses to waterways from the irrigation area. Wastewater irrigation at daily frequency was the most effective way to reduce nutrient leaching and avoid soil saturation, compared with irrigation at weekly frequency (i.e., identical total volume on a weekly basis). The higher volume of each wastewater application for weekly irrigation increased nutrient

percolation and leaching into the stream (see also Beets et al., 2013). No irrigation on high rainfall days, with reassignment to the first subsequent low-rainfall day, also reduced nutrient losses from the irrigated area despite the increase in volume immediately following rainfall delay. Other cases of increasing the irrigated area or ceasing irrigation altogether produced the expected reduction in nutrient loads to the Waipa Stream which drains the irrigated area.

The objective of Chapter 4 was to combine the improved hourly-routing catchment model (SWAT2012 rev629 from Chapter 3) with a lake model (DYRESM-CAEDYM version 4.0) to predict the response of polymictic, eutrophic Lake Rotorua to a projected 2090 climate and changes in catchment nutrient discharges. The Puarenga catchment was modelled using SWAT2012 and other catchments used measured hydrologic and water quality data as the lake model input. Concentrations of TN and TP in the Puarenga Stream simulated with the improved SWAT2012 model were better than those using SWAT2009 (from Chapter 2). However, in winter, after high rainfall events, discharge was overestimated by the SWAT2012 model, suggesting that it might not adequately represent exchanges between the river channel and the recently inundated area following the flood-water recession. Representation of water discharge from the river channel to the groundwater aquifer should be considered in the SWAT2012 model structure in order to better capture surface-groundwater exchanges generally (see discussion on this topic by Sun et al., 2016).

Precipitation from projected climate warming scenarios (2090) increased most in the months of January through April. This resulted in elevated rates of soil erosion and mobilisation of SS and particulate P and N in the model simulations of Puarenga Stream during quick flow in particular. Decreased precipitation from September to December caused a lagged response of discharge and decreases of discharge were found in October in particular. Elevated annual mean air temperature (2.7 °C in 2090) stimulated plant uptake of NO<sub>3</sub>-N, NH<sub>4</sub>-N and DRP from associated projected increases in soil temperature (annual mean 2.1 °C) but was counteracted by increased decomposition and mineralisation of organic matter. The net result was small increases in annual mean simulated DRP and NH<sub>4</sub>-N loads while increased denitrification likely contributed to the net balance of decreases in annual mean simulated NO<sub>3</sub>-N loads from the Puarenga catchment.

Simulations using the lake model (DYRESM–CAEDYM) showed that the combined effects of changes from catchment nutrient loadings and higher temperatures in a future (2090) climate would generally have negative impact on the water quality of Lake Rotorua. Lake Rotorua is shallow and polymictic, so mixing can occur throughout the year (Burger et al., 2008). Increased water temperatures should cause more extended periods (i.e., a few weeks) of thermal stratification in summer, resulting in an increase in anoxia of water adjacent to the bottom sediments (Wilhelm and Adrian, 2008; Özkundakci et al., 2012). An increase of thermal stratification may exacerbate internal sediment releases, resulting in greater nutrient supply to the water column to promote phytoplankton production (Burger et al., 2007; Adrian et al., 2009). Thus increased thermal stratification is the critical determinant of changes in trophic state of polymictic lake under the influence of climate warming. Our findings support work by Wilhelm and Adrian (2008) who studied the effects of increasing summer air temperature on thermal stratification in a polymictic German lake and found that longer thermal stratification resulted in increased anoxia and nutrient release as well as greater phytoplankton growth. A similar conclusion was also drawn in Adrian et al. (2009) where a polymictic lake was found to respond in the short term (i.e., months to a few years) to internal lake nutrient dynamics (i.e., sediment–water exchanges) to a greater extent than external nutrient loadings from the catchment.

### **5.3 Environmental implications**

The overarching outcomes of this thesis are:

- (1) the application of advanced modelling technologies, i.e., a process–based catchment model (SWAT) combined with the lake model (DYRESM–CAEDYM), to represent high–frequency (daily and hourly) variability of nutrient discharges;
- (2) application of the model to a mixed land use catchment (the Puarenga Stream) which includes an area which is spray–irrigated with wastewater to improve understanding of the relative effects of the spray irrigation, forestry and climate on stream discharge and nutrient and sediment loads; and
- (3) simulation of different land and wastewater irrigation management strategies, and predicting the response of the receiving waterbody (Lake Rotorua) to future climate and catchment nutrient discharge.

This thesis improves high-frequency simulation of suspended solids and nutrient loads from stream discharges to a receiving lake. It has important implications for the application of hydrological models to other catchments that have large fluctuations in stream discharge, particularly where there are substantial changes to the flow regime during the calibration period. High-frequency simulations will help to better identify the sources of sediments and nutrients entering streams and the lake, and target these areas as part of an overall strategy for eutrophication control in the lake.

This thesis proves the effectiveness of linking climate, catchment and lake models in better replicating hydro-biogeochemical processes and demonstrating opportunities to improve freshwater ecosystem management. The simulation results support the current strategy of reducing both N and P loads to Lake Rotorua. Although alum dosing of two inflows has reduced TP loads to the lake and the trophic level has improved (Smith et al., 2016), long-term dosing may not be sustainable due to the potential for adverse environmental consequences, e.g., ecotoxicological responses to alum (Tempero et al., 2015).

This thesis has also demonstrated how a lake responds both in terms of external loads and how it reacts internally, driven by climate, stratification and internal loads. Despite small changes in catchment nutrient loads with a projected 2090 climate, increased lake water temperatures could cause more frequent and longer periods of summer thermal stratification and anoxia generation, which enhances bottom sediment release of nutrients and accelerates phytoplankton production. These effects may intensify with a changing climate even though there are not obvious or consistent directional changes in catchment nutrient loading with climate change. This work has helped to identify how external restoration efforts (e.g., in the terrestrial catchment) may need to be taken of sufficient scale to offset the adverse in-lake effects of climate change.

## **5.4 References**

Abell, J.M., Hamilton, D.P., and Rutherford, J.C.: Quantifying temporal and spatial variations in sediment, nitrogen and phosphorus transport in stream inflows to a large eutrophic lake, *Environ. Sci.: Processes Impacts*, 15, 1137–1152, 2013.

- Adrian, R., O'Reilly, C.M., Zagarese, H., Baines, S.B., Hessen, D.O., Keller, W., Livingstone, D.M., Sommaruga, R., Straile, D., Van Donk, E., Weyhenmeyer, G.A., and Winder, M.: Lakes as sentinels of climate change, *Limnol. Oceanogr.*, 54, 2283–2297, 2009.
- Bain, D.J., Green, M.B., Campbell, J.L., Chamblee, J.F., Chaoka, S., Fraterrigo, J.M., Kaushal, S.S., Martin, S.L., Jordan, T.E., and Parolari, A.J.: Legacy effects in material flux: structural catchment changes predate long-term studies, *BioScience*, 62, 575–584, 2012.
- Beets, P.N., Gielen, G., Oliver, G.R., Pearce, S.H., and Graham, J.D.: Determination of the level of soil N and P storage and soil health at the Rotorua Land Treatment site, Scion Report 50659, New Zealand Forest Research Institute Limited, Rotorua, New Zealand, 39 pp., 2013.
- Böhlke, J., Smith, R.L., and Miller, D.N.: Ammonium transport and reaction in contaminated groundwater: application of isotope tracers and isotope fractionation studies, *Water Resour. Res.*, 42, W05411, 2006.
- Burger, D.F., Hamilton, D.P., Pilditch, C.A., and Gibbs, M.M.: Benthic nutrient fluxes in a eutrophic, polymictic lake, *Hydrobiologia*, 584, 13–25, 2007.
- Burger, D.F., Hamilton, D.P., and Pilditch, C.A.: Modelling the relative importance of internal and external nutrient loads on water column nutrient concentrations and phytoplankton biomass in a shallow polymictic lake, *Ecol. Model.*, 21, 411–423, 2008.
- Gabriele, W., Welti, N., and Hein, T.: Limitations of stream restoration for nitrogen retention in agricultural headwater streams, *Ecol. Eng.*, 60, 224–234, 2013.
- Guse, B., Reusser, D.E., and Fohrer, N.: How to improve the representation of hydrological processes in SWAT for a lowland catchment—temporal analysis of parameter sensitivity and model performance, *Hydrol. Process.*, 28, 2651–2670, 2014.
- Guzman, J.A., Moriasi, D.N., Gowda, P.H., Steiner, J.L., Starks, P.J., Arnold, J.G., Srinivasan, R.: A model integration framework for linking SWAT and MODFLOW, *Environ. Model. Softw.*, 73, 103–116, 2015.
- Jeong, J., Kannan, N., Arnold, J., Glick, R., Gosselink, L., and Srinivasan, R.: Development and integration of sub-hourly rainfall–runoff modeling capability within a watershed model, *Water Resour. Manag.*, 24, 4505–4527, 2010.
- Lindenschmidt, K., Fleischbein, K., and Baborowski, M.: Structural uncertainty in a river water quality modelling system, *Ecol. Model.*, 204, 289–300, 2007.
- Neitsch, S.L., Arnold, J.G., Kiniry, J.R., and Williams, J.R.: Soil and Water Assessment Tool theoretical documentation version 2009, Texas Water

Resources Institute Technical Report No. 406, Texas A&M University System, College Station, Texas, the United States, 647 pp., 2011.

Niraula, R., Kalin, L., Wang, R., and Srivastava, P.: Determining nutrient and sediment critical source areas with SWAT model: effect of lumped calibration, *T. ASABE.*, 55, 137–147, 2012.

Özkundakci, D., McBride, C.G., Hamilton, D.P.: Parameterisation of sediment geochemistry for simulating water quality responses to long-term catchment and climate Changes in Polymictic, eutrophic lake Rotorua, New Zealand, *Water Pollut. XI*, 171–182, 2012.

Rostamian, R., Jaleh, A., Afyuni, M., Mousavi, S.F., Heidarpour, M., Jalalian, A., and Abbaspour, K.C.: Application of a SWAT model for estimating runoff and sediment in two mountainous basins in central Iran, *Hydrolog. Sci. J.*, 53, 977–988, 2008.

Schmalz, B., Tavares, F., and Fohrer, N.: Modelling hydrological lowland processes in mesoscale river basins with SWAT—Capabilities and challenges, *Hydrolog. Sci. J.*, 53, 989–1000, 2008.

Smith, V.H., Wood, S.A., McBride, C.G., Atalah, J., Hamilton, D.P., and Abell, J.: Phosphorus and nitrogen loading restraints are essential for successful eutrophication control of Lake Rotorua, New Zealand, *Inland Waters*, 6, 273–283, 2016.

Sun, X., Bernard-Jannin, L., Garneau, C., Volk, M., Arnold, J.G., Srinivasan, R., Sauvage, S., Sánchez-Pérez, J.M.: Improved simulation of river water and groundwater exchange in an alluvial plain using the SWAT model, *Hydrol. Process.*, 30, 187–202, 2016.

Tempero, G.W., McBride, C.G., Abell, J.M., Hamilton, D.P.: Anthropogenic phosphorus loads to Lake Rotorua, Environmental Research Institute Report 66, the University of Waikato, Hamilton, New Zealand, 31 pp., 2015.

Wilhelm, S., and Adrian, R.: Impact of summer warming on the thermal characteristics of a polymictic lake and consequences for oxygen, nutrients and phytoplankton, *Freshw. Biol.*, 53, 226–237, 2008.

Zhang, Q., Ball, W.P., and Moyer, D.L.: Decadal-scale export of nitrogen, phosphorus, and sediment from the Susquehanna River basin, USA: analysis and synthesis of temporal and spatial patterns, *Sci. Total Environ.*, 563, 1016–1029, 2016.

# Appendix 1 Code modifications made in SWAT2012\_rev629

1-1 sched\_mgt\_done.f - Notepad

```

File Edit Format View Help
if (irrefm(ihru) < 1.e-6) irrefm(ihru)=1.0
if (irr_sc(j) <= 0) irr_sc(j) = irrsc(j)
if (irr_no(j) <= 0) irr_no(j) = irrno(j)
if (irr_sc(ihru) <= 0) irr_no(j) = hru_sub(j)
if (irr_sc(ihru) > 2) then    !! reach and res flag ??
call irrsb
endif

if (imgt ==1) then
write (143, 1002) subnum(j), hruno(j), iyr, i_mo,
iida,
* "IRRIGATE", phubase(j), phuacc(j), sol_sw(j), bio_ms(j),
* sol_rsd(1,j), sol_sumno3(j), sol_sumso1p(j), irramt(j),
* irr_sc(j), irr_no(j)
1002 format (a5,1x,a4,3i6,2a15,7f10.2,10x,f10.2,70x,2i7)

end if

case (3) !! fertilizer operation
ifrttyp = mgt1iop(nop(j),j)
frt_kg = mgt4op(nop(j),j) * hru_ha(j)
frt_surface = mgt5op(nop(j),j)
if (frt_surface <= 1.e-6) frt_surface = 0.2

call fert

if (imgt ==1) then
write (143, 1004) subnum(j), hruno(j), iyr, i_mo, iida,
* fertnm(ifrttyp),
* " FERT", phubase(j), phuacc(j), sol_sw(j), bio_ms(j),
* sol_rsd(1,j), sol_sumno3(j), sol_sumso1p(j), frt_kg,
* fertno3, fertnh3, fertorgn, fertso1p, fertorgp
1004 format (a5,1x,a4,3i6,2a15,7f10.2,20x,f10.2,10x,5f10.2)
endif

case (4) !! pesticide operation
hrupest(ihru) = 1
ipest = mgt1iop(nop(j),j)
pst_kg = mgt4op(nop(j),j)
pst_dep = mgt5op(nop(j),j)

call apply

if (imgt ==1) then

```

“sched\_mgt.f”

Note: \* hru\_ha(j) was added

fert\_done.f - Notepad

```

File Edit Format View Help
!! ~ ~ ~ SUBROUTINES/FUNCTIONS CALLED ~ ~ ~
!! SWAT: Erfc
!! ~ ~ ~ ~ ~ END SPECIFICATIONS ~ ~ ~ ~ ~

use parm

real, parameter :: rtof=0.5
integer :: j, l, ifrt
real :: xx, gc, gc1, swf, frt_t

j = 0
j = ihru

ifrt = 0
ifrt = ifrttyp

do l = 1, 2
xx = 0.
if (l == 1) then
xx = frt_surface
else
xx = 1. - frt_surface
endif

sol_no3(1,j) = sol_no3(1,j) + xx * frt_kg
& (1. - fnh3n(ifrt)) * fminn(ifrt)
sol_nh3(1,j) = sol_nh3(1,j) + xx * frt_kg
& fnh3n(ifrt) * fminn(ifrt)
sol_so1p(1,j) = sol_so1p(1,j) + xx * frt_kg
& fminp(ifrt)
sol_orgp(1,j) = sol_orgp(1,j) + xx * frt_kg
& forgp(ifrt)
sol_aorgn(1,j) = sol_aorgn(1,j) + xx * frt_kg
& forgn(ifrt)

end do

!! summary calculations
fertno3 = frt_kg * fminn(ifrt) * (1. - fnh3n(ifrt))
fertnh3 = frt_kg * (fminn(ifrt) * fnh3n(ifrt))

```

“fert.f”

Note: original carbon routine was used through the whole study, therefore only the statement of cswat=0 was remained.



```

2-3 rthsed_done.f - Notepad
File Edit Format View Help

do ii = 1, nstep
  if (hrtwtr(ii)>0. .and. hdepth(ii)>0.) then
    !! initialize water in reach during time step
    qin = 0.
    sedin = 0.
    qin = hrtwtr(ii) + hhstor(ii)

    !! do not perform sediment routing if no water in reach
    if (qin > 0.01) then

      !! initialize sediment in reach during time step
      if (ii == 1) then
        sedin = hhvaroute(3,inum2,ii) * (1. - rnum1) + sedst(jrch)
      else
        sedin = hhvaroute(3,inum2,ii) * (1. - rnum1) + hsedst(ii-1)
      end if

      if (sedin < 1.e-6) sedin = 0.
      !! initialize reach peak runoff rate
      peakr = prf(jrch) * hsdct(i1)

      !! calculate flow velocity
      vc = 0.
      if (hharea(ii) < .010) then
        vc = 0.01
      else
        vc = peakr / hharea(ii)
      end if
      ! if (vc > 5.) vc = 5.

      thbase = 0.
      thbase = ch_l2(jrch) * 1000. / (3600. * 24. * vc)
      if (thbase > 1.) thbase = 1.

      !! JIMMY'S NEW IMPROVED METHOD for sediment transport
      cyin = 0.
      cych = 0.
      depnet = 0.
      deg = 0.
      dep = 0.
      if (sedin < 1e-6) sedin = 0.
      cyin = sedin / qin !tons/m3
    end if
  end do
end do

```

**“rthsed.f”**

Note: those were adjusted

```

2-1 rtout_done.f - Notepad
File Edit Format View Help

! From this point, check each variables if it is simulated at subdaily interval before using the out
!
!
hhvaroute(1,ihout,ii) = 0.
hhvaroute(2,ihout,ii) = hrtwtr(ii)
hhvaroute(3,ihout,ii) = hsedyl(ii)
hhvaroute(4,ihout,ii) = horgn(ii) * hrtwtr(ii) / 1000.
hhvaroute(5,ihout,ii) = horgp(ii) * hrtwtr(ii) / 1000.
hhvaroute(6,ihout,ii) = hno3(ii) * hrtwtr(ii) / 1000.
hhvaroute(7,ihout,ii) = hso1p(ii) * hrtwtr(ii) / 1000.
hhvaroute(8,ihout,ii) = 0.
hhvaroute(9,ihout,ii) = 0.
hhvaroute(10,ihout,ii) = 0.
hhvaroute(11,ihout,ii) = hso1pst(ii) * hrtwtr(ii)
hhvaroute(12,ihout,ii) = hso1pst(ii) * hrtwtr(ii)
hhvaroute(13,ihout,ii) = hchl1(ii) * hrtwtr(ii) / 1000.
hhvaroute(14,ihout,ii) = hnh4(ii) * hrtwtr(ii) / 1000.
hhvaroute(15,ihout,ii) = hno2(ii) * hrtwtr(ii) / 1000.
hhvaroute(16,ihout,ii) = hbod(ii) * hrtwtr(ii) / 1000.
hhvaroute(17,ihout,ii) = hdisox(ii) * hrtwtr(ii) / 1000.
hhvaroute(18,ihout,ii) = hbactp(ii)
hhvaroute(19,ihout,ii) = hbactlp(ii)
hhvaroute(20,ihout,ii) = hhvaroute(20,inum2,ii) * (1. - rnum1)
hhvaroute(21,ihout,ii) = hhvaroute(21,inum2,ii) * (1. - rnum1)
hhvaroute(22,ihout,ii) = hhvaroute(22,inum2,ii) * (1. - rnum1)

varoute(3,ihout) = varoute(3,ihout) + hhvaroute(3,ihout,ii)
varoute(4,ihout) = varoute(4,ihout) + hhvaroute(4,ihout,ii)
varoute(5,ihout) = varoute(5,ihout) + hhvaroute(5,ihout,ii)
varoute(6,ihout) = varoute(6,ihout) + hhvaroute(6,ihout,ii)
varoute(7,ihout) = varoute(7,ihout) + hhvaroute(7,ihout,ii)
varoute(11,ihout) = varoute(11,ihout) + hhvaroute(11,ihout,ii)
varoute(12,ihout) = varoute(12,ihout) + hhvaroute(12,ihout,ii)
varoute(13,ihout) = varoute(13,ihout) + hhvaroute(13,ihout,ii)
varoute(14,ihout) = varoute(14,ihout) + hhvaroute(14,ihout,ii)
varoute(15,ihout) = varoute(15,ihout) + hhvaroute(15,ihout,ii)
varoute(16,ihout) = varoute(16,ihout) + hhvaroute(16,ihout,ii)
varoute(17,ihout) = varoute(17,ihout) + hhvaroute(17,ihout,ii)
end do
end if

!! set subdaily reach output - by jaehak jeong for urban project, subdaily output in output.rch file
if (ievent==3.and.iprint==3) then
  do ii=1,nstep
    !! determine sediment concentration in outflow
    sedcon = 0.
    if (hrtwtr(ii) > 0.01) then

```

**“rtout.f”**

Note: this assignment was added

2-2 route\_done.f - Notepad

```

File Edit Format View Help
    if (hrtwtr(ii) > 0. .and. hdepth(ii) > 0.) then
        hsedylid(ii) = hhvaroute(3,inum2,ii) * (1. - rnum1)
        sedrch = sedrch + hsedylid(ii)
        rch_san = 0.
        rch_sil = rch_sil + hsedylid(ii) !!All are assumed to be silt type particles
        rch_cla = 0.
        rch_sag = 0.
        rch_lag = 0.
        rch_gra = 0.
    end if
end do
end if
else
    if (ievent < 3) then
        if (ch_eqn(jrch) == 0) call rtsed
        if (ch_eqn(jrch) == 1) call rtsed_bagnold
        if (ch_eqn(jrch) == 2) call rtsed_kodatie
        if (ch_eqn(jrch) == 3) call rtsed_Molinas_wu
        if (ch_eqn(jrch) == 4) call rtsed_yangсанд
    else
        if (ievent==3) then
            do ii = 1, nstep
                hsedylid(ii) = hhvaroute(3,inum2,ii) * (1. - rnum1)
                sedrch = sedrch + hsedylid(ii)
            end do
        endif
        call rthsed
    end if
end if

!! perform in-stream nutrient calculations
if (ievent < 3) then
    if (iwq == 2) call watqual2
    if (iwq == 1) call watqual
    if (iwq == 0) call noqual
else
    if (iwq == 1) call hhwatqual
    if (iwq == 0) call hhnoqual
end if

!! perform in-stream pesticide calculations
call biofilm

!! perform in-stream pesticide calculations
if (ievent < 3) then
    call rtpest

```

**“route.f”**

Note: this statement was added

```

        if (ievent==3) then
            do ii = 1, nstep
                hsedylid(ii) = hhvaroute(3,inum2,ii) * (1. - rnum1)
                sedrch = sedrch + hsedylid(ii)
            end do
        endif

```

2-4 ysed\_done.f - Notepad

```

File Edit Format View Help
use parm

integer, intent (in) :: iwave
integer :: j
real :: c

j = 0
j = ihru

!! initialize variables
c = 0.
cklsp(j) = 0.

if (iwave > 0) then
    !! subbasin sediment calculations
    cklsp(j) = wcklsp(iwave)
else
    !! HRU sediment calculations
    cklsp(j) = usle_cfac(j) * usle_mult(j)
end if

!! compute sediment yield with musle
if (iwave > 0) then
    !! subbasin sediment calculations
    sedyld(j) = (sub_qd(iwave) * peakr * 10. * sub_km(iwave))
    & ** .56 * cklsp(j)
else
    !! HRU sediment calculations
    sedyld(j) = (surfq(j) * peakr * 10. * hru_km(j))
    & ** .56 * cklsp(j)
end if

if (isproj == 2) then
    sedyld(j) = sedyld(j) * dr_sub(j)
end if

if (sedyld(j) < 0.) sedyld(j) = 0.

!!adjust sediment yield for protection of snow cover
if (sno_hru(j) > 0.) then
    if (sedyld(j) < 1.e-6) sedyld(j) = 0.0
else if (sno_hru(j) > 100.) then
    sedyld(j) = 0.
else
    sedyld(j) = sedyld(j) / Exp(sno_hru(j) * 3. / 25.4)
end if

```

**“ysed.f”**

Note: those were adjusted

```

    sedyld(j) = (sub_qd(iwave) * peakr * 10. * sub_km(iwave))
    & ** .56 * cklsp(j)

```

```

2-4 ysed.f - Notepad
File Edit Format View Help
!! j | | | HRU number
!! bio_fr cov | none | fraction of cover by biomass - adjusted for
!! | | | canopy height
!! grcov_fr | | | fraction of cover by biomass as function of lai
!! rsd_fr cov | | | fraction of cover by residue
!! ~ ~ ~ ~ ~
!! ~ ~ ~ SUBROUTINES/FUNCTIONS CALLED ~ ~ ~
!! Intrinsic: Exp
!! ~ ~ ~ ~ ~ END SPECIFICATIONS ~ ~ ~ ~ ~

use parm

integer, intent (in) :: iwave
integer :: j
real :: c

j = 0
j = ihru

!! initialize variables
c = 0.
ck1sp(j) = 0.

if (iwave > 0) then
!! subbasin sediment calculations
ck1sp(j) = wck1sp(iwave)
else
!! HRU sediment calculations
ck1sp(j) = usle_cfac(j) * usle_mult(j)
end if

!! compute sediment yield with musle
if (iwave > 0) then
!! subbasin sediment calculations
sedyld(j) = (sub_qd(iwave) * peakr * 10. ** sub_km(iwave))
& ** .56 * ck1sp(j)
&
else
!! HRU sediment calculations
sedyld(j) = (surfq(j) * peakr * 10. ** hru_km(j)) ** .56 * ck1sp(j)
&
end if

if (isproj == 2) then
sedyld(j) = sedyld(j) * dr_sub(j)
end if

if (sedyld(j) < 0.) sedyld(j) = 0.

!! adjust sediment yield for protection of snow cover
if (sno_hru(j) > 0.) then
if (sedyld(j) < 1.e-6) sedyld(j) = 0.0
else if (sno_hru(j) > 100.) then
sedyld(j) = 0.
else
sedyld(j) = sedyld(j) / Exp(sno_hru(j) * 3. / 25.4)
end if

!! Particle size distribution of sediment yield
saryld(j) = sedyld(j) * det_san(j) !! Sand yield
silyld(j) = sedyld(j) * det_sil(j) !! Silt yield
clayld(j) = sedyld(j) * det_cla(j) !! Clay yield
sagylld(j) = sedyld(j) * det_sag(j) !! Small Aggregate yield
lagylld(j) = sedyld(j) * det_lag(j) !! Large Aggregate yield

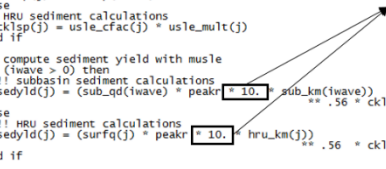
!! compute erosion with usle (written to output for comparison)
usle = 1.292 * usle_ei * ck1sp(j) / 11.8

return
end

```

“ysed.f”

Note: those were adjusted



```

soil_chem.f - Notepad
File Edit Format View Help

use parm

integer :: nly, j
real :: xx, dg, wt1, zdst, soldepth, sumno3, sumorgn, suminp
real :: sumorgp, solpst, soil_TP, labfrac, solp

j = 0.
j = ihru
nly = 0.
nly = sol_nly(j) - 1.

solpst = 0.
sumno3 = 0.
sumorgn = 0.
suminp = 0.
sumorgp = 0.

do ii = 1, nly
dg = 0.
wt1 = 0.
zdst = 0.
dg = sol_z(ii+1,j) - sol_z(ii,j)

!! calculate initial nutrient contents of layers, profile and
!! average in soil for the entire watershed
!! convert mg/kg (ppm) to kg/ha

sol_fop(1,j) = sol_rsd(1,j) * .0010 !! was 0.0003 Armen January 2009
sol_fon(1,j) = sol_rsd(1,j) * .0055 !! was 0.0015 Armen January 2009
sol_cov(j) = sol_rsd(1,j)

wt1 = sol_bd(ii,j) * dg / 10000. !! mg/kg => kg/ha
sol_hum(ii,j) = sol_cbn(ii,j) * wt1 * 1.72

zdst = Exp(-sol_z(ii,j) / 1000.)
sol_no3(ii,j) = 7. * zdst * wt1
sumno3 = sumno3 + sol_no3(ii,j)

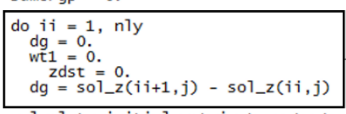
!! assume C:N ratio of 10:1
sol_orgn(ii,j) = (sol_cbn(ii,j) / 14.) * wt1 !! CN ratio changed back to 14 cbin 03022012
sol_aorgn(ii,j) = sol_orgn(ii,j) * nactfr
sol_orgn(ii,j) = sol_orgn(ii,j) * (1. - nactfr)

sumorgn = sumorgn + sol_aorgn(ii,j) + sol_orgn(ii,j) +

```

“soil\_chem.f”

Note: those were adjusted



```

soil_chem.f - Notepad
File Edit Format View Help
zdst = 0.
dg = sol_z(ii+1,j) - sol_z(ii,j)
!! calculate initial nutrient contents of layers, profile and
!! average in soil for the entire watershed
!! convert mg/kg (ppm) to kg/ha
sol_fop(1,j) = sol_rsd(1,j) * .0010 !! was 0.0003 Armen January 2009
sol_fon(1,j) = sol_rsd(1,j) * .0055 !! was 0.0015 Armen January 2009
sol_cov(j) = sol_rsd(1,j)
wt1 = sol_bd(ii,j) * dg / 10000. !! mg/kg => kg/ha
sol_hum(ii,j) = sol_cbn(ii,j) * wt1 * 1.72
zdst = Exp(-sol_z(ii,j) / 1000.)
sol_no3(ii,j) = 7. * zdst * wt1
sumno3 = sumno3 + sol_no3(ii,j)
!! assume C:N ratio of 10:1
sol_orgn(ii,j) = (sol_cbn(ii,j) / 14.) * wt1 !! CN ratio changed back to 14 cbin 03022012
sol_aorgn(ii,j) = sol_orgn(ii,j) * nactfr
sol_orgn(ii,j) = sol_orgn(ii,j) * (1. - nactfr)
& sumorgn = sumorgn + sol_aorgn(ii,j) + sol_orgn(ii,j) +
sol_fon(ii,j)
!! assume N:P ratio of 8:1
sol_orgp(ii,j) = .125 * sol_orgn(ii,j)
!! assume initial concentration of 5 mg/kg
sol_solp(ii,j) = 5. * wt1
sol_actp(ii,j) = sol_solp(ii,j) * (1. - psp) / psp
sol_stap(ii,j) = 4. * sol_actp(ii,j)
& summinp = summinp + sol_solp(ii,j) + sol_actp(ii,j) +
sol_stap(ii,j)
& sumorgp = sumorgp + sol_orgp(ii,j) + sol_fop(ii,j)
end do
basno3j = basno3j + sumno3 * hru_km(j) / da_km
basorgn = basorgn + sumorgn * hru_km(j) / da_km
basminp = basminp + summinp * hru_km(j) / da_km
basorgp = basorgp + sumorgp * hru_km(j) / da_km

```

“soil\_chem.f”

Note: those were adjusted

```

psed.f - Notepad
File Edit Format View Help
conc = 0.
if (iwave <= 0) then
!! HRU sediment calculations
& xx = sol_orgp(1,j) + sol_fop(1,j) + sol_mp(1,j) +
sol_actp(1,j) + sol_stap(1,j)
xxo = (sol_orgp(1,j) + sol_fop(1,j) + sol_mp(1,j)) / xx
xxa = sol_actp(1,j) / xx
xxs = sol_stap(1,j) / xx
wt1 = sol_bd(1,j) * sol_z(1,j) * 100.
conc = xx * erorgp(j) / wt1
sedp = 1000. * conc * sedyld(j) / hru_ha(j)
sedorgp(j) = sedp * xxo
sedminpa(j) = sedp * xxa
sedminps(j) = sedp * xxs
!! modify phosphorus pools only for HRU calculations
psedd = 0.
porgg = 0.
psedd = sol_actp(1,j) + sol_stap(1,j)
porgg = sol_orgp(1,j) + sol_fop(1,j) + sol_mp(1,j)
if (porgg > 1.e-3) then
& sol_orgp(1,j) = sol_orgp(1,j) - sedorgp(j) * (sol_orgp(1,j) /
porgg)
& sol_fop(1,j) = sol_fop(1,j) - sedorgp(j) * (sol_fop(1,j) /
porgg)
& sol_mp(1,j) = sol_mp(1,j) - sedorgp(j) * (sol_mp(1,j) /
porgg)
& sol_actp(1,j) = sol_actp(1,j) - sedminpa(j) * (sol_actp(1,j) /
psedd)
& sol_stap(1,j) = sol_stap(1,j) - sedminps(j) * (sol_stap(1,j) /
psedd)
end if
sol_orgp(1,j) = sol_orgp(1,j) - sedorgp(j)
sol_actp(1,j) = sol_actp(1,j) - sedminpa(j)
sol_stap(1,j) = sol_stap(1,j) - sedminps(j)
end if

```

“psed.f”

Note: those were adjusted

“enrsb.f”

```

3-3 enrsb_done.f - Notepad
File Edit Format View Help
!! ~ ~ ~ ~ ~
!! ~ ~ ~ ~ ~ END SPECIFICATIONS ~ ~ ~ ~ ~

use parm

integer, intent (in) :: iwave
integer :: j
real :: cy

j = 0
j = ihru

if (sedyld(j) < 1.e-4) then
  sedyld(j) = 0.0
  sanyld(j) = 0.0
  sllyld(j) = 0.0
  clayld(j) = 0.0
  sagyld(j) = 0.0
  lagyld(j) = 0.0
end if

!! CREAMS method for calculating enrichment ratio
cy = 0.
if (iwave > 0) then
  !! subbasin sediment calculations
  cy = 10. * sedyld(j) / (da_ha * sub_fr(iwave) * sub_surfq(iwave))
&
else
  !! HRU sediment calculations
  cy = 10. * sedyld(j) / (hru_ha(j) * surfq(j))
end if

if (cy > 1.e-6) then
  enratio = .78 * cy ** (-.2468)
else
  enratio = 0.
endif

if (enratio > 3.5) then
  enratio = 3.5
end if

return
end

```

Note: those were adjusted

“solp.f”

```

solp_done.f - Notepad
File Edit Format View Help

integer :: j
real :: xx, vap

j = 0
j = ihru

!! compute soluble P lost in surface runoff
!! compute soluble P leaching

xx = 0.
xx = sol_bd(1,j) * sol_z(1,j)
surqsolp(j) = sol_solp(1,j) * surfq(j) / (xx * phoskd)
!!units ==> surqsolp = [kg/ha * mm] / [t/m^3 * mm * m^3/t] = kg/ha

surqsolp(j) = Min(surqsolp(j), sol_solp(1,j))
surqsolp(j) = Max(surqsolp(j), 0.)
sol_solp(1,j) = sol_solp(1,j) - surqsolp(j)

nly = 0.
nly = sol_nly(j) - 1.

do ii = 1, nly

  dg = 0.
  wt1 = 0.
  vap = 0.

  dg = sol_z(ii+1,j) - sol_z(ii,j)
  wt1 = sol_bd(ii,j) * dg
  vap = sol_solp(ii,j) * sol_prk(ii,j) / (wt1 * pperco)
  vap = Min(vap, sol_solp(ii,j))
  sol_solp(ii,j) = sol_solp(ii,j) - vap
  sol_solp(ii+1,j) = sol_solp(ii+1,j) + vap

end do

!! summary calculation
if (curyr > nyskip) then
  wshd_plch = wshd_plch + vap * hru_dafr(j)
  wshd_ptile = wshd_ptile + vap_tile * hru_dafr(j)
end if

return
end

```

Note: those were adjusted



```

4-2 nminrl.f - Notepad
File Edit Format View Help
end if
ca = 0.
decr = 0.
rdc = 0.
ca = Min(cnrf, cprf, 1.)
if (idplt(j) > 0) then
  decr = rsdco_pl(idplt(j)) * ca * csf
else
  decr = 0.05
end if
decr = Max(decr_min, decr)
decr = Min(decr, 1.)
sol_rsd(k,j) = amax1(1.e-6,sol_rsd(k,j))
rdc = decr * sol_rsd(k,j)
sol_rsd(k,j) = sol_rsd(k,j) - rdc
if (sol_rsd(k,j) < 0.) sol_rsd(k,j) = 0.
rmn1 = decr * sol_fon(k,j)
rmp = decr * sol_fop(k,j)
sol_fop(k,j) = amax1(1.e-6,sol_fop(k,j))
sol_fop(k,j) = sol_fop(k,j) - rmp
sol_fon(k,j) = amax1(1.e-6,sol_fon(k,j))
sol_fon(k,j) = sol_fon(k,j) - rmn1
sol_no3(k,j) = sol_no3(k,j) + .98 * rmn1
sol_aorgn(k,j) = sol_aorgn(k,j) + .02 * rmn1
sol_solp(k,j) = sol_solp(k,j) + .98 * rmp
sol_orgp(k,j) = sol_orgp(k,j) + .02 * rmp
end if
!! septic changes 1/28/09 gsm
!! compute denitrification
wdn = 0.
if (i_sep(j) /= k .or. i_sep_opt(j) /= 1) then
  if (sut >= sdnco) then
    wdn = sol_no3(k,j) * (1. - Exp(-cdn * cdg * sol_cbn(k,j)))
  else
    wdn = 0.
  endif
  sol_no3(k,j) = sol_no3(k,j) - wdn
end if
!! summary calculations
if (curyr > nyskip) then
  wshd_hmn = wshd_hmn + hmn * hru_dafr(j)

```

“nminrl.f”

Note: those  
were adjusted